



## Durham E-Theses

---

### *Mid crustal thrust tectonic processes: examples from the Dalradian of N.W. Donegal*

Jolley, Stephen J.

#### How to cite:

---

Jolley, Stephen J. (1994) *Mid crustal thrust tectonic processes: examples from the Dalradian of N.W. Donegal*, Durham theses, Durham University. Available at Durham E-Theses Online:  
<http://etheses.dur.ac.uk/5884/>

#### Use policy

---

The full-text may be used and/or reproduced, and given to third parties in any format or medium, without prior permission or charge, for personal research or study, educational, or not-for-profit purposes provided that:

- a full bibliographic reference is made to the original source
- a [link](#) is made to the metadata record in Durham E-Theses
- the full-text is not changed in any way

The full-text must not be sold in any format or medium without the formal permission of the copyright holders.

Please consult the [full Durham E-Theses policy](#) for further details.

---

Academic Support Office, Durham University, University Office, Old Elvet, Durham DH1 3HP  
e-mail: [e-theses.admin@dur.ac.uk](mailto:e-theses.admin@dur.ac.uk) Tel: +44 0191 334 6107  
<http://etheses.dur.ac.uk>

MID CRUSTAL THRUST TECTONIC PROCESSES:  
EXAMPLES FROM THE DALRADIAN OF N.W. DONEGAL.

by

Stephen J. Jolley

The copyright of this thesis rests with the author.  
No quotation from it should be published without  
his prior written consent and information derived  
from it should be acknowledged.

A thesis submitted for the degree of Doctor of Philosophy  
at the Department of Geological Sciences, University of Durham.

January 1994.

i.



22 NOV 1994

To  
Catherine

## COPYRIGHT

The copyright of this thesis rests with the author. No quotation from it should be published without his prior written consent and any information derived from it, should be acknowledged.

No part of this thesis has been previously submitted for a degree at this university or any other university. The work described in this thesis is entirely that of the author, except where reference is made to previous published or unpublished work.

## ABSTRACT

A D2 ductile thrust imbricate stack has been identified within the mid greenschist facies (Appin Group) metasediments of the Breaghy Head area of Co. Donegal. Major stratigraphy parallel tectonic slides detach arrays of subsidiary ductile thrust imbricates, which display patterns of intensifying strain and minor structures generally regarded as being diagnostic of the much broader thrust sense shear zones (tectonic slides) which typify deformation within metamorphic parts of mountain belts. This commonality of structural associations implies that the Breaghy Head imbricates and their broader larger scale counterparts must share similar generative and propagative processes.

The imbricates have 'shaped' geometries with long bedding parallel flats and shorter 20-30° ramps preserved as hangingwall anticlines, footwall synclines or complex remnant zones of climbing vein arrays. At a number of localities, ramps have escaped direct incorporation into mature thrust profiles and have been preserved within thrust hangingwalls, 'frozen' at early or intermediate stages of development. This has enabled identification of three distinct ramp styles; "Vein array ramps" characterised by vein array complexes, and "fold ramps" & "fabric slip ramps", both hosted by primary F2 folds. These fold hosted ramps can be seen to nucleate or result from coalescent propagation of ductile thrust dislocation cells (FSR & FR respectively).

The concept of thrust dislocation cells is supported by the presence of D2 extensional flow within the imbricate stack, expressed by shear bands and boudinage. These structures are kinematically and temporally intimate, forming combinant structures at a number of localities. These structures characteristically intensify towards the thrust planes but are never seen to deform them, such that extensional flow is detached at the thrust plane to which it is seen to intensify.

The extensional and contractional flow clearly relates spatially and temporally to the generation and movement of individual imbricates and must, therefore, coexist kinematically as this takes place. This can be explained by rheologically focusing (localising) deformation to produce stratigraphy parallel dislocation cells. The development and subsequent propagation of these features produces the observed structural patterns and displacement connectivity via ramp generation to produce mature 'shaped' ductile thrust profiles.

Local polyphase fold and fabric histories are seen to be generated during continuum D2 ductile thrusting. These structures are temporally and spatially restricted, chiefly as hangingwall strains produced by local thrust stacking processes (eg. imbricate back-steepening and culmination extension). Local polyphase sequences are also generated by development of rare backthrusts, buttressing and footwall collapse of ramps and hard band block rotations. These structures are clearly D2 ductile thrust secondary structures, related to local kinematic processes and do not therefore reflect regional polyphase deformation.

## ACKNOWLEDGEMENTS

Special thanks to my supervisor, Donny Hutton, for his advice, guidance, encouragement and support over the years. His enthusiasm and discussion of the ideas communicated within this thesis is gratefully acknowledged. Thanks also to my other supervisor, Rob Butler, for useful discussion regarding strain localisation.

I would like to express gratitude to the people of Dunfanaghy, for welcoming me into their small community and their homes, making my time there an extremely happy one. Special thanks go to Martin O'Hara and Connie McGilloway for their company during two long field seasons; people of rare talent, who together with "Sugarfoot" and friends filled our house with a combination of R&B and traditional Irish music, life and laughter. Kenny Thompson is appreciated for alarmingly high speed lifts to work on his motorbike and his brother Dave for more sedate lifts to the pub on his moped. Thanks also to Eddie Gavin at the "Oyster" for logistical help, Jim Curran for weekly struggles over the chess board and Olly McGilloway for finding me unusual enough to interview on Ulster Television.

I would like to thank my office cohabitants at Durham, Ken McCaffrey, Chris Jones and Richard 'Trickie' England for their company, sense of humour and wide ranging discussions. Thanks also to Paul Jackson for company and discussions at Durham and in the field in Scotland, Gerald Roberts for mutual thrust tectonic trouble shooting sessions and Ian 'Thuggy' Alsop for discussions on Dalradian tectonics at Durham and in the field in Donegal. Thanks also to the post grads, Alick Leslie, Steve Mackin, John Henton, Pete Kealy, Simon Hook, and Kevin Brown for making Durham fun.

Thanks to Dave Asbery for supplying lights and performing regular surgery on my ghetto blaster, and to Karen Atkinson for advice and loans of drawing office equipment. Thanks also to Ron Lambert and George Randall for providing thin sections and to Gerry Dresser and Alan Carr for help with photography.

Special life-saving thanks to Marilyn Kendrick and Bert Askes at Anglovaal Ltd. (Johannesburg), for help draughting the maps.

## CONTENTS

<b>Copyright.</b>	iii
<b>Abstract.</b>	iv
<b>Acknowledgements.</b>	v
<b>Contents.</b>	vi
<b>Chapter 1: Introduction and previous research.</b>	1
1.1 Stratigraphy.	1
1.2 Structure.	2
1.3 Methodology.	4
<b>Chapter 2: Features diagnostic of ductile thrusting in the Dunfanaghy-Breaghy Head area.</b>	7
2.1 Thrust rationale.	8
2.2 Kinematic indicators.	12
2.2.1 Reliability of extensional crenulations and shear bands.	14
2.3 Nature of the thrusts.	20
2.3.1 Cleavage and strain profiles.	20
2.3.2 Boudinage and minor folds.	23
2.3.3 Syn-tectonic veining.	27
2.4 Summary.	29
<b>Chapter 3: Thrust sequence and imbricate geometry in the Dunfanaghy-Breaghy Head area.</b>	31
3.1 Knockduff, Dunrudian, Sessiagh, Lishagh and Kill.	31
3.2 Breaghy Head and Curragh Harbour.	45
3.3 The breaching thrusts.	53
3.4 The Middle Town stack and Sandhill imbricates.	71
3.5 Summary.	82
3.5.1 Sessiagh-Clonmass formation depositional environment.	83
3.5.2 Sessiagh-Clonmass Limestone and Quartzite thickness.	85
3.5.3 Structure.	86



<b>Chapter 4: Ramps.</b>	87
4.1 Ramps and folds.	87
4.1.1 Fabric slip ramps.	89
4.1.2 Fold ramps.	93
4.2 Vein array ramps.	96.
4.3 Summary.	99
<b>Chapter 5: Propagation of tectonic slides and the generation of "shaped" ductile thrusts.</b>	103
5.1 History.	103
5.2 D2 "associated" structures.	105
5.2.1 Kinematic classification of F2 folds.	106
5.2.2 "Primary" F2 folds.	109
5.2.3 D2 strain, S2 cleavage and bedding.	113
5.2.4 D2 stretching lineation.	114
5.2.5 Tectonic schists.	116
5.2.6 Boudinage.	117
5.2.7 Syn-tectonic quartz veins.	119
5.3 D2 secondary fabrics.	121
5.3.1 Secondary fabric timing.	121
5.3.2 Extensional crenulation orientation.	123
5.3.3 Extensional crenulation geometry and flow partitioning.	124
5.4 Propagation of tectonic slides and the generation of 'shaped' ductile thrusts.	128
5.4.1 Propagation of D2 thrust flats: a rheological control.	129
5.4.2 Flow kinematics associated with dislocation cells.	134
5.4.3 D2 extensional structures: support for a dislocation cell model.	138
5.4.4 Implications for D2 stretching lineations.	140
5.4.5 Implications for propagation of D2 thrust ramps.	141
5.4.6 Lateral structures.	145
5.5 Summary.	147

<b>Chapter 6: Discussion and conclusions.</b>	150
6.1 Section restoration and D2 ductile thrust displacement in the Breaghy Head area.	150
6.2 D2 ductile thrust dislocation cells.	152
6.3 Implications for polyphase deformation.	154
6.3.1 Penetrative deformation structures.	154
6.3.2 Local polyphase deformation histories.	155
6.3.3 D2 thrust and fold sequence.	156
6.4 Metamorphic implications.	157
6.4.1 Spatial and temporal focusing of greenschist metamorphism.	157
6.4.2 D2 'non-penetrative' fabrics.	158
6.5 Structure and age of metadolerite intrusives.	159
6.5.1 Evidence for pre-orogenic intrusion?	160
6.5.2 Evidence for syn-D2 intrusion.	161
6.5.3 Temporal interaction between metadolerite intrusions and D2 thrusting.	164
6.6 Significance of Dalradian Basin extensional faults.	165
6.7 Other discrete ductile thrust imbricate zones within the Dalradian belt.	166
6.8 Regional implications and concluding remarks.	167
<b>References.</b>	168

Two geological maps of the Dunfanaghy-Breaghy Head area are included at the rear of this thesis, primarily intended for use with chapter 3. A series of sequentially restored cross sections which summarise relationships discussed in chapters 3 & 6 are also included at the rear of this thesis.

## CHAPTER 1

### INTRODUCTION AND PREVIOUS RESEARCH

The study area lies within NW Donegal, on the western shores of Sheephaven Bay (Fig 1.1). The highest ground is the NE-SW chain of dissected ridges dominated by Muckish mountain, the summit of which reaches some 670m. The topography falls sharply to the NW from Muckish and then slopes gently, via a series of lee and scarp slopes, towards the coastline of Breaghy Head and Dunfanaghy. A sand choked tidal estuary separates Dunfanaghy from the relatively high ground (120-240m) of the Horn Head peninsula, whose hummocky topography is abruptly terminated on three sides by high cliffs. Originally surveyed by Kilroe & Nolan (1891), the rocks themselves are deformed mixed lithology greenschist facies metasediments and sill-like metadolerite sheets.

#### 1.1 Stratigraphy

In order to make accurate structural interpretations in complexly deformed sedimentary rocks, an understanding of the stratigraphy is vital. The lack of fossils or instantaneous time markers in these rocks has necessitated a lithostratigraphic approach. The stratigraphy of NW Donegal was described in detail from separate study areas by Iyenger et al (1954), McCall (1954), Knill & Knill (1961), Pulvertaft (1961) and Rickard (1962). This generated a confusing picture of geographically separated type successions with locally derived nomenclature. Pitcher & Shackleton (1966) reviewed and simplified the stratigraphy into a standard succession (Fig 1.2), and correlated it with the Ballachulish succession in the Scottish Appin (lower Dalradian)



Group. This correlation was originally suggested by McCallien (1937). Pitcher & Berger (1972) and Harris & Pitcher (1975) give this simplification and correlation a more detailed treatment.

With respect to the present author's study area, the lithologically varied Sessiagh-Clonmass formation, which contains metamorphosed limestones, pelites, silts and quartzites, has received detailed scrutiny from a number of authors. McCall (1954) and Rickard (1962) were in disagreement about the stratigraphic thickness of this formation. McCall had suggested the existence of "considerable repetition" by isoclinal folds and had therefore made allowances for this in his estimate. Whilst a combination of folding and facies diversity was favoured by Pitcher & Berger (1972), Hutton (1977a) adopted a strong facies variability to explain the complex and sometimes abrupt thickness and lithological changes presented by the Breaghy Head peninsula (Fig 1.3). This non layer-cake approach to the stratigraphic question is maintained in the present study.

## 1.2 Structure

McCall (1954) restricted his interpretation to that of the major structure. This he suggested, consisted of the NW verging and facing Marble Hill syncline and a similarly verging fold pair on Horn Head. These structures were envisaged to fold the Horn Head slide, which he correlated with the slide at Dunfanaghy and interpreted as being stratigraphically extensional, cutting out the complete Sessiagh-Clonmass formation between Dunfanaghy and Horn Head (Fig 1.4). This geometrical interpretation was in conflict with his view that the slide had developed in conjunction with the folding. Working in the Errigal area to the west, Rickard (1962) was in agreement with McCall's interpretation and recognised the Aghla anticline as the overlying return hinge to the Marble Hill syncline (which he renamed the Errigal syncline).

Rickard also suggested that a series of later cross cutting structures were related to the intrusion of the Thorr Granodiorite and the Main Donegal Granite.

His observations came at a time when the concept of polyphase deformation was gaining widespread acceptance in the geological fraternity. This developed into the technique of placing structures into chronologies of deformation 'events'. Employing this methodology, Pitcher & Berger (1972) were the first authors to establish a chronology of metamorphic and deformational events for the region (Fig. 1.5).

Pitcher & Berger (1972) interpreted the major structure in a very similar way to McCall (1954) and Rickard (1962), (Fig 1.4), but pointed out that the folding of the Horn Head slide presented a mechanical problem: how could a major dislocation be folded around the hinge of a fold and still be generated as a result of that folding? This was based on the understanding that slides were developed in strong causal connection with fold development (Bailey 1910, Fleuty 1964). The problem also rested with the paradox that the Horn Head slide apparently represented a strong thinning and removal of stratigraphy around a fold hinge, where stratigraphy would normally be expected to thicken. Pitcher & Berger therefore concluded that the Horn Head slide predated the folding.

Hutton (1977a, 1979a, 1983) interpreted the major structure not as a single extensional and folded slide, but as two separate thrust slides. Recognising the pelites on Horn Head as Ards Pelites, (and not Falcarragh Pelites), gave the Horn Head slide a thrust geometry and displacement, placing older rocks over younger (Figs 1.4, 1.6). Hutton was then able to demonstrate that the folding and thrusting were of similar (D2) age, and concluded that the Dunfanaghy slide to the south was also a thrust of D2 age.

Hutton (1977a, 1977b) also revised and updated (1982, 1983) the deformation chronology of Pitcher & Berger (1972), (Fig 1.5), and demonstrated a strong causal association of his D6-D9 structures with the emplacement of the Main Donegal Granite into a transcurrent sinistral shear zone to the south.

### 1.3 Methodology

One of the original briefs of this study was to investigate the extent to which polyphase deformation is generated during continuum ductile thrusting. An investigation was therefore undertaken, using the standard methodology as applied to polyphase deformation belts. This was carried out in order to establish which of the structures observed were of local kinematic significance and which of 'true' polyphase character. This is based on the cross-cutting relationships between structural elements, such that an earlier element is deformed by a later one. The resulting local chronology of elements is then pigeon-holed, such that folds (F) and cleavages (S) are allocated to a deformation 'phase' (D). A numerical subscript then denotes relative age in the chronological sequence, such that (D1) is post-dated by (D2), (S1) by (S2) and (F1) by (F2). These local chronologies of cross cutting structures are then correlated between outcrops across the area. Other abbreviations are utilized, but explanations are addressed where appropriate.

Fieldwork began by concentrating on major, identified ductile thrusts on Horn Head and at Dunfanaghy (Hutton 1977a, 1979a, 1983). These are broad ductile shear zones which are host to a complex series of structural elements. The chronology of cross cutting relationships established at these localities formed the basis for Hutton's (1983) regional chronology of events. It was found, however, that some of the fabrics in the chronology were extensional crenulations, belonging kinematically to D2 and not

part of any subsequent deformation. As will be discussed in detail in the following chapters, the Sessiagh Clonmass formation rocks of the Breaghy Head - Dunfanaghy area were found to contain a number of more discrete ductile thrust shear zones. These are also found to host fabrics which represent secondary shear zone crenulations. These thrusts are also seen to have 'shaped' profiles with ramp and flat segments. These geometrical features concentrate local fabric histories, which are kinematically linked to the thrusting and not therefore part of subsequent deformation.

In view of these discoveries, it was felt that a purely chronological approach to the structural investigation was inappropriate. Instead a geometrical approach was included in the investigation, similar to that applied to foreland fold and thrust belts. This involves identification of geometrical elements within the system (eg. hangingwall & footwall ramps, flats, hangingwall or footwall short-cuts, etc.), and identifying their geometrical (eg. triangle zones), and temporal inter-relationships (as in folded or breaching thrusts). This was greatly aided and supplemented by an emphasis on ductile kinematic behaviour, drawing on a range of cross cutting relationships and kinematic indicator criteria.

The approach therefore attempts to identify those structures developed in response to local processes as distinct from those related to polyphase deformation patterns. In this respect D1 and D2 were found to exist, although the deformation associated with the thrusting (D2) was seen to be far more complex than Hutton's (1983) D2, being found to contain his D3 and elements of his D4 and D5 deformation phases.

This geometrical approach was also favoured since the similarities and contrasts between thrust geometries found in this greenschist facies study area and the geometries of equivalent

structures within foreland thrust and fold belts might suggest the extent to which kinematic processes compare or contrast between the two crustal levels. Since the terminology applied to geometric features found in thrust belts is well documented in the literature (eg. Boyer & Elliott 1982, Butler 1982a) and seemingly commonplace in geological discussion, terminology explanations have not been repeated here.

The ductile thrusts within the Breaghy Head - Dunfanaghy area were found to display patterns of intensifying D2 strain and minor structures generally regarded as being diagnostic of the much broader thrust sense shear zones (tectonic slides) which typify deformation within metamorphic parts of mountain belts. Emphasis was placed on the details of nature and distribution of these minor structures, since the similarity of structural associations implied that the Breaghy Head - Dunfanaghy ductile thrusts and their broader larger scale counterparts must share similar generative and propagative processes. The attempt to identify these processes and those responsible for the generation of ramps in the thrust profiles was considered to be a vital aspect of the investigation.

The following chapters describe and investigate the geometries, sequencing and kinematic histories of ductile thrusts within the Breaghy Head - Dunfanaghy - Horn Head area, and processes responsible for the development of local polyphase fabric and fold histories during continuum D2 thrusting, ramp development and the propagation of ductile thrusts (tectonic slides).



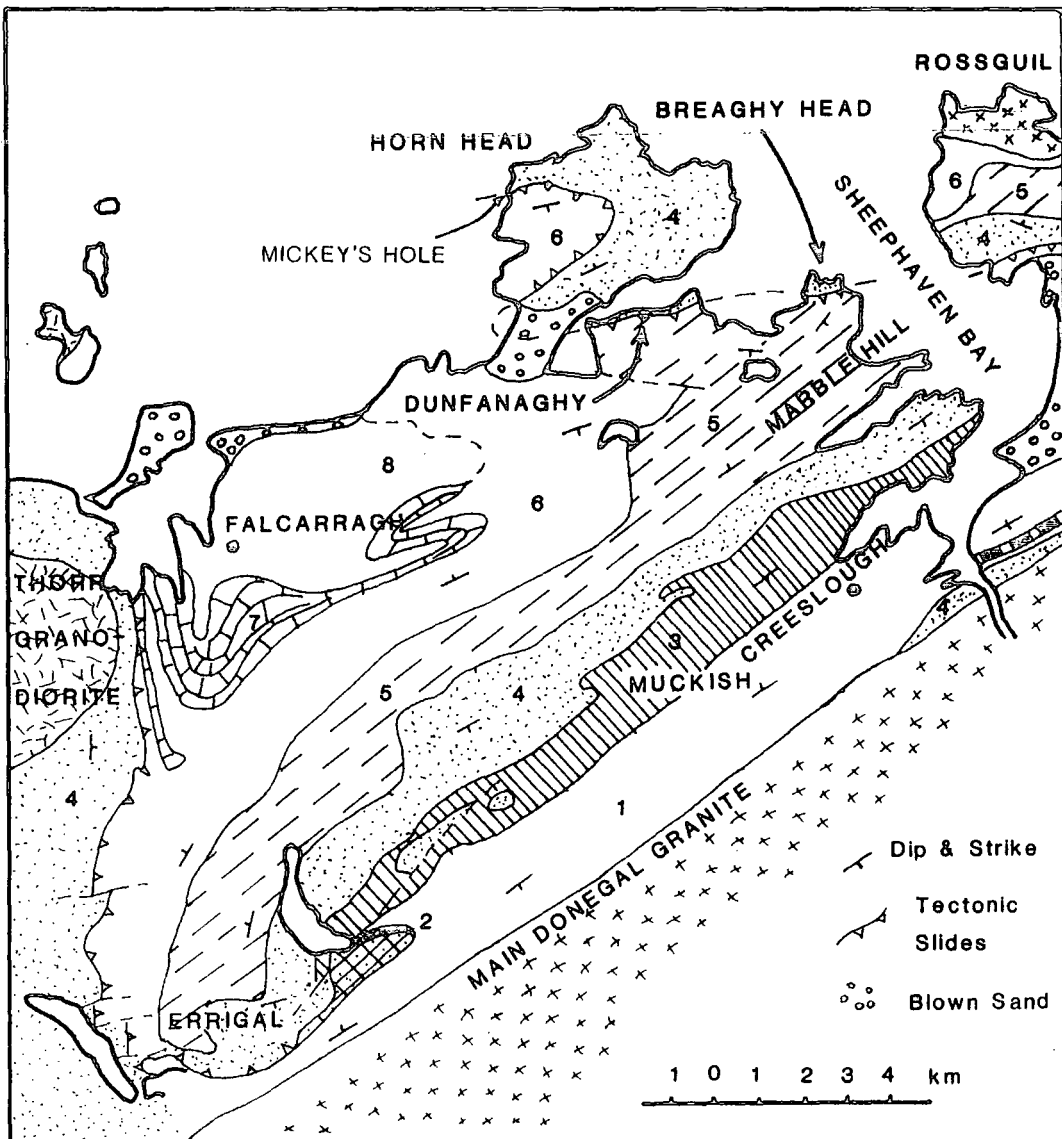
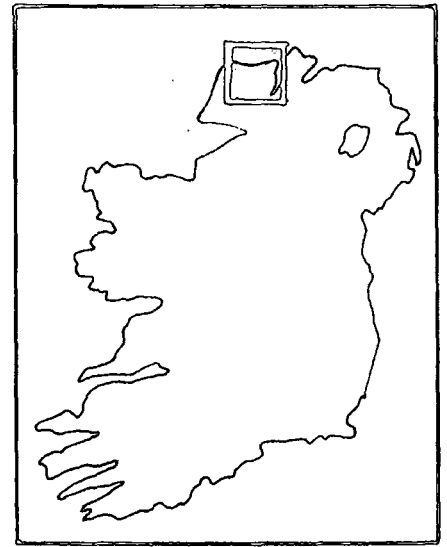
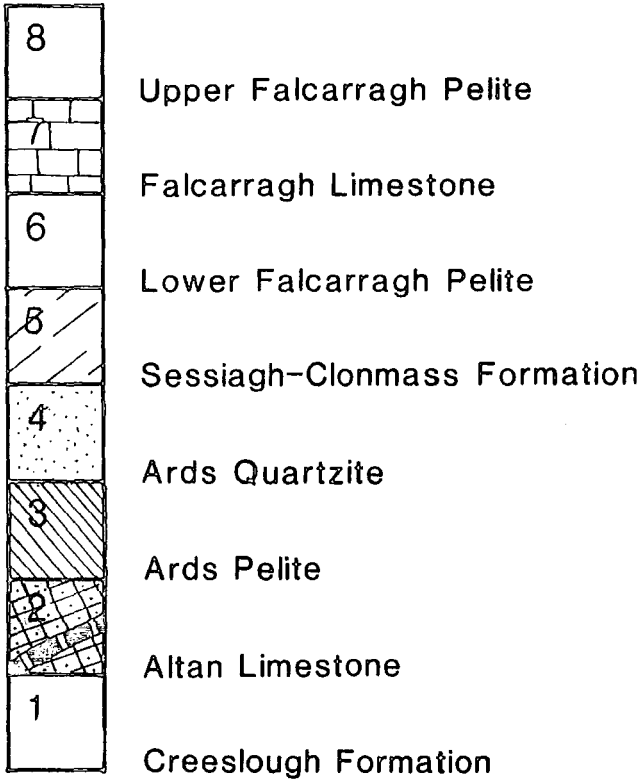


Figure 1.1 Location map and standard stratigraphic sequence in the region (after Pitcher & Berger 1972).

Upper Falcarragh Pelites

Falcarragh Limestone

Lower Falcarragh Pelites

Sessiagh-Clonmass  
formation

Ards Quartzites

Ards transition formation

Ards Black Pelites

Altan Limestone

Creelough Formation

In more detail:

Port Limestone

Sessiagh banded Quartzite

Marble Hill Limestone

Clonmass banded Quartzites

Clonmass Limestone

Figure 1.2 Standard lithostratigraphic succession of metasedimentary rocks in the study region (after McCall 1954, Pitcher & Shackleton 1966).

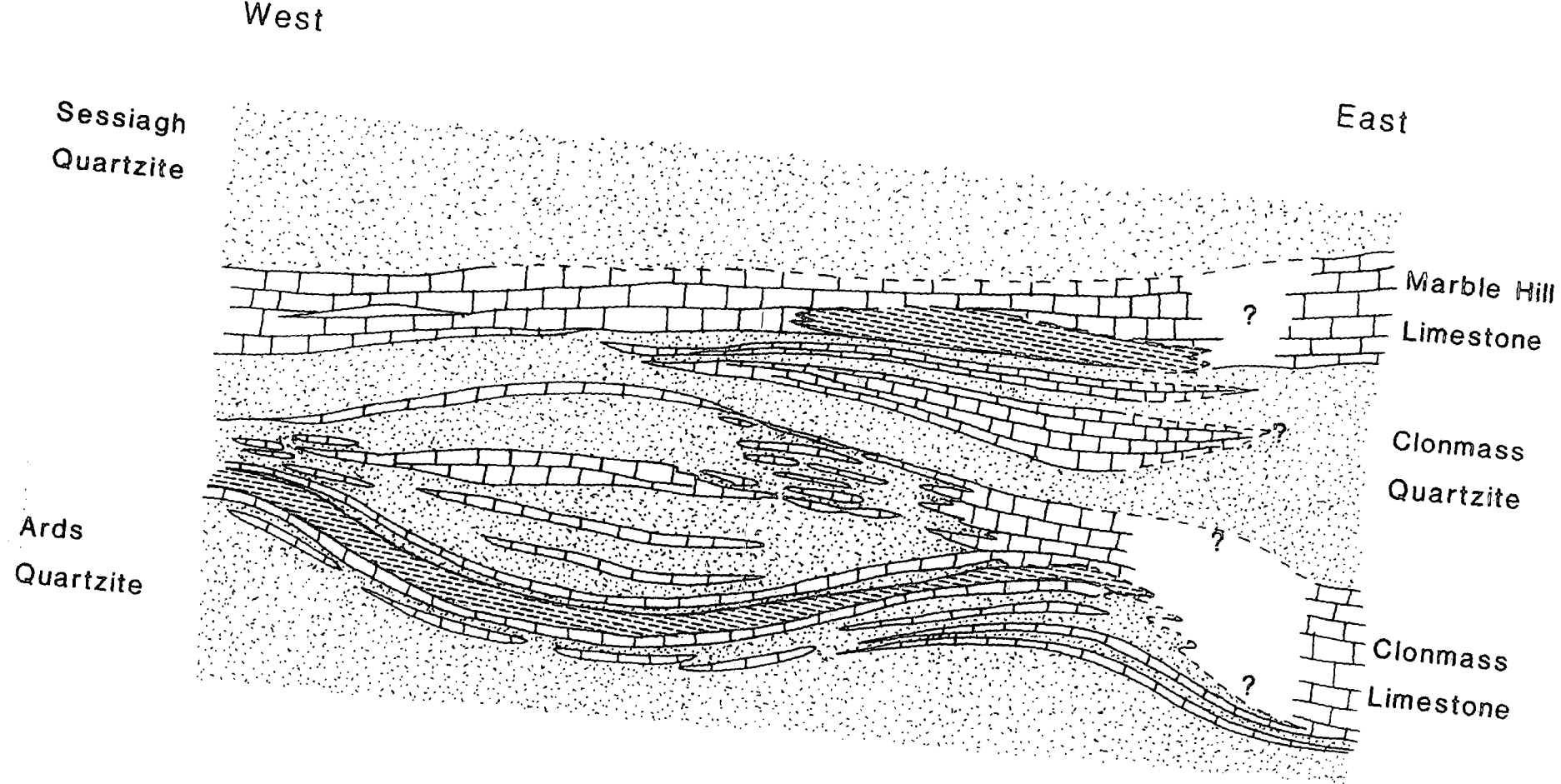


Figure 1.3 Schematic facies diagram of the Sessiagh-Clonmass formation in the Breaghy Head area, (after Hutton 1977a). Not to Scale.

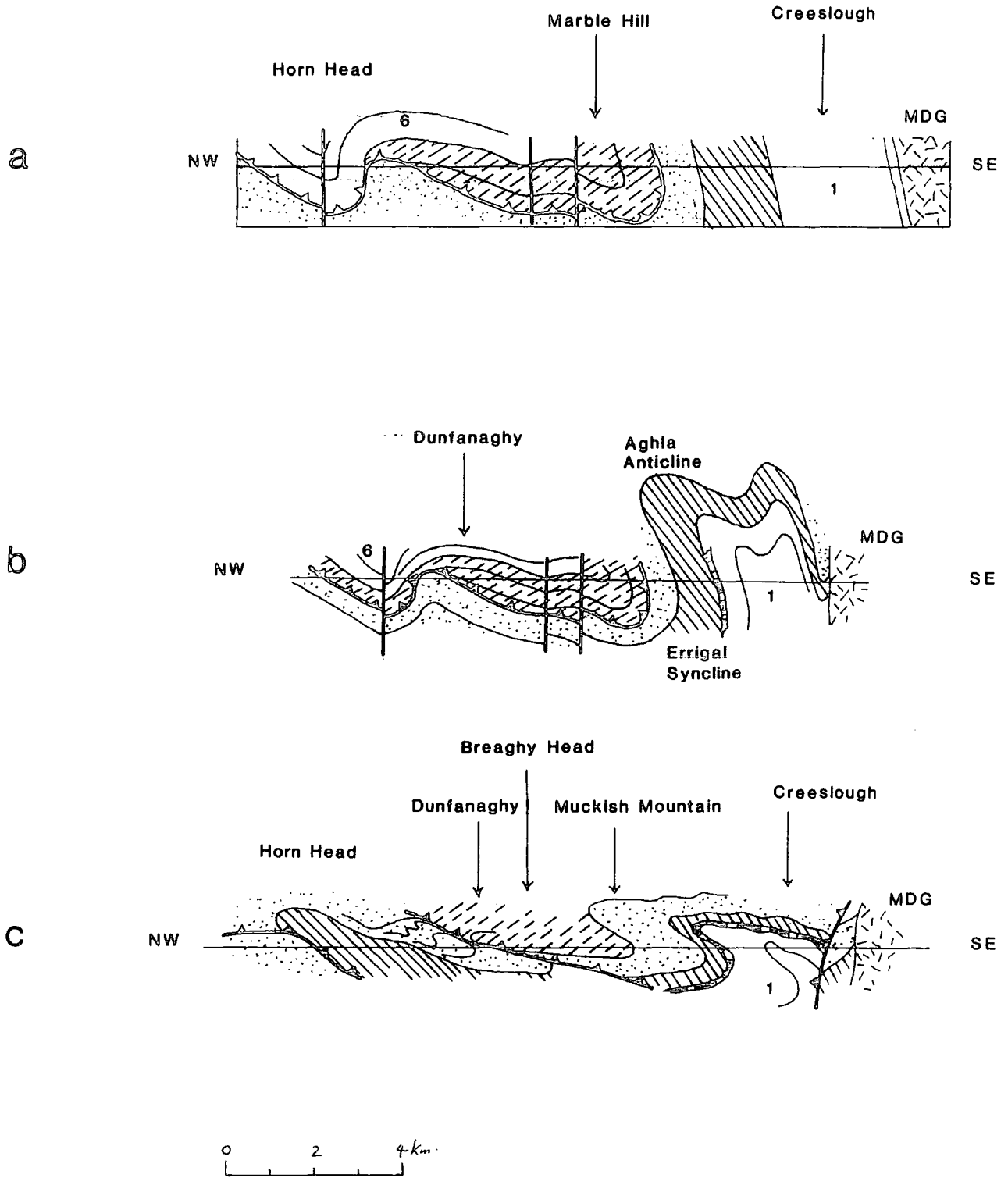


Figure 1.4 Comparison of regional cross sections produced by previous authors. (A) McCall (1954), (B) Pitcher & Berger (1972), (C) Hutton (1977a, 1983). MDG: Main Donegal Granite. (Ornament as for fig 1.1).

Pitcher & Berger (1972)

Hutton (1977b)

Hutton (1983)

D1 S1

D2-D3 { S2 F2  
S3

D4 { S4a  
F4b

Deformation associated with the Main Donegal Granite

DMG1 (Mineral alignment, mullions)

DMG2 SMG2 FMG2

?

DMG3 SMG3

D1 S1

D2 S2 F2

D3 S3 F3

?

D4 S4 F4

D5 S5 F5

D6 S6

D7 S7 F7

D1 S1

D2 S2 F2

D3 S3 F3

D4 S4 F4

D5 S5 F5

D6 S6 F6

D7 S7

D8 S8

D9 S9

Figure 1.5 Comparison of regional deformation chronologies according to Pitcher & Berger (1972), Hutton (1977a, 1983).

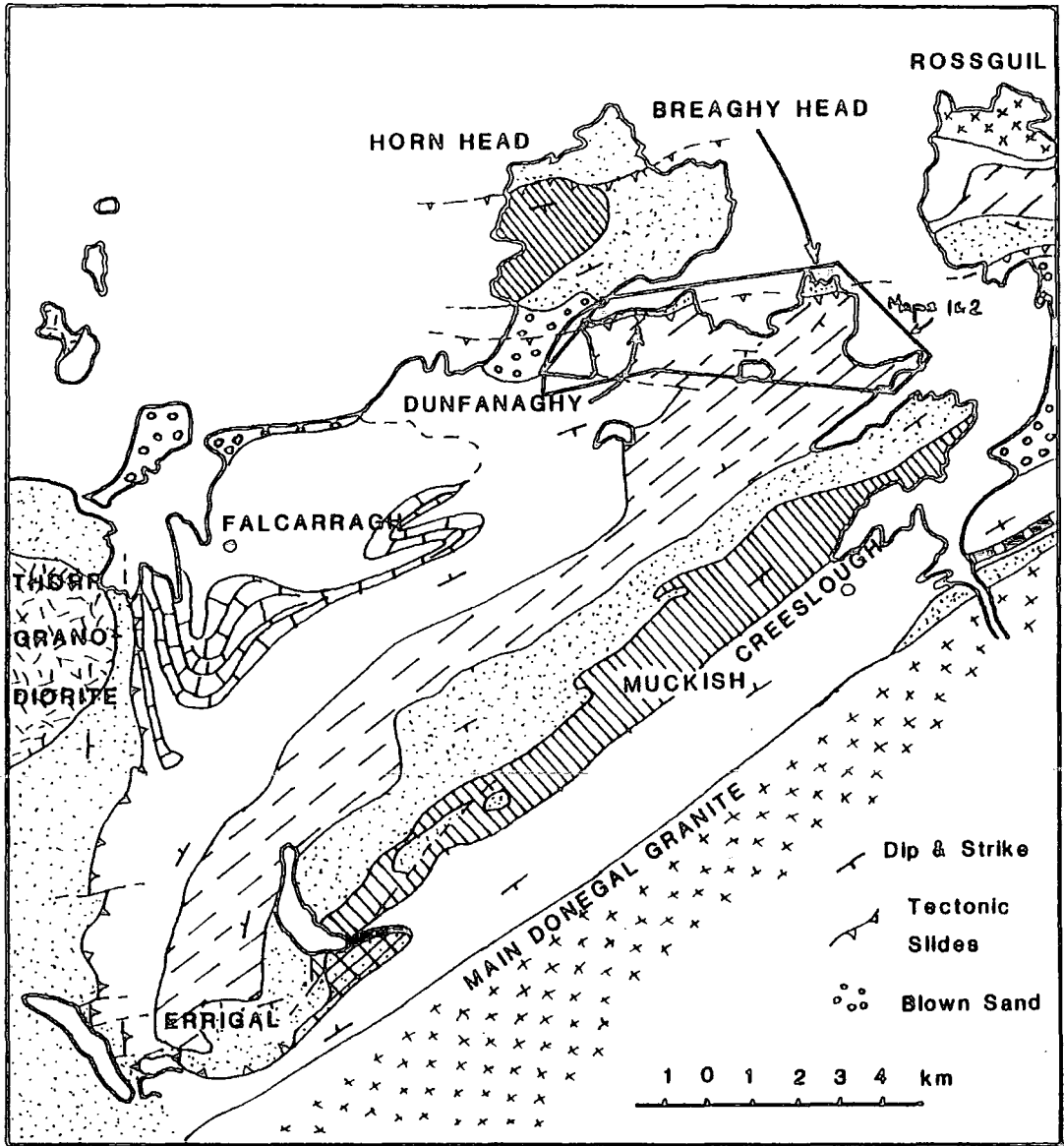


Figure 1.6 Regional map of NW Donegal modified from Pitcher & Berger (1972, cf. Fig 1.1), to incorporate Hutton's (1977a, 1979a, 1983) revision of major D2 structures. (Ornament as for Fig 1.1).

## CHAPTER 2

### FEATURES DIAGNOSTIC OF DUCTILE THRUSTING IN THE DUNFANAGHY-BREAGHY HEAD AREA

As indicated in Chapter 1, the rocks of the present study area are mainly composed of the Ards Pelite, Ards Quartzite and Sessiagh-Clonmass formation greenschist facies metasediments. As defined by McCall (1954), Rickard (1962) and Hutton (1977a), the Sessiagh-Clonmass formation rocks are a variable sequence of metamorphosed pelites, silts, quartzites, calcarenites and limestones, intruded by sill-like metadolerite sheets (Figs 2.1 & 1.3). This lithological variation of the Sessiagh-Clonmass formation is best developed and exposed on the Breaghy Head peninsula.

A reconnaissance of the Breaghy Head area led to the recognition of a large number of exposures displaying mylonitic strains, bedding cut-offs with thrust geometries and small scale kinematic indicators. The excellent exposure, (often in three dimensions), lithological variation and good primary way up evidence aided the recognition of a stack of imbricate ductile thrusts. Since this interpretation conflicts with the accepted interpretation which attributes the repetitive distribution of the Sessiagh-Clonmass lithologies to folding and the sedimentary history of the formation, it was decided to produce a detailed lithological map of the Breaghy Head peninsula and the surrounding environs.

The relatively small scale of the imbricate system and the excellent exposure tightly constrained observations and correlation of structural elements in the area. Whilst kinematic models will be discussed more fully in subsequent chapters, the main aim of this chapter and chapter three is to demonstrate ductile thrusting from the field evidence and to describe the geometry of the imbricates.

## 2.1 Thrust Rationale

The basic evidence that thrusts exist in this area is as follows: There are within the area relatively narrow zones of mylonitic fabric which must represent ductile displacement zones. There are clear duplications of stratigraphy across these zones. These repeat a relatively simple stratigraphic package which consists of a limestone, a quartzite and a limestone-quartzite transition. For example, N-S transects between (724100-633266) and (741100-707314), map 1.

With respect to bedding, these mylonitic zones have characteristic flat and ramp geometries similar to thrust faults from higher levels in the crust and are clearly visible and mappable in the field. These features support the contention that stratigraphy is duplicated across the mylonite zones.

Shear sense indicators (discussed in more detail below) are common and show a consistent NW directed overshear parallel to the well developed stretching lineation in the mylonites. Since the ramps are seen to incline in a variety of directions, with the general exception of NW, the kinematic indicators confirm that stratigraphy climbs the ramp segments and is not extended across them.



As will be discussed below, the mylonitic fabric has a non-mylonitic variant which is contractional in nature and is axial planar to westerly, northerly and easterly vergent folds. This shows that the mylonite zones were developed in a contractional environment and must, therefore represent contractional (thrust) dislocations of the stratigraphy.

The lithological map is similar in general appearance to maps of other thrust belts (maps 1 & 2) and the thrusts have been found to duplicate a relatively simple limestone-transition-quartzite stratigraphy (discussed in more detail below). McCall (1954) had suggested the existence of 'considerable repetition' in the Sessiagh Clonmass formation by isoclinal folding. However, the stratigraphic repetition is consistent with imbrication and not isoclinal folding (ie. abcabcabc compared with abcbabcba is asymmetric, Fig 2.2 & maps 1 & 2). In addition, primary way up criteria (such as cross stratification and ripples in the quartzites), reflect an overall constant right way up younging direction, and do not therefore record the repetitive younging reversals required by isoclinal folding. Furthermore, fabric (strain) characteristically intensifies towards basal limestone contacts, such that this is asymmetric with respect to stratigraphic repetition, consistent with intensification towards thrust planes and quite unlike the symmetrically disposed strain patterns of isoclinal folding (cf Fig 2.2 a & b).

In the study area, the earliest tectonic deformation is expressed as a weak, rarely developed bedding parallel to gently NW vergent slaty cleavage (S1) of very low metamorphic grade (Hutton 1977a, 1977b, 1983). In Central Donegal, D1 is associated with a major ductile thrust (Alsop 1987, 1992), but there is no evidence of D1 thrusting in the present study area and therefore the remaining discussion will concentrate on the post D1 deformation.

The thrust planes are easily identified in the field as localised zones of intense platy mylonite which contain a strong NW-SE mineral extension lineation and small scale sheath folds. As noted above, these mylonites strengthen the case for high strain dislocations of the stratigraphy, with small scale shear sense indicators (discussed below) showing predominantly NW directed overthrusting. The main mylonitic fabric can be traced away from the thrust planes, where the mylonitic character of the fabric is gradually lost. It is transitional with a gently inclined non-mylonitic pervasive fabric which is axial planar to W, N & E vergent folds, and is occasionally be seen to crenulate S1. The folds are therefore referred to as F2, the fabric as S2 and it's mylonitic variant at the thrust planes as S2m. Clearly, the thrusts and folds are penecontemporaneous D2 structures that belong to the same kinematic system. Since the thickness of the mylonitic zones is variable, (often between 1m and approximately 10m), the transition between S2 and S2m can be observed within individual exposures and cliff sections.

The mineralogy associated with S2 consists of quartz, plagioclase (probably albite), K feldspar, chlorite, muscovite, biotite, margarite, actinolite, epidote and occasionally garnet. The metamorphic grade is therefore interpreted as being within the quartz, albite, epidote, almandine subfacies of the Greenschist facies\* (Winkler 1967), or within the upper biotite, lower garnet Barrovian zone. The S2 fabrics are associated with the segregation and growth of quartz and micas in contractional cleavages indicating pressure solution of quartz and migration by diffusional mass transfer to the hinge regions of microlithon microfolds (Cosgrove 1976). S2 is also seen to wrap around chloritic polygonal knots which are probably pseudomorphs of garnet (Pitcher & Berger 1972, Hutton 1977a); Fresh garnets are sometimes seen in pelites (Fig 2.3). Feldspar porphyroblasts are occasionally seen to contain S2 crenulations of S1 (Hutton 1977a,

\* In a detailed review of the thermobarometry of metamorphic rocks, Essene (1989) indicates that temperatures under greenschist facies conditions are typically constrained to lie between 300-500°C. However, Essene also indicates that existing barometers for greenschist facies rocks are insufficiently calibrated to reliably constrain pressure estimates. Although an accurate estimate of P/T conditions for the study area lies outside the scope of this thesis, a crude estimate of 15-25 km depth can be achieved by assuming a geothermal gradient of 20°C per km.

pers comm. 1988), suggesting early crenulation of S1 preserved by rapid porphyroblast growth followed by intensification of S2 around the feldspars. These factors suggest that S2 and therefore the thrusting in the Breaghy Head and Horn Head area is synchronous with peak Greenschist facies metamorphism.

A qualitative estimate of the strain state of the rocks has been made, based on the spacing and intensity of S2 fabrics. The thickness of mylonitic and intensely cleaved rock is seen to be greater in the hangingwalls than in the footwalls. A good example of this can be seen on the eastern shore of Sessiagh Lough at (567110, maps 1 & 2). Here a thrust emplaces limestone in the hangingwall onto micaceous limestones of the transition beds in the footwall, the thrust being demarked at one position by a thin sliver of quartzite (see chapter 3 for detailed description of stratigraphy). Delicate trace fossils (worm burrows) are preserved some 2m into the footwall, allowing approximately 1m of intensely cleaved and mylonitized limestone below the thrust. By comparison, the hangingwall mylonite/high strain is in excess of 10-15m thickness.

Hangingwall dominant strain patterns have been described from other thrust belts, for example the Scandanavian Caledonides, where the broader hangingwall strain profiles are thought to result from transport of thrust sheets from deeper crustal levels where distributed shearing processes dominate into shallower levels characterised by more discrete shearing processes (R. Gayer, pers comm. 1994).

D2 strains are associated with and therefore generally localised around thrust planes such that mylonite (thrust) bound horizons can be identified. These are seen to contain easily identifiable lithologies with well preserved sedimentary structures as testimony to the low strain states of the horizons

interiors. This also equates well with observations in higher level thrust belts, where the deformation zones are the discrete horse-bounding thrust planes.

## 2.2 Kinematic Indicators

The high strain zones and mylonites of the thrusts frequently contain kinematic indicators. These were used to deduce the shear sense of thrusts and complemented other independent criteria, (such as stratigraphic repetition), in these deductions. These kinematic indicators are summarised in Fig 2.4, together with some of the terminology used below.

The sense of deflection of syn-thrusting S2 fabrics through the thrust strain profiles was used as a general guide to the shear sense. These fabrics have a general southerly dip and were found to curve asymptotically and intensify towards the thrusts, consistently indicating a NW directed overshear. As discussed below, this effect can also be clearly seen at bed margins, and is distinct from cleavage refraction since it is noted in uniform lithologies (eg. quartzites) and around 'banded' shears (see section 2.3.1) within metadolerite sheets. This enabled shear sense to be deduced at *exposure* level, being frequently supported by other kinematic criteria (eg. C band shears parallel to bedding or the planes of discrete shears within metadolerites). The asymmetry of deformed and rotated markers (eg. metadolerite sheets at Mickey's Hole discussed below and located on Fig 1.1), provided a reliable criterion for deducing the sense of shear. Displaced markers were also found to be reliable shear sense indicators. These include boudin necks and quartz veins displaced parallel to the shear planes (C shears) and in the R-1 direction within the thrust high strain zones (Fig 2.5). The margins of the displaced markers, especially the segregated vein portions, are seen to thin and tail to form asymmetric 'fish' (Lister & Snoke 1984), in the

direction of their displacement. This indicates localised ductile displacement rather than brittle offsets. With the notable exception of those exposed at Dunfanaghy harbour (Fig 1.1, maps 1 & 2), these displaced markers consistently indicated a NW overshear.

Asymmetric and rotated porphyroblast (generally pyrite) pressure shadows were uncommon, but useful additional kinematic indicators. They were used with caution since the pressure shadow asymmetry is different in rotated and non rotated porphyroblasts (Simpson & Schmid 1983). Again, with the exception of Dunfanaghy, (discussed below), these indicators supported a NW overshear (eg. Fig 2.6).

Mica 'fish' are also seen in the mylonites, and together with recrystallization of the host rock mineralogy with asymmetric alignment of elongate axes (especially calcite crystals in calc-mylonites), give a consistent indication of NW overshear (Fig 2.7).

Certain beds, or bands in the mylonites, were found to have deformed by fracturing or discrete shearing and 'domino' rotation of the shear-bound blocks (Fig 2.8). These features, similar to the 'asymmetric pull aparts' of Hammer (1986), are interpreted as R-2 shears and were found to consistently rotate towards the NW, indicating overshear in that direction. Strain slip (extensional) crenulations are frequently seen to emanate from the block delimiting shear zones into the surrounding rocks, especially where the 'dominos' are large. The most striking example of domino rotation occurs in the footwall of the Horn Head thrust (Fig 2.8). These large scale features generate open folding, sometimes with weak axial planar crenulation cleavage, at and around the corners of the blocks as a consequence of rotation. These folds and fabrics have previously been interpreted as D4 &

D5 structures (Hutton 1977a), they are however, clearly D2 kinematic structures.

### 2.2.1 Reliability of extensional crenulations and shear bands

The reliability of extensional crenulation cleavages (Platt & Vissers 1980) as shear sense indicators has become the subject of debate in recent years (eg. White et al 1980, Platt 1984, Brunel 1986, White et al 1986, Berhmann 1987, Dennis & Secor 1987). These crenulations, also known as shear bands (White et al 1980), are similar to the C bands of S-C mylonites (Lister & Snoke 1984), since they represent small scale shear zones (Platt & Vissers 1980). The displacement direction of the crenulations is taken to reflect the movement sense of the overall shear zone in the same way that C band displacement directions are used to determine shear sense (Lister & Snoke 1984). In the Breaghy Head area, these crenulations are seen to occur in the D2 high strain zones and mylonites. The cleavage displacements are predominantly towards the NW and are seen to offset the host S2m fabrics and markers such as thin quartz veins. These offsets are distinct from those noted in contractional crenulations since pressure solution features are absent and the microlithon structure thins into and is asymptotic with the cleavage planes in a consistently asymmetric direction across the outcrop width of a given cleavage zone (Figs 2.9, 2.10, 2.11). The extensional crenulations are therefore taken to represent R-1 shears (White et al 1986, Fig 2.4), and are clearly seen to be closely related to shear plane parallel C Shears and reverse P shears (Brunel 1986, Dennis & Secor 1987, Fig 2.12).

The occasional development in mylonites of a second, apparently conjugate set of crenulations with opposite dip and displacement direction has placed the reliability of extensional crenulations into debate (Platt 1984, Berhmann 1987). However,

White et al (1980) and White et al (1986) suggest that extensional crenulations may be used to determine shear sense where only one set is formed, a general rule of thumb now used by many field geologists. The exact geometrical nature of the crenulations, however, and that of the conjugacy between two sets is vitally important since it may allow shear sense to be determined from the extensional crenulations even when two 'conjugate' sets are developed. Using geometrical criteria, a regular field assessment of the reliability of the crenulations as kinematic indicators is possible, especially in the Breaghy Head area, where independent shear sense criteria can be used to verify shear sense deduced from the crenulations .

In extensional crenulation cleavages, the  $\sigma$ -fabric in the microlithons curves asymptotically into the cleavage planes, with one limb thinner than the other, defining the extensional micro-shear (Fig 2.10). In truly conjugate extensional crenulation cleavages, the microlithon structure should reflect the intersection of synchronously developed opposite sense shears and therefore be of augen or phacoidal geometry (Figs 2.10, 2.11, Platt & Vissers 1980). Such conjugate extensional crenulations would be unreliable as shear sense indicators. In the Breaghy Head area, conjugate sets with these geometries are rare. If a distinction between R-1 and R-2 extensional crenulations can be established, the crenulations may still be used to deduce shear sense even where both sets are developed. A geometrical approach to distinguishing between the two sets of extensional fabrics in the field was therefore used in the Breaghy Head area.

Gently NW dipping extensional crenulations are well developed within the thrust mylonites and high strain zones of the Breaghy Head and Horn Head area. They are best developed within micaceous lithologies or where  $S_2$  is intense enough to create sufficient anisotropy for their formation. The angle between these

crenulations and the host S2 fabrics rarely exceeds  $30^{\circ}$ . Since they crenulate the high strain S2 fabrics, are sometimes penetratively developed (eg. Mickey's Hole) and verge in the opposite direction to S2, they have previously been interpreted and correlated as S3 in NW Donegal (eg. Hutton 1977a, 1979a, 1983), with the implication that this cleavage is essentially contractional in nature. This work, however, has shown that the microlithon geometries maintain 'tail' asymmetry across outcrop width and are essentially extensional in character. If these fabrics were contractional, the microlithon asymmetry would be expected to change across the outcrop width (eg. as a result of minor folding), (Figs 2.9, 2.10). Furthermore, pressure solution has not been seen to be associated with these fabrics even when penetratively developed, and they are sometimes seen to clearly displace markers (eg. quartz veins). These displacements are not equal across the cleavage zone, but the apparent intensity of the individual cleavage plane development remains broadly constant, regardless of the difference in displacement recorded by adjacent cleavage planes (measured in mm or several cm). If these fabrics were contractional, the cleavage planes would be expected to be of greater intensity than adjacent planes where the marker offsets are greatest (by virtue of pressure solution). These cleavages also form multiple sets (cf. Platt 1984), which can be seen in the field to link in a similar way to fault systems, or cross-cut such that lower angle sets are seen to be cut by younger higher angle sets.

The crenulations are generally open microfolds of S2 fabrics with the NW dipping limbs (defining the extensional cleavage planes) being thinned with respect to the SE dipping limbs. This lends an asymmetric 'tail' or 'fish' geometry to the microlithons, indicating NW directed extensional shear displacements along the cleavage planes. The cleavage planes are seen to shallow out towards parallelism with S2m and are occasionally seen to change



orientation to cut up section with respect to S2m, producing P shears (Fig 2.12).

The evidence above strongly suggests that the crenulations represent secondary shear fabrics (R-1) developed in response to NW directed thrusting. This shear sense is confirmed by other criteria in the same outcrops as the crenulations (eg. asymmetric pyrite pressure shadows). These fabrics are also occasionally deformed by NW verging F2 warps which rework the S2 or S2m and clearly place the extensional crenulations in D2 (Fig 2.13, section 2.3). In conclusion, these fabrics are now recognised as D2 extensional crenulations (as defined by Platt & Vissers 1980) but were previously identified as S3 (Hutton 1977a, 1983) and correlated regionally between tectonic slide outcrops.

A less common second SE dipping set of extensional crenulations is sometimes developed in the thrust high strain zones. This set is generally not a 'true' conjugate to the NW dipping set (in the sense of Figs 2.10, 2.11 and Platt & Vissers 1980), since the opposing sets of the Breaghy Head area differ in geometry. As described above, the NW dipping (R-1) extensional crenulations are generally open microfolds of S2 fabrics with the NW limbs gently curving and tapering to define the cleavage planes. The SE dipping crenulation microlithons however, do not usually have this 'smooth' geometry (Fig 2.10). The S2 in the microlithons tends to make a far higher angle with the cleavage planes than noted for the R-1 crenulations and the asymptotic curve between the S2 and the extensional cleavage planes is tighter and narrower than in the R-1 crenulations. This suggests formation at a far higher angle (possibly up to 90°) to the S2 fabrics. In the final position the S2 in the microlithons dips NW and would therefore verge SE with respect to the surrounding bedding. S2 verges towards the NW on bedding in surrounding rocks unaffected by these extensional crenulations. This suggests that

the extensional crenulation microlithons and cleavage planes rotate towards the NW during formation.

The microlithons of the SE dipping extensional crenulations may sometimes display gentle internal crenulations which give the cleavage a superficially contractional appearance. Like the NW dipping R-1 extensional crenulations, however, the SE dipping second set also maintains the direction of 'tail' taper asymmetry across outcrop width. The cleavage is also seen to displace markers in a consistently SE direction and the cleavage planes are occasionally associated with fine quartz veining. These fabrics are therefore interpreted as extensional crenulations which have undergone rotation and experienced a contractional and dilatant deformation component during formation. These features all suggest that the SE dipping extensional crenulation set is a cleavage equivalent to rotational 'domino' (R-2) shears and is geometrically distinct from the R-1 crenulations. The extensional crenulations of the Breaghy Head area are therefore judged to be reliable shear sense criteria, even where both sets are developed together.

Where the two sets of crenulations are developed together, the R-2 crenulations are apparently slightly later than the R-1 set and wider spaced. At (200085, maps 1 & 2) the R-2 set deforms the early R-1 but at one position the microlithon geometries appear to show a more conjugate relationship. This suggests R-2 initiation took place towards the latter part of R-1 activity to take over as the dominant secondary shear. There are multiple sets of extensional crenulations in these exposures. The earliest set of closely spaced (1-2mm) R-1 crenulations is cut at a higher angle by a second set of wider spaced (56mm) R-1 crenulations. These are then deformed by R-2 crenulations (again some 5-6mm spacing). Occasional open NW vergent minor warps deform both of the R-1 sets but do not appear to deform the R-2 crenulations.

These warps may therefore be developed at the same time as the R-2 crenulations, although the warps are associated with a rare and weakly developed crenulation cleavage only seen in micaceous partings and this is distinct from the R-2 fabric. This would tend to suggest a change in deformation style of the shear zones over time from pervasive to more localised processes. The R-2 crenulations, however, are not the last fabrics to develop. At this locality all three sets of extensional crenulations are deformed by a final set of widely spaced (10-20mm) R-1 crenulations.

At (677146, maps 1 & 2) an early set of closely spaced (2mm) R-1 extensional crenulations is deformed by a set of wider spaced (5-6mm) R-2 crenulations. No conjugate geometries were seen here, but the R-2 crenulations are associated with fine quartz veins sub-parallel to the cleavage planes. As found at (509150, maps 1 & 2), small open NW vergent warps again deform the R-1 fabric, are associated with a separately developed weak crenulation but do not appear to deform the R-2 fabric.

Rotation of the extensional crenulations during formation and microshear (cleavage plane) displacement (Platt & Vissers 1980, Platt 1984, Kelley & Powell 1985, Dennis & Secor 1987) must ultimately lead to narrowing of the cleavage spacing, however, as described above, the later extensional crenulation sets may be as much as three or four times more widely spaced. One possible explanation to account for this additional spacing discrepancy is as follows: The extensional crenulations deform the pervasive mylonitic S<sub>2m</sub>, and since they represent micros shears in which the shear zone displacement is carried across spaced narrow zones, the extensional crenulations effectively represent localisation of displacement. This localisation of displacement will increase the ambient shear strain rate in the shear zone and will therefore promote further localisation. The wider spacing of successively

developed extensional crenulations may therefore reflect increasing localisation of the shear zone displacement with time.

## 2.3 Nature of the Thrusts

### 2.3.1 Cleavage and Strain Profiles

As described above, the strain profiles through the ductile thrusts were qualitatively estimated from the intensity, nature and spacing of S2 fabrics. Both these fabrics and the mineral extension lineations they contain are seen to intensify and curve asymptotically towards thrust planes. These estimates were supplemented where possible, by quantitative data in the form of pyrite pressure shadow aspect ratio measurements. These were measured in the S2 cleavage planes as the difference between pyrite width ( $l_0$ ) and total length of pyrite and pressure shadow ( $l_1$ ). However, these features are rare, pyrites in general lacking pressure shadows, suggesting late to post D2 crystallization.

The sporadic occurrence of pyrite pressure shadows precluded construction of a complete strain profile through any of the thrusts. As a general observation, however, aspect ratios ( $l_1/l_0$ ) increase towards the value of 8 in the vicinity of thrusts. However, these values are likely to be under estimates since the pyrites are likely to crystallize at different times during the deformation and may therefore only record relatively late strain increments. Furthermore, the closest pyrites with pressure shadows found to a thrust plane are N of Rincleven Point to the SW of Dunfanaghy (182218, maps 1 & 2). These are approximately 1m below the thrust plane and record a  $l_1/l_0$  of 8. The S2m host fabric to these pyrites, however, is seen to intensify over that distance to the thrust so that the spacing is reduced by some 50% in a constant silty quartzite lithology. This indicates that the

strain state nearest to the thrust is much higher than that recorded by the pyrites.

Hutton (1979c) demonstrated X/Y strains up to 9 in the footwall of the Horn Head thrust, using deformed quartz pebbles in the Ards Quartzite. Despite certain problems with overprinting footwall collapse structures here, this strain figure compares with those observed for other thrusts in the area. Since mylonitic strains closer to the thrust contact destroy all primary features of the quartzite, they are strong enough to obliterate any pebbles that might have been in the host rock. Strains are therefore liable to exceed 8 or 9 in the vicinity of the thrust planes.

The hangingwall dominance of strains has already been described, but the general character of strain increase is seen to be exponential; As a general feature, S2 is seen to intensify towards the thrust contacts, reducing its angularity to bedding ( $20^\circ$  to  $30^\circ$ ) to swing into parallelism with the contacts. The S2 becomes mylonitic as it approaches the thrusts so that S2 is transitional with S2m of the same generation. Bedding thickness is also reduced as the contact is approached and bedding becomes indistinguishable from S2m. The strain state of the rock seems to increase exponentially, escalating in the last metre or so nearest the contacts where intense S2m may be the only recognisable banding. This apparently exponential strain profile is supported in Fig 2.14a using data from the Horn Head thrust, (presented in Hutton 1977a & 1979c). A schematic strain profile through a thrust is suggested in Fig 2.14b.

This exponential trend suggests localisation of strains and displacement at the thrust contacts, so that the majority of thrust displacement is carried along thin high strain zones. This is analogous to the case in higher crustal levels where

displacements are generally carried on discrete thrust faults. This is evidenced by the lithological breaks which the ductile thrusts represent, sometimes seen to occur along thin (cm) zones of hybridised lithology or 'tectonic schist', the best examples of which are exposed at Mickey's Hole, W Horn Head and Lishagh (Figs 2.9, 2.15a).

The actual strain profiles, however, are not simple exponential increases. This is well illustrated by a thrust exposed in a road cut at (669228, maps 1 & 2), where hangingwall limestones are in contact with metadolerites in the footwall. The limestones are intensely cleaved by platy mylonite (S2m) which contains small (cm scale) sheath fold closures and a strong mineral extension lineation. This mylonitic deformation spans the 6-7m outcrop without any marked decrease in intensity and is likely therefore to be thick (in excess of 15m) at this location. Strain in the metadolerites, however, rises from undeformed crystalline rock to intense platy mylonite in under 10m as the thrust is approached. This is accomplished via a series of localised bands of high strain containing C-band shears (discussed above) of the chloritised mineralogy which support a NW directed thrust displacement. These zones increase in thickness and intensity towards the thrust plane, suggesting a more 'dog tooth' strain profile in the thrust zones (Figs 2.14c, 2.15b).

A similar situation is seen in a series of low cliffs around Lishagh (410112, maps 1 & 2). Here the character of hangingwall strains is well recorded in quartzitic and silty lithologies. Bedding thickness reduces towards a thrust at the base of the cliffs, and bands of high strain increase in intensity and thickness. Furthest away from the thrust, strains are recorded in certain horizons as micro-shears which anastomose when viewed in the stretching direction, suggesting a component of layer-parallel shearing of the bedding. This anastomosing habit intensifies

towards the thrust, increasing the density of shears and apparently attenuating the shear-bound 'pods'. These give way to bands of platy strains as the dominant strain expression, which increase in thickness and intensity (Fig 2.16). It should be noted at this juncture that the platy strain habit is by far the more common observation.

Bedding/S2 angles decrease towards the thrusts and bedding becomes thinner. Where bedding is preserved between platy zones, S2 can be seen to be transitional at the bed margins with the platy S2m. This might suggest that as shearing progresses, the S2 intensifies, becoming transposed and mylonitic at the bed margins. Also at the bed margins, occasional C-band shears deform the emerging S2/S2m, but appear to be S2m-planes themselves. This supports a syn-thrusting component of layer parallel shear and supports the notion of a 'dog tooth' character to the thrust strain profiles (Fig 2.14c). This 'banded' shearing, however, is also noted from crystalline metadolerites (as described above), so that bedding/banding anisotropy may not be the primary cause for developing the effect of 'banded' shearing.

### 2.3.2 Boudinage and Minor Folds

Hutton (1979b) noted that the "degree of boudinage" increases close to tectonic slides, given the presence of adequate rheological contrasts within the near-slide lithologies. In the Breaghy Head area, boudinage, especially of metadolerite sheets and quartzites close to the ductile thrusts is not an uncommon feature. The boudinage is generally of symmetrical geometry with neck long axes lying close to perpendicular to the mineral extension lineation. This suggests that the boudinage expresses a non-flattening L-S type deformation synchronous with thrust motion. Intensification of S2 fabrics around boudins supports a syn-thrusting D2 age for their formation, and was also observed by

Hutton (1977a) as evidence for syn-D2 boudinage.

Although generally of overall symmetrical geometry, some boudins contain internal 'domino' fractures which indicate a NW or NNW overshear direction (Fig 2.17). This is compatible with the shear sense of the majority of the thrusts and therefore provides supportive evidence for a syn-thrusting age for boudin formation. It also suggests a layer-parallel (simple) shear component to the deformation. The exact nature of boudinage intensification however, enables a more accurate assessment of the temporal relationship between boudinage and thrust motion to be made. The set of outcrops around Lishagh has already received partial description above, where the nature of bed thinning and fabric intensification was discussed. Boudins here become smaller and more frequent towards the thrust as bedding thickness decreases. This suggests that boudinage must have begun to initiate after the main phase of bed thinning near the thrust (associated with the increase of strain). The thrust strain profile must therefore have been at an advanced stage in it's development at the time of boudinage initiation. Significantly, the boudinage in the Breaghy Head area is never seen to deform the thrust planes despite intensifying towards them. This strongly suggests that the extensional strains which these structures represent is effectively detached at the thrust planes to which they intensify during thrust motion.

Asymmetric minor folds which verge W, NW, NE & E, and which frequently have an intrafolial geometry have S2 and S2m axial planar cleavages. These folds are therefore minor F2 folds. In a similar way to the boudinage, F2 minor folds are seen to become smaller as the thrust planes are approached and bedding thickness is reduced. Also as the thrusts are approached and strain increases, the fold hinges swing towards parallelism with the stretching lineation and the fold closures tighten to become



isoclinal, sheath-like or rootless closest to the contacts (eg. Fig 2.18). Folds are not always developed throughout individual strain profiles, but are sufficiently numerous and well developed at some localities (eg. 568209, maps 1 & 2) to see these relationships clearly. These observations indicate that the minor fold development took place after the main bedding thickness reduction phase, but whilst the thrusts and their mylonitic mantle were still in motion. That the folds are an integral part of the thrust motion kinematics is also strongly suggested by these relationships.

Whilst the minor folds are usually restricted to the thinned bedding, this is not always the case. Near to the thrusts, S2m domains are sometimes seen to be folded by minor folds which have a mylonitic axial planar cleavage. When fully developed, this fabric is indistinguishable from the S2m surrounding the folds. These folds may become sideways closing and 'crenulate', disharmonic or sheath like in appearance. In some examples the axial planar fabric is clearly transitional with S2m along the axial plane (Fig 2.19). These folds must therefore express reworking of the thrust mylonites during motion, analogous to reworking noted by Bell (1978), Bell & Hammond (1984), Evans & White (1984).

Occasionally, folds are found within thrust strain profiles which have become transposed by the high strain S2 fabrics (eg. 448154, maps 1 & 2, Fig 2.18). At (578162, maps 1 & 2) intensely cleaved micaceous limestones contain a tight fold closure associated with SE vergence (Fig 2.20). The fold axial plane steepens to the SE, appearing to have been deformed by a gentle NW vergent refold. The fold axial planar crenulation cleavage is seen to have symmetrical (contractional) microlithon geometries at the mid point of the axial plane. As the cleavage shallows at the lower (NW) end of the axial plane, the microlithons take on an

extensional (to the NW) geometry (regardless of which fold limb they occur in), before shallowing into near parallelism with the intense S2, which becomes mylonitic in the lower parts of the exposure. Thin section investigation showed that a calcite, muscovite, quartz/ feldspar mineralogical banding is crenulated by the fold axial planar cleavage. This banding is expressed by segregation and growth of the mineral phases (eg. large muscovite laths and calcite crystals). The muscovites have reaction coronas which appear to be related to altered feldspars in the quartz rich domains. This schistosity is uncharacteristic of S1, which where preserved, is an alignment of small mineral grains involving negligible segregation or mineral growth. It is likely to represent strongly thinned bedding and sub-parallel S2 frequently found within the high strain parts of the thrust strain profiles. The cross cutting fabric causes strong deformation of the earlier schistosity with quartz grain size reduction, kinking and bending of muscovite, lattice distortions in the feldspars and deformation twinning in the calcite. The fabric is also associated with growth of large chlorite bundles and renewed growth of muscovite along the cleavage planes and in pyrite pressure shadows. Being fresh and euhedral, this 'new' muscovite is distinctive from the earlier growth.

Since the fabric is associated with phyllosilicate porphyroblast growth, crenulates S2 and is axial planar to an apparently SE verging fold, the fabric and fold would be S3 & F3 as defined by Hutton (1977a, 1983). The fold axial plane, however, is deformed by a NW vergent refold, implying a return to NW overshear. The fabric, a mylonitic strain slip cleavage, is reactivated and modified as an extensional crenulation consistent with NW overshear. A correlative of the fabric in the lower parts of the exposure is also seen to be in mutual interference with S2m so that it appears to crenulate and be crenulated by S2 fabrics. This implies that the two cleavages have negligible time

separation, and must share part of a single progressively evolving kinematic system of D2 age. Indeed, the reaction relationships between the different mineral constituents of the rock and the apparent syn-tectonic rejuvenation of phyllosilicate growth probably reflects a cyclic scavenging and recrystallisation process similar to that described within mylonites by Knipe & Wintch (1985). These relationships are therefore interpreted as an expression of reworking of S2 and S2m fabrics. As described and discussed in detail in chapter 3, similar relationships have been observed elsewhere in close connection with rare D2 backthrust development.

### **2.3.3 Syn-tectonic Veining**

Quartz veining sub-parallel to S2m is frequently seen to develop close to the ductile thrusts (eg. at 200220, 405157, 420113, maps 1 & 2). These are sometimes seen to be related to boudinage necks, tension gashes and veins parallel to F2 axial planar S2. These veins appear to be contemporary since they are seen to be both interconnected and mutually cross cutting in a number of outcrops (Fig 2.21). These veins are seen to be folded by F2 folds and are also seen to cross cut F2 folds, suggesting vein opening during D2 deformation; The further significance of veins parallel to F2 axial planes will be discussed in chapter 4.

Veins parallel to S2 fabrics and bedding have a large lateral extent and often occur in swarms of ten, twenty or more. These swarms represent displacement zones across which thrust displacements of markers are seen to occur. It is interesting to note here that similar features have been described from foreland thrust belts as a precursor to discrete thrust fault development, during progressively localising deformation (Beach 1981).

Beach (1981) suggests that such veins are developed by

"...very large, lateral extension, opening and infilling of short, subvertical cross-cleavage boudin necks". This produces oblong, lozenge or 'beaded' vein geometries and would be expected to produce inclusion (opening) trails in the vein material parallel to the host cleavage. In the Breaghy Head area, although 'beaded' geometries are occasionally seen, the veins generally have smooth walls and where developed, opening trails run obliquely across the veins such that the upper vein margin must have moved forward and upwards to the NW in the direction of D2 thrust transport. Where associated with boudin necks, opening trails remain oblique. These veins are therefore interpreted as fabric parallel dilatant fractures developed in the thrust strain profile during the later stages of the localisation history, (and therefore at relatively high strain rates), since they are occasionally associated with boudinage which deforms S2m and must, therefore, have formed after the main stage of S2m development. Furthermore, the vein margins are occasionally sheared so that the S2m at the margin becomes intensified, suggesting that the veins may catalyse discrete displacement surfaces in the strain profile during this localisation.

This suggests a different mechanism of vein development to that proposed by Beach (1981). Indeed, the S2m parallel veins described above are morphologically and causally closer to fabric parallel veins described by Roering & Smit (1987) to be restricted to narrow layer (bedding) parallel thrust shear zones within quartzites metamorphosed to greenschist facies grades (Phillips 1987). Similar 'smooth' veins with large lateral extent and oblique opening trails/fibres are not uncommon in foreland areas of thrust belts. For example, the Moine Thrust zone (S. Bowler pers. comm. 1989), the external French Alps (R. Butler, S. Bowler, G. Roberts pers. comm. 1989) and the External Sierras (Spanish Pyrenean foreland).

## 2.4 Summary

The Breaghy Head peninsula contains a number of high strain (mylonitic) zones across which stratigraphy is thrust dislocated and repeated. The high strain zones contain reliable kinematic indicators which show that the thrust hangingwalls are displaced towards the NW. Some of the structural elements associated with the high strain zones and interpreted here as being diagnostic of ductile thrusts in the Breaghy Head area are cited by Hutton (1977a, 1979b) and Rathbone et al (1983) as being diagnostic of broader, larger scale tectonic slides (for partial summary see Fig 2.22). The high strain zones in the Breaghy Head area are generally less than 20m thick and as such are more discrete structures than the tectonic slides to which Hutton (1979b) and Rathbone et al (1983) refer. In most other respects however, the ductile thrusts of Breaghy Head conform to the definition of tectonic slides proposed by Hutton (1979b):

"A tectonic slide is a fault which forms in metamorphic rocks prior to or during a metamorphic event. It occurs within a zone of coeval penetrative (ie. microscopic) deformation that represents an intensification of a more widespread, often regionally developed deformation phase. Within this zone of high strain slides may lie along and be sub-parallel to (although they will cross cut on a large scale) the boundaries of lithological, tectonic and tectonic-metamorphic units".

It would perhaps be unwise however, to label the structures of Breaghy Head 'small' tectonic slides, since this would imply a lesser displacement magnitude than slides of wider visible expression. As noted above (and described in chapter three), the Breaghy Head thrusts display marked similarity to thrusts from higher crustal levels where fault zone width bears little relation

to fault displacement.

The term "tectonic slide" (Fleuty 1964, Hutton 1977a, 1979b) is intended to describe strike-slip syn-metamorphic dislocations (eg. that bounding the Main Donegal Granite) or dip-slip syn-metamorphic dislocations where the shear sense and therefore extensional or thrust nature of the shear zone is unknown. We are however, aware of the thrust nature of the Breaghy Head dislocations, so that they may be termed 'thrusts'. Furthermore, the thrusts are seen to be marked by an intensification of the regional D2 fabric (essentially zones of mylonitic S2), and therefore represent part of a distributed (regional) deformation. The thrusts therefore conform with the definition of 'ductile' proposed by Rutter (1986). It follows, therefore, that the Breaghy Head tectonic slides might best be referred to as discrete D2 "ductile thrusts".

(McCall 1954)

(Rickard 1962)

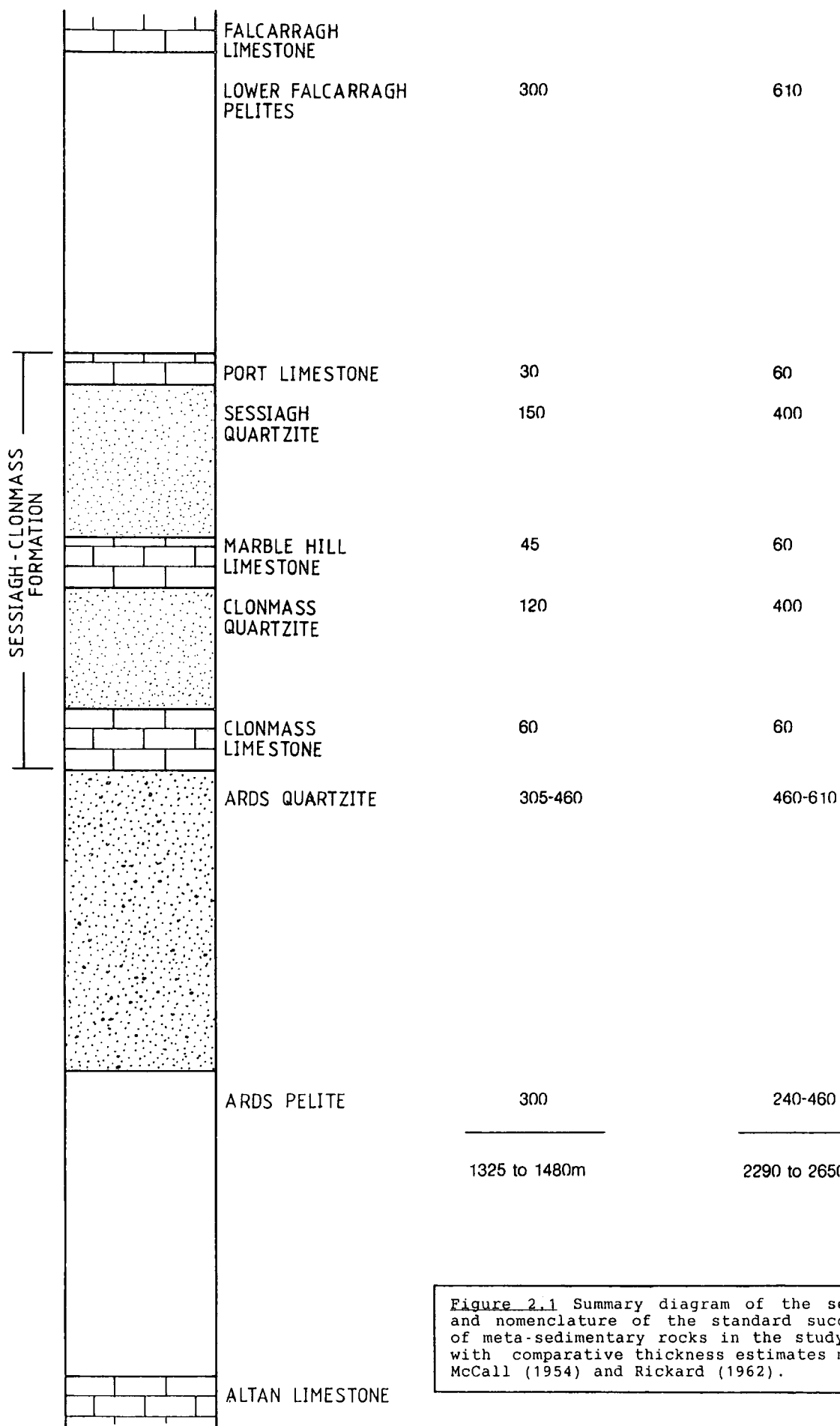
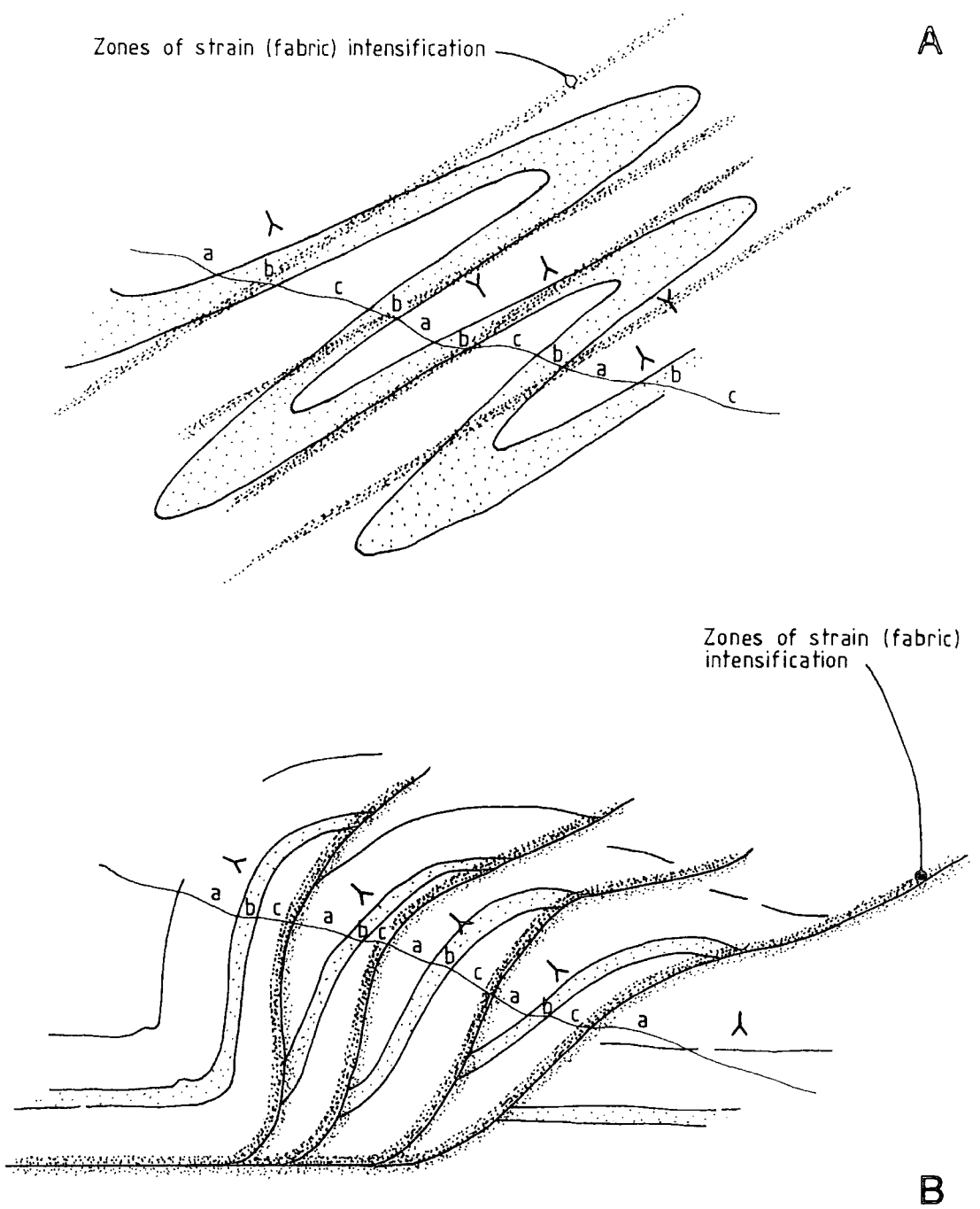
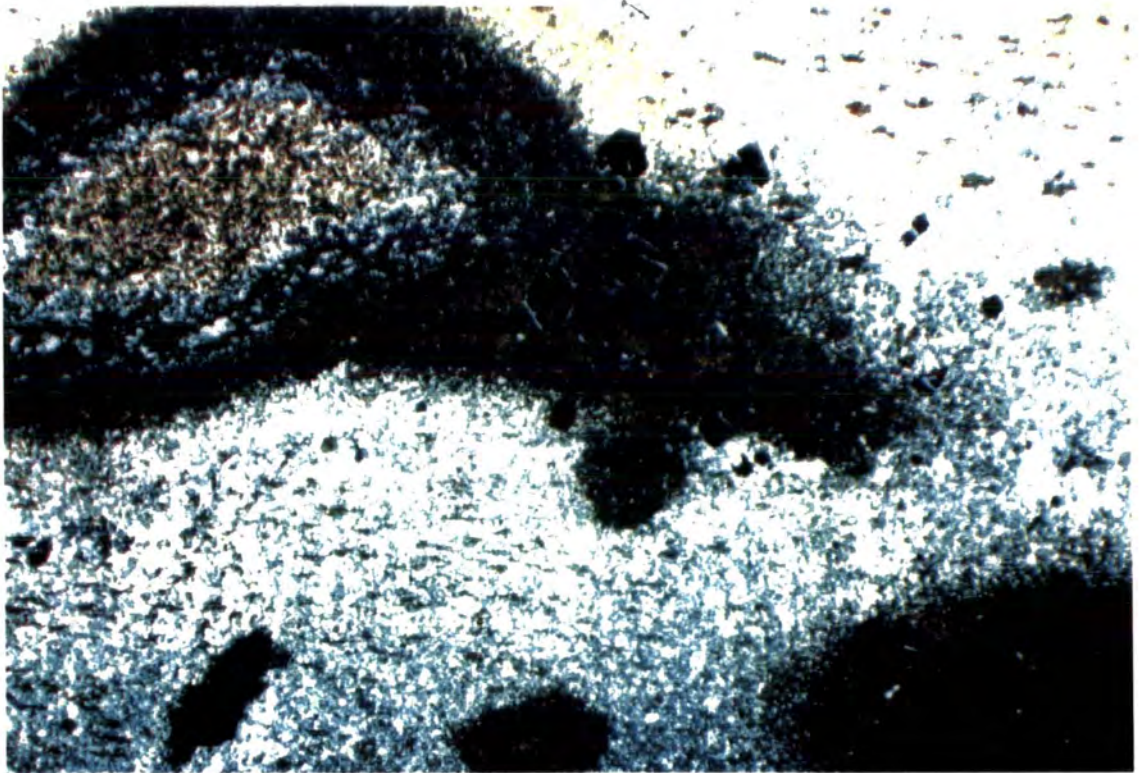


Figure 2.1 Summary diagram of the sequence and nomenclature of the standard succession of meta-sedimentary rocks in the study area, with comparative thickness estimates made by McCall (1954) and Rickard (1962).



**Figure 2.2** The disposition of stratigraphic and strain repetition associated with folding and thrust imbrication. (A) Folding produces symmetric repetition of rock units (abcbabcba), concentration of intensified fabric in limb areas (symmetric distribution with respect to rock units) and reversals in younging direction and cleavage vergence. (B) Thrust imbrication produces asymmetric repetition of rock units (abcabcabc), concentration of intensified fabric near thrust planes (asymmetric distribution with respect to rock units) and constant younging direction and cleavage vergence.

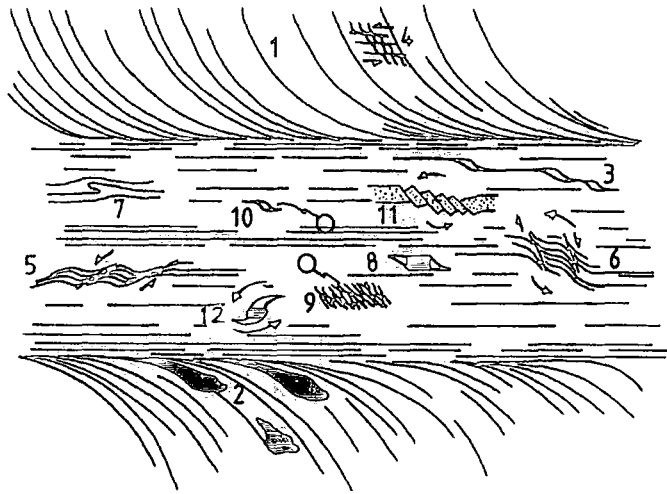




0.5mm

Figure 2.3 Garnets associated with hornfels spots in Ards Pelites close to a large metadolerite sheet, located near Pollaquill Bay, western Horn Head (O.S. sheet 1 B990390).

A



- 1) Rotation/curvature of a generated (S<sub>2</sub>) foliation into the thrust plane.
- 2) Rotation and 'tail' asymmetry of deformed markers.
- 3) Displaced markers (eg. veins).
- 4) C shears.
- 5) R-1 Shear bands or extensional crenulation cleavages.
- 6) R-2 Shear bands or extensional crenulation cleavages.
- 7) Asymmetry of intrafolial folds (only used as supplement to other criteria).
- 8) Asymmetry of pressure shadow trails growing around non-rotating 'hard grains'.
- 9) Asymmetry of elongate recrystallized grains (eg. calcite).
- 10) Asymmetry of mica 'fish'.
- 11) R-2 'domino' rotation of hard bands.
- 12) Asymmetry of rotated porphyroblast pressure shadows.

B

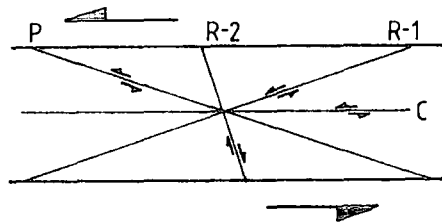


Figure 2.4 Diagrams summarising ductile kinematic/shear sense indicators used in the Breaghy Head area. (A) Kinematic indicators in a hypothetical shear zone. (B) Riedel terminology applied to the various types of secondary or strain slip/shear cleavages encountered in the area. (modified from White et al., 1986).

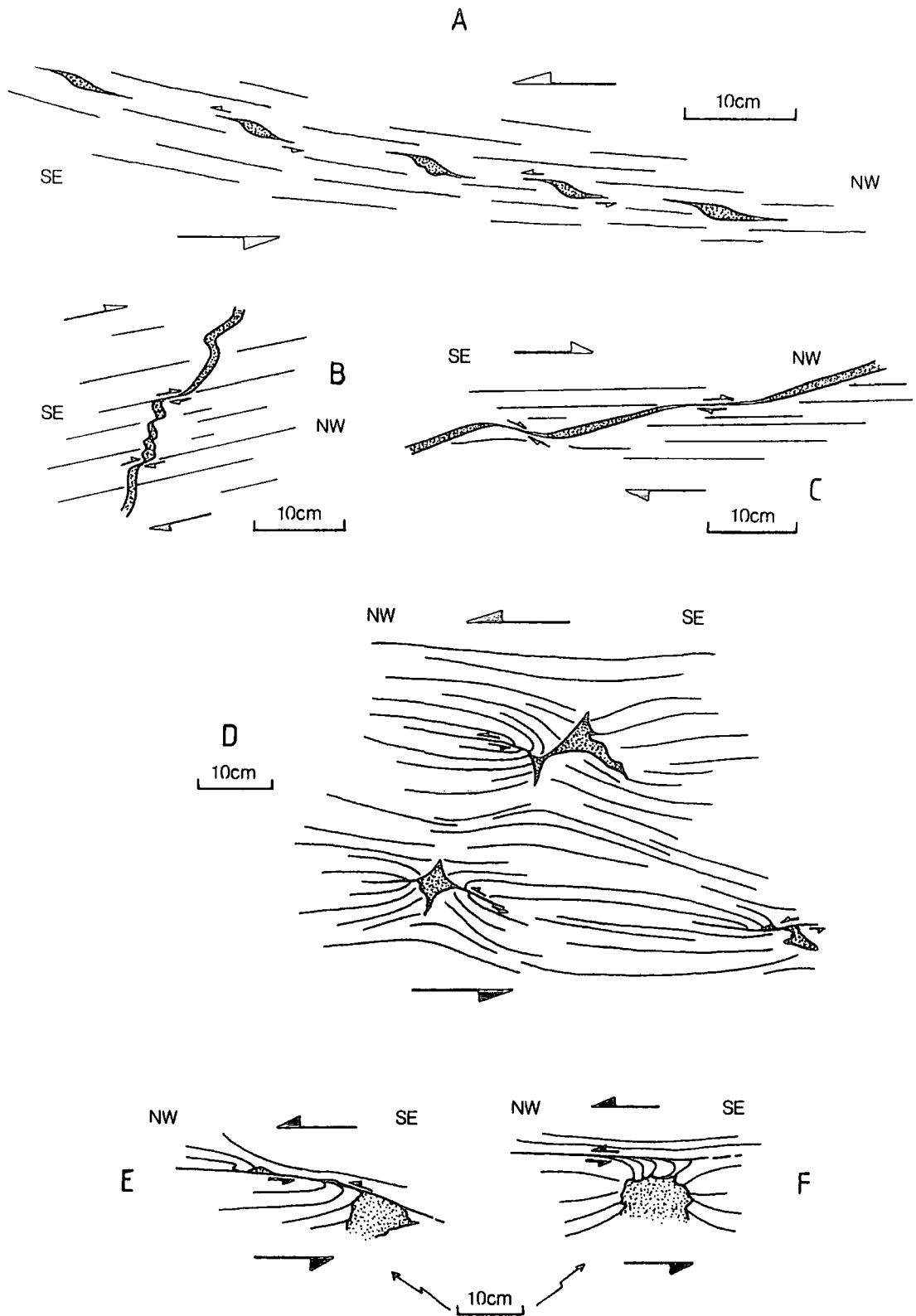
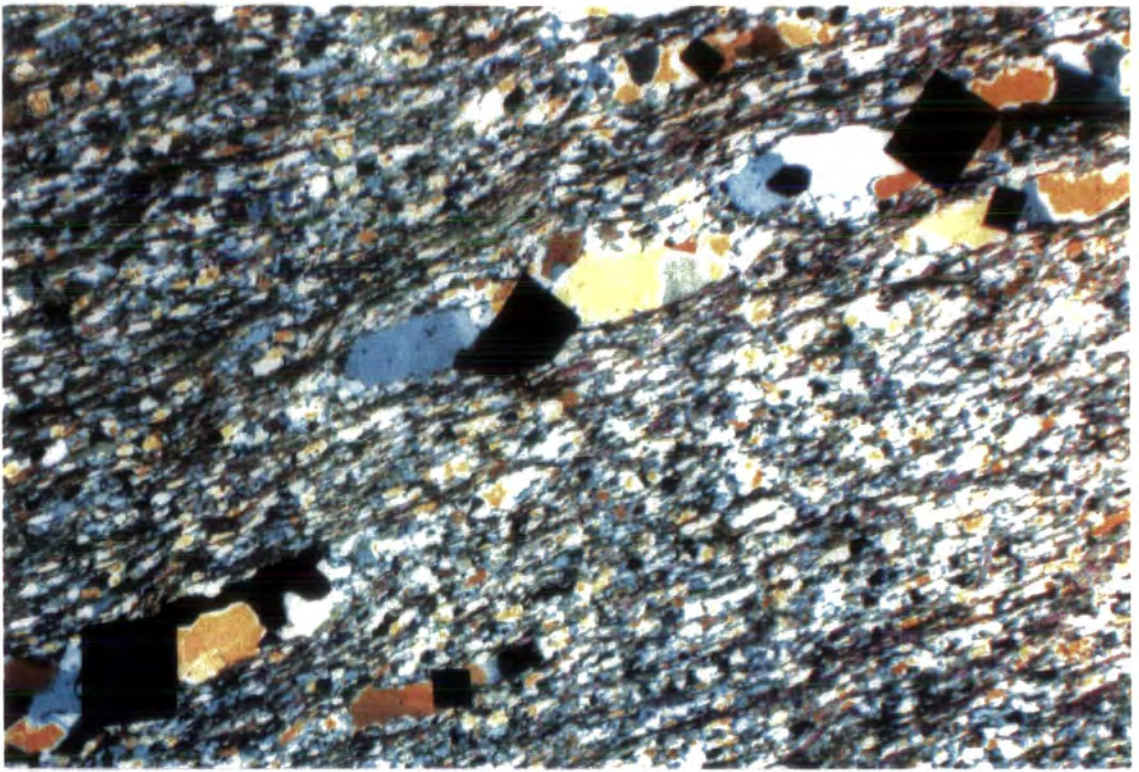
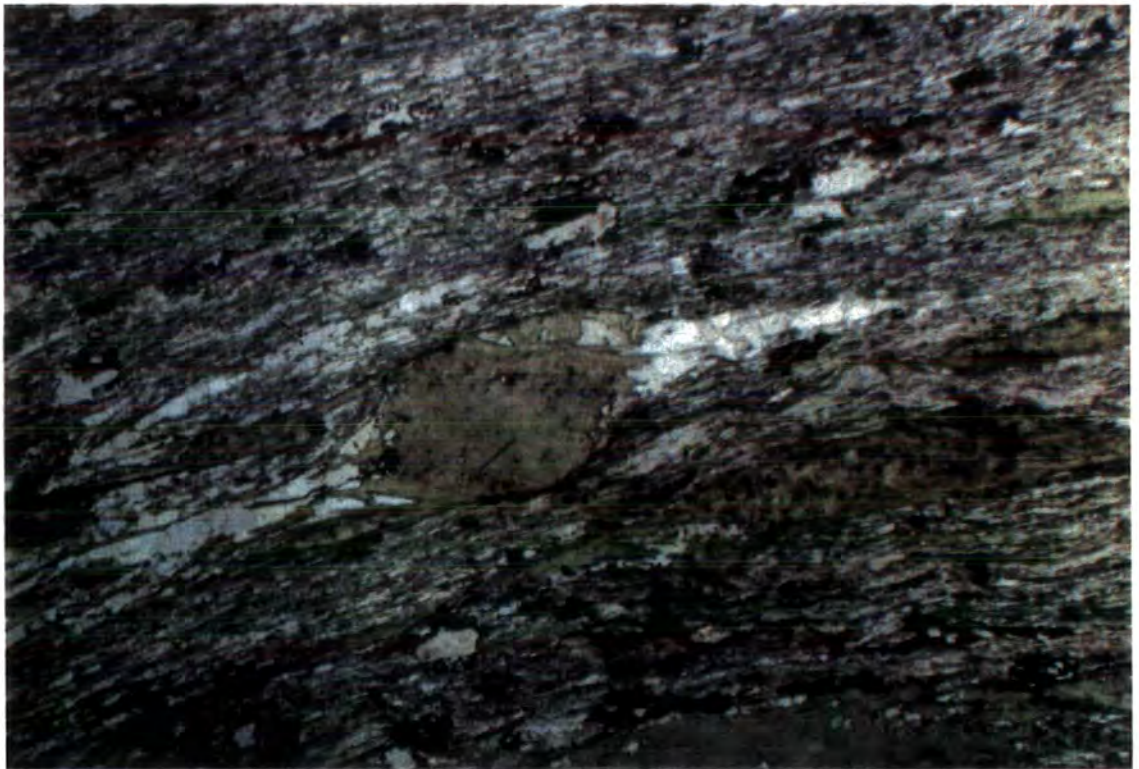


Figure 2.5 Field sketches of displaced markers (veins and boudin necks). (A) Displaced vein within  $S2m$  of the Dunfanaghy Slide pelites. (B) Displaced vein in mylonitised limestones at (691200). (C) Displaced vein in mylonitised quartzites at (607170). (D, E & F) Displaced boudin necks in metadolerite pervaded by intense  $S2$  and  $S2m$  near Dunrudian (677146). All diagrams subparallel to  $D2$  stretching direction.



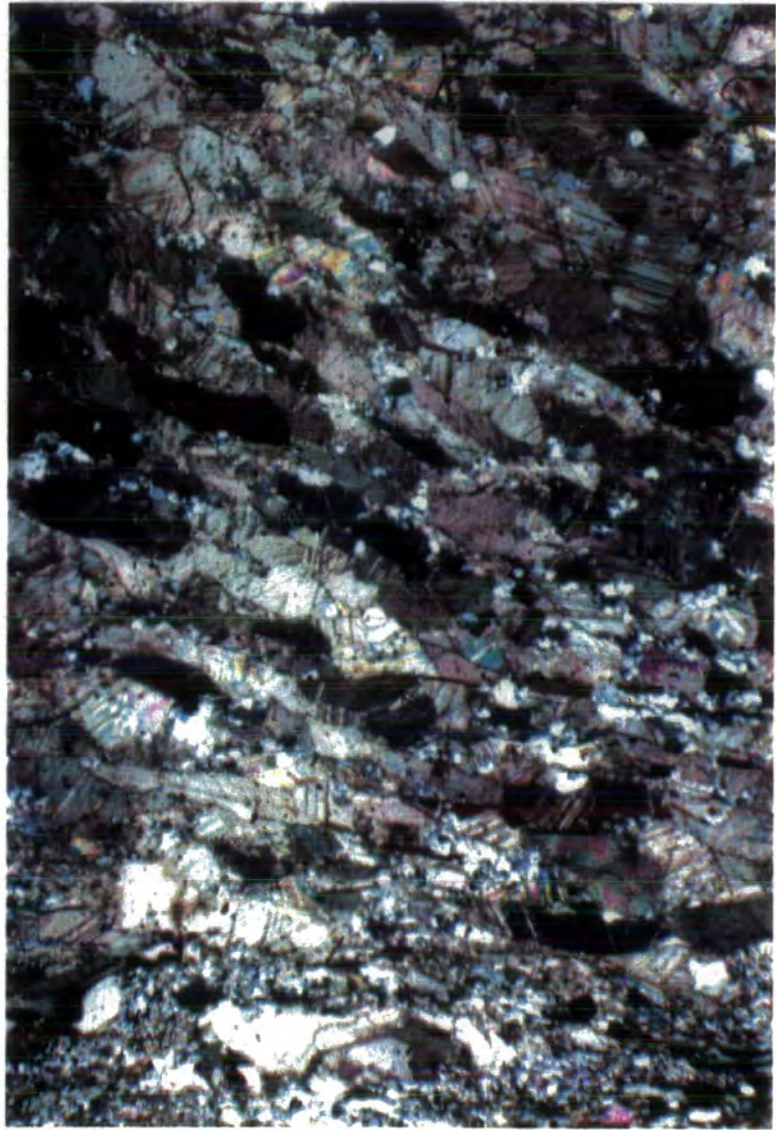
A



B

0.5mm

**Figure 2.6** Photomicrographs of asymmetric pressure shadow trails. (A) Pyrites with asymmetric pressure shadow trails indicating NW directed overthrust (top to the right), from 189095 (maps 1 & 2), near Ringleven Point. (B) A chlorite 'knot' with asymmetric pressure shadow trails indicating NW directed overthrust (top to the right), from 470200 (maps 1 & 2), north of Sandhill. This porphyroblast appears to be a pseudomorph, possibly of a garnet or feldspar, the chlorite growing in optical continuity with a central ovate structure which represents the original porphyroblast. Chlorite fibres can be seen to have grown into the pressure shadow area, indicating chloritisation during D2 shearing.



0.5mm

Figure 2.7 Elongation and alignment of calcite grains within mylonitised limestones at 845126 (maps 1 & 2), on the south shore of Marble Hill. Note that in this example the grain alignment swings asymptotically into a zone of increased grain size reduction at the base of the photomicrograph (a C shear). The alignment indicates NW directed overshear (top to the left).



A

sill ~ 2m thick



B

**Figure 2.8** Photographs of R-2 hard band 'domino' rotations. (A) Quartzite outcrop near Lishagh with dominos indicating NW directed overthrust (photograph's top to the right). (B) Large scale R-2 disruption of a major metadolerite body on the NW coast of Horn Head. These dominos produce folds and fabrics which cross-cut D2 structures but are clearly of a similar D2 age (see text for details). The rotations indicate NW directed overthrust (photograph's top to the left) and are located just north of Mickey's Hole in the footwall to the Horn Head thrust (OS sheet 1, B990405).

NNW

SSE

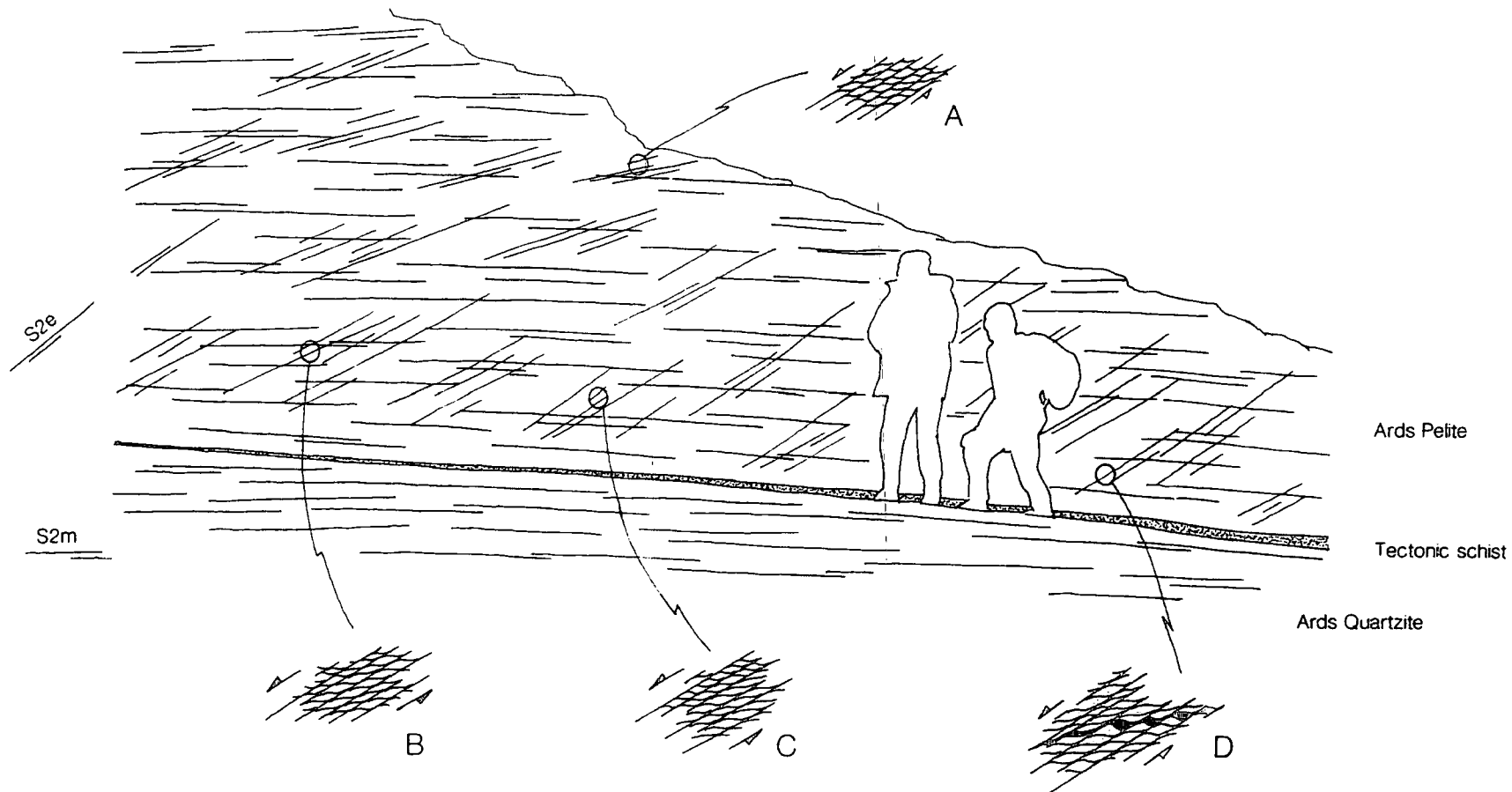
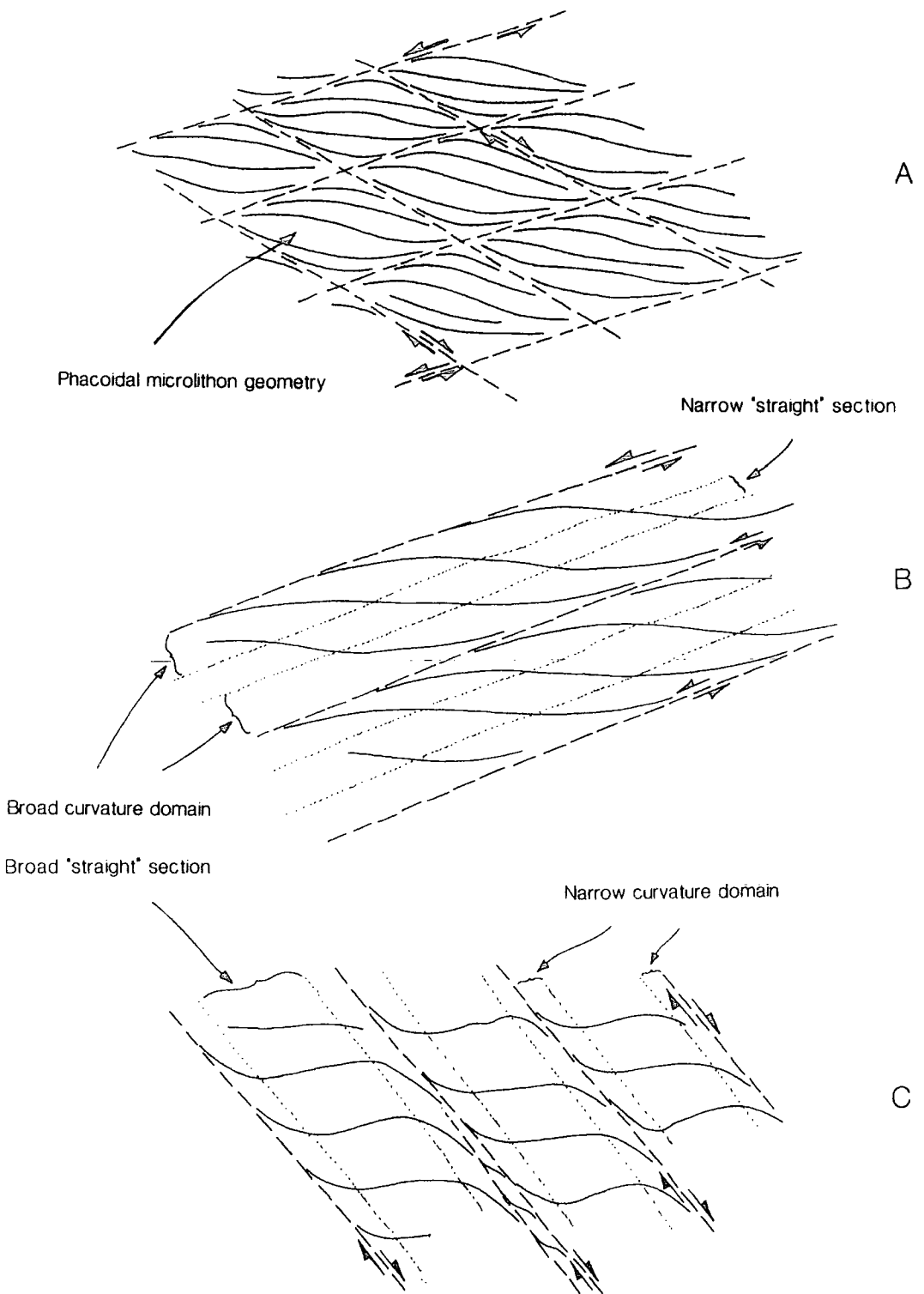


Figure 2.9 Line drawing from a photograph (Hutton 1983, fig 3a) illustrating constant nature of extensional crenulation asymmetry across an outcrop (Mickey's Hole, west Horn Head). (A) to (D) represent the constant slip direction of R-1 extensional crenulations in the exposure and (D) illustrates the direction of marker offsets (eg. fine quartz veins) across the crenulations seen at positions.

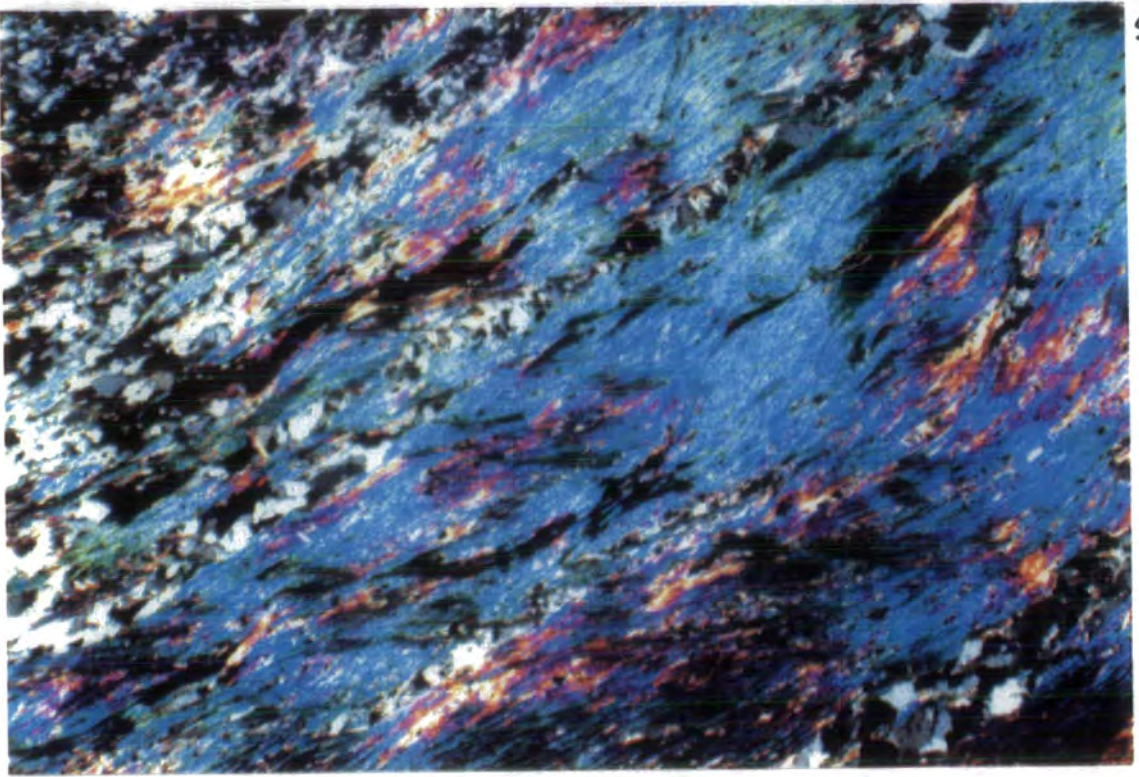


**Figure 2.10** Extensional crenulation cleavage geometries. (A) The augen or phacoidal microlithon geometry created by synchronously developed R-1 & R-2 extensional microshears (B) R-1 extensional crenulations. Note the broad curvature domains and narrow 'straight' sections in the microlithon structure which create 'smooth' asymptotic curvature of the deformed fabric into the cleavage planes. The cleavage planes which are defined by the attenuated microfold limbs represent extensional microshears. (C) R-2 extensional crenulations. Note the narrow curvature domains and broad 'straight' sections in the microlithon structure. The asymptotic curvature of the deformed fabric into the cleavage planes is far 'sharper' than in the R-1 crenulations and the 'straight' sections are at a higher angle to the cleavage planes. Also by comparison to the R-1 crenulations, the microshears (defined by the attenuated limbs of the microfolds) are narrower.



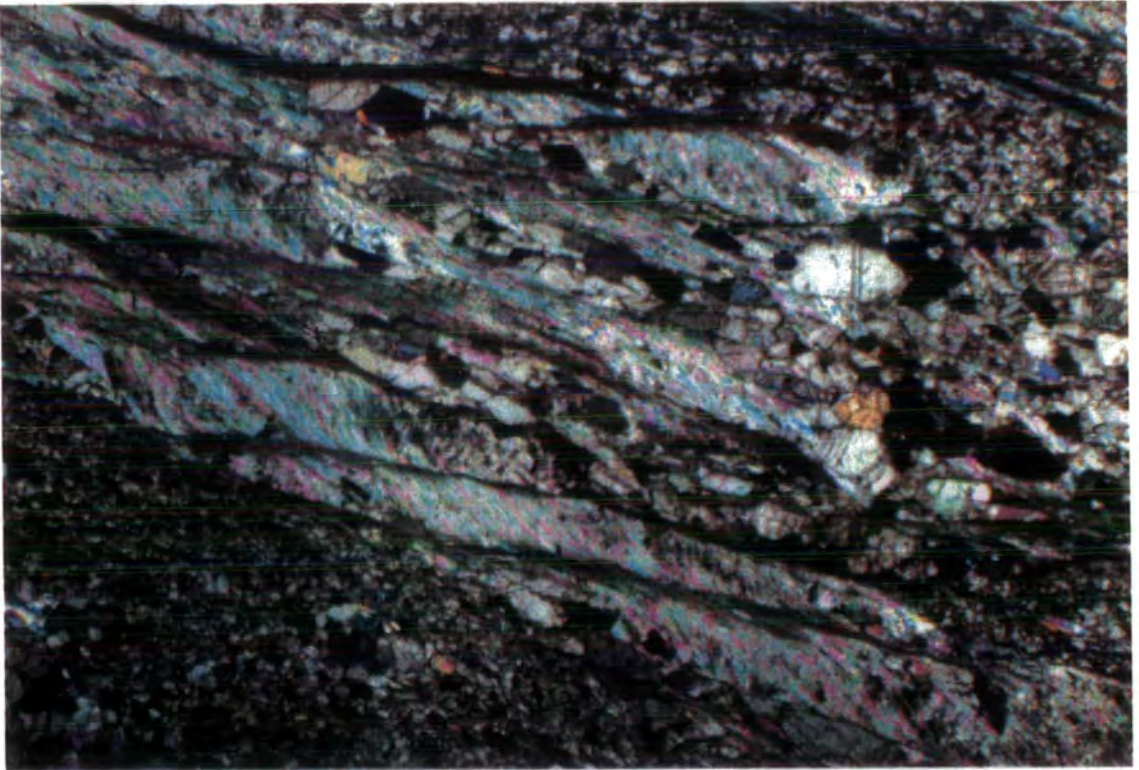
NNW

SSE  
A



NNW

SSE  
B

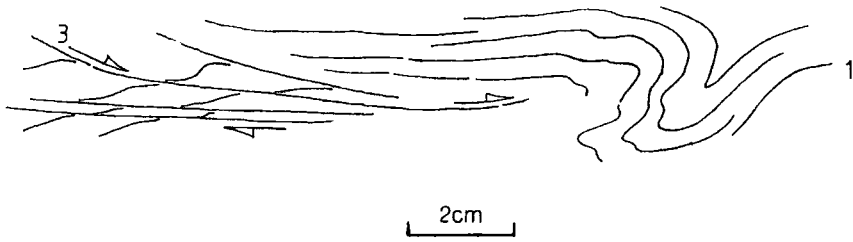


0.5mm

**Figure 2.11** Photomicrographs of extensional crenulations. (A) An example of the rare phacoid geometry associated with synchronously developed R-1 and R-2 extensional crenulations, from 597216 (maps 1 & 2). R-1 is represented by the crenulations aligned with the upper and lower frames of the photomicrograph. R-2 is less well developed, wider spaced and near vertical in the photomicrograph. Compare with figure 2.10a. (B) R-1 extensional crenulations indicating NW directed overshear, from 593157 (maps 1 & 2). Note the smooth asymptotic curvature of the microlithon S2m into the cleavage planes.

SE

NW

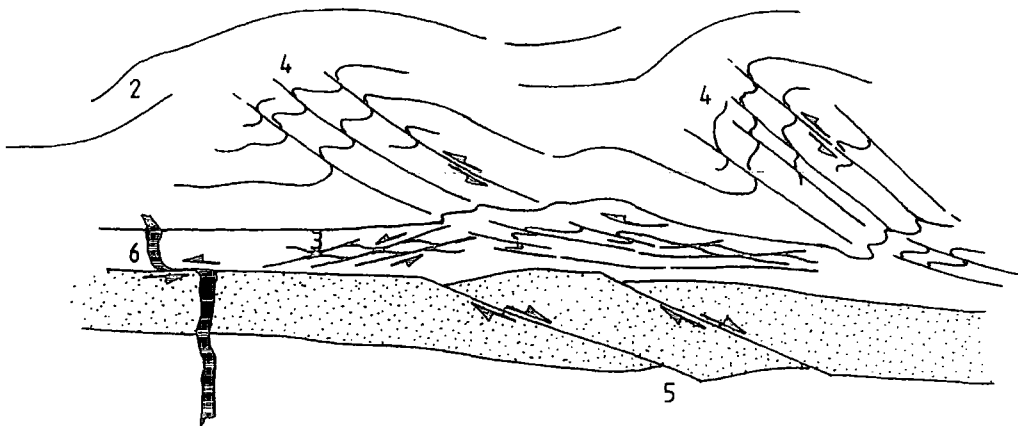


A

NW

2cm

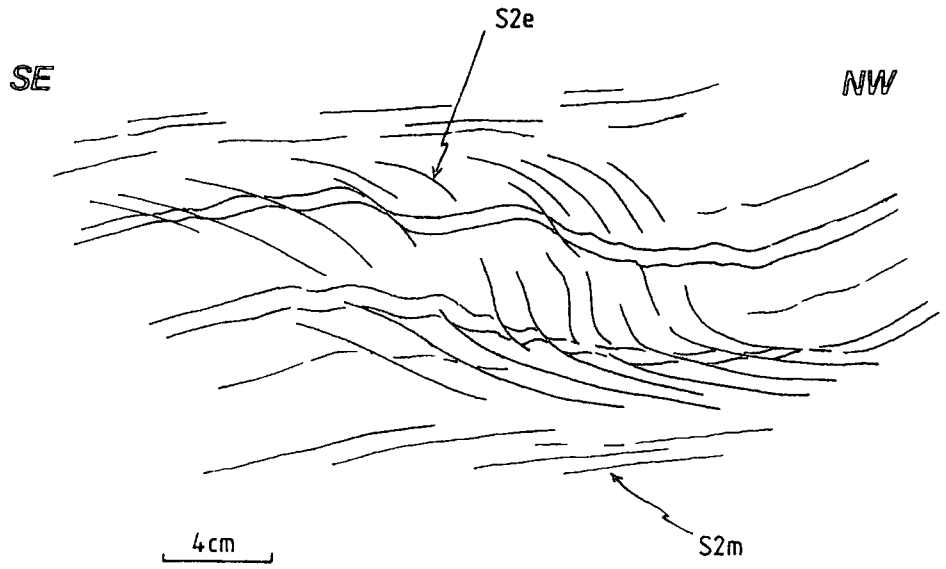
SE



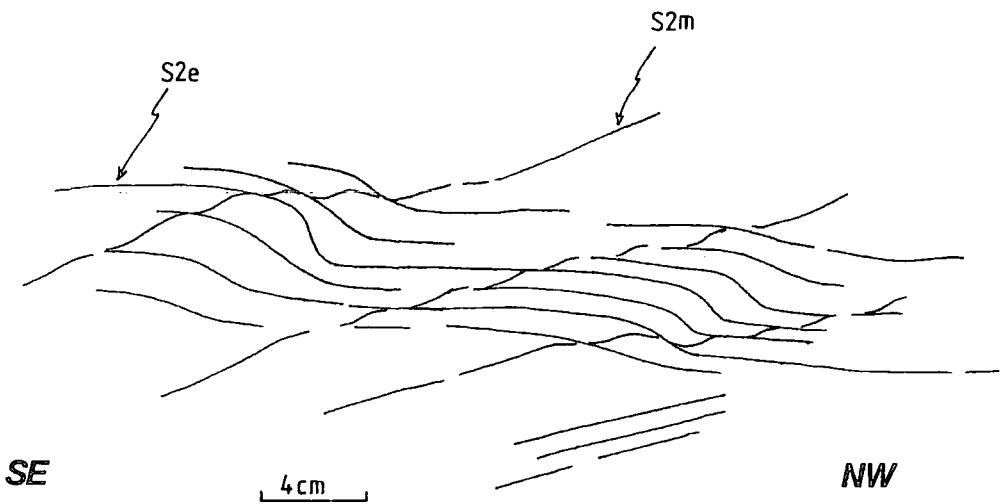
B

Figure 2.12 Simplified field sketches of the transitions between R-1 shear bands and P shears. (A) An example where the extensional crenulation displacements appear to sum together and become a P shear, analogous to a thrust fault tip fold. (locality at 546160). (B) A more complex example containing a number of shear sense criteria. In this case the R-1 extensional crenulations are continuous with a P shear fabric and folds. (locality at 525156).

(1) S2m. (2) Bedding/S2m. (3) R-1 extensional crenulations. (4) P shears. (5) R-2 'domino' rotations in hard band. (6) C shear displacement of vein.

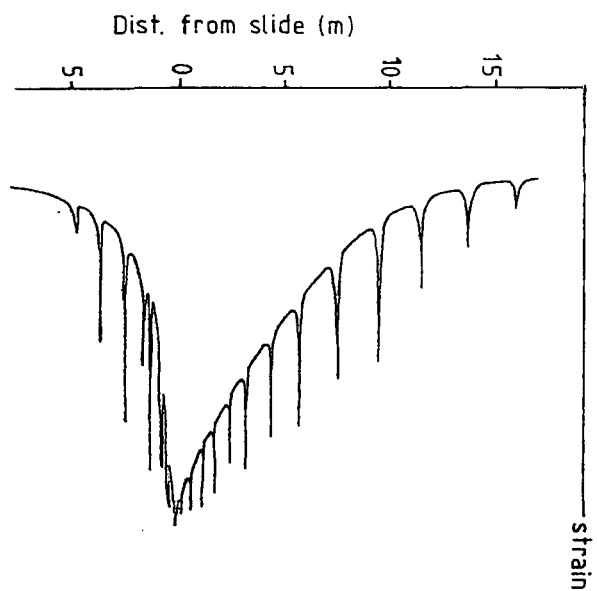


A

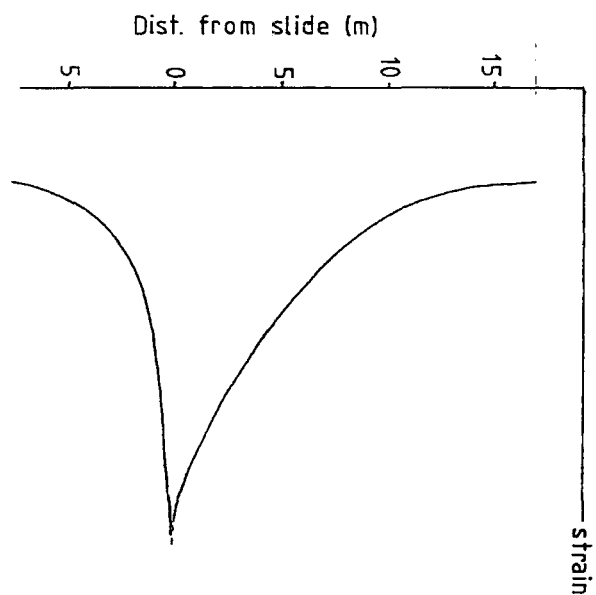


B

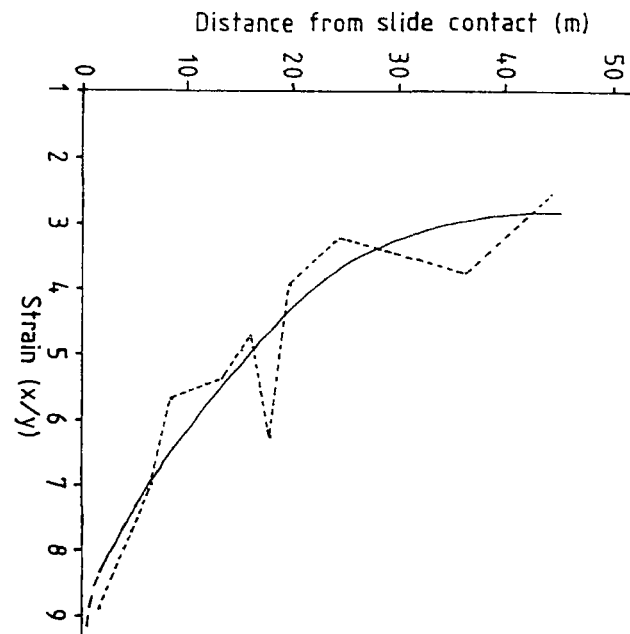
Figure 2.13 Simplified field sketches of folding of R-1 extensional crenulations by NW verging F2 folds. (A) In calc-mylonites at 590225, (B) In calc-mylonites at 525156 maps 1 & 2.



C.



B.



A.

**Figure 2.14** Graphs illustrating the nature of strain profiles through ductile thrusts. (A) Graph illustrating the 'exponential' nature of strain increase towards the Horn Head Thrust (modified from Hutton 1979c). (B) A schematic strain profile through a ductile thrust, with scales appropriate to the thrusts found on the Breaghy Head peninsula. (C) A more realistic 'dog-tooth' strain profile through a ductile thrust. This strain character is manifested at outcrop as 'banded' shear strains of increasing intensity within the overall 'background' strain increase profile. (see text for details).

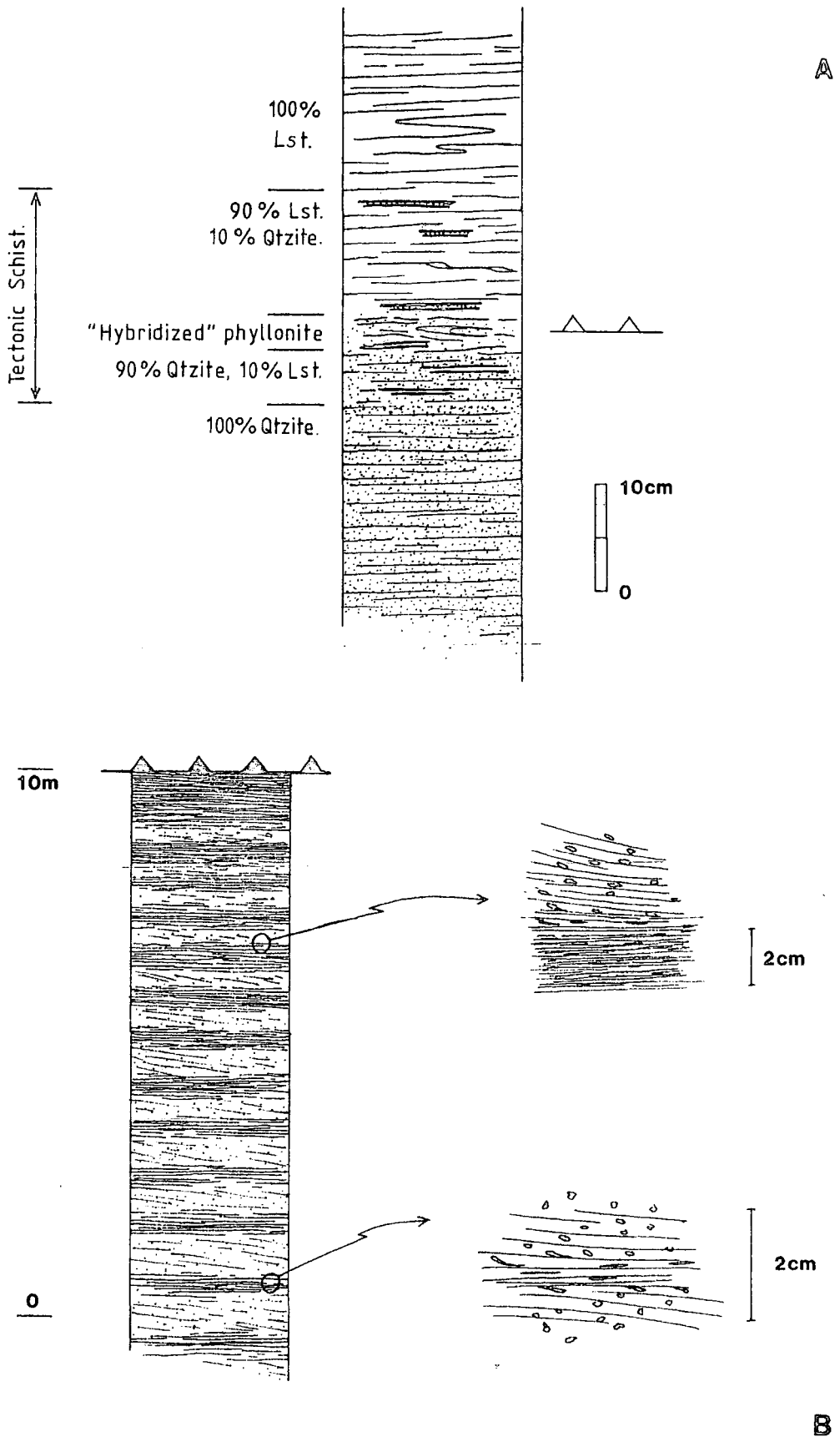


Figure 2.15 (A) Sketch log through a thrust contact at Lishagh, showing compositional details of the tectonic schist zone. Limestone and quartzite is tectonically interbanded (seen as colour and hardness changes) on a (mm) scale, giving the rock a streaked appearance. A central 5-6cm thick zone is a micaceous hybrid lithology which acts as a matrix for rootlessly folded or C shear displaced thin quartz veins. (B) Sketch log through the footwall of a thrust at 669228, maps 1 & 2, indicating the "banded" nature of strains at this locality. There is a "background" strain here against which the "banded" strains appear as spaced zones of (in a relative sense) anomalously high strain.

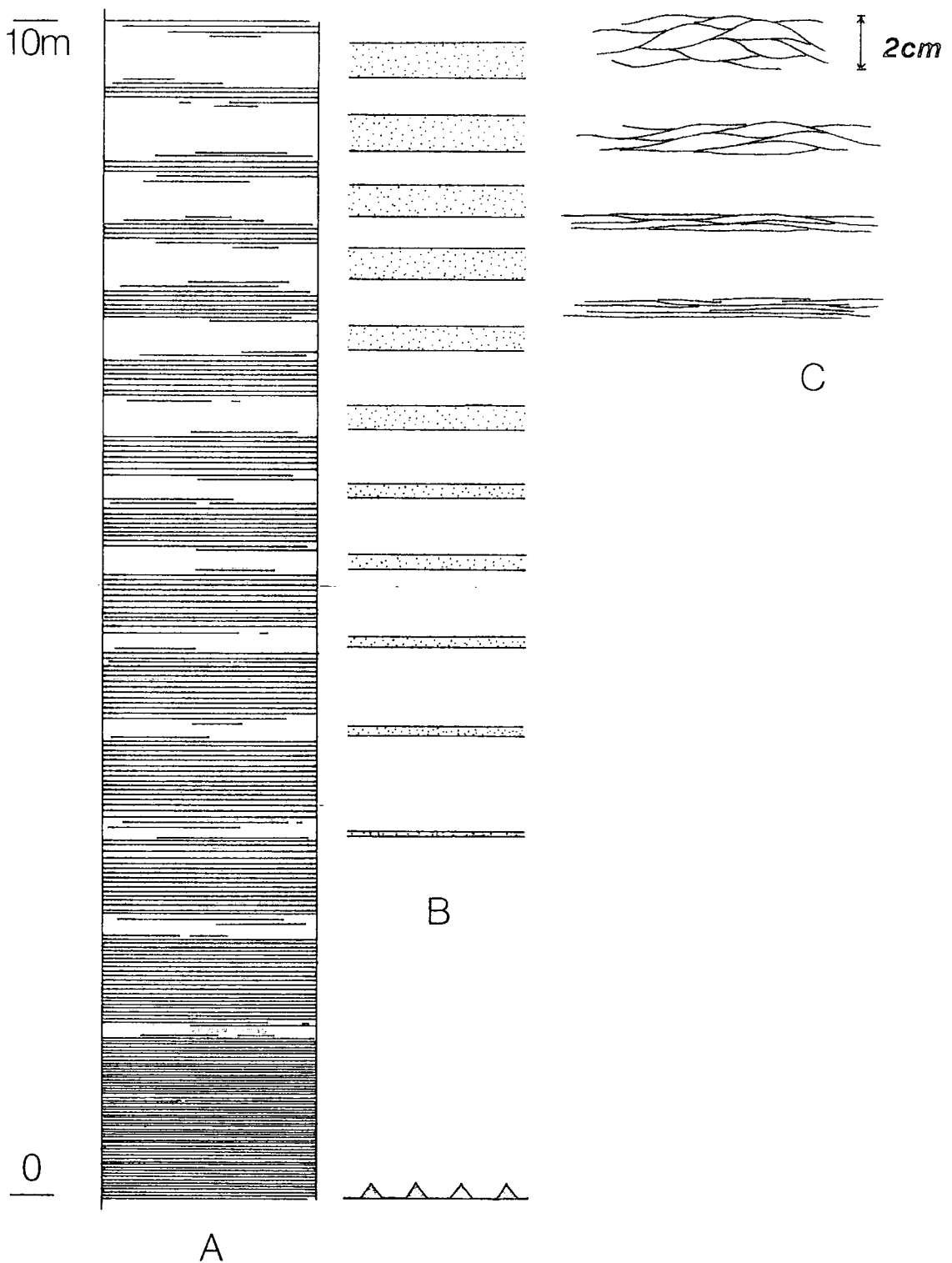
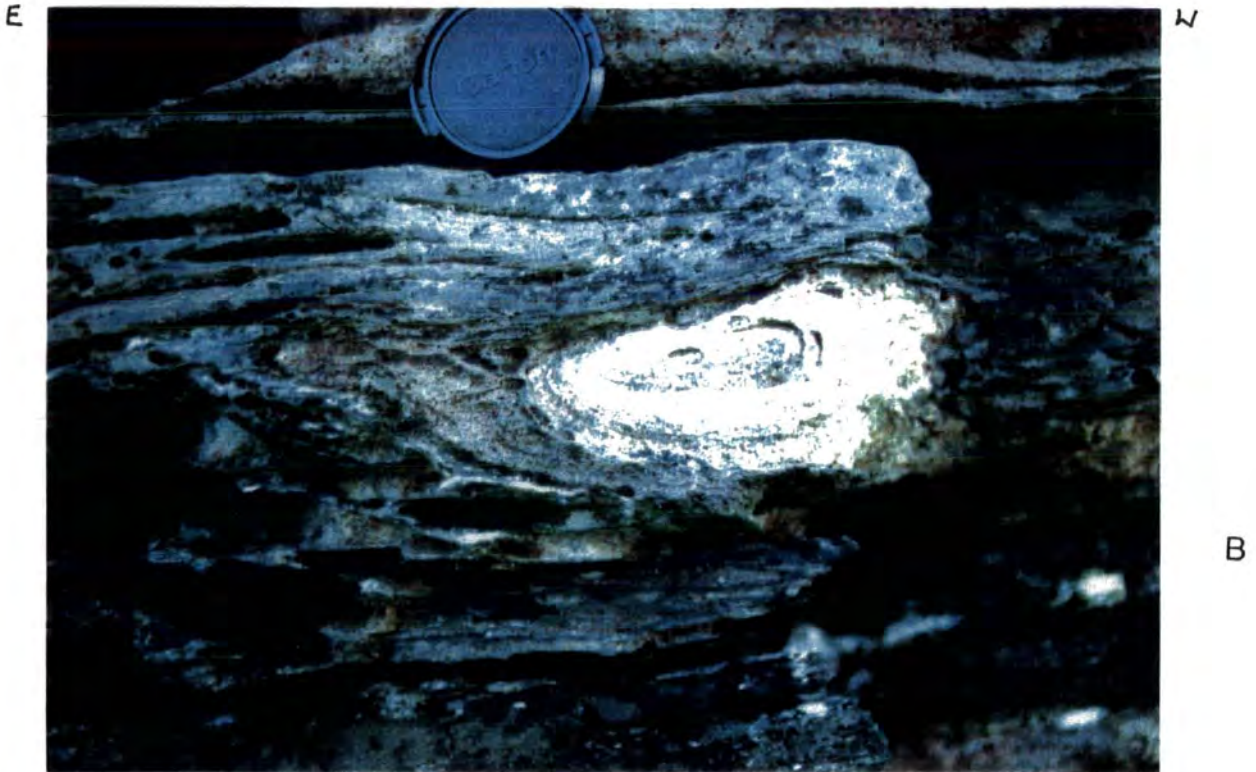


Figure 2.16 Diagrammatic representation of the strain increase and bed thinning associated with a ductile thrust at Lishagh. (A) Strain 'bands' increasing intensity and thickness towards the thrust plane. (B) Progressive reduction in bed thickness towards the thrust plane. Bedding becomes obliterated and therefore indistinguishable from  $S_2m$  close to the thrust plane. (C) Occasionally, microshears are seen between beds in the marginal areas of the thrust-related strain. These microshears anastomose when viewed down the stretching direction and intensify towards the thrust so that the shear-bound 'pods' become rapidly attenuated and the geometry indistinguishable from planar  $S_2$  fabrics.



Figure 2.17 Photograph of symmetric boudins in mixed dolomitic lithologies with long axes orthogonal to the stretching lineation. These boudins contain internal R-2 'dominos' which indicate NW directed over-shear (photograph's top to the left). Located at 648249, maps 1 & 2.



**Figure 2.18** Photographs of rootless and sheath fold closures within calcareous D2 thrust mylonites. (A) Rootless folds: the hinges are orientated at an acute angle to the stretching lineation. Located at 448154, maps 1 & 2. (B) Sheath fold closure: note that the axial planar S2m is the pervasive horizontal fabric visible in the photograph, not bedding. Located at 648249, maps 1 & 2.



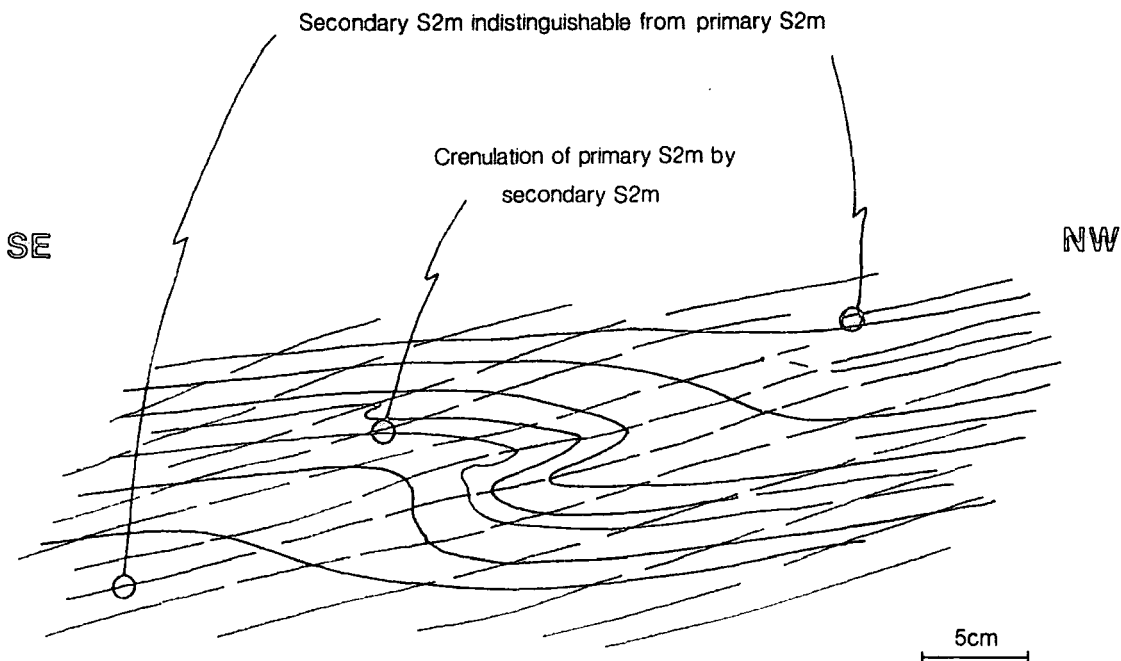


Figure 2.19 Simplified field sketch of a minor fold which folds S2m in calc-mylonites at 568209, (maps 1 & 2), displaying the transitional nature of the fold axial planar cleavage with the surrounding S2m. In the central portion of the fold, the axial planar cleavage produces contractional crenulations of the S2m, but becomes mylonitic and indistinguishable from the S2m up and down the axial surface.

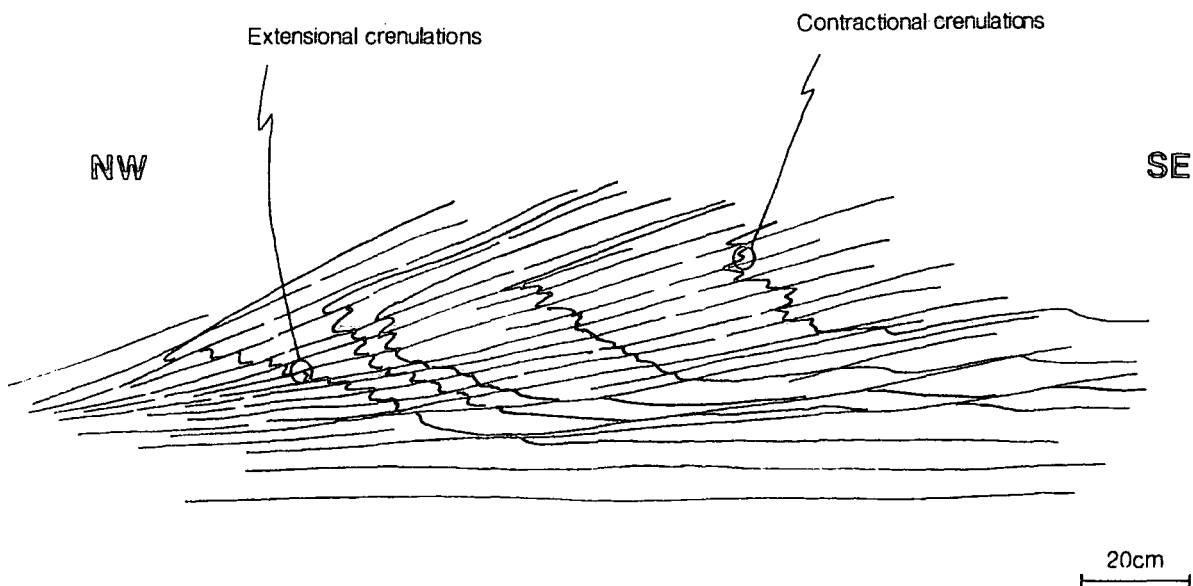
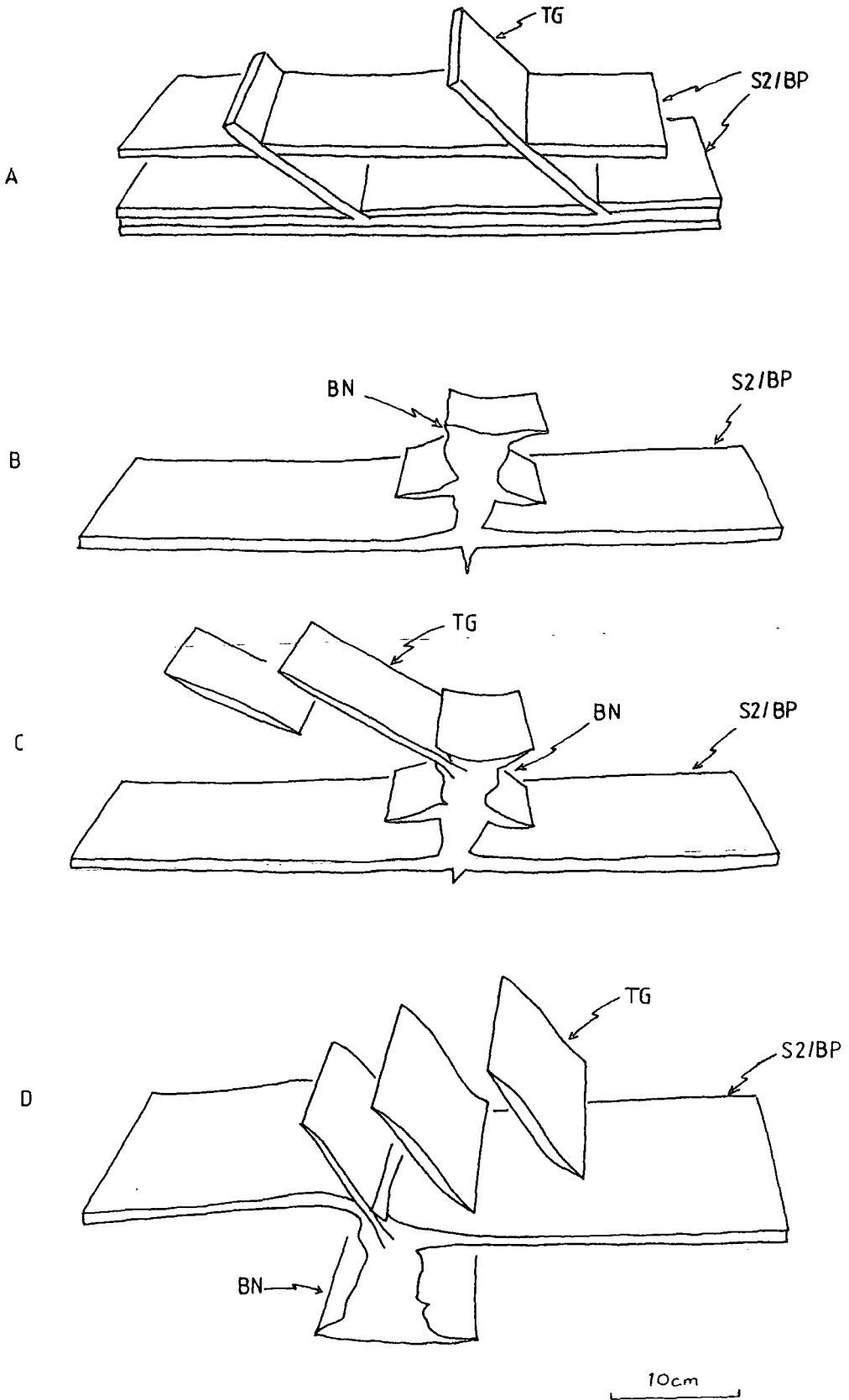


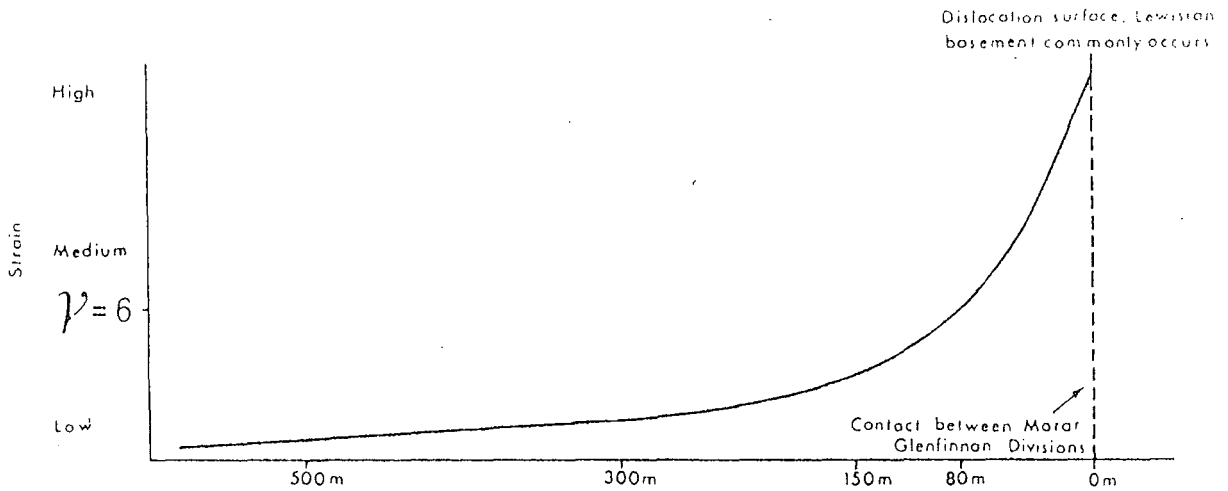
Figure 2.20 Simplified field sketch of a SE verging minor fold from 578162, (maps 1 & 2), which displays reactivation of its axial planar cleavage as R-1 extensional crenulations which are indicative of NW directed overshear and are of D2 age. The axial planar cleavage creates contractional crenulations of intense S2, (alternating 'tail' asymmetries within the microlithon structures), which become extensional in character down the axial plane to the NW (constant 'tail asymmetries regardless of position in minor fold limbs). (see text for details).

SE

NW



**Figure 2.21** Diagram illustrating the contemporaneity of vein types: (TG) tension gashes, (BN) boudinage necks, (S2/BP) S2/bedding parallel. The veins are seen at outcrop to be mutually cross cutting or interconnected. (A) 405157, (B) 200220, (C) & (D) 420113 maps 1 & 2.



Associated features

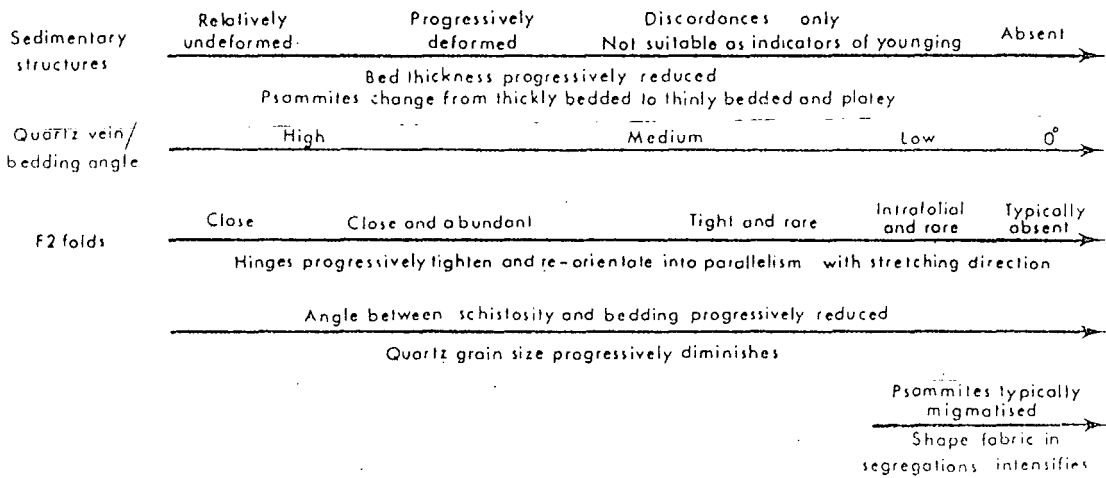


Figure 2.22 A summary of strain increase and associated features approaching the Sgurr Beag Slide (after Rathbone et al., 1983). Note that the structural elements summarized here are similar to those summarized for the Breaghy Head thrusts. Also, compare the strain-distance curve with that of fig 2.14a from the Horn Head thrust.

## CHAPTER 3

### THRUST SEQUENCE AND IMBRICATE GEOMETRY IN THE DUNFANAGHY-BREAGHY HEAD AREA

This chapter aims to describe the main aspects of the imbricated stratigraphy and the geometry, sequencing and kinematic histories of the Breaghy Head ductile thrusts. This chapter also aims to describe and discuss processes responsible for development of local polyphase fabric and fold histories during continuum D2 ductile thrusting. In the interests of clarity this is approached in a similar way to a field excursion guide, so that locality numbers quoted in brackets in the text refer to the circled numbers displayed on map 2.

#### 3.1 Knockduff, Dunrudian, Sessiagh, Lishagh and Kill

The low flat rocks and stepped cliffs at (1) provide a section through the lower contact of the Knockduff metadolerite sill and the underlying gently SE dipping stratigraphy, summarised in Fig. 3.1. The lowest units exposed at this locality are well bedded green pelites and pink fine grained quartzites. Pelitic content decreases upwards, the quartzites become cream coloured (purer) over some 2m and are overlain by 2m of white fine grained quartzite. Metre scale shear bands are developed across the contact between the white and pelitic quartzites and indicate overshear to the NW (Fig. 3.2a). Gently NW vergent S2 which is seen in the pelitic lithologies is lost in the white quartzite, presumably in response to lack of micaceous content. However, the upper metre of quartzite displays S2m sub-parallel to bedding which gives the rock a fissile and flaggy appearance. These are

overlain by white limestones with intense platey S2m development. This limestone gradually becomes dolomitic over some 3-4m upwards and the S2m decreases in intensity. Metre scale shear bands, again extending to the NW, are well developed and restricted to a zone 1m above the limestone-quartzite contact.

The dolomite is overlain by 2-3m of intercalated thin calc-silts and quartzitic bands which are rapidly replaced upwards by green phyllites. In the final metre of section these phyllites become intercalated with pink quartzites which increase in thickness and frequency upwards as the phyllitic content of the sequence decreases. This suggests a stratigraphic transition from limestone to quartzite. The S2 at this position has lost mylonitic character, verges gently NW and contains a NNW-SSE mineral extension lineation. The base of the metadolerite above this contact displays discrete intense shearing (cm scale thickness); The contact is also deformed by a well developed domino shear extending towards the SE and deflecting the stratigraphy below the sill, indicating NW overshear (Fig 3.2b). These features suggest that a NW directed thrust shear zone is located at the base of the limestone and that this thrust duplicates a limestone - quartzite transition - quartzite stratigraphic package. The lithologies are sub-parallel across the contact indicating hangingwall and footwall flat geometry.

Further NW at (2), the cream limestone (which at this locality contains grey banding), shallows and changes dip to 5° or less to the west, whilst the footwall quartzites dip at approximately 10-12° to the northwest. The quartzite is clearly seen to be cut off against the limestones above showing the geometry here to be that of a hangingwall flat resting on a gentle footwall ramp. The contact itself is a highly fissile schistose band some 2cm thick (tectonic schist). S2m decreases in intensity rapidly down into the quartzites (in under 1m), but the quartzite

is host to numerous high strain zones which are subparallel to bedding and which contain (cm) scale anastomosing shears. These anastomosing shears are occasionally offset by small shear bands which indicate NW directed overshear. These high strain zones must therefore have sheared the footwall towards the NW (ie. layer parallel shear), and must therefore have reduced the ramp angle from an originally higher angle.

The hangingwall limestones are dominated by intense platey S2m which parallels the thrust contact. Approximately 1m above the contact, the mylonites contain bands of asymmetric NW verging minor folds with sheared and displaced mid limbs. Minor folds with sheath closure geometries are also developed. Some of the mylonites contain bands of domino shears and fractures extending to the SE and indicating NW overshear (Fig 3.3). Some of these dominos are seen to have been reactivated as P bands following rotation into a shallow angle with S2m. The S2m here is also host to dense bands of micro-boudins. Above these features the limestone deformation state reduces although still remaining fairly platey. Again the limestones become dolomitic and pass up into mixed pelitic and silty lithologies, which in turn pass up into quartzites where the strain decays rapidly and the quartzites become massively bedded. The strain profile in the hangingwall is therefore some 6-7m thick. At the uppermost part of the cliff here, another thrust is found with platey limestones again with an angular discordance to the quartzites below. This is a similar hangingwall flat and footwall ramp relationship to that described in the previous paragraph. Again S2m development is greater in the hangingwall and the footwall massive quartzites are disrupted by high strain zones of anastomosing shears.

Within the limestone between (1) and (2), a zone (approx. 1m thick) contains S2m which is visibly more intense than the surrounding parallel S2m. This is likely to be the expression of

a branch point between the two thrusts.

Further north at (3), grey limestones are overlain by cream limestones. The limestones overly pink quartzites and green pelites in thrust contact. Again, intense platey mylonite (S2m) is concentrated around the contact and is thicker in the hangingwall. The intense platey mylonite tends to obliterate bedding near the thrust, but it is clearly preserved 1m above the thrust as thin bands of cream limestone within the grey limestone. The bedding in the limestones is seen to be folded into a NW vergent monofold with axial planar S2m and curvilinear minor hinges. The contact between the cream and grey limestones defines the smooth outer arc of the fold and shows that the grey limestone thins to the NNW by some 2m. Furthermore, the bedding within the grey limestone follows a trajectory which will intersect the contact with the quartzites. When traced towards the NNW, bedding can be clearly seen to become parallel to S2m and the thrust contact, dipping gently SE. This represents a hangingwall ramp of smooth trajectory resting on a gentle footwall ramp (the quartzites appear to thicken as the limestones thin). The ramp geometry is very similar to 'classic' ramp geometries seen in foreland thrust zones (Fig 3.4).

Further to the north and below this thrust at (4), a second thrust is exposed emplacing platey limestones onto platey quartzites. The platey S2m is transitional up section with gently NW vergent non mylonitic S2 in the pelitic mixed lithologies which overly the limestone. These pass up into pink and green pelitic quartzites over some 7-8m. Bedding, which dips shallowly to the south, is parallel across the thrust contact intimating a hangingwall flat, footwall flat geometry.

The quartzites and to a lesser extent the limestones form low ridges which enable the lithologies and therefore the thrusts to be traced westwards towards (5). Here the upper thrust sheet is partially exposed in nearby fields and drainage ditches, and again shows increasing intensity of the S2 to become S2m closer to the thrust contact. The lower thrust sheet is more generously exposed in road cuts, enabling a near complete section through the thrust to be examined: Pelitic impure pale to iron stained quartzites contain weak S2 crenulations which verge gently NW and contain a NW-SE stretching lineation. Silty micaceous limestones exposed nearby to the NW are pervasively deformed by extensional crenulations of equally intense S2 and indicate NW overthrusting. These extensional crenulations are superseded approximately 1m down section by C-bands (Fig 2.4), which displace S2 and small quartz veins towards the NW. Below this zone (approx. 1m), the S2 becomes intense and mylonitic. The limestones become pure and crystalline below this level and the S2m becomes less prominent. Fresh faces in the limestone, however, show strong asymmetric alignment of the calcite crystals in the limestone indicating NW overthrusting and dynamic recrystallization. The loss of the micaceous component in the limestones presumably enables secondary recrystallization (recovery) to proceed uninhibited and thereby overprints and obscures S2m fabric planes.

The thrust contact is exposed further NW, where the rocks are intensely cleaved by S2m which gives the footwall micaceous quartzites a fissile papery habit. A strong NW-SE stretching lineation is developed in the S2m and late boudin necks are displaced to the NW along C-shears. S2m has obliterated bedding here, however the general attitude of surrounding bedding suggests concordance and therefore flat on flat geometry.



The thrusts can be traced SW via a series of low linear exposures towards Dunrudian at (6) where the lower thrust is exposed in a small cliff. Here SE dipping grey limestones have some  $35^\circ$  discordance with near horizontal footwall quartzites. As noted at (2), the thrust contact generates a narrow zone of intense platy S2m in the quartzites. The limestones are heavily recrystallized which masks the S2m in them, however where the limestones have a micaceous content intense S2m is preserved. Also as noted at (2), the footwall quartzites feature bedding parallel shears which here are not as intense as at (2), but which displace quartz veins to the NW. This is therefore a hangingwall flat on footwall ramp geometry. This exposure will be described and discussed in detail in chapter four.

The limestones pass up into pelitic and micaceous limestones where intense S2m is preserved. These limestones shallow by some  $20^\circ$  along strike to the SW, suggesting a decrease in ramp angle towards the SW. At (7) both quartzites and limestones dip  $15^\circ$  ESE, giving the thrust a flat on flat geometry.

Above the pelitic and micaceous limestones at (6), silty impure dolomitic limestones pass up into mixed thin intercalations of dolomite, silt, quartzite and pelite, with the pelites making up the greater part of the percentage lithology log. These become platy up section and contain pyrites with asymmetric pressure shadows indicating NW overshear. Above this, highly deformed white and grey crystalline limestone marks the position of the upper thrust. Away from the thrust, the limestone becomes pelitic and micaceous, passing up into silty dolomitic limestones, which in turn pass up into intercalations of dolomite, silt, quartzite and pelite. These contain shear bands, P-bands and dominos indicating NW overthrusting.

The limestones of the upper thrust are here in concordance with the sequence below and are therefore in a flat on flat relationship. However, the quartzites separating the two thrusts at (5) are missing here, suggesting that the upper thrust gently climbs section to the NE in the footwall.

At (8) towards the SW, the footwall quartzites to the upper thrust reappear, containing dominos and extensional crenulations which indicate NW directed overthrusting. The limestones become very platy towards the base where they are in thrust contact with the quartzites which thicken towards the south. This thrust therefore climbs section to the south and indicates a hangingwall flat on a footwall lateral ramp geometry. SW towards (7) the quartzites and mixed lithologies are gradually cut out against the limestone indicating another footwall lateral ramp.

The branch point between the two thrusts is visible in a set of low exposures at (7). The footwall quartzites here are highly strained with alternating zones of anastomosing shears and platy S2m containing a strong NNW-SSE stretching lineation. This footwall strain is some 3m thick here. The basal part of the limestones are affected by intense platy S2m which decreases in intensity up section rapidly and the limestone becomes more crystalline (as noted at (6)). A zone (some 1m thick) of very intense S2m gently climbs across the exposure towards the NE, above which two sets of extensional crenulations are well developed in a band some 1m thick. Broad (2cm spacing) crenulations apparently extensional to the W intensify towards the NE and swing to apparently extend to the WSW. Remnants of this crenulation are occasionally seen in the intense S2m zone, where the extensional crenulations are apparently reworked where the S2m crosses them. The reworking S2m is indistinguishable from S2m in the surrounding rocks. A low angle closely (2-5mm) spaced set of extensional (to the NW) crenulations cross cuts both the earlier

set of crenulations and the S2m. Veining is also present in this outcrop and is generally fabric parallel, but is also seen to transgress the S2 in places, and to cross cut the earlier broad extensional crenulations. These veins are deformed and sheared out in the mid exposure high strain S2m zone and deformed by the later lower angle crenulations.

The above observations strongly suggest that the higher thrust is the later of the two, being a break-back thrust, the displacement of which is likely to be responsible for the anomalous strike and strike swing in the earlier broad extensional crenulations, which appear to have been rotated towards the X direction. The total thickness of the hangingwall shear strains here is in excess of 8m. These relationships are summarised in Fig 3.5.

Further SW at (9) a number of subsidiary thrusts in the footwall to the limestone thrust bring metadolerite over quartzite. As illustrated in Fig 3.6, the geometry at exposure level is that of a leading edge branch point in the metadolerite resting on a footwall ramp in the quartzites. Above and to the south of the branch point there are a number of warps and folds in the metadolerite-quartzite contact and changes in the thickness of the metadolerite. These features are most satisfactorily explained by structurally necessary folds above ramp-flat thrust geometries (Fig 3.6).

The limestone thrust swings westward towards (10) south of (9). The thrust contact is not exposed between the localities, however, a series of cliffs at (11) bring the erosion level down to the lower structural levels and S2 is seen to intensify transitionally into S2m as the thrust is approached. Here pink and grey limestones pass upwards into white and buff to grey limestones with a general upwards increase in micaceous content.

At the thrust contact between micaceous limestones and quartzites exposed at (10), a 30cm zone of intense shearing (relative to surrounding shear strains) contains apparent lithological mixing between the hangingwall and footwall (tectonic schist).

South of (10) at (12), a second higher thrust is exposed. This thrust emplaces limestone onto limestone and, (as described in chapter 2), has a hangingwall dominant strain profile, being some 1m thick in the footwall and some 10-15m thick in the hangingwall. A thin sliver of quartzite which defines the thrust contact at this location is seen to thicken towards (13) to become 3m thick. The mixed lithologies noted between limestone and quartzite are absent here, instead the quartzites are intercalated with common pelitic partings. This thrust swings NE from this locality and may branch with the lower thrust near (9). This suggests that the thrust climbs and descends the stratigraphic section very gently across strike. The lower thrust can be traced westward from (10) to (14) where it can clearly be seen to climb through the quartzites towards the west to form a hangingwall flat resting on a lateral footwall ramp. Again strain (S2m) increases towards the mapped contact. In cliffs to the south of (12) and (13), quartzites contain well developed cross bedding which indicates that the stratigraphy is right way up.

This thrust can be traced westward to (15) as lying between isolated exposures and breaks of slope, and NW through increasing numbers of exposures towards (16) at Kill. Bedding attitudes across the mapped contact remain virtually parallel from (14) to (16) indicating a flat on flat geometry over this distance. Also over this distance, the exposures show a consistent intensification of S2 fabrics towards the mapped thrust contact between limestone and quartzite. South of (16) at (17), limestones become dolomitic up section, containing strong S2. These are overlain by interbedded impure quartzites and grey

pelites. These pass up into pure white quartzites with intense platy S2m. Approximately 1m above these quartzites, platy limestones are seen to show a decrease in S2m intensity up section. The quartzite can be traced westward from here into dead ground using the break of slope it creates for up to 700m before this feature disappears. This is interpreted as being cut out by the thrust in that direction. The quartzites are clearly seen to be cut out to the east and the thrust, which then emplaces limestone onto limestone, is demarked by a zone several metres thick of S2m which is highly intensified relative to that in the surrounding outcrops.

This higher strain zone (thrust) is easily traced southwards to (18) at Lishagh. Here the quartzites reappear and the thrust climbs section briefly to the east before descending section once more. These outcrops are more fully described above in chapter two, however, both limestone and quartzite here are highly strained and contain intense S2m. These mylonites contain extensional crenulations, C-bands, P-bands and dominos indicating NW directed overshear.

East of (18), exposure is more sporadic, however, a high strain zone in the limestones traces east towards the shore of Sessiagh Lough, where it is logical to correlate the thrust to the east shore at (12) and is here considered a continuation of this thrust along strike.

Both thrusts are traced westward from (16) and (17) via breaks of slope. The lower thrust apparently cuts down section to emplace limestone onto metadolerite. As described above, the break of slope representing the quartzites of (17) can be traced westward towards (19) before disappearing at (20). This is accompanied by the disappearance of scrub vegetation in the same area. The break of slope representing the limestone and

metadolerite interface of the lower thrust swings to the southwest in such a way that this and the quartzite break of slope are aligned to intersect. This suggests that the upper thrust branches into the lower thrust near (21).

Further west at (22), limestones and metadolerites are in contact with intense platy S2m developed in both lithologies, dipping shallowly SE. Quartzites crop-out in a small exposure 10m west of here in contact with the metadolerite. This quartzite and metadolerite contact runs due west from (22) whilst a break of slope runs SW to intersect the coast at (23) where platy micaceous limestones containing several generations of extensional crenulation are in contact with platy quartzites. This indicates that the thrust climbs section to the SW from (22) to (23) to create a footwall ramp. The platy S2m in these lithologies decays away from the contact in a hangingwall dominant pattern, being some 10-15m thick in the hangingwall and only some 3-4m thick in the footwall. The limestones, exposed in shoreline cliffs can be traced westwards to (24) where they pass gradationally upwards into grey pelites. Above and to the west of (24), these pelites become intercalated with thin fine grained iron stained quartzites. These quartzite intercalations become more important upwards so that in the area of (25) they occupy some 60-80% of the stratigraphic log. At this position 10-15cm thick quartzite beds show a variable vertical spacing so that in places evenly spaced quartzite-pelite intercalations are replaced by closely stacked quartzite beds separated by thin pelite veneers. This may suggest that the quartzites were deposited in pulses against a background pelitic sedimentation.

Above the quartzites of (25) a bedding parallel metadolerite sill is coarsely crystalline and contains sub-horizontal igneous banding. This indicates negligible strain at this position, supported by undeformed hornfels spots in the quartzites near the

sill contact. Southwest of (25) at (26), the top of the sill is exposed in contact with iron stained and pelitic fine grained quartzites. At the contact the metadolerite is very fine grained, containing a ghost banding and the quartzite bedding is locally disrupted to form open domes. Inside these domes, bedding is contorted and apparently autobrecciated with fragments of quartzite suspended in a fine grained metadolerite matrix. These structures (Fig 3.7) resemble sedimentary de-watering features with buckling of bed fragments being highly disharmonic and pygmatic in geometry. There are no fabrics associated with these buckles and since the surrounding rocks are unstrained, these bedding disruptions must be original (pre-deformation) features associated with the sill intrusion. It is possible that they represent locally developed volatile escape structures and they are therefore used here to indicate right way up stratigraphy.

Above and south of (26) at (27), cream and buff fine grained quartzites have negligible pelite content. These have a high strain with intense S2 parallel to bedding and a NW-SE extension lineation. Boudinage occasionally showing crude domino rotations and extensional crenulations in the outcrops suggest a SE directed overshear. These features represent a strain increase from the negligible strain of (26) and imply the existence of a thrust above and to the south of (27). At (28) to the east, inverted igneous banding in the metadolerite dips  $75^{\circ}$  to the NE and is overprinted by gently SSW dipping S2. Further east at (29), the metadolerite contains intense S2 and a NNW-SSE extension lineation. These outcrops indicate that a high strain zone (thrust) can be traced from the upper part of the quartzite at (27) eastwards into the metadolerite. The thrust therefore has a lateral footwall ramp at this position. Atypically the kinematic indicators suggest SE overthrusting, so that the thrust is a backthrust (regionally D2 structures verge NW).

Returning to the outcrops around Lishagh, we can examine the stratigraphy in the hangingwall to the thrust exposed at (18). At (30), platey grey micaceous limestones overly the platey more crystalline limestones of (18). The micaceous limestones pass upwards into silver grey pelites which contain thin bands of limestone and calcpelite, together with thin silt and quartzite bands. The quartzite bands become more important upwards so that quartzite makes up some 80% to 90% of the log thickness. This transition between limestone and quartzite is some 4-5m thick at this locality but appears to reduce thickness and disappear westwards. This is accomplished by a westward increase in the quartzite component in the transition beds so that micaceous limestones rapidly pass upwards into quartzite-pelite intercalations. Above these outcrops, cream to light grey and iron stained fine grained quartzites, exposed in a series of cliffs are in excess of 100m thick. These cliffs dominate the skyline south of Dunfanaghy and Sessiagh Lough so that the quartzites are easily traced westwards from Lishagh to (25) south of Rincleven Point and eastwards to the south of Sessiagh Lough, the type section for the Sessiagh Quartzite.

Southeast of Sessiagh Lough at (31), the gradational limestone-quartzite contact is exposed in a cliff face. Pelitic grey and dolomitic limestones pass up into approximately 1m of intercalated pelites, thin limestones, porous iron rich silts and thin fine grained iron stained quartzites. Above these beds grey pelites are intercalated with heavily iron stained quartzites which become more important upwards so that pelite is only present as rare thin veneers. The quartzites become less iron stained as the pelitic content of the sequence diminishes and well developed cross bedding indicates right way up stratigraphy. At (32) to the NE, the limestone to quartzite transition is a 3m sequence of intercalated grey pelites, green pelites and grey iron stained fine grained quartzites. These quartzites become the dominant



lithology up sequence. Here a metadolerite sill is intruded into the quartzites, above which the quartzites contain cross bedding indicative of right way up stratigraphy. These quartzites are easily traced westwards to the cliffs south of Sessiagh Lough.

West of Dunrudian at (33) the upper part of the limestones are dolomitic and pass rapidly upwards into silver grey pelites which contain thin quartzite partings and thin iron rich silts. Approximately 15-20m above these beds grey phyllitic pelites are in contact with the Dunrudian metadolerite sill. These pelites contain thin quartzite partings and thin (up to 2cm) more laterally persistent quartzite bands. The pelites, which contain hornfels spots and appear 'baked' near to the sill contact, make up around 80% of the sequence at this position. These rocks also contain NW vergent minor folds with sheared mid limbs and broad shear bands which indicate NW directed overshear. Exposed at a similar stratigraphic level at (34), grey pelites contain thin intercalations of iron stained quartzite and green pelite, with some quartzite bands being very dark grey and chert-like in appearance. Above the sill at (35), silver grey pelites contain occasional thin quartzite veneers and both R-1 & R-2 extensional crenulations indicative of NW directed overshear. Above this the pelites, which are rich in biotite porphyroblasts, contain thin bands of pale calcpelite and quartzite. The quartzite bands become more frequent over some 20m upwards, so that at (36) iron stained and grey quartzites are the dominant lithology (80-90%), containing intercalations of thin grey and green pelite and rare thin calcsilt veneers. Up sequence from (36) the silt component is lost and the pelitic component further reduced.

Along strike to the NE at (37) the upper contact of the Dunrudian sill<sup>#</sup> is exposed again. Intercalations of iron stained quartzite, buff silts and grey and green pelite pass upwards over 5-10m into massively bedded iron stained quartzite. The Sessiagh

\* Dunrudian Sill (Synon) = Knockduff Sill.

Clonmass quartzites are characteristically fine grained, however at this location some of the lower quartzite beds contain thin bands of medium to coarse grain size with calcareous clasts. Above these beds a complete 30-40m coastal section through the quartzites shows a consistent fine grain size. This suggests that at least in part the early quartzite sediment load was supplemented by locally derived detritus. The base of the quartzites may therefore in places be erosive in character.

An open synclinal feature with a crude 'spoon-like' geometry exists between Dunrudian and Knockduff, as evidenced by bedding attitudes in the area (map 1). This is consistent with hangingwall accommodation to movement over the 'shaped' footwall topography so far described in the area. This fold produces multiple exposure of the mid part of the transition beds at (38) & (39). At both localities silver grey pelites contain thin calc pelite veneers and silt bands.

In summary, it has been shown that both the limestone and the quartzite are laterally persistent units, whilst the transition beds between the limestone and quartzite are variable in both lithological content and thickness. These variations are summarized in Fig 3.8. This suggests that the thrusts duplicate a non layer-cake stratigraphy.

### **3.2 Breaghy Head and Curragh Harbour**

The quartzites exposed around Breaghy Head are massively bedded, white to light blue-grey, coarse grained and contain well developed cross bedding. These quartzites also contain occasional feldspathic grit and pebble bands. In all these respects the quartzites are identical to and are therefore correlated with the Ards Quartzite.

East of Breaghy Head at (40), cross bedding indicates that south dipping Ards Quartzite is inverted. These inverted beds occupy the mid limb of a major NW vergent F2 fold. A metre scale platy S2m (high strain) zone in the mid limb can be traced SW from this position to disappear in the direction of Curragh Harbour. This high strain zone can also be seen to disappear down the cliff to the south, however, the treacherous slopes and sheer faces of the cliffs at this location prevented direct observation of this high strain zone in the fold profile plane. Cut-offs and shear bands indicating NW overshear were found to be clearly visible, however, from a boat (Fig 3.9a). This structure represents a fold with a thrust middle limb, a relationship commonly described from foreland thrust and fold belts.

To the west at (41), Ards Quartzite contains cross bedding indicative of inverted stratigraphy. This inversion is also indicated by cross bedding in other outcrops between (40) & (41). The contact between the Ards Quartzite and the metadolerite sill below (41) is undeformed, since cross bedding is preserved close to the contact and a nearby pebble bed records negligible strain. The metadolerite at (42) to the SW, however, is pervaded by high D2 strains, implying sill intrusion prior to deformation. The metadolerite must therefore be inverted with the Ards Quartzite by the F2 folding and thrusting.

At (42), limestone containing numerous small isoclinal and sheath fold closures overlies the metadolerite in thrust contact. Both these lithologies are pervaded by intense platy S2m with a strong NW-SE extension lineation and large (m scale) shear bands are developed in the metadolerite indicating NW directed overshear. The limestones become micaceous upwards, passing into intercalations of buff silty dolomite, buff silt, pale green and grey pelite and thin quartzite. These rocks resemble the transition beds described elsewhere, however, at this location

silty lithologies dominate the sequence. Strain appears to decrease upwards through these beds. Above these rocks to the south, exposed in a cliff face, cream and pink to iron stained fine grained quartzites interbed with the silty and pelitic transition beds. Strain appears to increase upwards once more into an intense zone below a panel of strongly folded transition beds which overlie a quartzite body. These rocks are overlain by a second thick (4-5m) quartzite body which is cloaked by high strains containing S2m and tight to isoclinal minor folds with sheared out mid limbs. This quartzite is also cut by more discrete high strain thrust shear zones (Fig 3.9b). The limestone and transition sequence thin out and taper towards the NE where they disappear into a high strain zone within the Ards Quartzite. Ards Quartzite also overlies the transition beds to the SE and appears to taper out towards a position beneath the Sessiagh Clonmass quartzite body described above. The disposition of high strains and outcrop pattern indicate that the limestone and transition beds represent a NW directed forethrust-backthrust wedge. Similarly, the Ards Quartzite above the transition beds represents a wedge remnant of the backthrust hangingwall, cut out by an overlying forethrust. These relationships are summarised in Fig 3.10.

The western limit of the Sessiagh Clonmass quartzite body (described in the above paragraph), is folded into a syncline so that the quartzite bedding is cut out against the upper high strain zone (Fig 3.9b). Silty transition beds rest in a hangingwall flat relationship against the quartzite footwall syncline. Along strike to the east, these rocks are in a footwall flat against hangingwall flat relationship. Down dip to the south towards (43), the quartzite body tapers out so that transition beds rest on top of transition beds. Here the high strain zone can be traced towards an anticline-syncline pair with a sheared out mid limb (Fig 3.11). It is significant to note at this

junction that the fold pair have a westerly vergence and imply the opposite sense of overthrusting to that implied by the quartzite footwall syncline and nearby minor fold vergence. Another narrower high strain zone in the lower normal limb of the fold pair appears to trace out towards the quartzite footwall syncline. This high strain zone traces westwards from the anticline-syncline pair around the Curragh Harbour anticline to a position above an easterly facing footwall syncline on the west limb of the anticline (Figs 3.11, 3.15). This footwall syncline faces in the same direction as the one in the quartzite, suggesting that a folded thrust climbs section to the east in a footwall ramp hangingwall flat relationship.

An E-W trending sub-vertical late normal fault was mapped to intersect Curragh Harbour. This fault has previously been used to explain the juxtaposition of Ards Quartzites and Sessiagh Clonmass rocks here (McCall 1954, Hutton 1977a). It should be noted, however, that a normal fault in this area would not explain the presence of the wedges of Sessiagh Clonmass rocks to the N and NE of the harbour. This normal fault branches into two strands to trace to the N and S of an Appinite body west of the harbour (cf. Elsdon & Todd 1989). The fault is therefore expressed in the cliff line surrounding the SE shore of the harbour as two faults. Neither fault is seen to exceed a displacement of a metre or so, since distinctive lithologies and the above described high strain zones can be matched across the faults; (these observations were greatly aided by an excursion in an inflatable boat). These normal faults do not, therefore, explain the Ards Quartzite - Sessiagh Clonmass juxtaposition and consequently do not affect the above or following observations.

The core of the Curragh harbour anticline must, therefore, be occupied by the limestones and transition beds exposed at (42), since these thrust hangingwall lithologies follow a dip trajectory

across the narrow harbour to this position.

On the western limb of the anticline above the folded thrust, platy limestones reappear in high strain thrust contact with the transition beds at (44). A thrust near to the upper part of the limestones forms an easterly facing footwall syncline and hangingwall flat. This thrust contains multiple shear bands, extensional crenulations and domino shears indicating NW directed overshear (Fig 3.12). The limestones thin out to the east (hangingwall ramp) so that above the (43) cliff exposure, at (45), transition beds are once more emplaced onto transition beds. The rocks here are highly strained with intense S2 and S2m development. A metadolerite sheet is domino sheared here and boudins in the sediments contain well developed internal domino shears indicating NW overshear (Figs 3.13 & 2.17).

The exposures at (45) also contain sheath fold closures with west vergent (on surrounding bedding) axial planar S2 cleavage. An east vergent cleavage crenulates this S2 and would be interpreted as S3 in the deformation chronology of Hutton (1977a, 1982, 1983). Near to one of the sheath fold closures, a thin (5cm) metadolerite sheet is intruded across bedding, parallel to S2. The metadolerite sheet contains S2 and occupies the mid limb of a west vergent F2 fold. These relationships suggest that the metadolerite was intruded during D2 deformation. The F2 fold and the associated axial planar S2, fold and crenulate the east vergent cleavage. The two cleavages, which face and verge in the opposite direction to one another, therefore mutually overprint in a conjugate relationship and cannot therefore be separated into S2 & S3 (D2 & D3), (Fig 3.14).

Thrust hangingwall cleavage which verges in the direction of thrust transport is a familiar feature of thrust belts (e.g. Mitra & Elliott 1980, Cooper & Trayner 1986, Boyer & Mitra 1988). The

development of forethrusts and backthrusts therefore offers an environment conducive to the development of two sets of cleavage with an opposing sense of vergence and facing, especially where the forethrusts and backthrusts face one another (eg. Morley 1986, Seago & Chapman 1988). In the Curragh Harbour area, these relationships are seen where the mid limb sheared fold pair of (43) lies below and north of the outcrops of (45). This fold-thrust feature appears to overshear in the opposite direction to the lower folded thrust and the thrust of (44) & (45). These relationships support the suggestion that the conjugate folds and fabrics are penecontemporaneous and representative of forethrust and backthrust strains associated with continuum D2 thrusting. These relationships are summarized in Fig 3.15.

The thrust of (44) & (45) can be traced NE above the Sessiagh Clonmass quartzite body (Fig 3.9b) to the NE of which at (46) it emplaces transition beds onto Ards Quartzite. Another thrust emplaces Ards Quartzite above the transition beds of (46) so that the transition beds taper and disappear into a high strain zone in the Ards Quartzite to the NE. This suggests the existence of another NW directed forethrust-backthrust wedge cored by transition beds. The Ards Quartzite backthrust here is cut out against the intense platy S2m of a limestone thrust at (47). Below this thrust and above the Ards Quartzite backthrust, an intensely platy limestone is exposed at (48). Highly strained Ards Quartzite lies above and below this limestone, which can be traced eastwards to (49). Hutton (1977a) described anomalously high local strains recorded by stretched pebbles in the Ards Quartzite close to limestones near (49). Kinematic indicators associated with this limestone remained elusive, however, it is logical (in view of the relationships described above) to interpret this feature as a further forethrust-backthrust wedge. In a similar way to the Ards Quartzite thrust, these thrusts are clearly seen to be cut out against the breaching limestone thrust

(bt1) at (47), as described in detail below.

On the western limb of the Curragh Harbour anticline, south of (44) at (50), the intercalations of silty dolomite, silt, green and grey pelite and thin quartzite pass upwards into intercalations of green and grey pelite and cream to pink or iron stained fine grained quartzite. The quartzites lose their pink colour and become the dominant lithology up section to occupy in excess of 80% of the sequence. This limestone to quartzite succession is summarized in Fig 3.16. Also at (50), the quartzites are in thrust contact with overlying grey limestones. Both lithologies are intensely cleaved by platy S2m which lies parallel to the steeply west dipping contact. In the footwall the S2m reduces intensity downwards to the east over approximately 8m to be transitionally replaced by gently west verging non mylonitic S2. Above the contact in the hangingwall, however, S2m remains intense for approximately 10m of section, crossing the contact with metadolerite which overlies the limestone with no apparent loss of intensity. The S2m shallows dip and loses intensity upwards over the next 10m to be replaced by a more gently westward inclined non mylonitic S2 fabric. Extensional crenulations, P-shears and C-shear offsets of small quartz veins are well developed close to the thrust contact all of which indicate NW overshear. These relationships show that the thrust shallows to the west and is therefore folded to become downward facing by the Curragh Harbour anticline (Fig 3.17).

To the south at (51), the downward facing thrust is still steeply west dipping and is cut out by a higher thrust which dips shallowly to the SE. This thrust is a correlative of the breaching thrust at (47) to the NE. At (51) this breaching thrust has intense platy S2m characteristic of the ductile thrusts in the area and is therefore of D2 age. Thus a D2 thrust clearly breaches other D2 thrusts so that time separation between the



thrusts is short lived and local in significance. Furthermore, the downward facing thrust is folded by the Curragh Harbour anticline prior to being breached by the new thrust which cuts down through the fold to the NE. The breaching thrust therefore cuts the Curragh Harbour anticline. This anticline is associated with upright contractional and strain slip cleavages which crenulate the S2 fabrics at (50) and the 'conjugate' S2 fabrics at (45). The anticline and associated minor folds and fabrics have been interpreted (Hutton 1977a) as a large F4 fold with subsidiary conjugate F5 & S5 elements. These fabrics and the folds cannot, however, reflect post D2 deformation since this would create the inescapable paradox of a D2 structure (the breaching thrust) cross cutting D2, D3, D4 and D5 structures.

In summary, it has been described how Ards Quartzite and Sessiagh Clonmass rocks tectonically interdigitate in the Curragh Harbour area. The stratigraphically younger Sessiagh Clonmass rocks are found in the forethrust hangingwalls and the stratigraphically older Ards Quartzites in the backthrust hangingwalls. This strongly suggests that the Ards Quartzites and the Sessiagh Clonmass lithologies were at a similar datum level at the time of D2 thrusting. This stratigraphic juxtaposition does not indicate the presence of an F1 fold since there are no refolding structures associated with the F2 folding noted between (40) & (41). Furthermore, this F2 fold would not bring Sessiagh Clonmass rocks into a position favourable to emplace them into the Ards Quartzite via a forethrust-backthrust complex. The most likely explanation is that an original basin fault is responsible for bringing Sessiagh Clonmass rocks and Ards Quartzite into a similar position. It is considered therefore that the forethrust-backthrust complex and the Curragh Harbour anticline were developed as buttressing structures in response to the rheological interface which this fault must almost certainly have presented to propagating thrusts. As illustrated in Fig 3.18, the

(cf. structural sections @ rear of thesis),

structures of the Curragh Harbour area are very similar to buttressing structures seen in foreland fold and thrust belts (eg. Gillcrist et al 1987, Welbon 1988, Butler 1989a, 1989b). The Curragh Harbour folds and fabrics therefore represent a complex fold and fabric history of local kinematic significance in which individual structural elements are developed with negligible temporal separation. This local polyphase fold and fabric history is therefore developed during progressive D2 thrusting deformation.

### 3.3 The Breaching Thrusts

The thrust which breaches thrusts at (47) near Curragh Harbour, contains in its hangingwall, cream and grey limestones which are highly strained with intense platy S2m containing a strong NW-SE stretching lineation and small isoclinal and sheath fold closures to which the S2m is axial planar. The platy S2m of the limestone forethrust -backthrust wedge of (48) is folded over in the footwall to the breaching thrust. Despite recrystallization of the fabric, it can be seen to be crenulated by the breaching thrust's S2 fabrics as the contact is approached (over approximately 3m) these crenulations in both limestone and quartzite take on a crude SC-like character before the earlier fabric rapidly swings into parallelism with the new S2m. Eastwards from (47), the thrust ramps in the hangingwall through pelite, silt and quartzite intercalations (transition beds) to the base of an overlying metadolerite sheet at (52). Further east, the thrust ramps back down into limestones and can be traced to follow the base of cliffs between (49) & (53). Southwest of (47) the thrust ramps upwards in the hangingwall to the base of the metadolerite and back down into the limestones towards (51). The thrust therefore gently climbs and descends section between (49) & (51) to form a series of gentle lateral to oblique hangingwall ramps. The footwall geometry appears to be fairly concordant (flat) from

(49) to (47), however, between (47) and (51) this thrust breaches an earlier thrust and the Curragh Harbour anticline, making the footwall geometry difficult to determine.

At (51) the thrust on the western limb of the Curragh Harbour anticline is cut by the breaching thrust. Fabric relationships here are similar to those noted at (47), so that despite recrystallization, the S2m of the breaching thrust is seen to crenulate and shear out the earlier S2m which swings into parallelism with the new fabric. Also at (51) another thrust appears to branch from the breaching thrust and ramp eastwards in the footwall to emplace limestone and metadolerite onto metadolerite, quartzite and metadolerite towards the east (the metadolerite bifurcates near (54)). This produces an oblique footwall ramp and hangingwall flat geometry.

The breaching thrust ramps upwards in the hangingwall from limestone into metadolerite SW of (51) at (55). Further west towards (56), the thrust ramps upwards in the footwall from metadolerite into quartzites. Between (55) & (56), the thrust ramps upwards in the footwall from metadolerite into quartzites. Between (55) & (56) the quartzites in the footwall are folded into an east facing syncline with S2 axial planar cleavage and vertical bedding in the mid limb. The thrust must breach this fold, since highly sheared hangingwall metadolerite is present in the adjacent field to the south, leaving insufficient room to fit in the anticlinal return hinge below the metadolerite thrust.

At (57) folds and a discrete thrust in the footwall quartzites display a complex array of different kinematic features, summarised in Fig 3.19. These include domino shears in massive quartzite beds which 'leak' strain slip crenulations into pelites which occasionally interbed with the quartzites. These crenulations sometimes follow a listric trajectory onto the

interface between the pelite and the next quartzite bed in the sequence. Quartz veins parallel the fold axial planar cleavage in mid limb regions and occasionally show thrust sense offsets of bedding across individual veins. The axial planar cleavage (S2) is also deformed by flexural shearing along bedding and deformed by shear bands and extensional crenulations indicating NW overshear. Some shear bands are apparently associated with the flexural shear and indicate eastward overshear in the fold long limbs. A discrete (approximately 20cm thick) thrust shear zone at the leading (eastern) end of the fold train displaces bedding and an anticline-syncline fold pair. The outcrops here are orientated E-W so that the section view they afford is oblique to the thrust transport direction indicated by a NNW-SSE stretching lineation. Fold hinges are sub-parallel to this stretching direction, however, this sub-parallelism is not viewed as resulting from high strain passive rotation of the fold hinges towards the X direction. This is because the high strains required to accomplish such rotation are not present in these rocks, as evidenced by the presence of well preserved cross bedding (which indicates right way up stratigraphy). The deformation here is mainly associated with folding which contains veining parallel to the axial planar cleavage across which thrust sense displacements are recorded. The discrete thrust at the eastern end of the exposure is parallel to the axial planar S2 and shows an intensification of this fabric towards the thrust. These features are characteristic of 'fabric slip ramps' (see chapter 4). Significantly, Coward & Potts (1983) have discussed the development of asymmetric folds with hinges sub-parallel to the stretching direction, in response to local wrench strains formed by thrust sheet differential movement, possibly leading to the development of lateral or oblique ramp segments.

The structures around (57) are interpreted as being associated with an oblique fabric slip ramp segment. The

breaching thrust, which is traceable from (56) to (57) lies above this ramp and is folded by folds associated with the ramp. This therefore represents a D2 thrust being deformed by D2 thrust related folding. In terms of thrust sequence, movements on the ramp must post date movement on the breaching thrust.

Just west of (57) the platey strain of the breaching thrust bifurcates so that platey S2m is seen to follow the metadolerite base and is also seen to form a 3m thick zone within the metadolerite, traceable for some distance to the SW. Gently westward dipping S2 intensifies to become platey S2m and shallows into the mid point of this shear zone. Sediment 'rafts' (limestone and silt) are contained within the shear zone approximately 50cm to 1m into the hangingwall. The lower contact of the largest of these rafts is folded by minor easterly vergent folds with axial planar S2 which intensifies downwards to become the thrust shear zone S2m. Certain parts of this raft's lower contact contain metadolerite 'tails' which transgress bedding and wispy zones of altered iron rich mineralogy. These features, which apparently catalyse the folds in the lower contact, may represent structures developed during the metadolerite intrusion, indicating right way up rocks (Fig 3.20). Similar rafts are seen at (58) near the base of the metadolerite body. The margins of these rafts appear to concentrate an igneous flow fabric in the metadolerite and show gradational contacts with iron rich altered mineralogy at the margins. Veins containing this iron rich mineralogy emanate from the rafts. These features may suggest that fluids escaping from the sediment rafts have altered the host metadolerite metasomatically. The presence of these rafts near the base of the metadolerite sill suggests that the thrust west of (57) detaches and branches from the sill base to emplace it as a hangingwall flat onto a metadolerite footwall ramp.

North of (57) and (58) the main breaching thrust takes the form of two closely spaced (approximately 10m) imbricates which ramp downwards and upwards along strike in their hangingwalls into limestone and impure quartzites below the metadolerite sill. The higher imbricate is a more discrete shear zone than the lower one, with both zones containing a NNW-SSE stretching lineation, isoclinal fold closures and extensional crenulations indicating NW directed overshear. Small quartz veins are displaced parallel to the zones' platey S2m and confirm NW overshear. A small discrete forethrust-backthrust complex is developed between the two imbricates (Fig 3.21). West of (58) the platey S2m of the lower imbricate rejoins the base of the metadolerite.

The metadolerite forms a prominent rocky hill covered in scrub vegetation distinct from the surrounding grassy area. To the west a break of slope is coincident with a change from rocky scrubland to grassy pasture. It is considered that the breaching thrust is itself breached by a new thrust along the line of this break of slope at (59). The evidence for this breaching by a new thrust is as follows:

Northwest of (59) at (60), metadolerite is in thrust contact with limestone. In the hangingwall the limestones are overlain by 2-3m of interbanded silts, pelites and dolomites which are overlain by quartzites. In the footwall, highly deformed quartzite 'rafts' are contained within the uppermost parts of the metadolerite. Further NE at (61) the base of the metadolerite is exposed in the walls of a blow hole where transition beds similar to those in the thrust hangingwall are seen to directly underlie the sill. The stratigraphic sequence is therefore thrust repeated across the limestone-metadolerite thrust contact. The metadolerite contains S2 fabrics which become penetrative, intensify and become mylonitic (S2m) upwards over 10-15m towards the thrust contact. This S2m contains a strong NNW-SSE stretching

lineation and is axial planar to tight, isoclinal or rootless folds. In the hangingwall quartzites, the folds are open to tight with an intrafolial geometry and axial planar S2. The folds tighten and the S2 becomes S2m as the thrust is approached. The fold hinges are sub-parallel to the stretching lineation in the hangingwall and footwall, swinging towards greater parallelism closest to the thrust where the highest strains are developed. Reworking of the S2m fabric is also seen in the higher strain parts of the thrust, where S2m is folded by intrafolial F2 folds with axial planar S2m which crenulates the folded S2m, but is indistinguishable from and transitional with the S2m up and down the axial plane (Fig 3.22). The limestones at the western end of the exposure contain a complicated set of recumbent fold closures with curvilinear hinges which thicken the limestone at this position and may represent a highly deformed hangingwall anticline (Fig 3.22).

This thrust strikes NE-SW at the western end of the exposure at (60) and is clearly seen to be re-exposed on a series of small rocky islands to the SW. Moving eastwards, the strike of the thrust swings to E-W and ESE-WNW. This thrust must continue to swing strike into a NW-SE orientation since good exposure (80 to 90%) in the ground to the east and southeast contains quartzites and pelitic quartzites with a consistent N-S to NNE-SSW strike. These quartzites overly the metadolerite east of (60) and (61) and are therefore in the thrust footwall. The thrust cannot trace eastwards into these quartzites since there is insufficient room between the quartzite exposures to facilitate such a violent strike swing or to accommodate its thick (approximately 20m) high strain zone without being noticed. Field relationships therefore point towards a NW-SE strike swing in the thrust towards alignment with the break of slope around (59). This break of slope follows the bottom of a small valley to the southeast where limestone is in thrust contact with quartzites at (62). This thrust displays a

strain gradient in the hangingwall and footwall from bands of anastomosing shears to intense platy S2m near the limestone-quartzite contact. The footwall quartzites contain domino shears which 'leak' strain slip crenulations beyond the domino margins and indicate NW overshear. This thrust is considered to be the correlative of the thrust at (60). Between (60) and (62), this thrust carries a coherent hangingwall flat across a footwall which crosses from the footwall to the hangingwall of the lower breaching thrust and must therefore breach the lower thrust at (59).

The thrust can be clearly seen to swing strike to a NE-SW orientation and is easily traced NE along low cliffs to (56). Between (62) and (56), S2m is axial planar to small sheath closures and is deformed by extensional crenulations (both R-1 and R-2) indicating NW overshear. Further NE at (56), similar shear bands are associated with recumbent F2 folds and discrete shear zones in the limbs of these folds (Fig 3.23). A steep west vergent cleavage (S4 in the chronology of Hutton 1983) cross cuts these crenulations. This steep cleavage is, however, deformed and offset by shear bands which are closely related to the S2m and indicate NW overshear. This suggests that the steep cleavage was developed during the D2 thrust motion and is not representative of any subsequent deformation. Instead this cleavage, which is only locally developed, must be an expression of an unidentified but spatially and temporally local D2 kinematic process.

It has been suggested above that the thrust traced between (60), (62) and (56) breaches the lower breaching thrust at (59). This is confirmed at (56), where the lower breaching thrust, (bt1), is updomed into a gentle warp. Above this the platy S2m of the new breaching thrust (bt2) is planar so that (bt2) cuts across the updomed (bt1). Furthermore, the warp in (bt1) is related to the oblique ramp in its footwall at (57) described



above. The motion on (bt2) therefore not only breaches (bt1), but also post-dates the activity on the oblique ramp.

South of (56) at (63), another thrust is exposed above (bt2) emplacing grey and impure micaceous limestone onto cream and iron stained fine grained quartzites. This thrust contains intense S2m (which is axial planar to F2 folds) and low angle shear bands indicating NW overshear. This thrust, (bt3), gently ramps downwards to the NE through the footwall quartzites. The hangingwall limestone appears to maintain thickness to the NE to produce a hangingwall flat on a gentle lateral footwall ramp geometry. The limestones of (bt2) and (bt3) are of similar thickness and appear to converge (branch) near (64) so that (bt3) does not pass into the footwall of (bt2). Unfortunately sporadic exposure in the area of the branch prevents relative timing between (bt2) and (bt3) to be established using fabric criteria. Southwest of (64), however, (bt3) occupies a higher topographic position than (bt2) whilst maintaining a hangingwall flat on footwall flat geometry near and SW of (63). This may suggest that (bt3) is elevated by stacking (bt2) in it's footwall so that (bt2) follows (bt3) in piggy back sequence.

East and southeast of (64) towards (65), (bt3) can be seen to cut down from metadolerite into limestone to form a gentle frontal ramp in the footwall with a flat in the hangingwall. To the E and NE of (65), (bt3) appears to laterally cut up and then down section to (66). These are not true ramp features, however, since at (66) (bt3) breaches the imbricate which branches from (bt1) at (51). The apparent footwall topography is an artifact of (bt3) cutting straight across the oblique/trailing culmination wall of the imbricate in the footwall. The platy S2m of the breached imbricate swings towards parallelism with that of (bt3) but is poorly exposed in boggy ground here, preventing more detailed observations.

Further NE at (67), (bt3) is more accessible and better exposed in a small road cut. Here platy S2m is axial planar to small sheath fold closures and contains a strong NW-SE stretching lineation. S2m in the limestone hangingwall only appears to decrease intensity marginally upwards over 6-7m where the exposure ends, suggesting that high strains in the hangingwall are in excess of 15m thick. In the metadolerite footwall, however, strain decreases downwards from intense platy S2m to spaced bands of localised shearing to crystalline metadolerite in under 10m (see Fig 2.15). In the hangingwall, grey limestones become micaceous upwards to be overlain by intercalated grey pelites and thin iron stained quartzites of the transition beds. These underlie a metadolerite sill and appear to maintain a 2-3m thickness from (67) as far SW as (63) and beyond. These transition beds pinch out against the sill base near (67). The sill is overlain by cream and iron stained fine grained quartzites with less than 20% pelitic content. NE of (67) at (68) (bt3) reaches the coast apparently maintaining a hangingwall flat geometry. East of (68) the thrust rapidly ramps upwards in the hangingwall towards (69) to cut out the limestone. This must be a true ramp feature since limestone would be expected to be exposed above the sill to the south and east if the feature represented transgression of the sill through the stratigraphy.

Eastwards of (69) towards (70), the thrust ramps downwards in the hangingwall laterally and frontally back into platy limestones. In the footwall, interbedded silts, pelites and thin quartzites of the transition beds also thicken eastwards so that the thrust ramps upwards laterally to the east in the footwall (Fig 3.24). East of (70) a flat on flat geometry is maintained. In the footwall, pelites and thin quartzites overly metadolerite. The contact between these lithologies is deformed by open domes similar to those associated with sill intrusion at (26) south of Rincleven Point (compare Figs 3.7, 3.25). As suggested before,

these primary structures are interpreted to indicate right way up stratigraphy. This is confirmed approximately 8m above the contact, where graded bedding between silt and pelite occurs in 10cm beds indicating right way up stratigraphy. This graded bedding is approximately 8m below the thrust so that strain in the footwall rises from relatively undeformed sediments to intense platy S2m in approximately 5m as the thrust is approached. In the hangingwall, however, the limestones and the metadolerite above are intensely deformed for at least 10m upwards into the hangingwall, with well developed intense S2 and S2m fabrics. The limestone also contains intensely sheared and contorted metadolerite pods which may have originated as a small metadolerite sheet below the main sill. The hangingwall therefore displays a thicker strain profile than the footwall.

At (71) above the metadolerite sill, silver grey pelites pass rapidly upwards across a short exposure gap into intercalated grey and green pelites and cream and iron stained fine grained quartzites. The quartzites occupy 60 to 70% of the log sequence, rising to over 80% as individual quartzite beds increase in frequency and thickness relative to the pelites.

Returning SE to the branch point between (bt2) and (bt3) at (64), (bt3) is easily traced SW to (63). To the SW of (63), (bt3) is exposed in a cliff face and easily traced SW to (72) where the thrust and the thrust's hangingwall stratigraphy follow the topographic contours around the top of a small valley. The gently SE dipping grey limestones of the thrust are overlain by micaceous limestones which pass upwards into intercalations of pelite, silt and thin quartzite over some 4m. intercalations of pelite and quartzite replace these mixed lithologies upwards over the next 2m and the pelite content decreases so that quartzite makes up over 80% of the log sequence (Fig 3.26). S2 intensifies to swing into parallelism downwards through the micaceous and grey limestones

towards the thrust contact. Moving to the NW towards (73) at the bottom of the valley, progressively lower structural levels are exposed. The limestones' bedding and intense S2 fabrics swing strike towards a N-S orientation to dip gently to moderately to the west. The limestones contain intense S2 and S2m fabrics which are axial planar to tight to isoclinal recumbent minor F2 folds. Moving into the hangingwall, the transition beds and quartzites dip more steeply to the west and at one position near (73) quartzites contain cross bedding which indicates westward younging of the sediments. Here the beds are locally overturned to dip steeply east.

The gross structure between (72) and (73) is therefore that of a west vergent monoform, passing from the upper normal limb at (72) through the anticlinal hinge to the lower part of the mid limb around (73). The upper structural levels are mainly exposed in quartzite and S2 cleavage, in the absence of micas, is only weakly expressed. Moving towards the anticlinal hinge, however, thin beds and partings of pelite contain S2 which is clearly seen to be axial planar to neutral vergent minor folds related to the monoform. The monoform must therefore be of D2 age. The S2 increases intensity towards the mid limb where it is well developed in both quartzite and pelite. This must therefore represent a 'true' rather than apparent (lithologically controlled) intensification of S2 in the mid limb. Lower stratigraphic levels are exposed towards the lower part of the mid limb, where interbedded quartzites, silts and pelites (transition beds) dip moderately westwards, marking the approach of the return synclinal hinge of the monoform. Minor west vergent folds are well developed here, and contain a pervasive axial planar S2. The mid limbs of the minor folds are sheared out along discrete (10cm) thrust shear zones where S2 intensifies to become mylonitic. Small intrafolial folds, displaced markers (fine quartz veins) and the direction of bed thinning into the shear zones indicate

north-westerly directed thrusting. The lowest of these imbricates lies on pure quartzite, suggesting that part of the transition sequence is emplaced into the quartzites along this lower thrust (Fig 3.27).

A number of interesting features are displayed by the attitude and position of structures at this structural level of the monoform. Firstly, the minor folds verge westwards, and since the synclinal hinge has not yet been crossed, they are still within the mid limb and should, therefore, be neutral or easterly vergent. Secondly, bedding, the imbricate shears and fold axial planar cleavage dip westwards so that the folds and imbricate thrusts face downwards to the west. At the lowest structural levels where the limestone of (bt3) is exposed, bedding and the thrust S2m dip to the west. These features suggest that the major F2 monoform folds a major D2 ductile thrust and a small ductile imbricate stack in its hangingwall, during progressive D2 deformation (Fig 3.28). Also, as illustrated in Fig 3.28, the monoform is breached by further ductile imbricates, (described and discussed below).

Northwest of (73), (bt3) can be traced through exposures in private gardens and a break of slope west of that of (bt2) to coastal exposure at (74). Here limestone is in thrust contact with interbedded quartzites and pelites (quartzite in excess of 80% log sequence). These limestones are overlain by approximately 6m of intercalated limestone, dolomite, silt, pelite and thin quartzite. The limestones, dolomites and silts become less important upwards through this 6m so that quartzites and pelites become the dominant interbedded lithologies, with quartzites becoming increasingly important upwards to make up in excess of 90% of the log sequence (Fig 3.29). The limestones and footwall quartzites are intensely deformed and contain opposed vergence (E and W) minor F2 folds and minor F2 folds with curvilinear hinges

are well developed near the thrust contact suggesting sheath type closure geometries. Open folds are also developed here with upright axial planes (equating with F4 and F5 of Hutton 1983). These folds tighten upwards along curved (convex) axial planes which curve into the west or east vergent F2 folds. These folds have axial planar S2m or else they rework the S2 fabric in the more inclined portions of the axial plane and swing into parallelism with the S2 fabric up the axial planes (Fig 3.30). The above fabrics and folds are therefore part of a progressive D2 thrusting deformation. Higher up in the hangingwall, the quartzites are dominated by a complex of boudinage and large shear bands indicating NW overshear. The shear bands form shear zones in their own right and contain synthetic extensional crenulations which shallow listrically into the shear zones. Some of the shear bands appear to form composite structures with the boudinage, with folded shears across which cut offs can be seen. These features are sometimes spatially associated with SE vergent folds with a SE vergent axial planar cleavage rising listrically from the shears. These cleavages appear to be hybridised with extensional crenulations associated with the shear bands in certain positions, suggesting negligible time separation and therefore development during D2 thrusting (Fig 3.31). Bedding and the S2 fabrics dip gently southwards in the hangingwall but steepen towards the thrust. This appears to steepen (bend) the boudins above and may be responsible for the development of detaching SE vergent folds and fabrics. A similar process of SE vergent fabric and fold development related to D2 thrust hangingwall back-steepening is described from the Middle Town area later in this chapter.

At the western end of the exposure, (bt3) swings strike to a more southerly direction and is clearly in alignment with a series of linear rocky islands within the bay, so that (bt3) is easily traced SW to the cliffs at (75). Here (bt3) is folded by an easterly vergent monoform. Hutton (1977a) suggested with

reservations that the monoform might be of D3 age, principally on the basis of the structure's easterly vergence, however, F2 folds which verge in opposite directions have been described above (eg. Curragh Harbour). Furthermore the structural relationships presented at (75) are remarkably similar to those noted within the D2 monoform at (73):

The monoform, which for the most part is exposed in quartzite, is of similar dimension and geometry to that of (73) and contains a comparable intensification of the axial planar fabric into the mid limb. Also, two minor thrusts emplace part of the transition sequence into the quartzites and are then folded around the monoform. These thrusts are at a comparable structural and stratigraphic level to those at (73) and are considered to be laterally equivalent to the thrusts exposed at (73). Narrow (30-40cm) zones of high strain are concentrated at the thrust contacts, away from which strain rapidly decays. In the immediate thrust footwalls, the quartzite is finely laminated. This is not thin bedding however, since close inspection reveals occasional small (cm scale) intrafolial folds and sheath closures. At one position, a tight closure is apparently 'rootless', however, by carefully tracing banding on one limb for a metre or so along strike, a complimentary hinge is discovered. This confirms the tectonic origin of the fine laminations and bears testimony to the high strains involved.

Over most of the exposure, the axial planar cleavage at (75) is a strong biotite - muscovite - quartz fabric with no discernable microlithon structure. This strongly resembles S2 fabrics elsewhere in the study area. Indeed, Hutton (1977a) expressed difficulty in including this monoform in D3, despite its easterly vergence, (in view of the syn-metamorphic nature, and therefore close resemblance of the axial planar fabric to S2). In summary of these observations, Hutton (1977a) suggested that

the monoform and its axial planar cleavage might, therefore, represent a late D2 to pre-D3 structure, thereby implying short geological time separation between its D2 & D3 deformation phases.

The axial planar cleavage to this monoform is seen to be transitional downwards with the S2m of (bt3), demonstrating a D2 age for this structure. Similar to the D2 monoform noted at (73), therefore, the D2 monoform at (75) folds D2 thrusts during progressive D2 deformation (Fig 3.32).

In the mid limb, the monoform's axial planar cleavage crenulates the minor thrusts' high strain fabric. In both the upper normal limb and the mid limb of the monoform, the high strain (mylonite) zones of the minor thrusts are of comparable width (30-40cm). In the mid limb, however, the expression of the cleavage 'transition' zones (ie. mylonitic to background cleavage strength) outboard of the mylonitic strain zones are apparently narrower. These features might be best explained by: (A) intensification and transposition of minor thrust fabrics in the upper normal limb by the development of the axial planar cleavage, and (B) heightened crenulation of minor thrust fabrics in the mid limb by the axial planar cleavage so that the latter has a more visible expression at exposure level (Fig 3.32). (A and B being primarily a result of appropriate orientation of the minor thrust fabrics with respect to the newly developing fold axial planar cleavage).

A further similarity between the structures at (73) and (75) is that the monoform at (75) is breached by a further ductile thrust imbricate. This structure is parallel to the fold axial planar fabric (which intensifies into it) and is associated with shear bands indicating a northerly directed overshear. These shear bands also intensify the S2 axial planar fabric and are associated with more symmetrical boudinage of the cleavage in the



mid limb. This shear banding and boudinage is very similar in dimension and geometry to that deforming S2 and S2m fabrics at (74), (compare Figs 3.33 & 3.31). The boudinage at both (74) and (75) have similar orientations (mean boudin axes  $078^{\circ}$  and  $086^{\circ}$  respectively), with a sub-perpendicular extension lineation (mean  $161^{\circ}$  at both localities). This suggests that these structures are of the same (D2) generation and are likely to be related to the thrust breaching of both monofolds ((73) and (75)). The structure of these rocks is summarised in Fig 3.34.

Moving into the footwall of (bt3), west of (75), (bt2) is re-exposed at (76). This thrust is easily traced SW from (60) along the line of a series of rocky islands and long thin peninsulas orientated NE-SW. At (76) white and grey intensely platy limestones reduce in strain upwards over 12m and pass upwards into limestones containing thin (less than 1cm) partings of grey calcpelite. These calcpelite bands increase in frequency and thickness upwards over 2m to become 3-4cm thick and spaced 15-20cm. At this position in the sequence thin (cm scale) grey brown quartzite beds appear. These quartzites increase thickness (to 10cm) and frequency upwards over the next 2m of stratigraphy, as do the calcpelites, at the expense of limestone which steadily reduces in importance. Over the next 2m of the sequence, the quartzites rapidly increase thickness to some 20-30cm to become more persistent whilst the proportion of limestone decreases to disappear altogether. The calcpelite bands increase thickness between the more persistent and regularly spaced quartzites and thin pale silts and grey pelites appear in the sequence. As the calcpelites increase thickness, the pelites and silts increase in proportion up section so that a combination of calcpelites, pelites and silts appear to replace the limestones in the sequence. These calcpelites, pelites and silts reach similar frequency and thickness (5-10cm) upwards over the next 1m of section. Although occurring mostly as 'individual' beds, these

lithologies occasionally show diffuse boundaries with the top of quartzite beds in an upward fining relationship to indicate right way up stratigraphy. Upwards over the next 1-2m of section, the grey pelites increase in frequency to replace the calcpelites and silts in the sequence. The sequence therefore becomes one of interbedded grey pelites and grey cream quartzites. Also in this part of the log, the quartzites become more important, increasing thickness (to 30-40cm) as the pelites reduce thickness (to less than 5cm). This stratigraphic section is summarized in Fig 3.35).

The limestones of (bt2) are in thrust contact with pink micaceous quartzites and green grey pelites. The quartzites and limestones near to the thrust contain intense platy S2m which gives the lithologies closest to the contact a 'paperly' appearance. Strain decreases away from the thrust to 'background' S2 intensity in less than 5m in the footwall and approximately 8-10m in the hangingwall, where S2 is seen to verge gently NNW on bedding. The strain reduces up section via a series of highly strained horizons containing NW vergent intrafolial minor folds with axial planar S2. These folds become smaller, more frequent and isoclinal as the thrust is approached. Extensional crenulations (mostly R-1 with some R-2) are also present in these strained zones and indicate NW overshear. Quartzite beds are also occasionally disrupted into R-2 domino style boudins, with strain slip crenulations 'leaking' from the domino slip shears. These features also indicate NW directed overshear. Higher in the sequence, quartzite beds are symmetrically boudinaged. Both the domino boudinage and the symmetrical boudinage intensifies S2 fabrics and in a few places veins associated with both styles of boudinage can be seen to link as a continuum. These features imply a common D2 age for both boudin types as suggested at (74) and (75). These features also indicate non plane strain, as suggested at (45), (Figs 2.17 & 3.13).

Moving west from (76) into the footwall of (bt2), sheer cliffs prevent direct observation of the rocks until accessible exposure is regained in the small cove around (77). Here limestones containing platy S2m lose strain upwards to the SE and pass up into pelites, silts and cream grey and iron stained quartzites. The platy limestones are in thrust contact with grey and phyllitic pelites containing thin beds of pale iron stained quartzite and grey silty pelite. The quartzitic and silty bands are lost downwards into the footwall to be replaced by a relatively thick (in excess of 18m) sequence of finely bedded grey phyllitic pelites. This thrust is lost to the west in non exposure, however, the strike of bedding and S2m suggests that the thrust intercepts (bt2) near (78). The exact relationship between (bt2) and this thrust remains hidden in the non-exposure. The trace of (bt2) can be easily followed SW for several hundred metres from a roadside exposure above (78), using the break of slope and vegetation change it creates. These features peter out towards Sandhill where the further course of the thrust is tentatively mapped using sub-crop material surrounding newly cut drainage ditches.

Moving inland to the SW, (bt3) can be traced towards (79). Here bedding in the hangingwall of (bt3) strikes NE and dips gently SE. Strain increases upwards so that the hangingwall quartzites contain platy S2m with extensional crenulations and larger scale shear bands indicating NW directed overshear. Immediately above these exposures, platy limestones indicate the presence of a further thrust contact. This thrust has a more E-W strike and is seen to ramp upwards across the quartzites in the footwall to the east. The thrust is also seen to cross into the footwall of (bt3) to the west and therefore breaches (bt3) around (79). This thrust, (bt4), also runs straight across the western and eastern contacts between quartzites and the metadolerite body exposed between the monofoms of (73) and (75). This creates

apparent footwall ramps cutting up section eastwards to (80) and down section towards (72). It is clear, however, that these geometrical features are a consequence of (bt4) breaching (bt3) and the monoform structures on either side of the metadolerite (Fig 3.34). Shear bands indicating NW directed overshear in the quartzites and strong S2 fabrics in the metadolerite are associated with (bt4).

### 3.4 The Middle Town Stack and Sandhill Imbricates

East of (72) at (81), the grey limestones and micaceous limestones of (bt4) become silty and interbedded with dolomitic limestones upwards over 1-2m. These buff dolomitic and silty beds pass upwards abruptly into grey and white quartzites containing thin pelite interbeds. The lower 1m of these quartzites contain banded shear strains manifested as discrete shears which deform strong S2 and anastomose when viewed down the NNW-SSE stretching lineation. Also in these quartzites, and exclusive to the lower 1m, are occasional fragments of limestone which measure up to 5cm x 0.5cm. These do not represent tectonically disturbed thin limestones since they occur in beds containing relatively low strains between the bands of high shear strain. These fragments may represent rip-up clasts derived from the limestones below. The quartzites here contain good examples of cross bedding (indicating right way up stratigraphy) which, in conjunction with the limestone fragments, may suggest a sudden deposition of quartzites into the relatively quiescent 'limestone environment' and a resultant slightly erosive base to the quartzites not noted elsewhere.

The strains associated with (bt4) become more localised eastwards from (72) where (bt4) can be seen to branch into a number of more discrete ductile imbricates just east of (81). These imbricates appear to form an antiformal stack, the higher

imbricates achieving successively greater dips. The magnitude and direction of these dips also appears to conform well with position in the stack and the geometry of individual imbricates (Fig 3.36).

At (82), the hangingwall of the lowest of the imbricates is composed of very platy grey crystalline limestones which overly grey-cream fine grained quartzites in thrust (flat on flat) contact. The hangingwall limestone, although of generally high strain, contains 'banded' shear strains, where the relatively higher strain zones are host to reworked quartz vein material. Shear bands and asymmetrical pull-aparts (domino hard band rotations) of some hangingwall quartzite beds indicate NW directed overthrusting. The limestones pass upwards into micaceous limestones, micaceous and silty limestones, intercalations of quartzite with 'mixed' silty lithologies and finally micaceous quartzites. This transition sequence is 2-3m thick and is lost in under 25m along strike to the east and the west where it is cut-out against the next higher thrust. This thrust at this position therefore contains two lateral footwall ramps which dip away from each other. One of these ramps can be clearly seen in a small cliff where a (m) scale footwall syncline (with axial planar S2) overturns beds to the west. Beds in the overturned mid limb can be seen to terminate within the thrust high strain zone.

The hangingwall of the thrust does not appear to contain any transition beds, instead the limestones and the quartzites are separated by a small (approx. 4m thick) metadolerite sheet. This metadolerite, like the quartzite above it is relatively undeformed, with strains increasing towards the base of the limestone where platy S2m is the only discernable banding. In the hangingwall, the thrust ramps gently up stratigraphic section towards the east, but ramps upwards rapidly towards the west where the metadolerite is thrust onto quartzites.

A number of hangingwall strains are associated with the position of this western ramp/culmination wall, expressed as local fabric development and vein opening: In the higher strain parts of the limestone, nearer to the thrust, shear bands and a strain slip fabric are present and are extensional to the SW (Fig 3.36). Similar, but more intense south-westerly extending shear bands are developed further west in the micaceous mylonitic limestones of (bt4) at (81). These shear bands are deformed by R-1 extensional crenulations of D2 age which record NNW directed overshear and indicate that the southwesterly extending shear bands were developed during D2 thrust motion. The shear band and strain slip fabrics can be correlated with a steeper cleavage higher in the stack. This cleavage has tighter asymptotic curves in the microlithon geometries (similar to R-2 shear bands described above) and would be interpreted as S4 or S5 on the basis of superficial appearance and orientation, but it is clear that this cleavage is of D2 age.

Summarised in Fig 3.37, these fabrics collectively represent a broad shear zone with a crude listric geometry which is interpreted as extension in the western culmination wall of the stack in response to differential uplift created by imbricate accretion. In the lower strain areas of the hangingwalls, planar steeply dipping quartz veins are present in swarms (sub-perpendicular to bedding) which record bedding parallel extension around the 'outer arc' of individual culminations and the outer arc of the stack. These veins are restricted to the area of the thrust stack and many extend in a similar direction to the shear bands in the western culmination wall. The above features are therefore interpreted as structures analogous to hangingwall drop faults seen in foreland thrust belts and similar to culmination wall extension described from these higher crustal level belts (Fig 3.37, Butler 1982c, Coward & Smallwood 1984).

At (83), the penultimate thrust in the stack (below (bt4)) emplaces grey massive limestones onto quartzites. The strain increases towards the thrust contact in both the hangingwall and the footwall, with 3-4m platy S2m and intense S2 in the limestones and 1-2m of these fabrics in the quartzites. The footwall quartzites contain swarms of steep planar veins consistent with culmination extension. Some of these veins cut the thrust S2m indicating that the thrust had ceased movement at the time of vein generation and further suggesting that the veins are developed in response to culmination development during accretion of the thrust below in piggy back sequence. The hangingwall limestones also contain veins, however these are in the form of a network of irregular shapes which in places give the limestones a 'chicken-wire' textural appearance.

Moving up through the hangingwall, the limestones become buff coloured, dolomitic and more thinly bedded. In a roadside quarry approximately 5m of 'mixed' lithologies represent the transition beds between the limestones and quartzites (both of which are exposed here). Buff crystalline dolomitic limestones interbed with thin layers of very iron rich silt which readily disintegrates when touched. Occasional thin beds of pale silty limestone are seen in the sequence and green-grey pelite beds appear. The limestones gradually disappear upwards over 3m as iron content increases and the green pelites become more important in the sequence. The limestones are replaced by thin grey-brown or 'rusty' quartzites which increase in frequency and thickness and become paler (purer) upwards over 2m as the silty beds disappear and iron content diminishes (see Fig 3.38).

Bedding in the thrust sheet has steepened markedly from the thrust contact so that the roadside quarry is positioned somewhere towards the rear of the imbricate stack. There is also a weak cleavage in these rocks which dips and verges towards the SW (see

Fig 3.36). This fabric shallows and intensifies downwards and eastwards towards the thrust where it can be correlated with a cleavage near (84) which is axial planar to a S & SW closing synform. The limestones here are closer to the thrust and therefore contain relatively high strains. An isoclinal minor fold with intense axial planar S2 is folded around the synform and the S2 crenulated by the synform's axial planar cleavage. This cleavage and syncline would be interpreted as S3 & F3 in the deformation chronology of Hutton (1983) on the basis of cleavage appearance, the southerly vergence and fold morphology. There is, however, a clear association between the cleavage and the antiformal stack.

The cleavage loses strength upwards to (85) and downwards from (84) and also along strike, so that the cleavage is seen to form a 'belt' which follows and is restricted to the steep rear of the stack. This strongly suggests a causal relationship between the growth and back steepening of the stack and the development of the cleavage and associated fold, making the fold and fabric D2 structures (see Fig 3.39). Further, this also implies that the thickening and back steepening of the antiformal stack is not entirely accomplished by imbricate accretion, there being at least some ductile strain involved.

Moving upwards to the SW to (85) across (bt4), the highest imbricate in the stack, bedding steepens further to become near vertical before shallowing again to form a broad syncline which demarks the rear of the stack. The cleavage which is axial planar to the syncline at (84) weakens and steepens to dip and face downwards towards the SW in the roadside quarry. The cleavage steepens further with bedding as (bt4) is crossed, before shallowing with bedding to face upwards to the NW at (85). This cleavage is therefore deformed by the broad syncline and can be seen to be crenulated by a relatively upright fabric which is



axial planar to the syncline. This upright cleavage would be interpreted as S4 in the chronology of Hutton (1983) on the basis of the fabric's appearance, upright nature and westerly vergence. As with the cleavage it crenulates, however, the upright fabric can be seen to form a 'belt' which follows and is restricted to the steep rear of the stack. The fabric weakens and disappears rapidly upwards and downwards from the immediate hangingwall of (bt4) and along strike. Again, the inference is a causal relationship between the growth and back steepening of the stack and the development of the cleavage, so that the fold and fabric are locally generated D2 structures (see Fig 3.39). The warping of the earlier cleavage and development of a second upright fabric may be the result of hinge tightening at the rear of the stack and onset of a more flexural shear dominated folding process.

It is clear that east of (81) (bt4) branches into a number of imbricates which form a piggy back sequence antiformal stack. The lower imbricates breach a thrust (likely to have originally been part of bt4), at (86) & (87). Bedding in the hangingwall to this breached thrust contains right way up stratigraphy (cross bedding) which dips inwards to form a 'basin' or 'spoon' geometry. Bedding strikes at near right angles to the lower imbricates of the stack and is seen very close to the map trace of the imbricates. This suggests that the spoon geometry was, at least in part, developed prior to breaching by the lower imbricates of the stack.

Some of the imbricates appear to branch onto the base of a metadolerite sheet towards the east around (88), whilst the highest imbricate, (the map trace of bt4), appears to localise onto the top of the metadolerite. From (85), (bt4) ramps up section along strike in the hangingwall towards (88), then down into transition beds (not seen around (81) or (85)), and back up into quartzites to the NE of (88). The presence of all the imbricates is lost approximately 200m to the NE of (88) in a zone

of diminishing S2 & S2m strength and complex of multiple fabric development and large (m) scale shear bands which indicate NW directed overshear.

Where the imbricates have branched onto the base of the metadolerite, S2 & S2m forms intensity 'bands' similar to those described around Lishagh and (67) (see Fig 2.15). These bands become less well defined to the NE as overall S2 & S2m intensity diminishes and the S2 fabrics become deformed by C-shears and extensional crenulations which indicate NW directed overshear. Also in this area, a number of discrete minor thrusts with south-westerly dipping lateral ramps are clearly visible, onto which S2 rapidly intensifies (in less than 10cm) to become S2m. These discrete features contain ramp-flat geometries, a hangingwall short cut complex (Knipe 1985) and deformed asperity fragments are contained within the narrow but intense thrust mylonites (Fig 3.40). This is analogous to terminations of shear zones described by Simpson (1983) to have developed under greenschist conditions in granodiorites. In the case of the granodiorite shear zones, as the shear zone tips are approached, the C-planes of SC mylonites occur with less and less frequency and the S-planes diminish intensity and disappear so that the tips are "...essentially brittle fractures" (Simpson 1983).

Above and including part of the metadolerite, two large (m) scale shear bands are developed which extend towards the NW. These shear bands appear to be responsible for the development of a number of local fabrics. Extensional crenulations are developed near the rear of the structures and a contractional fabric in the frontal part of one. On the flanks of the shear bands, strain slip cleavages with a strike slip sense of shear are developed (see Fig 3.41). These fabrics and overall bedding disposition define the margins of the structures which have an extensional 'tongue' geometry.

These structures and the imbricate stack are believed to represent the tip line of (bt4).

Re-tracing (bt4) westwards to (79) where (bt4) breaches (bt3), we arrive at a position west of (79) where the hangingwall of (bt2) lies in the footwall of (bt4). Here (bt4) emplaces platey grey limestones onto quartzites. The platey S2m of the limestones dips at  $30^{\circ}$  to the SE and contains common R-1 extensional crenulations indicating NW directed overshear. The limestones rapidly pass upwards into micaceous limestones which in turn pass up into dark grey pelites containing occasional quartzite beds which become dominant upwards to make up over 80% of the log sequence. The transition between micaceous limestones and quartzites is approximately 5m thick. Bedding in the quartzites dips  $30^{\circ}$  to the SE in a very similar way to the platey S2m in the limestones near to the thrust. This suggests that at this position the hangingwall of (bt4) has a flat geometry. At (89) the limestones thin out towards the SW and are emplaced onto a metadolerite sheet containing intense S2m. This suggests a lateral ramp in both the hangingwall and footwall of (bt4) at this position.

Following the trace of (bt4) further towards the west, transition beds are in thrust contact with quartzites and at (90), thin interbeds of pelite, calc pelite, silt, calc silt and quartzite contain a NE verging fold with a thrust mid limb and discrete subsidiary shears (this exposure is described in detail in chapter four and illustrated in Fig 4.2). This structure appears to ramp material towards the NE, but contains a NW-SE stretching lineation and must therefore represent an oblique ramp in the hangingwall of (bt4) which failed to reach maturity and incorporation into the profile of (bt4).

Moving further west to (91), (bt4) emplaces transition beds

similar to those of (90) onto the metadolerite body described at (89). For some 250m between (90) and (91), the quartzite appears to maintain thickness in the footwall of (bt4) and assuming the metadolerite sheet to be bedding parallel, (bt4) must have a flat on flat geometry between (90) and (91).

To the W and NW of (91), (bt4) ramps downwards in it's hangingwall to include platey grey limestones containing occasional thin beds of silt, well exposed at (92). Here, a series of folds with axial planar S2m are exposed in a small cliff (some 4m high). The lower two thirds of the cliff is dominated by relatively flat lying intense S2m which contains many minor (15-20cm scale) recumbent rootless folds (illustrated in Fig 2.18a) and streaked-out S2m parallel vein material. Strain decreases marginally upwards towards the upper third of the cliff, which contains a (m) scale fold pair. This folds S2m, but has an axial planar cleavage which is indistinguishable from the S2m in surrounding rocks away from the fold pair. A series of veins within the fold pair are parallel to the axial planar cleavage. The limestones are overlain by metadolerite.

Platey limestone debris in a N-S drainage ditch near to (92) indicates an outcrop width of 80-100m for the limestones in this area. Breaks of slope and vegetation changes indicate that the hangingwall of (bt4) ramps upwards into transition beds at a point nearly equi-distant between (91) and (92).

The exposures in the area around (92) are scattered and sporadic, however, to the south of (92), the metadolerite above the limestones climbs section towards the NW and SE into transition beds and is cut out against a higher thrust which emplaces limestones onto the metadolerite and thrust duplicates the hangingwall stratigraphy of (bt4). This thrust also ramps

upwards in its hangingwall into transition beds towards (93) in the NW and (94) in the SE to form a 'pip' of limestone with lateral culmination walls. To the east of (94), the thrust emplaces transition beds onto transition beds in an apparently flat on flat relationship, the thrust being marked as a zone of intensified strain (S2m) within the transition beds' outcrop. At the east of (95), the thrust ramps upwards into quartzites in both hangingwall and footwall and is apparently lost within a zone of boudinage, large and small scale R-1 & R-2 shear banding and vein swarms around (96) where S2m rapidly loses intensity. This is believed to represent a tip region of the thrust.

The outcrop of the thrust (which lies structurally above bt4), appears to follow the outcrop of (bt4), suggesting that (bt4) is the later of the two thrusts to develop (in local piggy back sequence). Other structural observations at (91) and (97) to the south would seem to agree with this development sequence.

At (97), a sequence of silts, pelites, calc pelites and occasional thin quartzites are exposed in a broad cliff some 6m high. In the central part of this cliff the beds are folded by an easterly verging fold pair. At first glance the fold appears to be paradoxically associated with a westerly vergent S2 cleavage. On close inspection, however, the exposure is seen to contain two cleavages, the later of which is weaker, axial planar to the fold and dips towards the SW. The earlier westerly verging cleavage is rotated into parallelism with the fold axial plane, but the original westerly vergence is preserved at some bed margins where the later cleavage crenulates the earlier (Fig 3.42).

Also within the exposure are a number of extensional features which disrupt some of the thicker silt beds or quartzites. These features have geometries very similar to structures generated by lystric extensional basin faults. Discrete high angle fractures

in the beds shallow downwards to detach within pelite beds beneath, where bedding subparallel C shears take up the displacement and deform the early westerly verging S2 cleavage (Fig 3.43). In a similar way to the layer parallel extensional features (veining) within the Middle Town Stack, the extensional structures at this locality are interpreted as an expression of culmination extension developed during D2 thrusting.

The C shears associated with the culmination extension structures at (97) are seen to be folded by the easterly verging fold pair and to have been crenulated by the axial planar cleavage. Furthermore, in some parts of the exposure, these features have become re-closed or 'inverted' (Fig 3.43).

This is spatially associated with development of the NE vergent fold axial planar cleavage and easterly vergent minor fold trains in the normal limbs of the major fold pair. Where the structures are inverted, the weaker NE verging cleavage crenulates S2 and the C shears and is axial planar to tightened rollover geometries (Fig 3.43). This inversion therefore reflects a return to contractional deformation and is temporally associated with the development of the major fold pair and axial planar cleavage.

Passing down structural level northwards between (97) and (91), the NE verging cleavage becomes stronger and S2 intensifies to become platey S2m. This locates the thrust above (bt4). Further north, S2m decreases intensity briefly before increasing intensity once more as (bt4) is approached at (91). The NE verging cleavage, however, steadily increases intensity from (97) to (91) where it shallows towards parallelism with S2m, the two cleavages becoming indistinguishable, except where S2m is folded or rare extensional 'rollover' features are inverted. A small west vergent fold with axial planar S2 is preserved in a pod within the composite mylonitic cleavage (Fig 3.44).

Occasional bands appear to contain S2 which has become steepened to dip more steeply towards the west or even overturned by the re-working. This is associated with a banding parallel mylonitic fabric and must therefore represent layer parallel shearing related to the NE and E verging structures further south (Fig 3.44).

The NE and E verging structures described above would be F3 and S3 in the chronology of Hutton (1983), however, they are clearly related to movement of (bt4) rather than a separate post D2 deformation. The structures are restricted to the hangingwall of (bt4) and clearly intensify towards (bt4). This suggests a direct relationship between the structures and (bt4) and indicates that the thrust above (bt4) had become inactive before movement on (bt4). The cleavage appears to form a hybrid fabric with and to partially rework the S2m of (bt4) with an apparent shear towards the NE. As described above and in chapter four, a NE verging F2 fold with a thrust mid limb is exposed further east at (90). NE or E verging structures are not found to the east of this thrust fold.

It is considered that the structures described above and the thrust fold represent the aborted propagation of an oblique ramp into the hangingwall (bt4). Also, the hangingwall of (bt4) contains structures from the thrust's early history, (as part of bt3?), and it is therefore to be expected that these early structures may be at least partially reworked during the breaching movement of (bt4) and the attempted propagation of a ramp into the hangingwall of (bt4).

### 3.5 Summary

As described above, the Breaghy Head peninsula contains a number of D2 ductile thrust imbricates, developed under

greenschist metamorphic conditions. These thrusts have geometries very similar to those in foreland thrust and fold belts, with long stratigraphy parallel flats and shorter ramp segments. With only a few exceptions, the thrusts overshear towards the NW.

The thrusts duplicate a relatively simple limestone, quartzite-transition, quartzite stratigraphy, such that the various elements of the standard Sessiagh-Clonmass succession in the area, (Fig 2.1), are thrust duplications of the same stratigraphic package. The Clonmass & Marble Hill Limestones are therefore the same limestone and the Clonmass and Sessiagh Quartzites are the same quartzite. It seems reasonable, therefore, to suggest that the stratigraphy in the area be unified under a common label. Since "Sessiagh-Clonmass Formation" is now entrenched within the literature (Pitcher & Shackleton 1966, Pitcher & Berger 1972, Harris & Pitcher 1975, Hutton 1983), it would be sensible to term the limestone, quartzite-transition and quartzite as "Clonmass Limestone", "Sessiagh-Clonmass Transition Beds" and "Sessiagh Quartzite" respectively. This will hopefully dispense with spurious nomenclature and avoid confusion.

### **3.5.1 Sessiagh-Clonmass Formation Depositional Environment**

As described above, the Sessiagh Clonmass sequence in the Breaghy Head area consists of a laterally persistent limestone and quartzite between which transition beds are laterally changeable in both thickness and lithological make up. The transition beds do, however, characteristically become more detrital and less calcareous upwards in a smooth transition from limestones to quartzites, with the exception of locality (81) where quartzites rapidly replace limestones and appear to contain small limestone rip-up clasts (suggesting a more erosive transition by comparison with the depositional transition noted elsewhere).



A number of features within the calcareous part of the sequence suggest a low energy shallow water depositional environment. The limestones at locality (12) on the shores of Sessiagh Lough contain delicate worm tracks/burrows which are bundles of bedding parallel cylindrical spines. Although these structures are not reliable evidence of shallow water, they may indicate a low energy environment since they are quite unlike 'bio-escape' structures which are indicative of higher energy conditions. Collaborative evidence for quiet shallow water comes from stromatolitic (algal mat) structures described by Bliss et al (1978) in Sessiagh Clonmass limestones near Maas further to the west in Donegal. Dolomitic limestones at Ballymore, several kilometres south of the study area, contain polygonal desiccation cracks, described in detail by Bliss et al (1978). This suggests that the Sessiagh Clonmass sediments may have been subject to occasional sub-aerial exposure. Indeed, White & Hutton (1985) describe the presence of 'cargneules' within rocks higher in the stratigraphic column further east on West Fanad. These are brecciated and heavily calcite-dolomite veined dolomites derived from dehydrated and metamorphosed evaporite/dolomite interbeds. There are a few locations in the study area (eg. 100m NE of (7) and near the northern shore of Sessiagh Lough), where saccharoidal dolomites are heavily veined by calcite-dolomite veins. These veins have highly random and sinuous geometries, may make up as much as 60% of the rock volume, are clearly not tectonic in origin and may therefore represent 'cargneules'.

The transition beds occasionally contain upwardly fining graded bedding and the quartzites only occasionally contain small cross beds or ripples. The vast majority of these rocks are planar bedded, with thin intercalations of the various lithologies, (especially within the transition beds and lower quartzite section), again suggesting low energy deposition.

It would appear, therefore, that the Sessiagh Clonmass rocks of the study area may have been deposited in a lagoonal to lacustrine or estuarine environment; a similar setting to that suggested by McCall (1954).

### 3.5.2 Sessiagh-Clonmass Limestone and Quartzite Thickness

An un-tectonised contact between the base of the Sessiagh Clonmass formation and the underlying Ards Quartzite has not been discovered within the study area. A directly observed estimate of the maximum thickness of the Clonmass Limestones is therefore not possible. As described above, however, and argued in chapter 5, the Breaghy Head imbricates appear to detach from the Ards Quartzite - Sessiagh Clonmass formation boundary. The thickest limestone development is seen to be within the hangingwalls to the highest and apparently furthest travelled thrusts. Assuming, therefore, that these thrusts bring limestones from detachment level to surface exposure, maximum limestone thickness is estimated from localities with poorest transition sequence development to be between 45m (S of Marble Hill) and 60m (Sessiagh Lough).

Diachrony between areas of depositional transition and local non-deposition to erosive low angle unconformities at the basal part of the quartzite section suggests that whilst the quartzites should be lithologically constant, they may vary in thickness at the expense of the transition beds. This certainly appears to be the case within the higher thrust sheets between Knockduff, Dunrudian and Sessiagh Lough. The maximum observed thickness of the Sessiagh Quartzites is therefore estimated (at localities where the transition beds are only poorly developed), to be between 90m (SW of Dunrudian) and 100m (S of Marble Hill). Unless it is assumed that the top of the quartzites represents an upper detachment (roof thrust) to the Breaghy Head imbricates,

however, these figures must be regarded as under-estimates.

### 3.5.3 Structure

The majority of the thrusts on the peninsula are breaching thrusts arising from a common detachment within the Clonmass limestones. These thrusts originate from the hangingwall of the previous structure and are therefore in break-back sequence, (as defined by Butler 1987). The thrusts are, however, locally in piggy-back sequence (eg. Middle Town Stack), such that:

The first clearly identifiable breaching thrust, (bt1), breaches structures south of Curragh Harbour, (bt1) is then breached by (bt2) in break-back sequence, whilst (bt2) post dates (bt3) in piggy-back sequence. Thrust (bt3), however, is breached by (bt4) in break-back sequence. The two imbricates north of Knockduff and Dunrudian are in break-back sequence, but their timing with respect to thrusts in their collective footwall and hangingwall is possibly piggy-back, since their outcrops follow these thrusts for considerable distance.

It has also been shown in this chapter that fabrics and folds in the area, previously categorised chronologically into D2, D3, D4 and D5 (Hutton 1977a, 1982, 1983), are contained within D2 and that local polyphase fold and fabric histories can be related to local kinematic inhomogeneities created during continuum D2 thrusting (eg. antiformal stacking, backthrusting, culmination extension, buttressing).

The propagation of D2 ductile thrusts, the generation of syn-kinematic contractional and extensional structural patterns in the study area and the generation of shaped ductile thrust profiles are discussed in chapters 4 & 5.



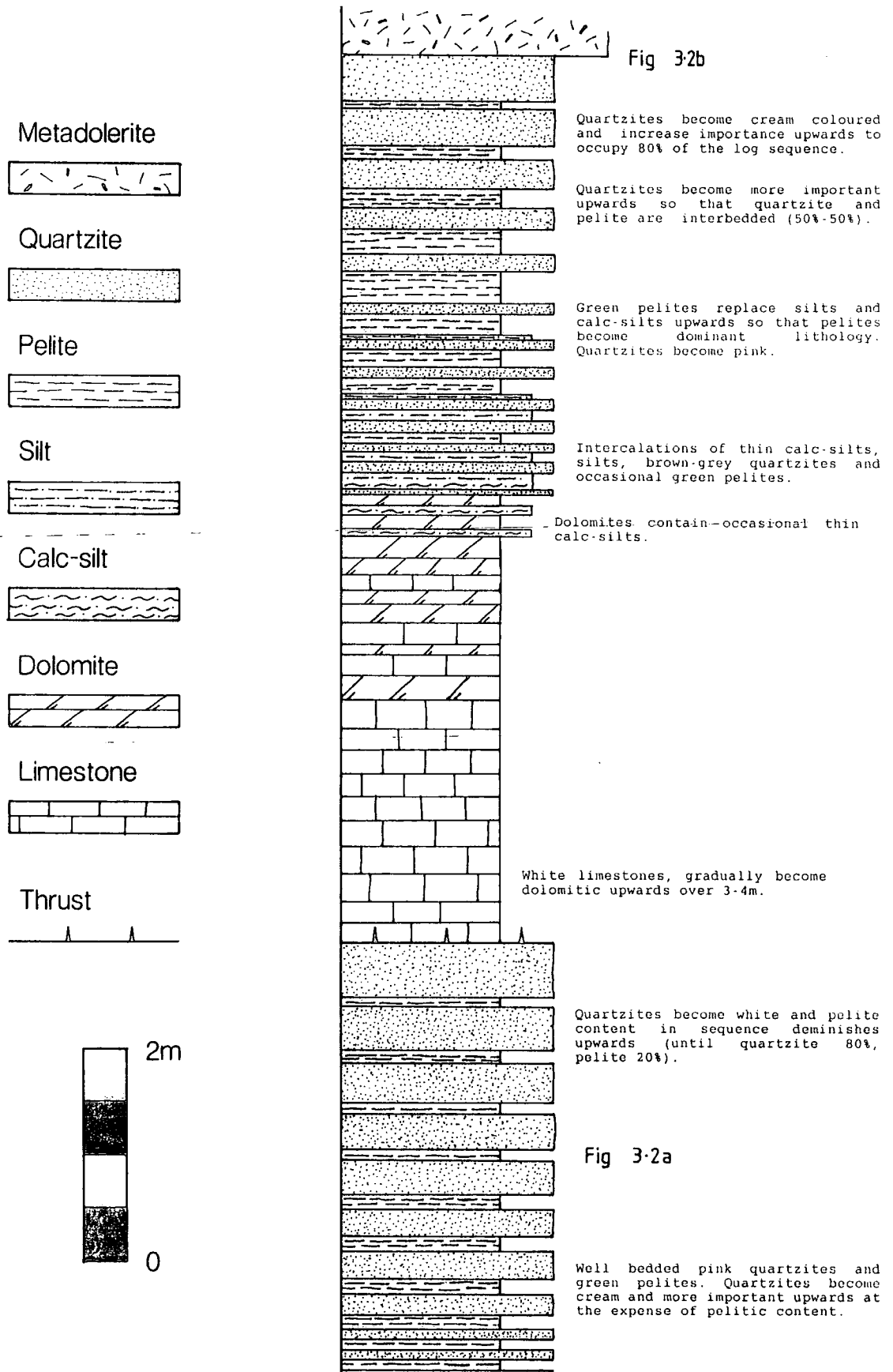


Figure 3.1 Summary lithological log of sediments exposed at 765205, (locality 1, maps 1 & 2). Location of figs 3.2 a & b are indicated (see text for details).

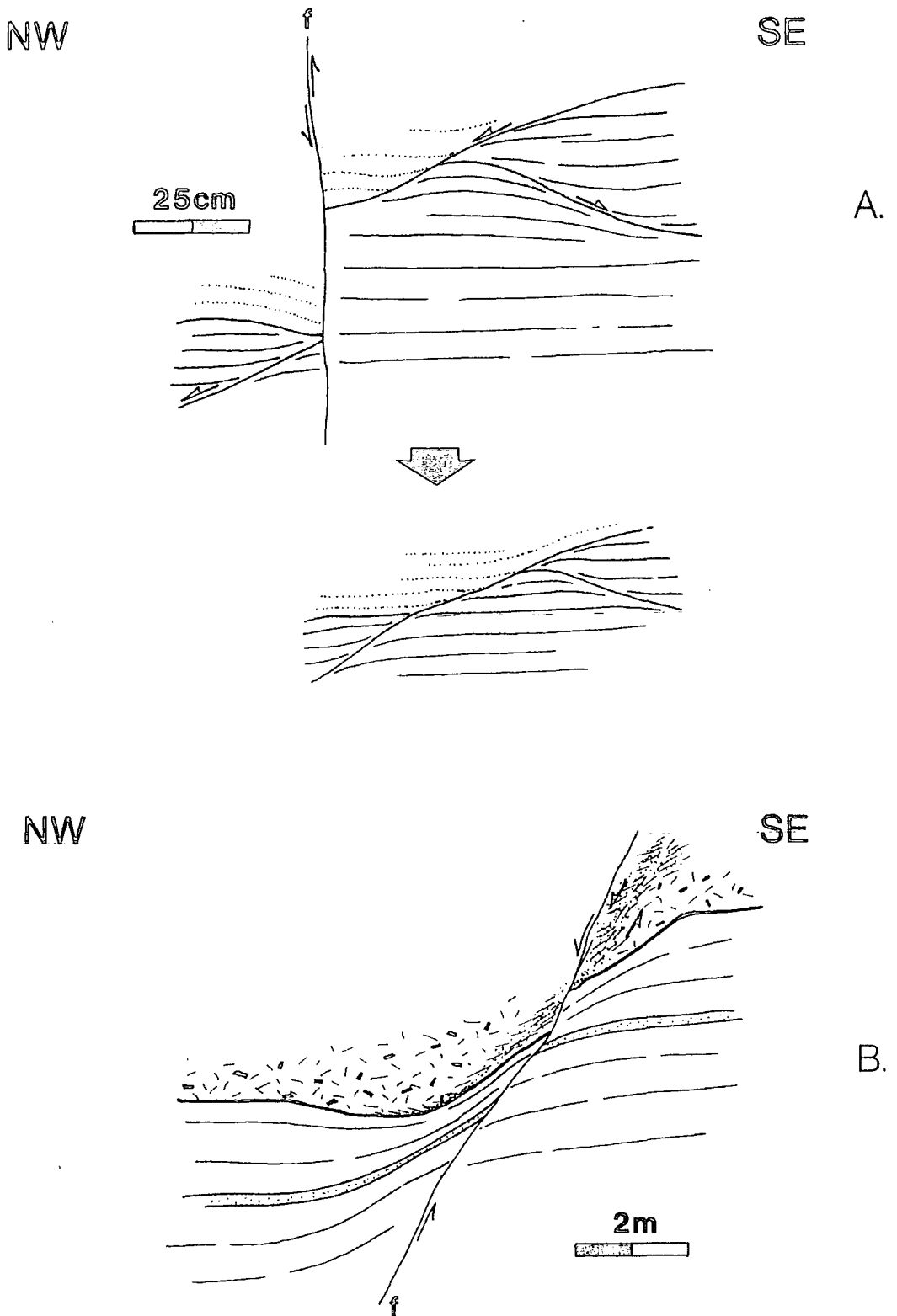
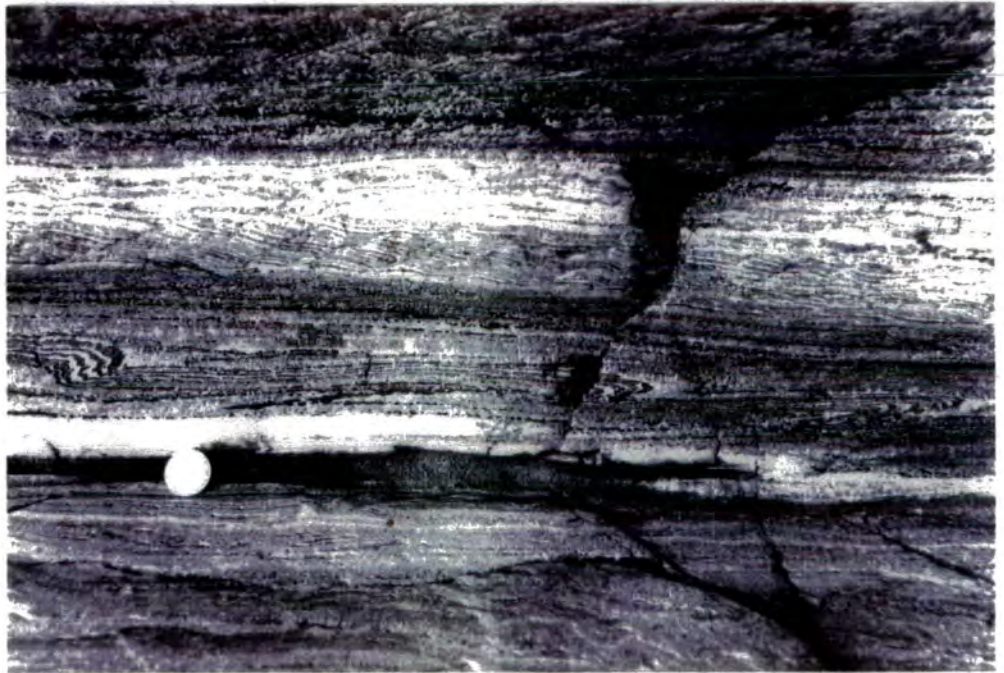


Figure 3.2 Simplified field sketches of shear bands in quartzites and 'domino' offset of the base of the Knockduff metadolerite at locality 1, map1. (A) Shear bands indicating NW directed overshoot which cross the boundary between pelitic quartzites and purer white quartzites (see fig 3.1). Note the apparent ramp-flat geometry of the NW extending shear band. (B) Domino offset of the base of the metadolerite indicating NW directed overshoot. This offset takes place across a fairly discrete shear zone in the metadolerite which can be seen to shallow into the base of the metadolerite. This offset deflects and locally thins the country rock bedding and is the catalyst for a late normal fault.



**Figure 3.3** Deformation in limestones at locality (2), map 1. (A) Photograph, looking south, of highly curvilinear and sheath fold closures. (B) Photograph of extensional domino rotations (at middle bottom of photograph), indicating NW directed overshear (NW to right of photograph). NW verging fold trains are visible in centre of photograph.

A

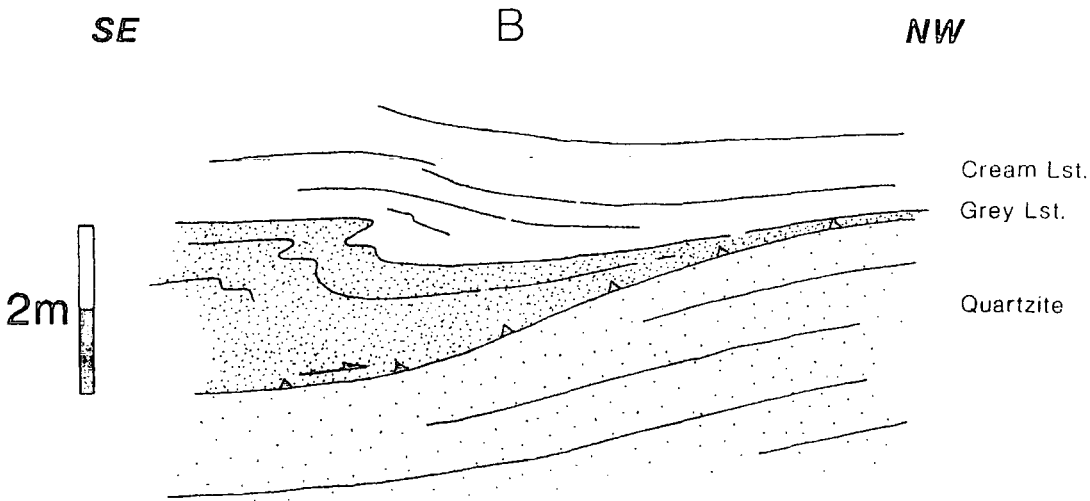
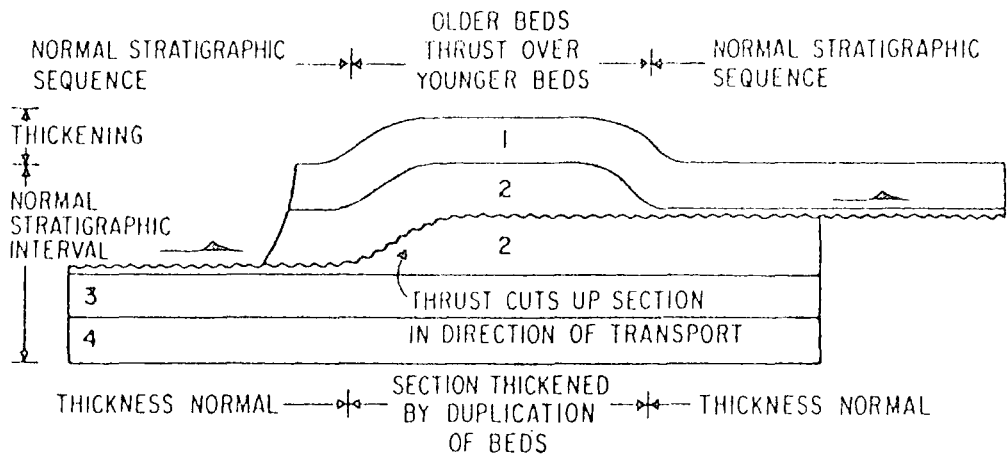
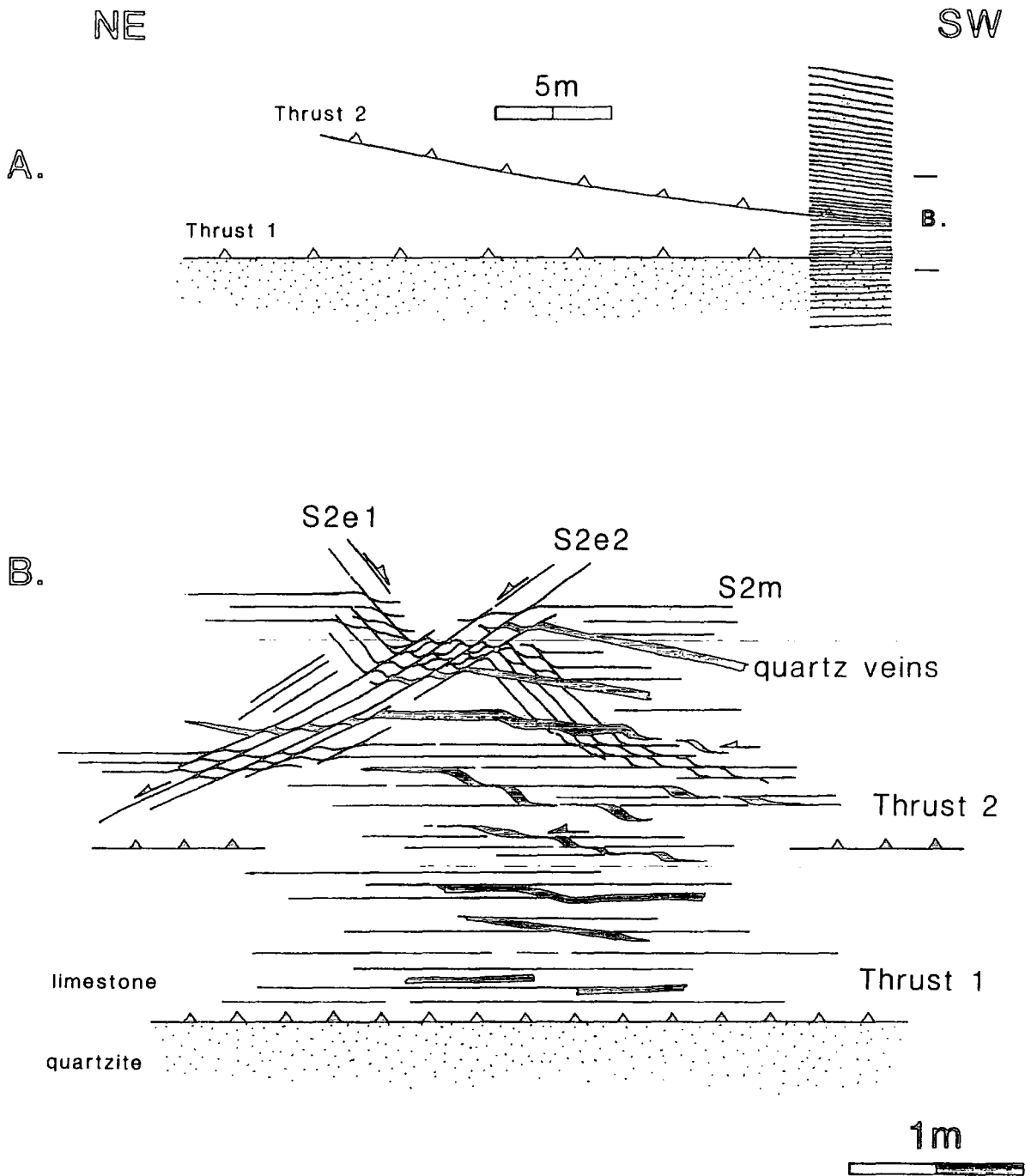


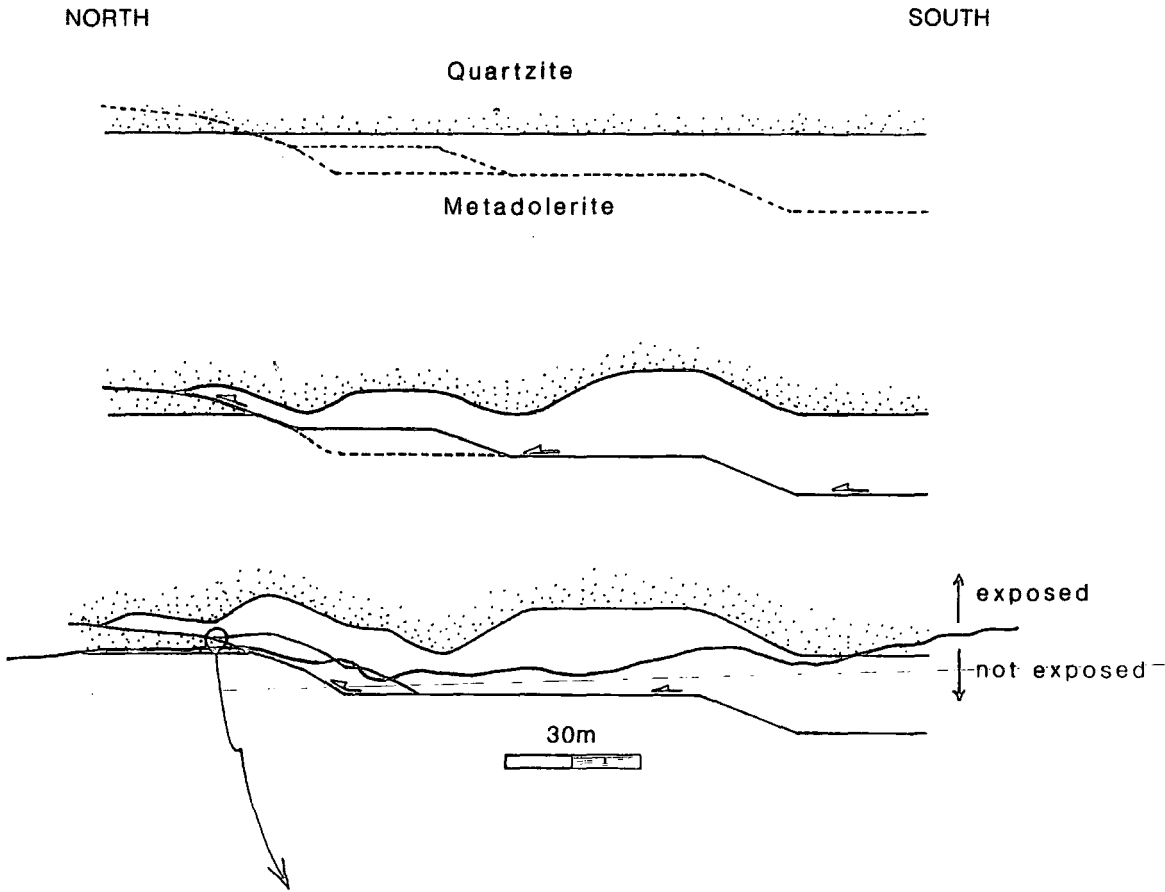
Figure 3.4 Diagram comparing a hangingwall ramp-flat geometry from Breaghy Head with a 'classic' high crustal level geometry. (A) The ramp-flat geometry of an "ideal thrust fault" (after Dahlstrom 1970). (B) Simplified field sketch of an example of a D2 ductile thrust with ramp-flat geometry from near Knockduff, locality 3, map 1.



**Figure 3.5** Diagrams illustrating fabric and veining relationships developed within the break-back sequence branch point at 662169, locality 7, map 1. (A) Schematic summary of the main structure and vertical strain distribution (intensity of S2 fabrics) at locality 7. Note that intense platy S2m is associated with both thrust 1 and thrust 2. Thrust 2 and its associated platy S2m climb across the exposure to the northeast. (B) Summary of fabric and vein relationships. An early set of extensional crenulations (S2e1) deform the S2m associated with thrust 1. This crenulation and the S2m are cross cut by narrow (cm) quartz veins which must therefore have been intruded as or shortly after displacement ceased on thrust 1. These veins and S2e1 are sheared out by the rejuvenation of S2m associated with thrust 2. Finally, a second set of extensional crenulations (S2e2) deform S2e1, the quartz veins and the S2m associated with thrust 2. These relationships indicate that thrust 2 is the later structure to be developed, (during progressive D2 deformation), so that the thrust sequence is break-back in nature.



a.



b.

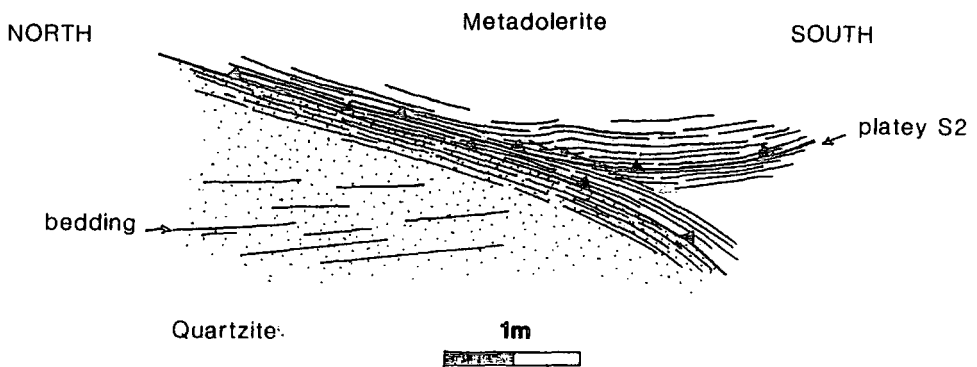


Figure 3.6 Minor ductile thrusts displaying ramp-flat geometries, structurally necessary folding and a leading edge branch point in the area between 647127, (locality 9) and 640140, map 1. (A) Schematic N-S cross section illustrating the ramp-flat thrust geometries and structurally necessary folding of the metadolerite-quartzite contact. (B) Simplified field sketch of the leading edge branch point and footwall ramp 100m NW of locality 9. The upper thrust is folded by the lower, indicating development in piggy-back sequence. Note that the mylonitic fabric of the upper thrust swings into general parallelism with that of the lower thrust but is also partially cross cut by the lower thrust's fabric.

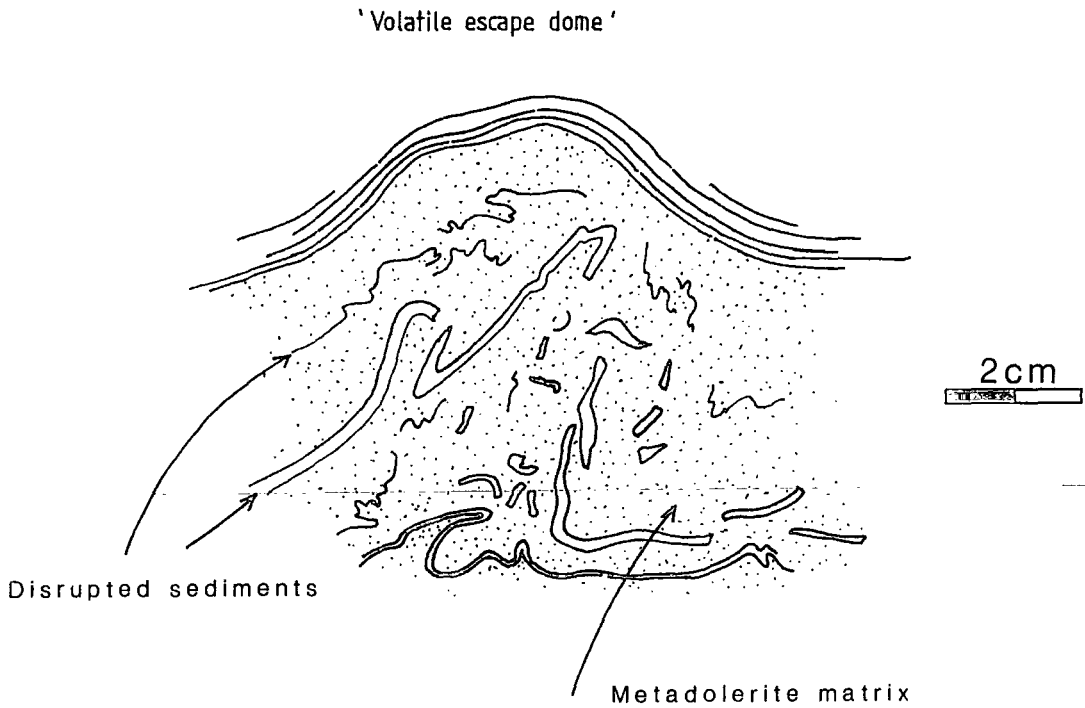


Figure 3.7 A simplified field sketch of a volatile escape (?) structure at the upper contact between the metadolerite sheet and country rock SW of Rincleven Point (locality 26, map1). The undeformed 'volatile escape dome' contains contorted fine sediment rafts suspended within fine grained metadolerite. This and similar structures found at sill contacts elsewhere in the area were tentatively used as way up criteria, since the vast majority of the metadolerites are considered to be pre-deformational (see text chapters 3 & 4 for details).

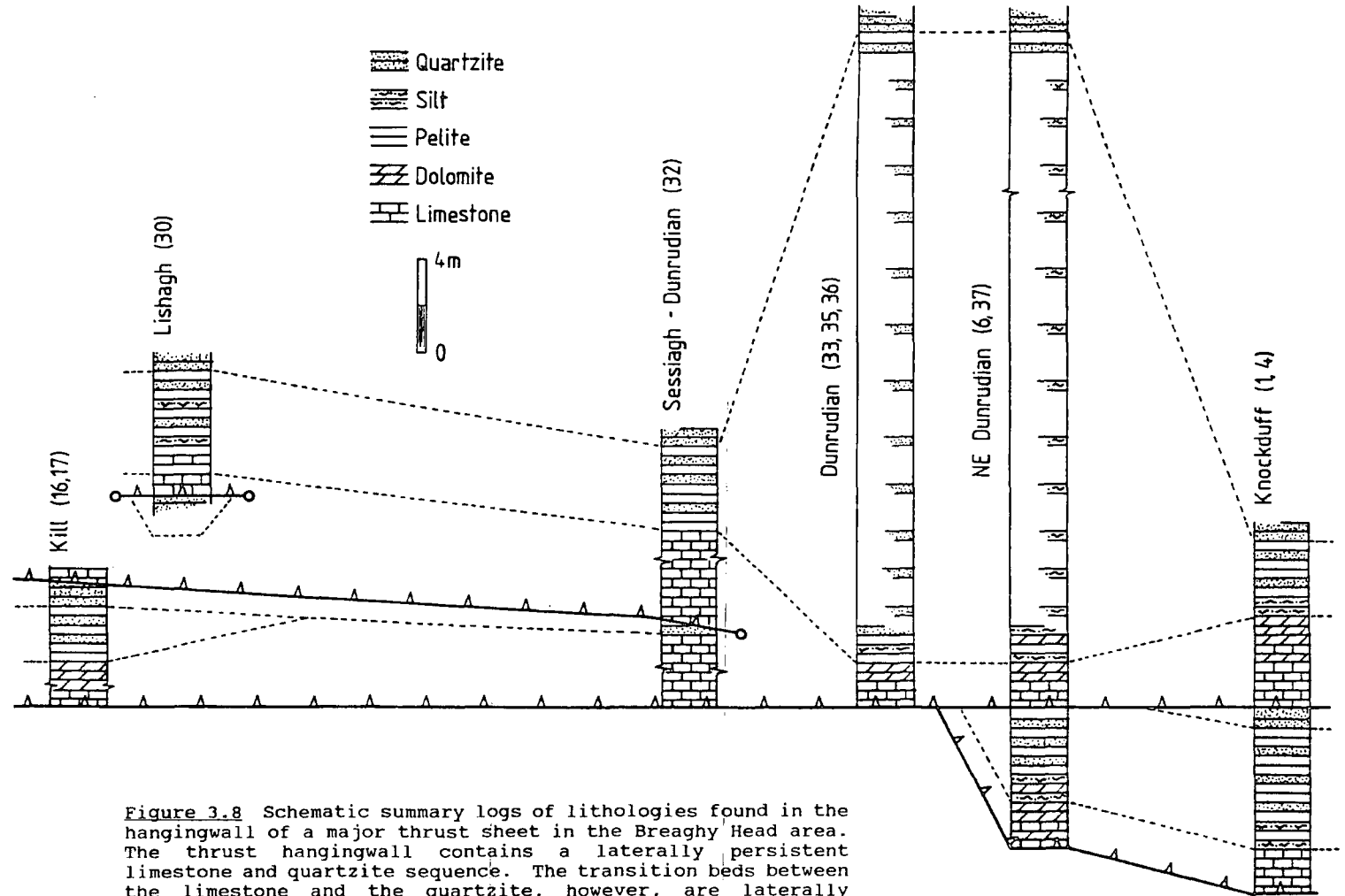
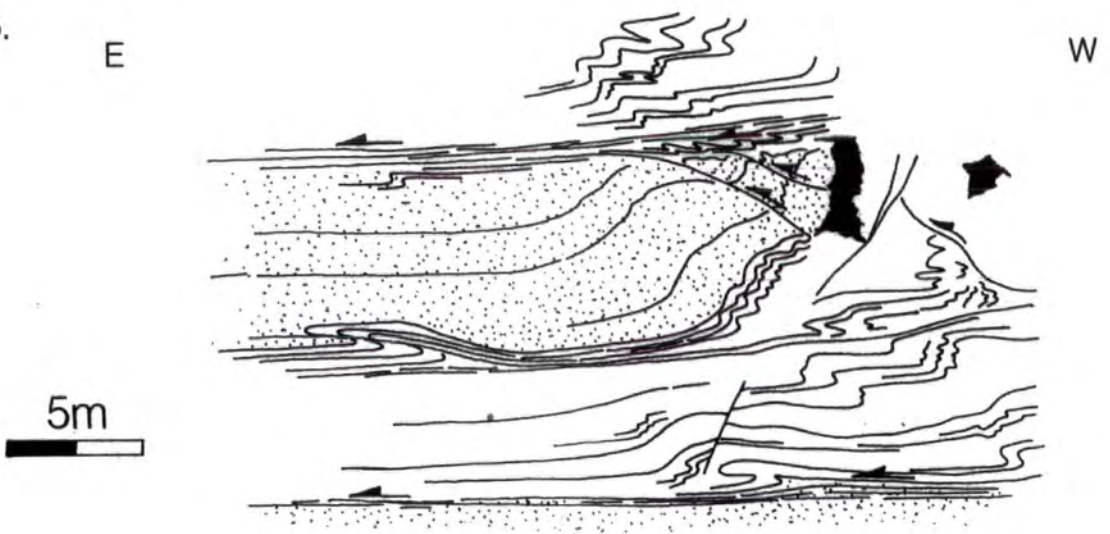


Figure 3.8 Schematic summary logs of lithologies found in the hangingwall of a major thrust sheet in the Breaghy Head area. The thrust hangingwall contains a laterally persistent limestone and quartzite sequence. The transition beds between the limestone and the quartzite, however, are laterally changeable in both thickness and lithological make-up. The dashed lines indicate the boundaries between limestone, transition and quartzite sequences. (Detailed examples of transition sequences from the Breaghy Head area are illustrated in Figs. 3.1, 3.16, 3.26, 3.29, 3.35, 3.38).

A.



B.



**Figure 3.9** (A) A photograph of the F2 fold with thrust middle limb exposed in the coastal cliff at 716293, locality 40, map 1. (B) Simplified field sketch of two minor thrusts exposed in a cliff face at 647255, between localities 42 and 43, map 1. Note the footwall ramp-syncline in the upper thrust.

E

W

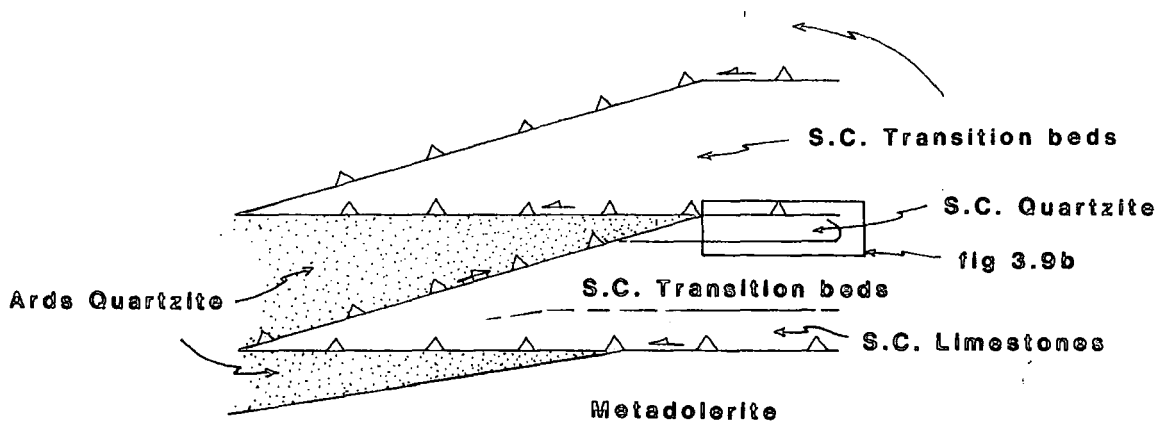


Figure 3.10 Diagram summarising the position of Ards Quartzite in the forethrust-backthrust complex east of the Curragh Harbour Anticline.

E

W

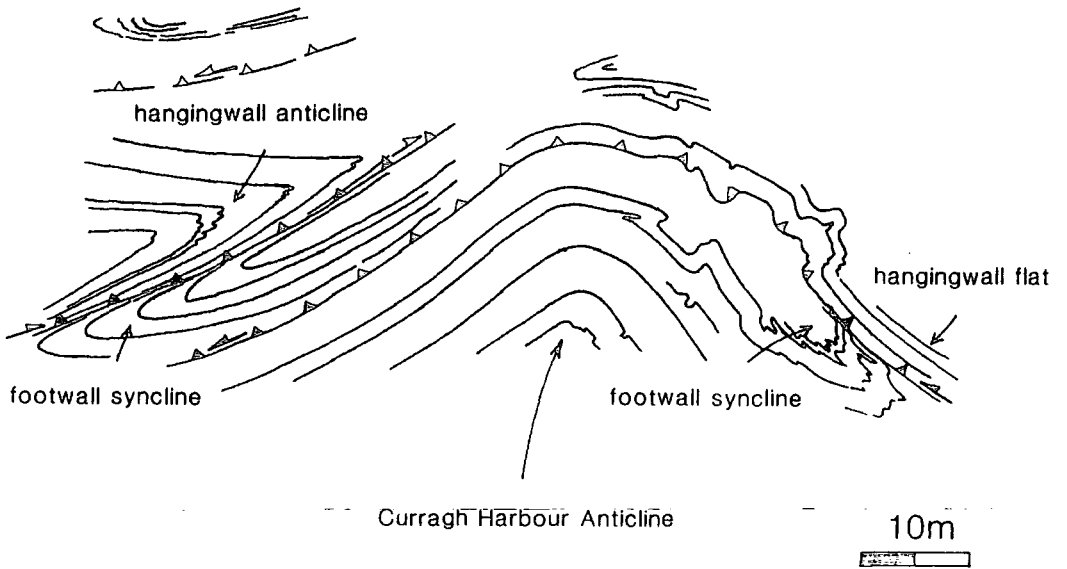


Figure 3.11 Simplified field sketch of fold-thrust structures exposed in a coastal cliff at Curragh Harbour (at and to the west of locality 43, map 1). Note the opposing throw directions of the two lower thrusts. Note also that the folded thrust can be traced northwards to overlie the quartzite footwall syncline of fig 3.9b (see also fig 3.15).

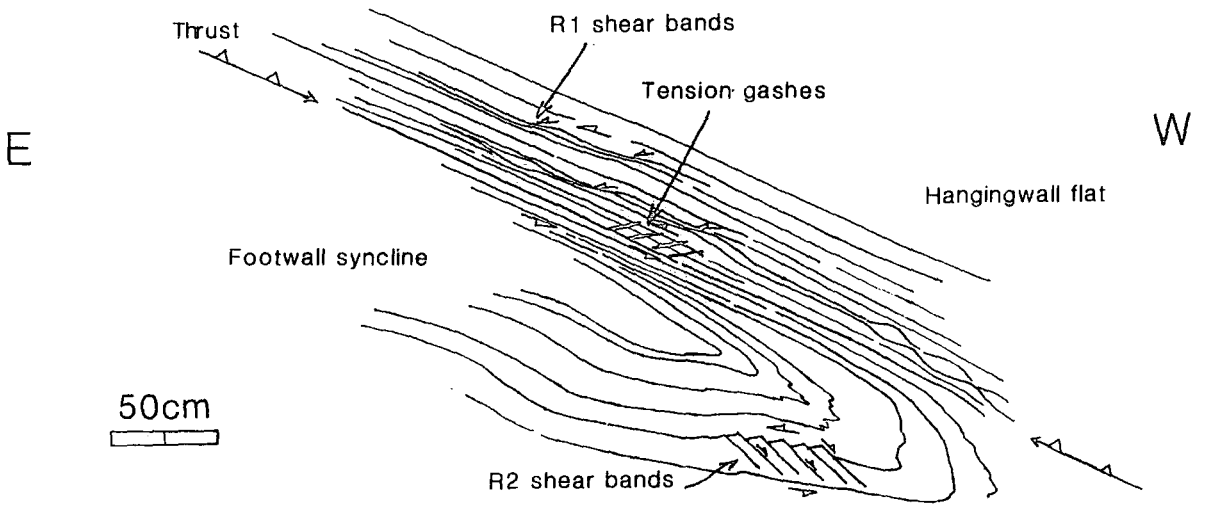


Figure 3.12 A D2 thrust with footwall syncline, hangingwall flat geometry and containing numerous shear bands, extensional crenulations and tension gashes indicative of an apparent thrust motion across the syncline to the east. However, the view is highly oblique to D2 stretching lineations indicative of NNW directed overshear. Locality 44, map 2.

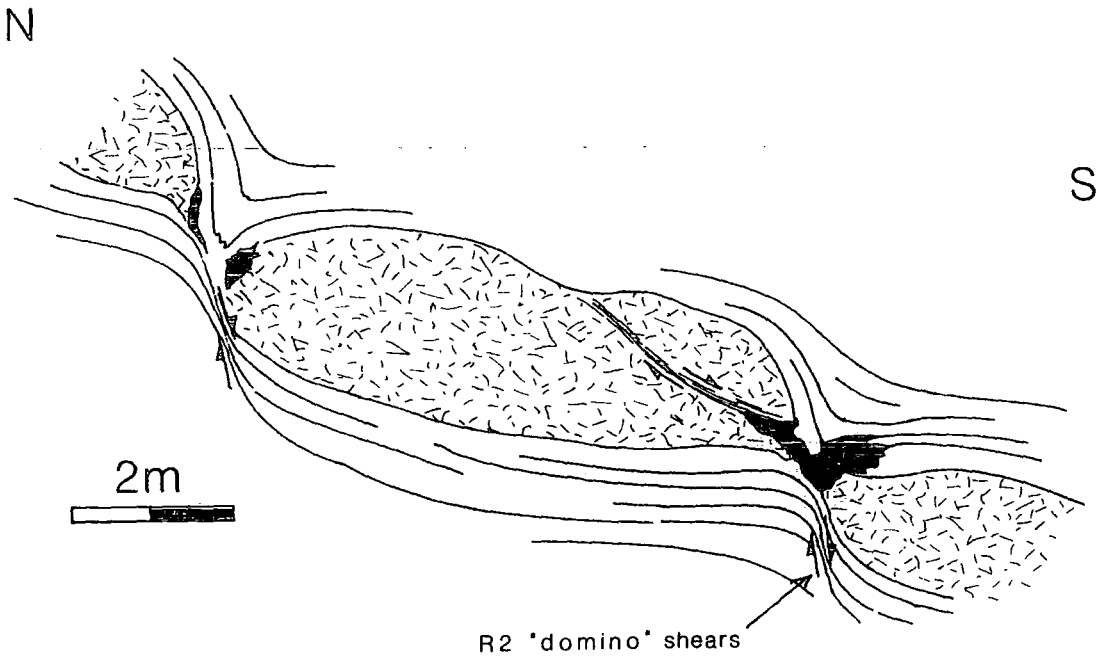
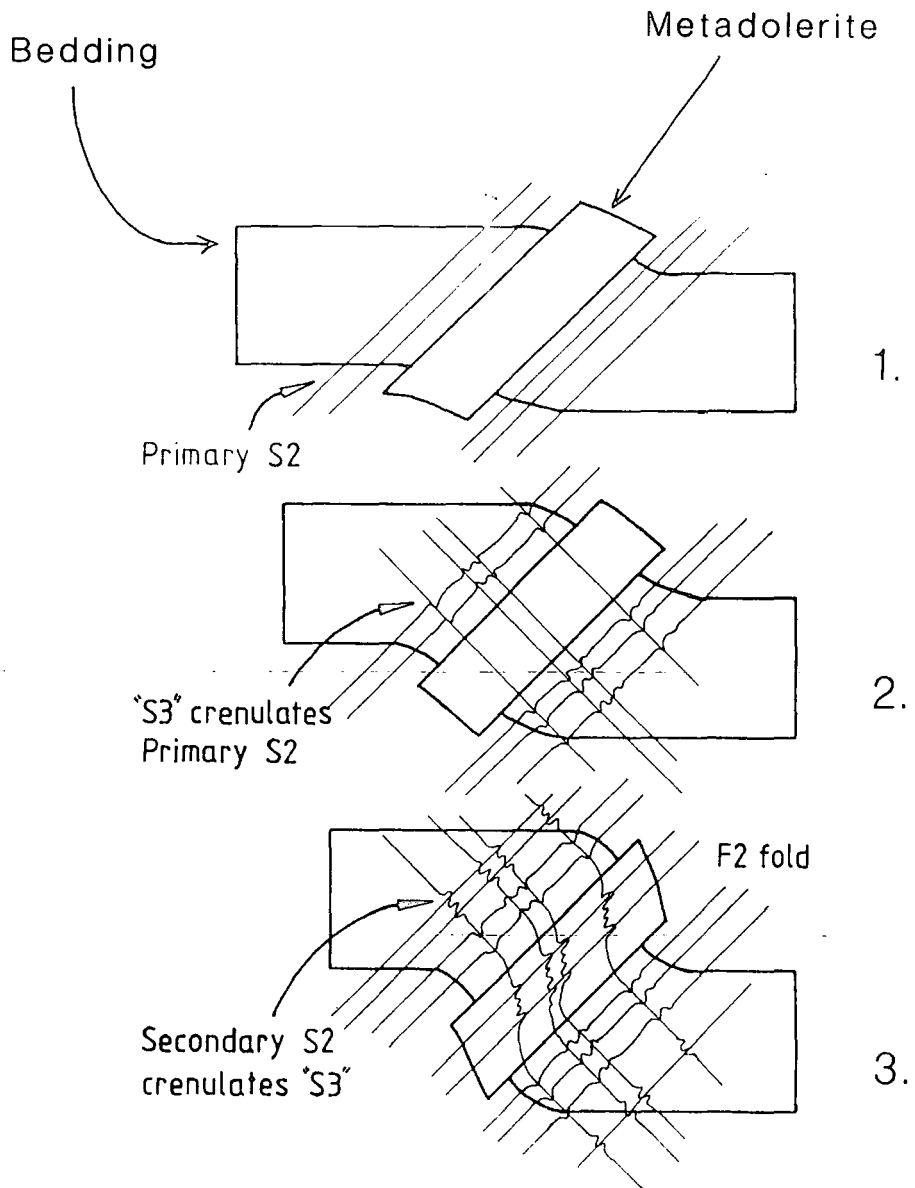


Figure 3.13 Large scale 'domino' rotations of a metadolerite and within country rock boudins (see fig 2.17) at locality 45, (map 1) indicate NW directed overshear of the thrust in fig 3.12.



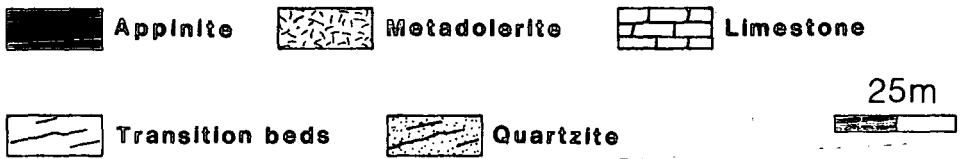
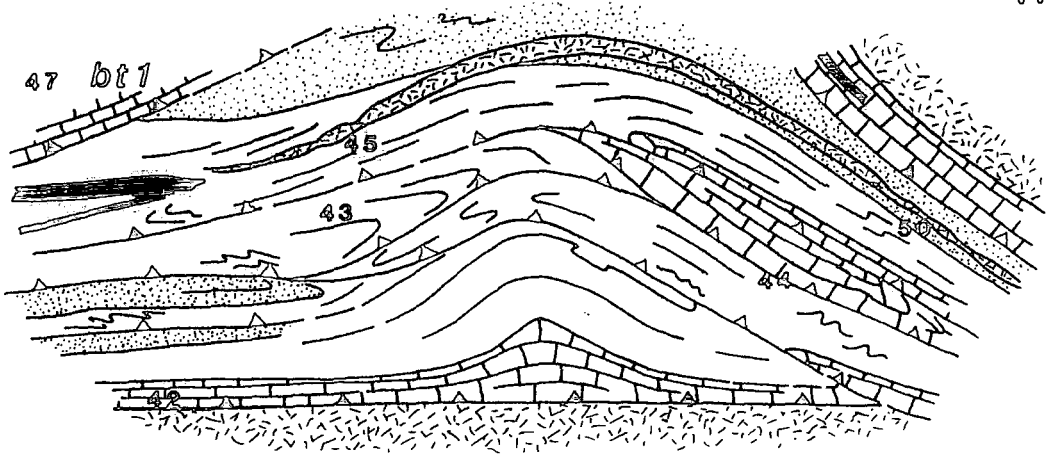
**Figure 3.14** Diagram illustrating the development of an F2 fold and conjugate S2 fabrics previously identified as S2 and S3 at 647248, location 45, map 1.

(1) Thin metadolerite sheet intruded during D2 parallel to primary S2 in the mid limb of an F2 fold. (2) Development of the 'conjugate' S2 ("S3" in the chronology of Hutton 1977a, 1982, 1983). This forms a new cleavage within the metadolerite and crenulates S2 in the country rock. (3) Resumption of S2 development (secondary S2) which crenulates the 'conjugate' S2 in both metadolerite and country rock. Tightening of the F2 fold also deforms the 'conjugate' S2.



E  
A.

W



B.

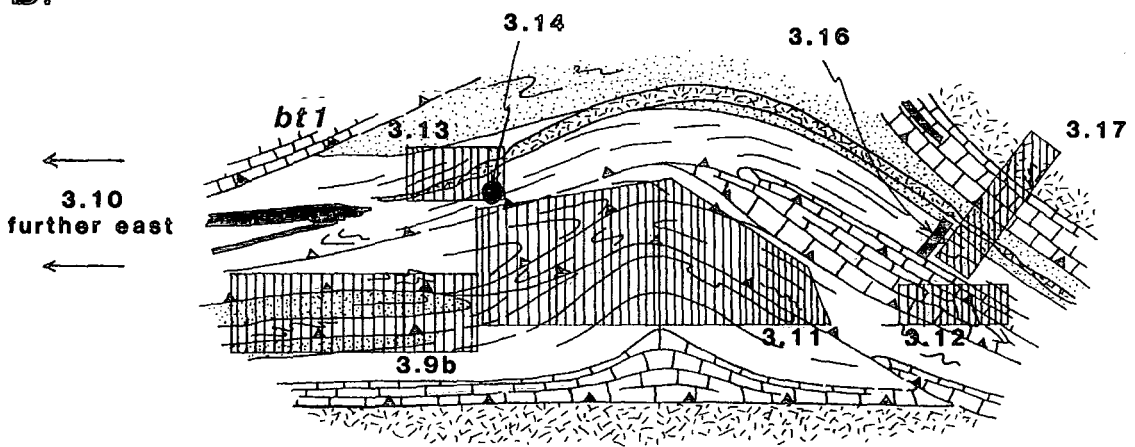


Figure 3.15 (A) Schematic east-west section across the Curragh Harbour anticline. Positions of field localities are indicated. (B) Location within the structure of figures 3.9b to 3.17.

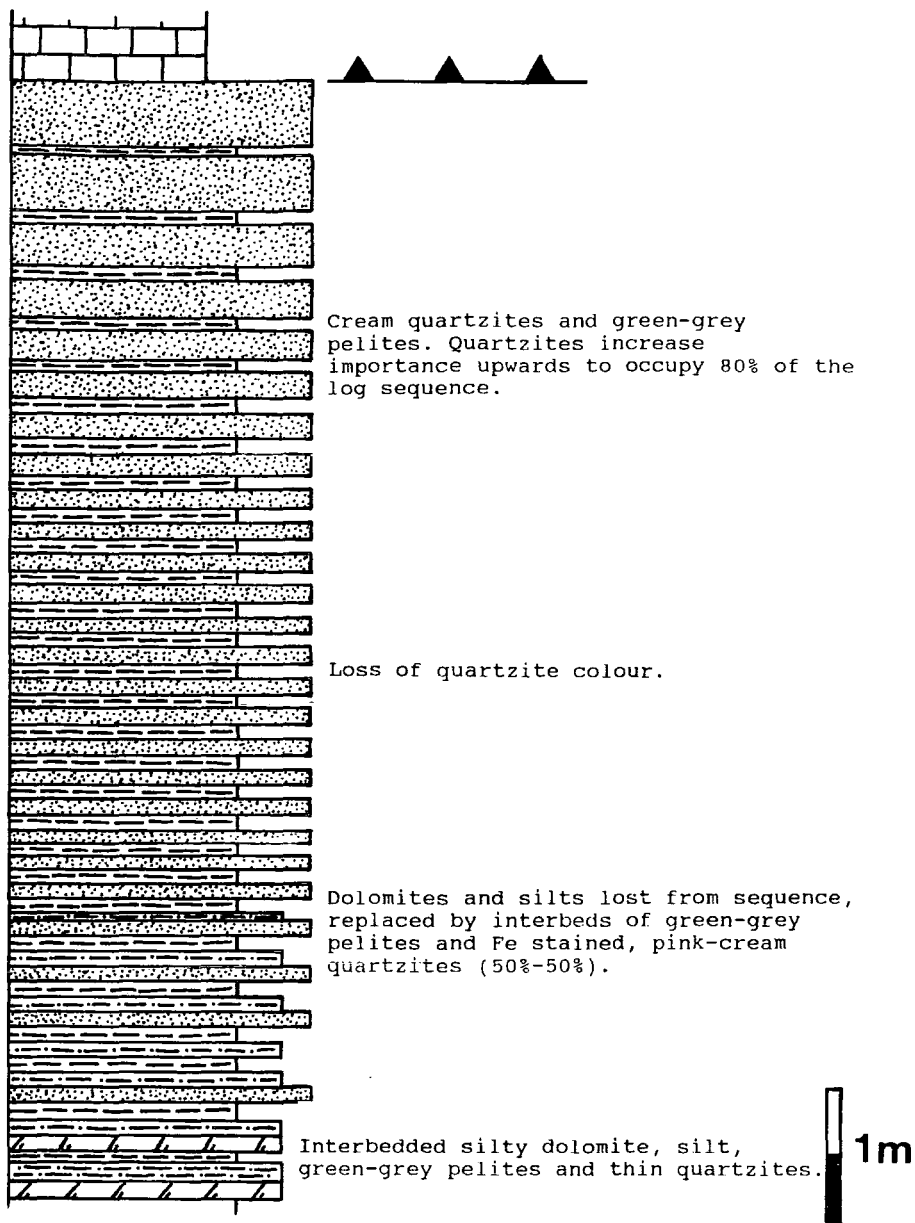


Figure 3.16 Summary lithological log of transition beds at 637240, locality 50, map 1. Ornament as for Figure 3.1.

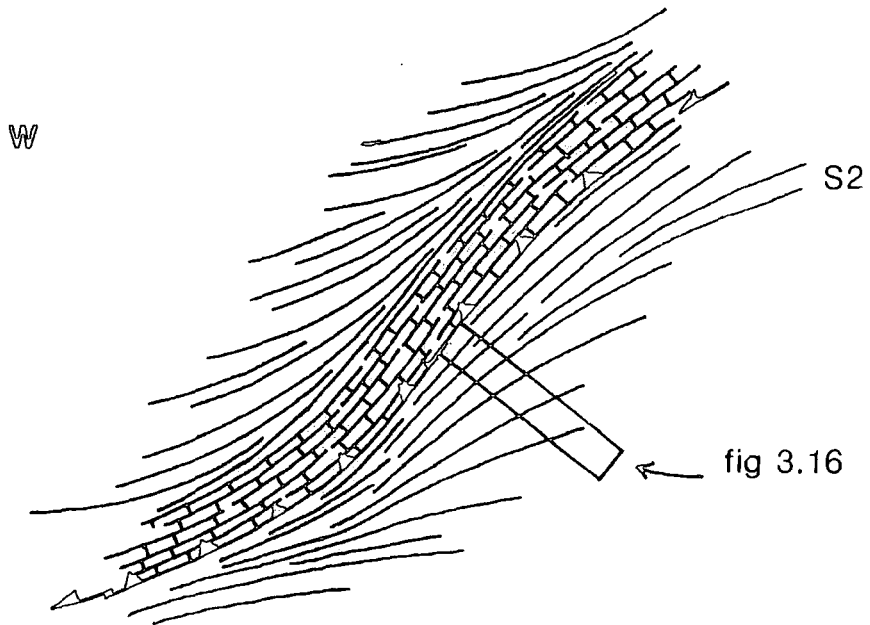
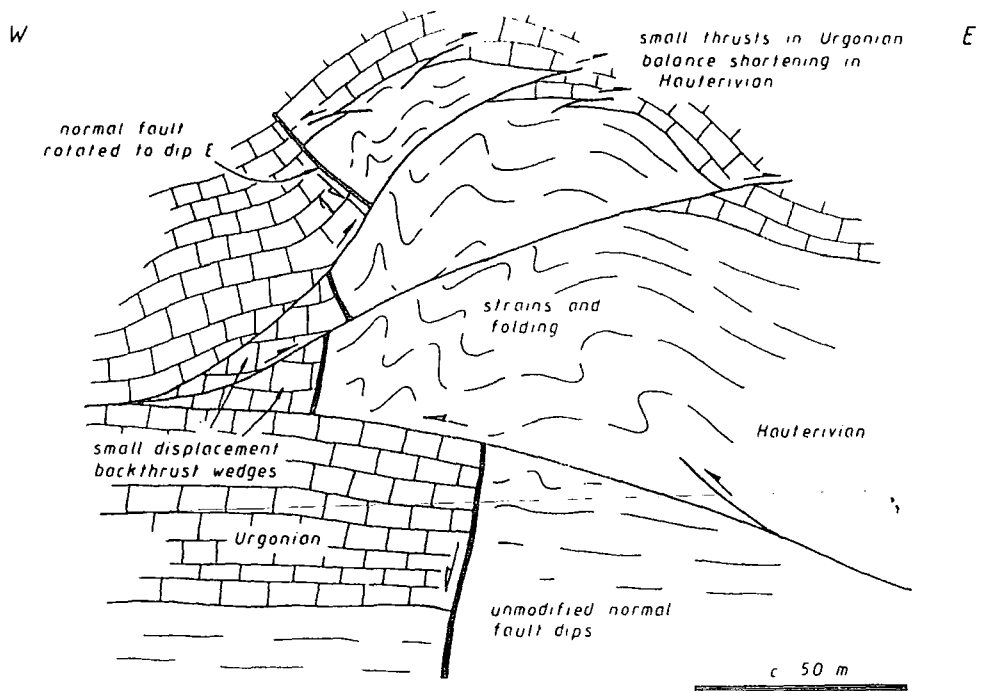


Figure 3.17 Fabric relationships surrounding the western-most thrust to be folded by the Curragh Harbour Anticline. The direction of the swing of S2 into the thrust, numerous extensional crenulations, P-shears and C-shears indicate that the thrust overshears towards the NW and is therefore downward facing at this position.



**Figure 3.18** Schematic section through a butressing structure from the Col de la Bataille area of the Vercors, western Alps. This structure is developed by a thrust attempting to propagate across a normal fault from relatively weak Hauterivian limestones and shales into massive Urgonian limestones. (from Butler 1989a).

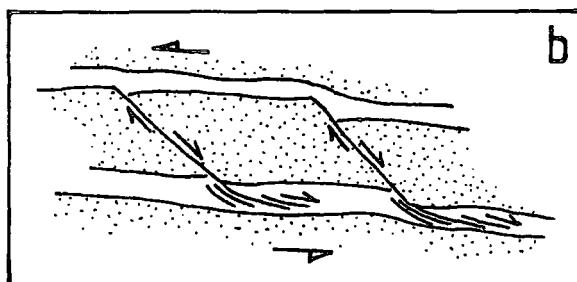
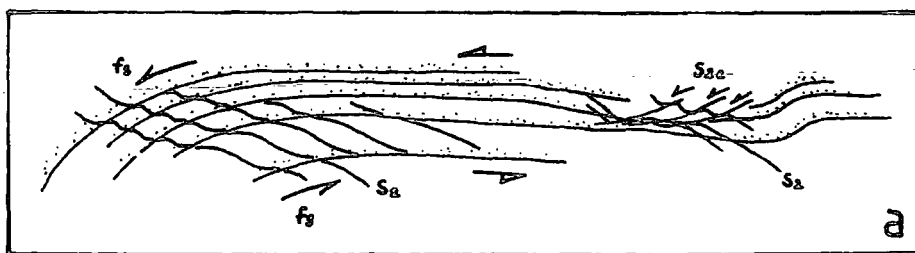
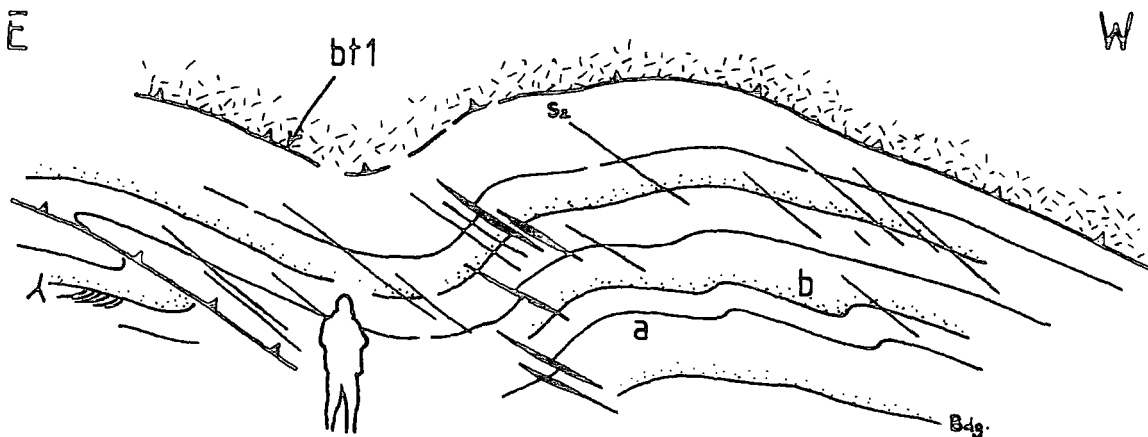


Figure 3.19 Simplified field sketches of minor structure relationships in an easterly verging F2 fold pair in quartzites which deforms breaching thrust (bt1), at locality 57, map 1. Mineral extension lineations in S2 plunge into the page, so that thrust transport is out of the page. S2 parallel quartz veins are present in the fold mid limb. Bedding is thrust displaced across some of these veins. (A) S2 is deformed by bedding parallel flexural shearing (fs) and extensional crenulations and shear bands (S2e). Some shear bands appear to have a lystric geometry and link to flexural shears. (B) R2 'domino' rotations are present in some quartzite beds, from which extensional crenulations 'leak' into pelite interbeds, lystrically detaching the rotation displacements onto the quartzite bed below.

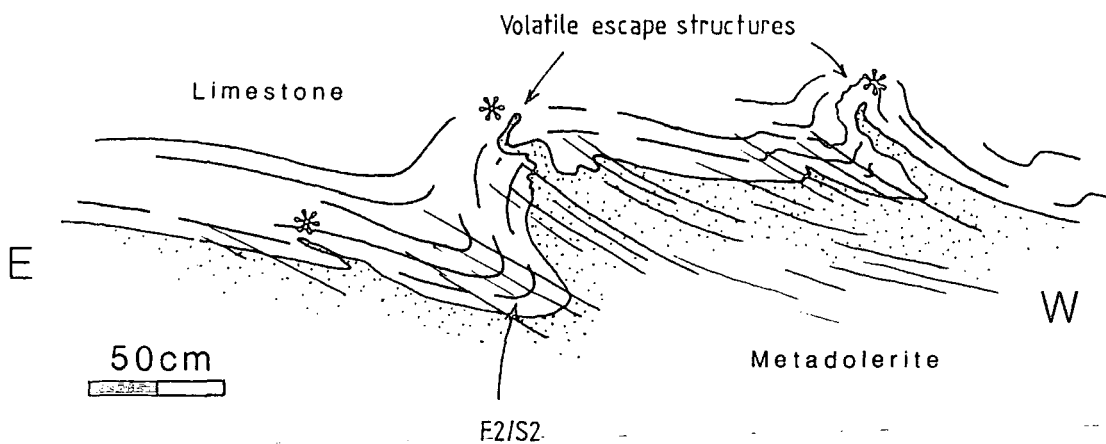
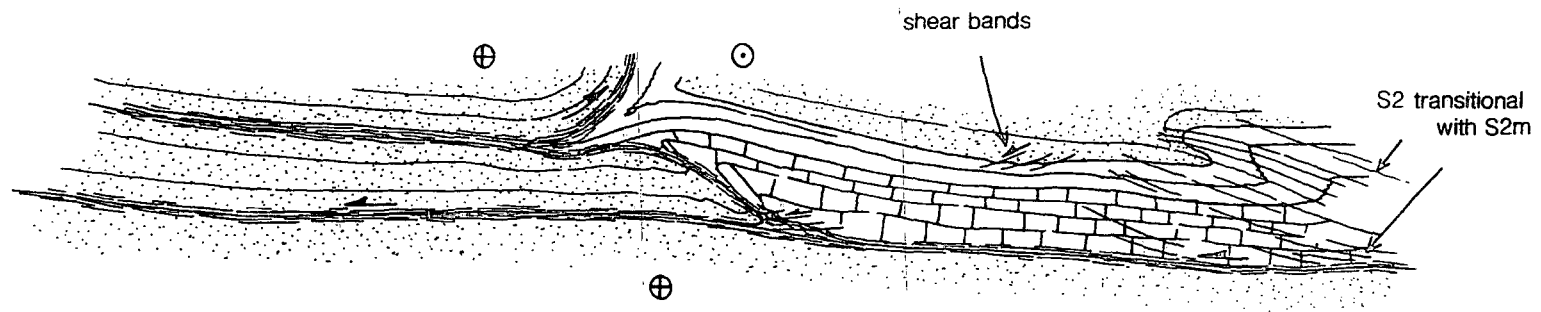


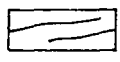
Figure 3.20 A simplified field sketch of the lower contact of a sediment raft in host metadolerite. Certain parts of the contact are intruded by finger-like 'tails' of metadolerite (asterisked) which transgress/buckle bedding and contain wispy zones of altered mineralogy. These features appear to catalyze minor F2 folds and may represent deformed examples of volatile escape (?) structures (see also fig 3.7).

E

W



**Limestone**



**Pelite**



**Quartzite**

1m



**Figure 3.21** Simplified field sketch of two discrete minor ductile thrusts in a forethrust-backthrust relationship. These minor thrusts are located between two splays of (bt1) at 597214, locality 58, map 1. The actual movement direction of the thrusts is obliquely out of the page, so that the limestones have been emplaced onto/within the quartzites from a footwall ramp some distance to the south (behind the page). S2 is axial planar to an F2 fold and is transitional with platy S2m associated with the thrust planes.

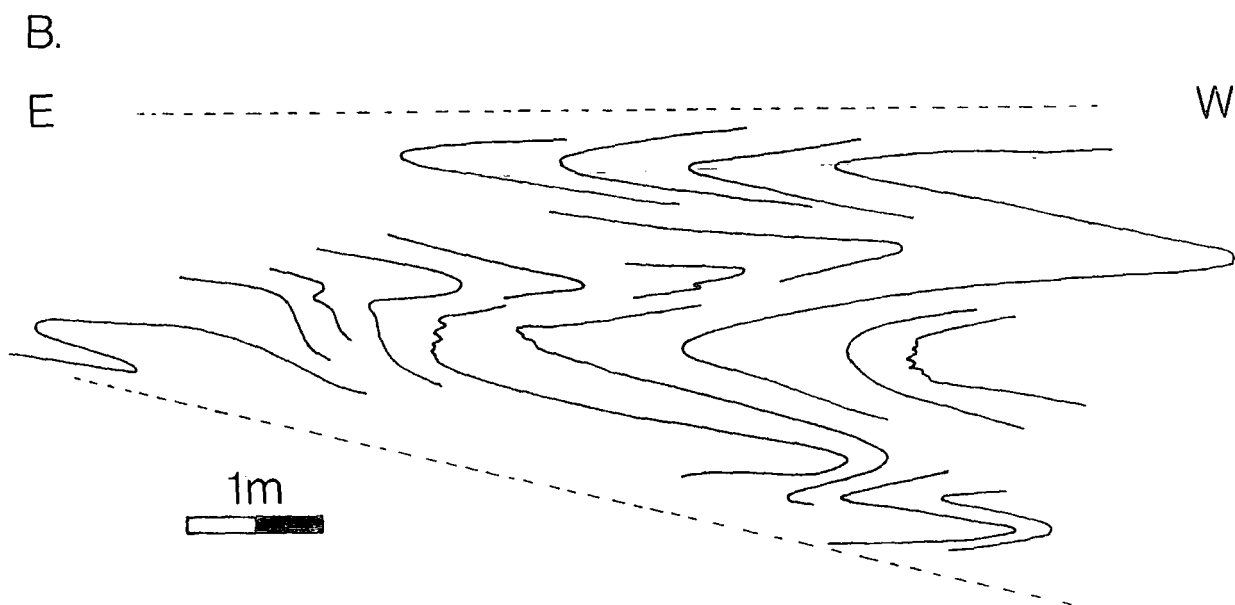
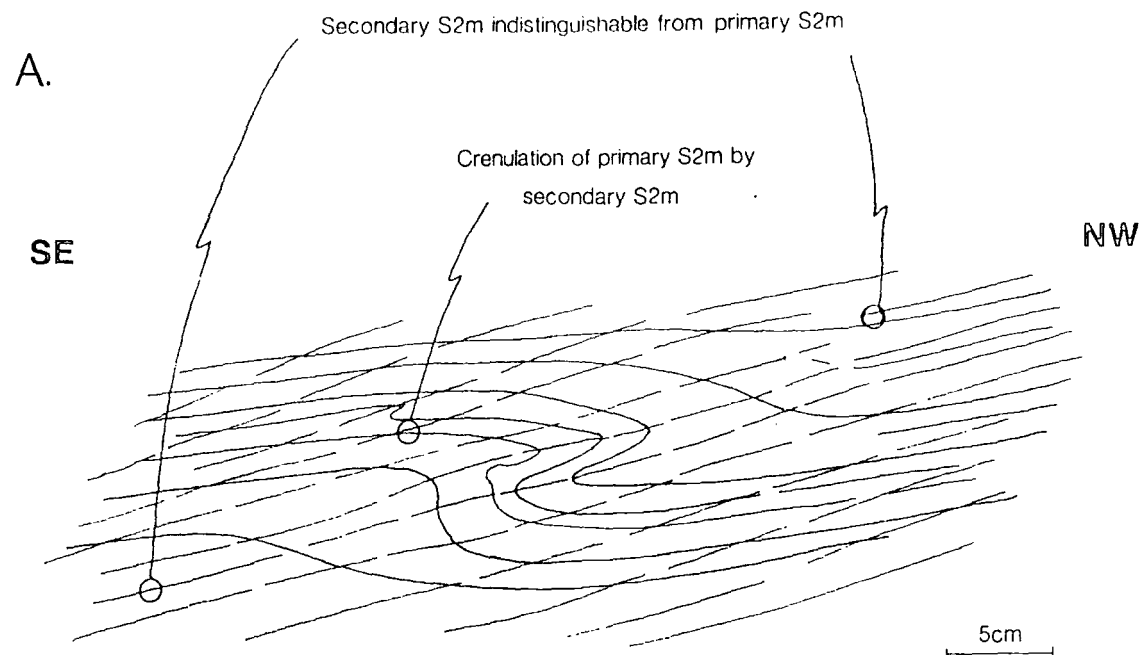


**Figure 3.22** Simplified field sketches of fold reworked S2m in limestones at 568209, locality 60, map 1. (A) Minor fold of S2m, showing the transitional nature of the fold axial planar cleavage with surrounding S2m. In the central portion of the axial plane, the axial planar cleavage produces contractional crenulations of S2m, but becomes mylonitic and indistinguishable from the surrounding S2m up and down the axial plane. This particular example is located 3-4m east of figure 3.22b. (B) A series of recumbent to isoclinal folds of bedding/S2m which have highly curvilinear hinges and appear, in part, to have sheath geometries. As indicated, these folds thicken the limestone towards the west and may collectively represent a highly deformed hangingwall anticline.



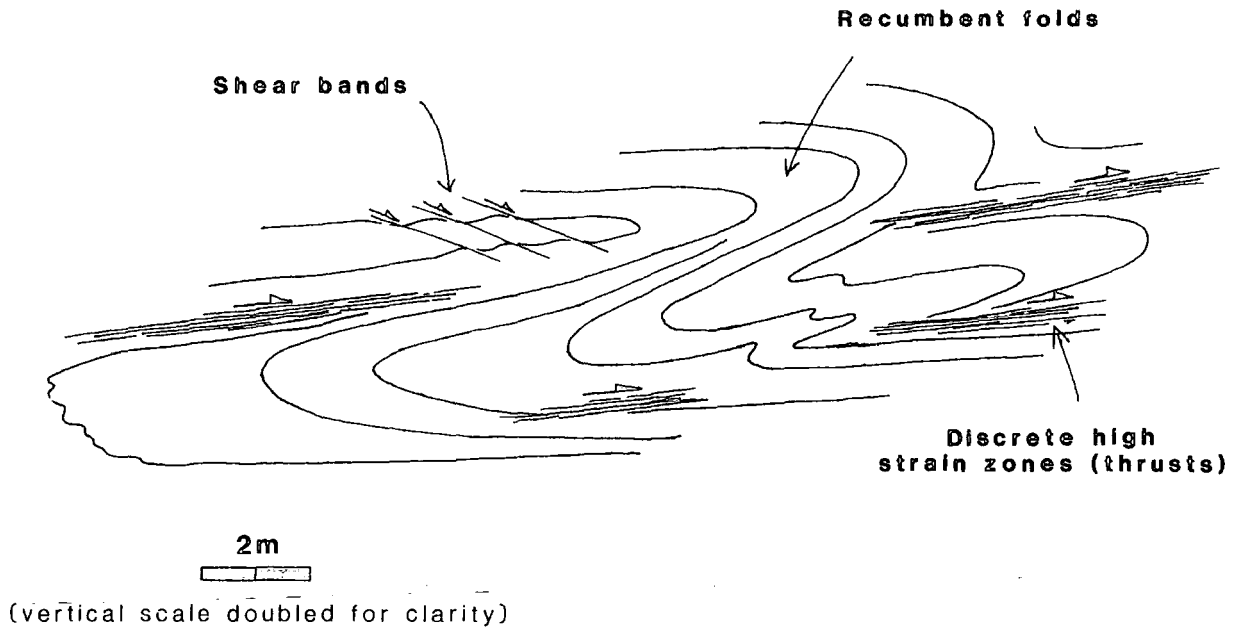
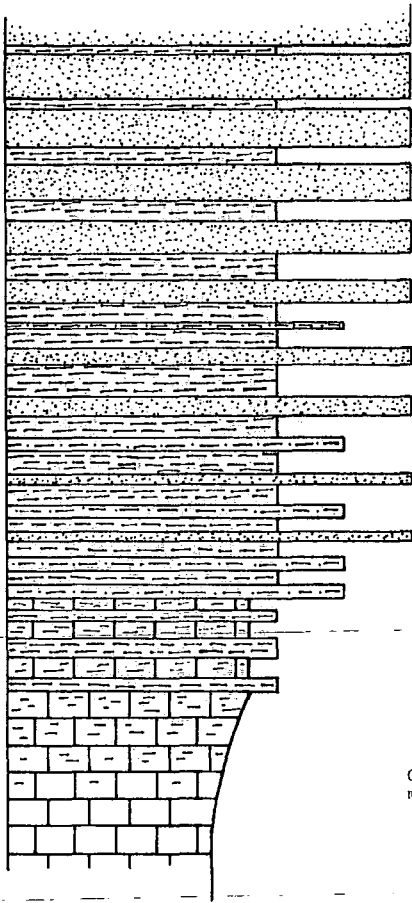


Figure 3.23 Schematic field sketch of the inter-relationship between recumbent F2 folds, discrete thrust shear zones and shear bands at 612200, locality 56 map 1. Note that the fold mid limbs at this locality effectively represent ramps between thrust flats.

Figure 3.24 Photograph looking due west at locality 70, map 1. This shows a frontal ramp in (bt2/3) in the background emplacing limestones and metadolerite in the hangingwall onto a veneer of quartzitic transition beds above a metadolerite in the footwall. The thrust also ramps eastwards (out of the page) in the footwall across quartzitic transition beds and quartzites from the background to a position just above the head of the gentleman on the far right. This is visible from the marked increase in thickness of the footwall beds from the background to the foreground.



Figure 3.25 Photograph at locality 70, map 1, of an open dome in the country rocks above a metadolerite sill, caused by volatile escape (?), being a similar structure to that described south of Rincleven Point (compare with fig 3.7).



Silts become replaced by quartzites, and sequence becomes a series of pelite and quartzite interbeds with quartzite proportion increasing to 80%.

Mixed intercalations of pelite, silt and thin quartzites (3m).

Grey limestones, become increasingly micaceous (1m).

Micaceous Limestone

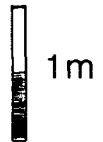


Figure 3.26 Summary lithological log of transition beds at 588164, locality 72, map 2. Ornament as for Figure 3.1 (with exception indicated).

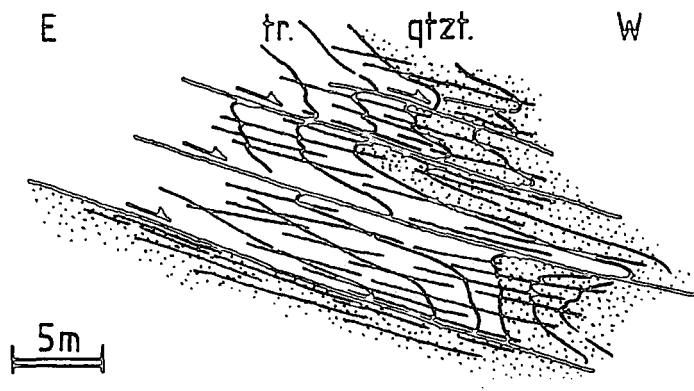


Figure 3.27 Simplified field sketch of minor ductile imbricates at locality 73, map 1. These minor thrusts are localised in the mid limbs of westerly vergent minor folds and displace the transition beds - quartzite contact. The lowest thrust emplaces transition beds onto pure quartzites, indicating displacement in tens of metres. The folds, S2 cleavage and the thrusts all face downwards to the west.

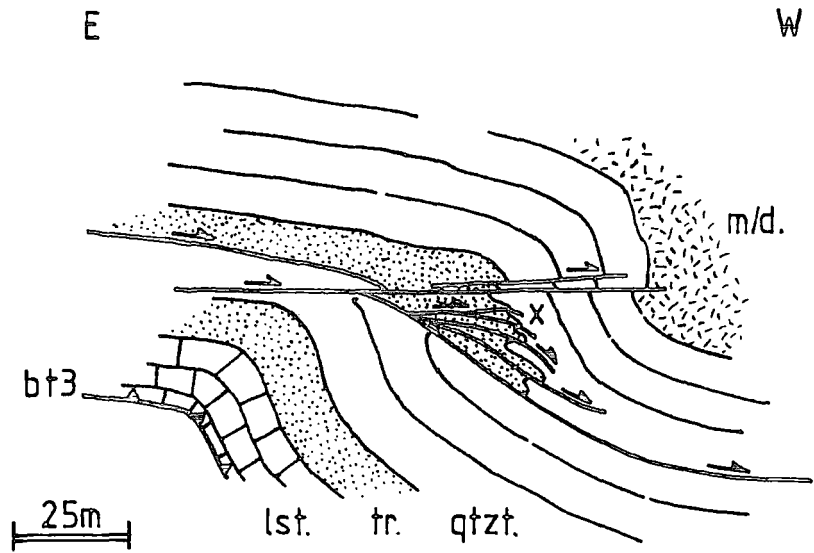


Figure 3.28 Schematic diagram of the fold-thrust structure at locality 73, map 1. The fold deforms limestones, transition beds, quartzites, a metadolerite body, major thrust (bt3) and a minor ductile imbricate stack in its hangingwall (x), illustrated in Fig 3.27. The fold and folded thrusts are breached by further minor ductile thrusts.

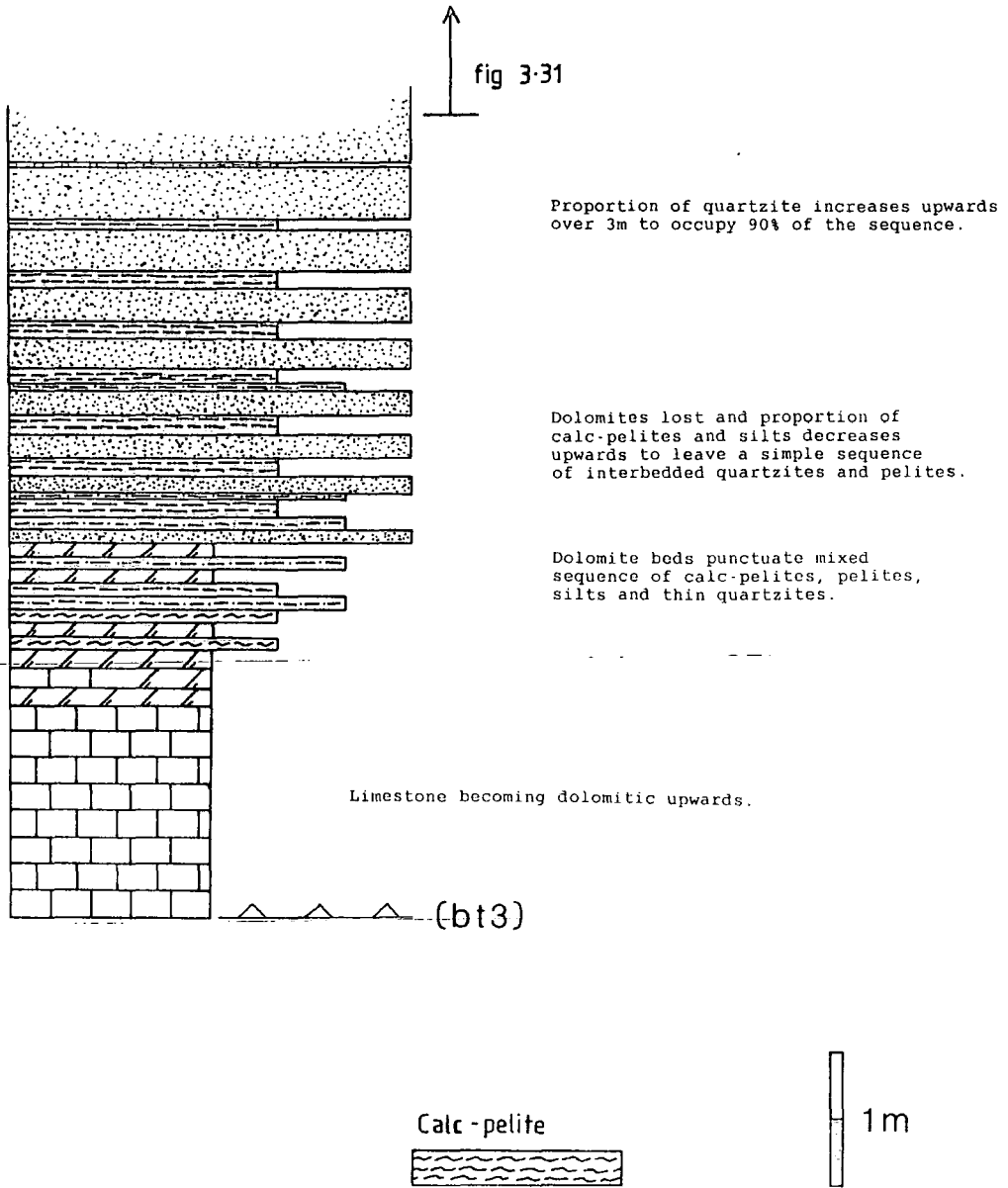


Figure 3.29 Summary lithological log of transition beds at 565202, locality 74, map 2. The boudinaged quartzites of Figure 3.31 occur immediately above the logged sequence as indicated. Ornament (with exception indicated) as for Figure 3.1.

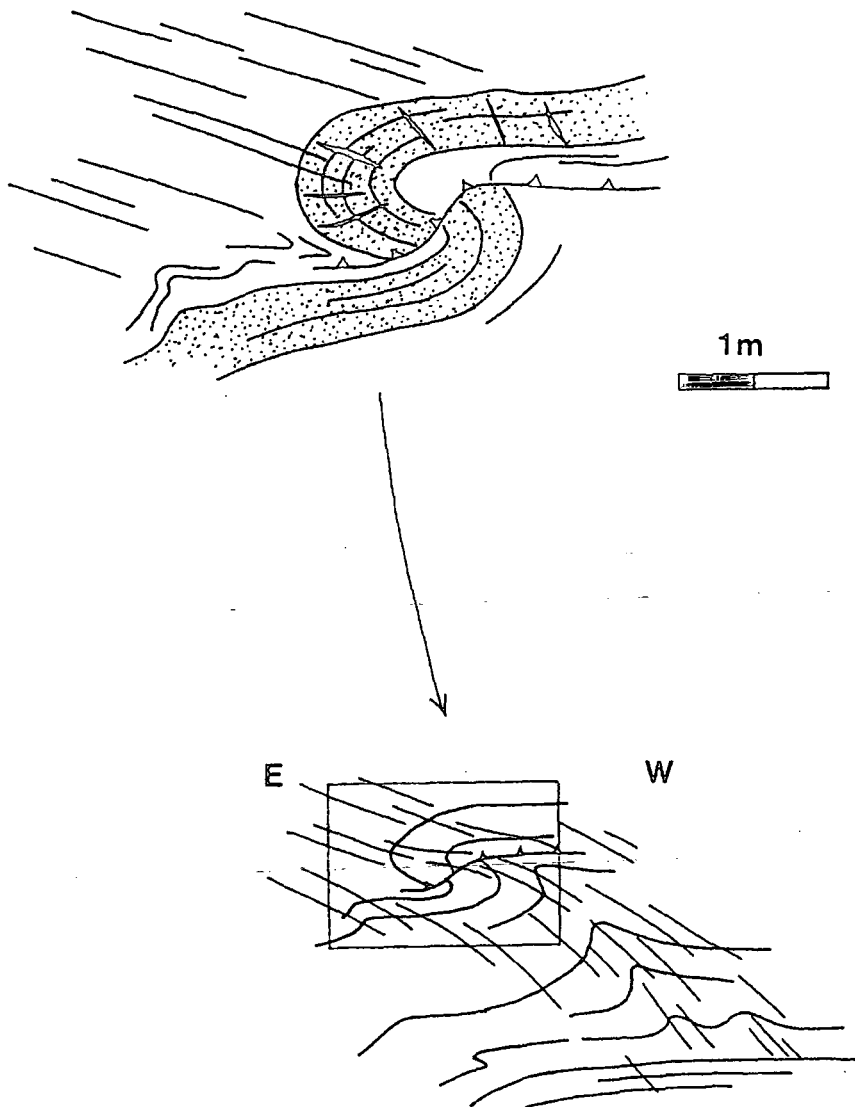


Figure 3.30 Simplified field sketch of upright folds which tighten upwards along shallowing axial planes. The folds have axial planar S2 & S2m which reworks the S2 fabrics in the upright regions of the folds, but is parallel to and indistinguishable from S2 fabrics higher up the axial plane. The folds are developed during D2 but partially rework S2.

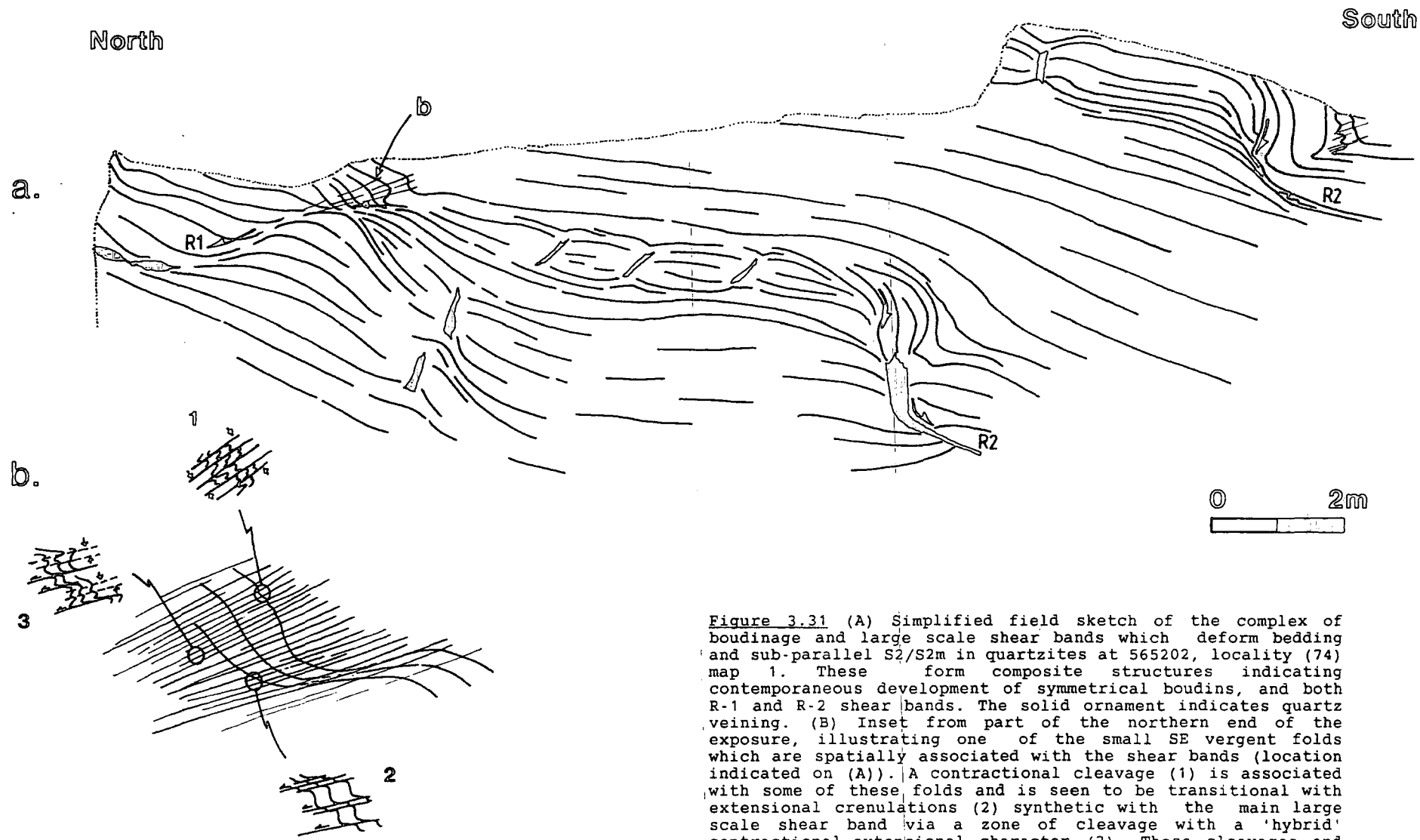
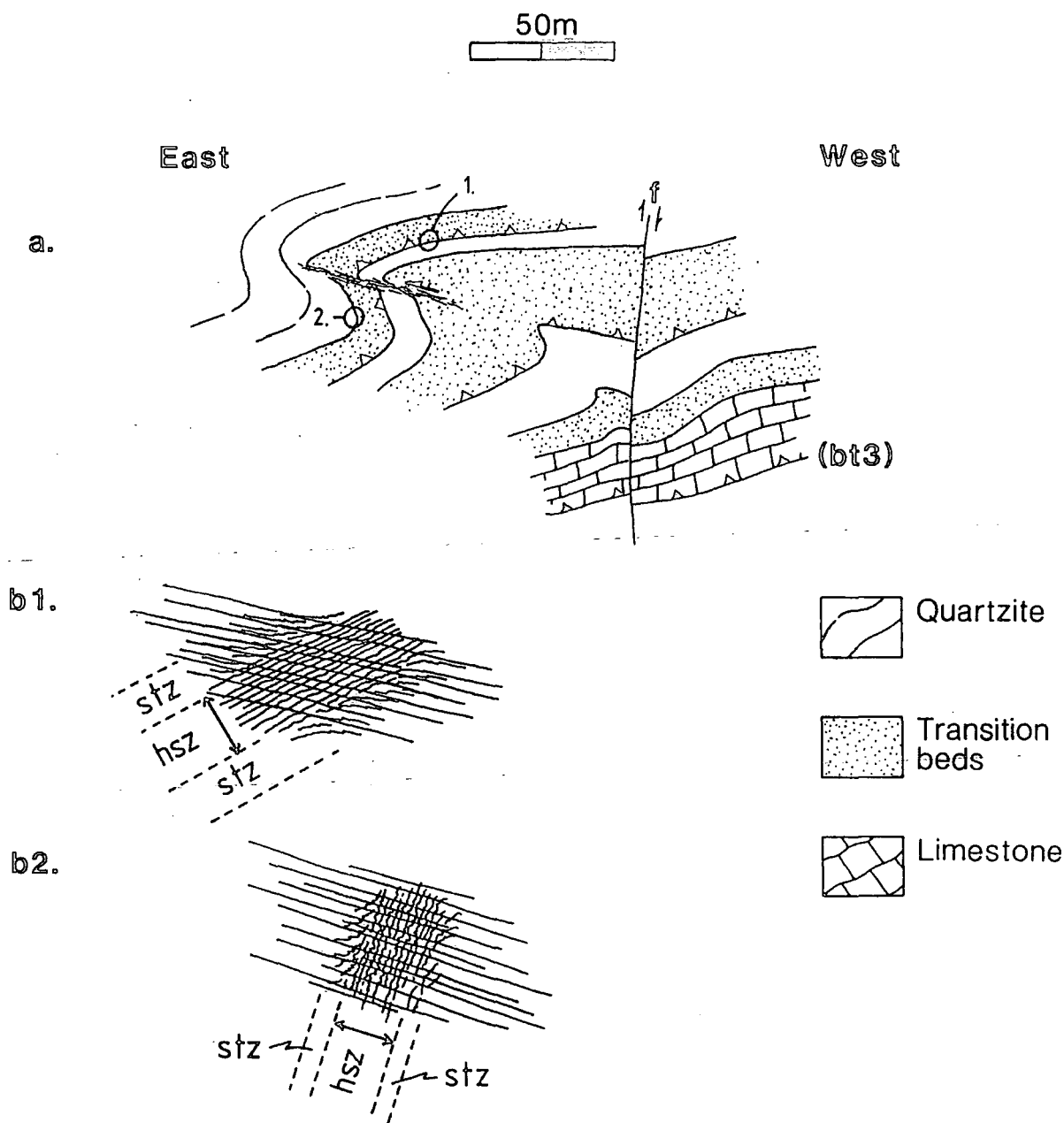
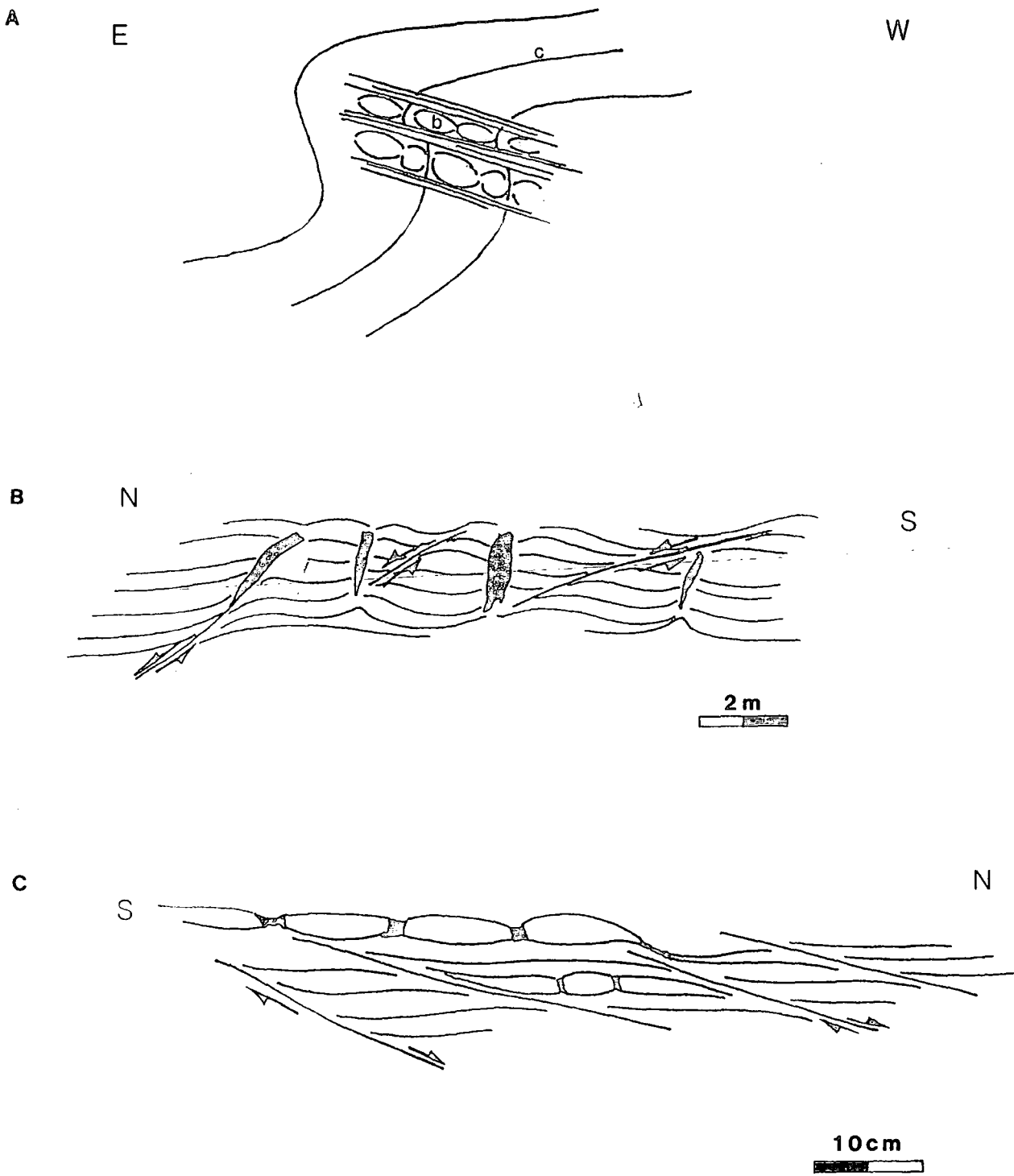


Figure 3.31 (A) Simplified field sketch of the complex of boudinage and large scale shear bands which deform bedding and sub-parallel S<sub>2</sub>/S<sub>2m</sub> in quartzites at 565202, locality (74) map 1. These form composite structures indicating contemporaneous development of symmetrical boudins, and both R-1 and R-2 shear bands. The solid ornament indicates quartz veining. (B) Inset from part of the northern end of the exposure, illustrating one of the small SE vergent folds which are spatially associated with the shear bands (location indicated on (A)). A contractional cleavage (1) is associated with some of these folds and is seen to be transitional with extensional crenulations (2) synthetic with the main large scale shear band via a zone of cleavage with a 'hybrid' contractional-extensional character (3). These cleavages and folds are clearly developed in strong causal relationship to the development of the large scale D<sub>2</sub> shear bands.

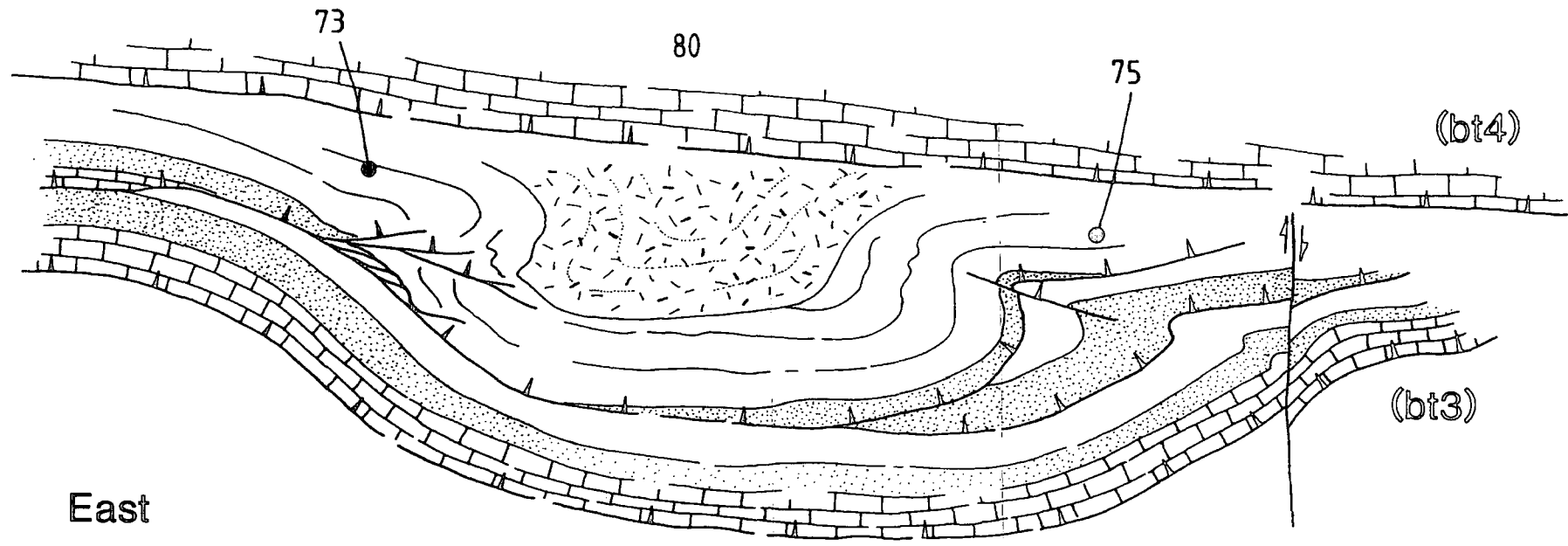


**Figure 3.32** Simplified field sketches of the monoformally refolded minor thrusts at 550173, locality (75) map 1. (A) Overall morphology of the easterly vergent F2 monoform which appears to lose amplitude downwards towards (bt3). Note that the minor thrusts are refolded by the structure and that the higher of the two has been offset by a further minor thrust. This thrust is parallel to and lies within a zone of intensification of the monoform's axial planar cleavage (cleavage omitted for clarity). (B1 & B2) Diagrammatic comparison of the relationships between minor thrust fabrics and the fold axial planar cleavage in the upper normal limb and the mid limb of the monoform. In both cases the high strain zone (hsz) is of similar width. The width of the strain transition zones (stz) outboard of the minor thrust mylonites, however, is narrower in the mid limb. (The stz is the transition between mylonitic and 'background' cleavage intensity associated with an individual ductile thrusts).





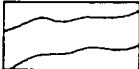
**Figure 3.33** Simplified field sketches of composite shear band & boudinage structure within the monoform at 550173, locality 75, map 1 (see fig 3.32). (A) Diagrammatic representation of the monoform with (B) & (C) located. Note that it is the bands of intensified S2 associated with a minor fabric slip ramp (chapter 4), which provides the anisotropy to catalyse boudinage in (B), and bedding in the case of (C). Note also that both (B) & (C) are morphologically very similar to the composite shear band & boudinage structures at 565202, locality 74, map 1 (compare this figure with figure 3.31).



East

West

 Metadolerite

 Quartzite

 Transition beds

 Limestone

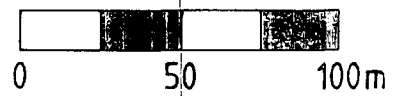


Figure 3.34 Schematic east-west section viewed down the transport direction, summarising the major structure between locations (73), (80) and (75) (maps 1 & 2). Note the opposing vergence of the two D2 antiforms at (73) and (75) and the breaching nature of (bt4).

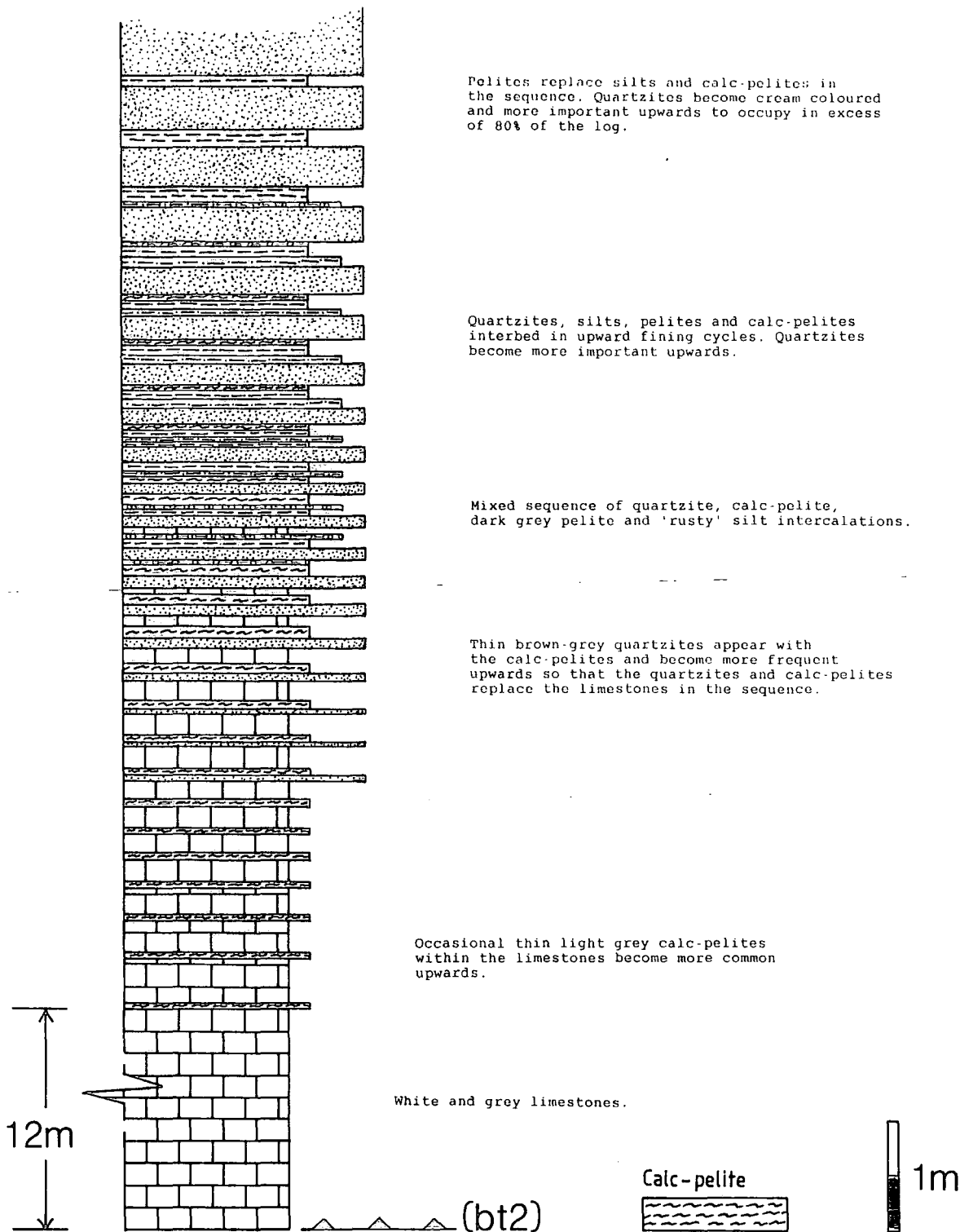
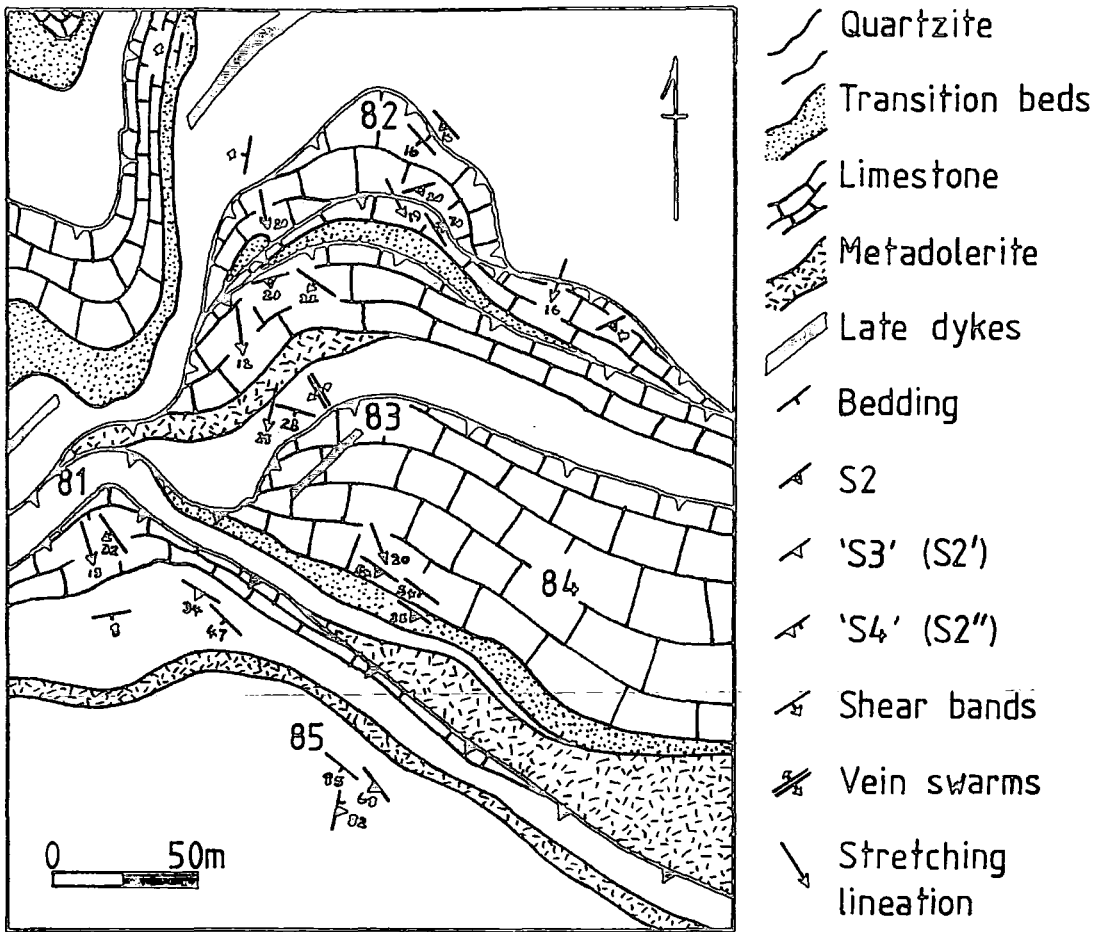


Figure 3.35 Summary lithological log of transition beds at 532175, locality 76, map 1. Ornament as for figure 3.1 (with exception indicated).



**Figure 3.36** Detail map of the Middle Town ductile thrust stack. Bedding and S2 dips increase towards the rear (south) of the stack in response to footwall collapse and back-steepening of the higher thrust sheets during accretion of younger thrust sheets to the collective footwall. Note the development and restriction of secondary S2 fabrics to the rear of the stack during this back-steepening. These fabrics would be S3 and S4 in the regional chronology of Hutton (1983), but are more appropriately labelled S2' and S3" (see Fig. 3.39). Details in text.

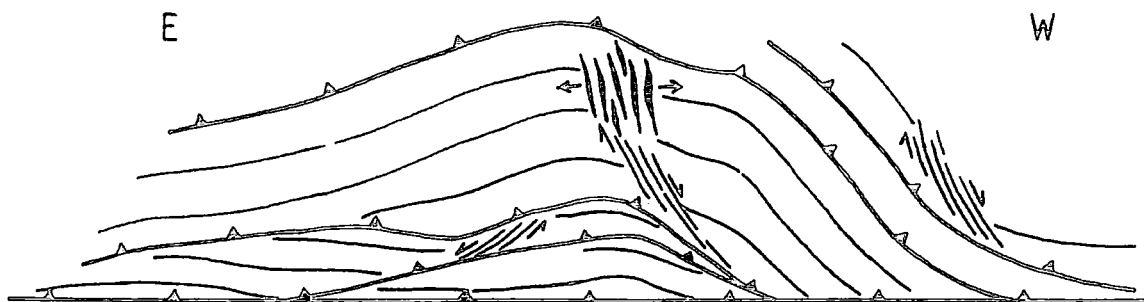
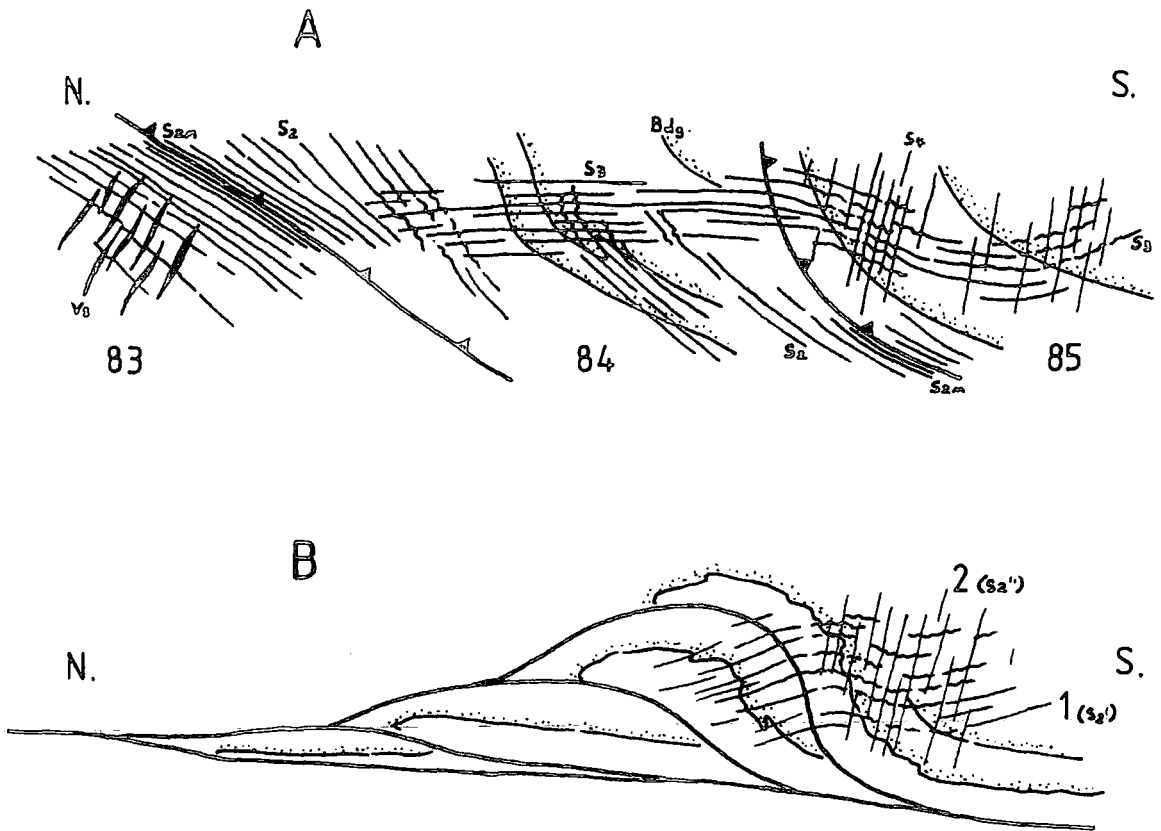


Figure 3.37 Schematic E-W structural section across the Middle Town stack illustrating culmination wall extension structures. These are shear bands and extensional crenulations on the culmination walls which form shear zones with lystric geometry. These structures are well developed on the western side of the stack where the imbricates have marked lateral hangingwall ramps. These fabrics would be S4 and S5 in the regional chronology of Hutton (1983), but are clearly secondary S2 fabrics. High in the stack, swarms of quartz veins accommodate stretch around the outer arc of the culmination.





**Figure 3.39** (A) Schematic diagram of structural relationships in exposures at the rear of the Middle Town stack (see also Figs. 3.36 & 3.37). In addition to S<sub>2</sub>, a shallow SW vergent cleavage and steep W vergent cleavage are developed, being restricted to a 'belt' at the rear of the stack. The cleavages would be S<sub>3</sub> & S<sub>4</sub> in the chronology of Hutton (1983). vs: Vein Swarm bdg: Bedding. (B) Schematic summary cross section through the Middle Town stack, illustrating the restricted distribution of the 'S<sub>3</sub>' and 'S<sub>4</sub>' fabrics. These fabrics are clearly D<sub>2</sub> in age, however, being causally related to the back-steepening of the stack rear. These secondary D<sub>2</sub> cleavages are therefore more appropriately labelled S<sub>2'</sub> and S<sub>2''</sub>. Details in text.

NE

Quartz veining in H.W. only

SW

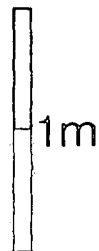
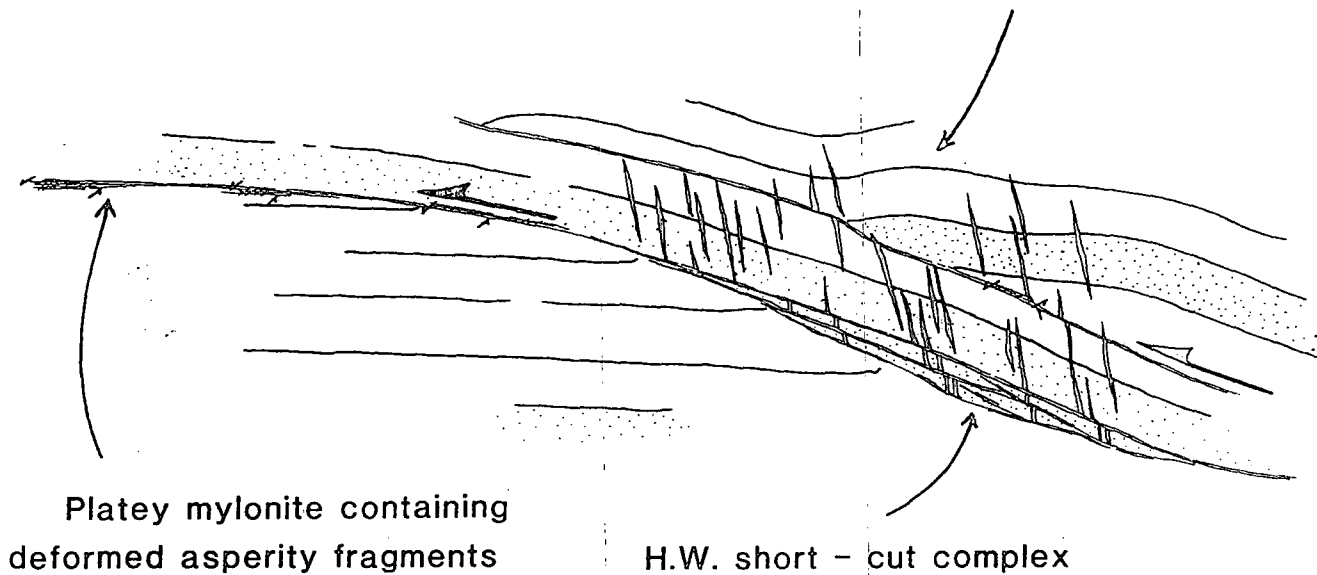
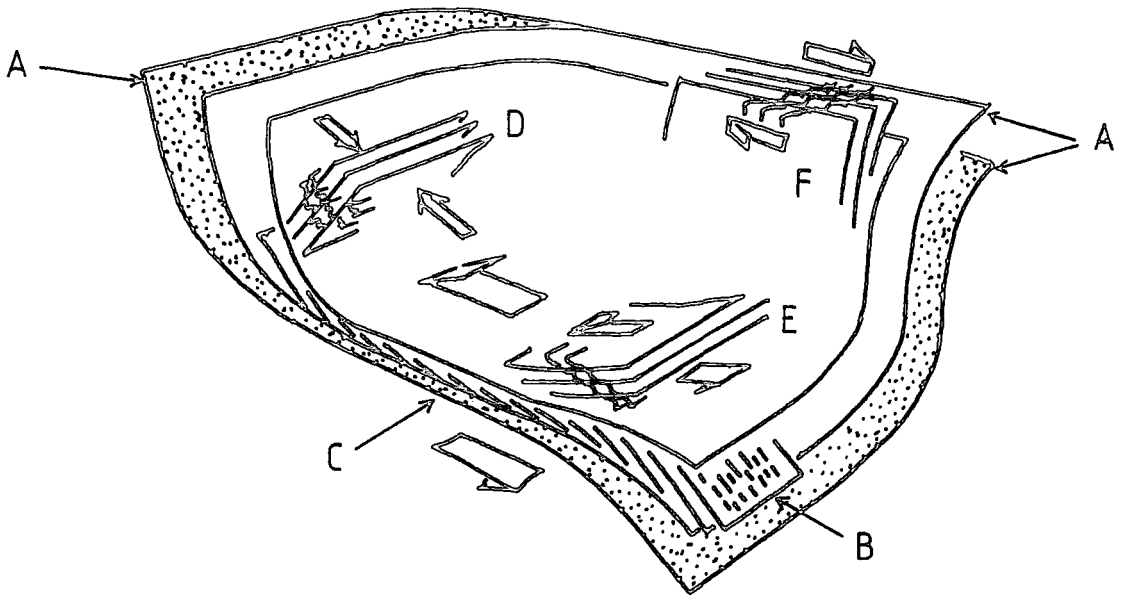


Figure 3.40 Simplified field sketch of discrete minor thrusts at 637157, locality 88, map 1. Note the ramp-flat geometries and hangingwall short cut (Knipe 1985) complex. Also of note at this locality is the presence of hangingwall restricted quartz veins (which have been cut by the short cut complex). These features are likely to represent progressive hangingwall deformation associated with ramp climb.



NNW



**Figure 3.41** Schematic 3D diagram of distribution of secondary fabrics associated with (m) scale 'tongue'-shaped shear bands at 637157, maps 1 & 2. (A) Bedding. (B) S2 containing mineral extension lineation. (C) S2 rotates and intensifies to S2m, bedding rotates and thins. (D) Secondary contractional fabric crenulates S2. (E) S2e extensional crenulation fabric. (F) Secondary strain slip fabric, deforms S2-bedding intersection lineation.

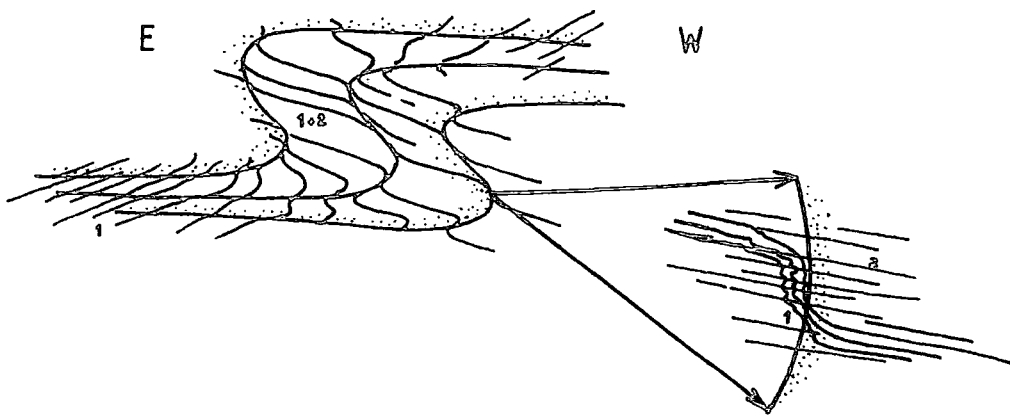


**Figure 3.42** Schematic diagram illustrating the apparent vergence anomaly in the fold pair at locality 97, map 1. The cleavage (1), verges west on long limbs, but is axial planar to the fold pair in the mid limb. Close examination reveals a second weaker cleavage (2), which is axial planar to the fold pair: the earlier cleavage (1) is transposed into the axial planar orientation, except at some bed margins where original vergence is preserved and (1) is crenulated by (2).

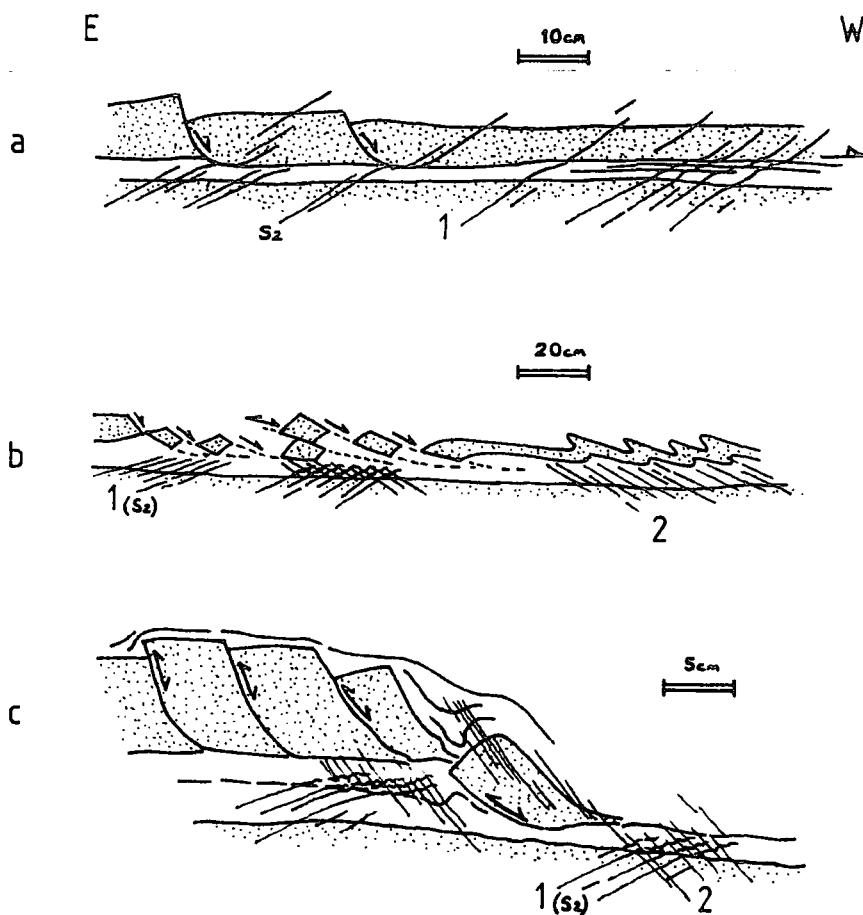


**Figure 3.43** Simplified field sketches of extensional structures in long limbs of the easterly vergent fold pair of locality 97, map 1. These structures disaggregate individual silt or quartzite beds with geometries reminiscent of listrically detaching graben structures. These structures appear to be associated with S<sub>2</sub> development, since S<sub>2</sub> is deflected by the rotations, but is also seen to cut straight across them. (a) Discreet high angle fractures in the disaggregated beds shallow and detach within zones of C shears in pelite beds below. (b,c) In some parts of the exposure, these extensional structures have been re-closed or 'inverted', indicating a shear sense reversal. These re-closed zones are spatially associated with development of a second cleavage (2), which is axial planar to the fold pair and crenulates S<sub>2</sub> (1). (See Fig. 3.42).

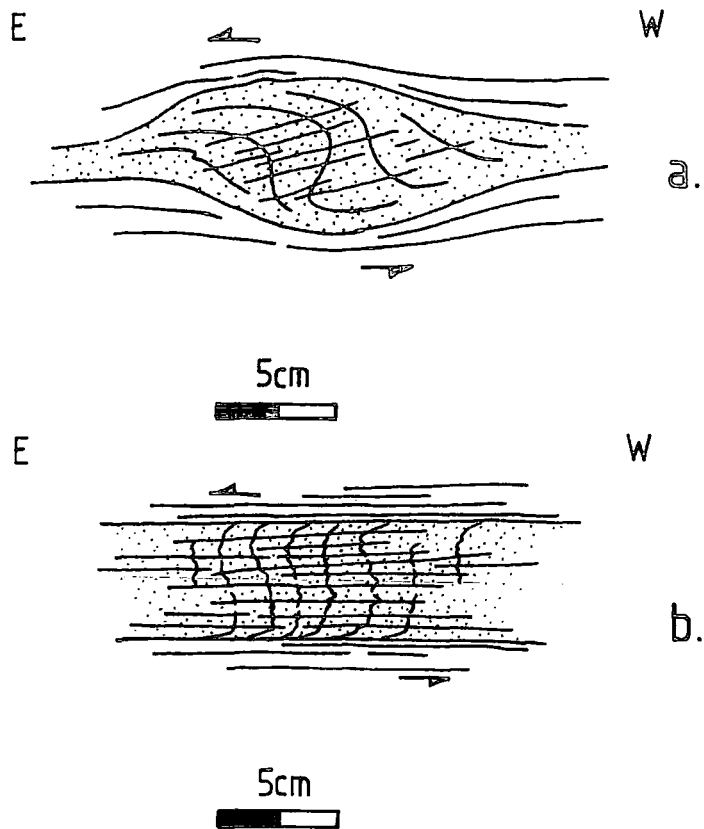


**Figure 3.44** Simplified field sketches of early structures preserved in the mylonitic banding of thrust (bt4), locality 91, map 1. (A) An F2 fold and axial planar S2 preserved in an asymmetric augen-like 'pod' of quartzite bedding. (B) Crenulated S2, apparently over-steepened to subvertical dip by viscous drag in a thinned bed.

## CHAPTER 4

### RAMPS

As described in chapters 2 & 3, the Breaghy Head peninsula contains a number of ductile thrusts which are morphologically very similar to thrusts from higher crustal levels. With only a few rare exceptions, the thrusts on Breaghy Head overshear towards the NW and generally have smooth geometries with long bedding parallel flats and shorter ramps which transgress stratigraphy at 20-30°. Some of the ramps have modest strike swings and a number of ramp strike directions are present on the peninsula, but no ramp segment dips away from the hinterland such that it might become extensional. It is the aim of this chapter to describe and discuss the nature and propagation of ductile thrust ramps.

Many of the ramps seen and mapped strike NW-SE or NNW-SSE, sub-parallel to the D2 stretching lineation, and are therefore lateral or very oblique structures. The intensification of S2 and S2m follows these geometries, but where the ramps are lateral or very oblique, F2 folds do not appear to be commonly developed as a precursor to the ramp. Folds, it would seem, are more commonly related to the development of less oblique or frontal ramp segments.

#### 4.1 Ramps and Folds

The thrust planes in the Breaghy Head area are associated with intense platy mylonite containing a strong NW-SE to NNW-SSE mineral extension lineation, small scale sheath folds and shear sense indicators. The main mylonitic fabric (S2m), can be traced

away from the thrust planes, where it's mylonitic character is lost, being transitionally replaced by non-mylonitic S2, which is axial planar to W & NW vergent F2 folds. This indicates that the thrusts and folds are part of the same D2 kinematic system. Less common easterly verging folds of identical style, dimension and geometry are also found within the penetrative deformation. Like their NW vergent counterparts, their axial planar cleavage becomes mylonitic in character towards thrust planes. This would suggest that the westerly and easterly vergent structures share a common kinematic origin related to the ductile thrusts. Indeed, Pitcher & Berger (1972) concluded that these structures were "...genetically related". The significance of the westerly and easterly vergence of these structures will be discussed in detail in chapter 5.

The geometry and style of the penetrative deformation folds is akin to that frequently described in the literature as 'intafolial' where hinges tighten and shallow along their axial surfaces viewed in profile section (Fig 4.1). Here the anticlinal hinge region is displaced forward and upward relative to the synclinal hinge region. In profile section this displacement dies out as the hinge tightness and amplitude decays both up and down the axial surface. Since these folds die out along strike, a displacement gradient also exists normal to the profile plane. These folds therefore represent biconvex discs of distributed displacement which effectively ramp material upwards and forwards such that they may be considered as being shear zones kinematically equivalent to thrust ramps. As described in the following sections, these structures frequently have thrust middle limbs and feature displacements of bedding cut offs parallel to the axial planar cleavage. This fabric parallel displacement is along an azimuth oblique to thrust flats, since it occurs between them where the pervasive axial planar cleavage is inclined with respect to the S2m of the flats. The displacements

therefore have a true ramp attitude with respect to flat-parallel datum lines (see Fig 4.1).

#### 4.1.1 Fabric Slip Ramps

Figure 4.2 illustrates folds with thrust middle limbs. In both cases, strain increases towards the thrust plane concomitant with intensification on the fold axial planar cleavage. A mineral extension lineation within the cleavage also intensifies and the cleavage becomes a (m) scale mylonite. Bedding is overturned and attenuated into this high strain zone where displaced tight to isoclinal rootless minor fold hinges are present. (The significance of augened vein quartz material in this zone will be discussed later). Although a transect into the mid limb appears to follow a smooth strain gradient, this is not the case. Within the gradient, more discrete (cm) scale mylonite zones are associated with the mid limbs of minor folds and produce stepped cut offs of beds near to the main mid limb shear zone (Fig 4.2). This produces a 'dog-tooth' strain profile similar to that described in chapter 2 (see Fig 2.14).

The sequence of development begins with formation of the mesoscopic asymmetric fold and its axial planar cleavage. This is followed by intensification of the cleavage, overturning of bedding in the mid-limb region, and development of a (m) scale mylonite (the main mid limb shear zone). Locally, the more discrete (cm) scale zones gently climb up and down section with respect to the pervasive fabric. This gives them a subtle ramp-flat geometry and suggests that they post date the fabric and (m) scale mylonite development. Shear bands associated with the (m) scale mylonite, however, either link with the discrete (cm) scale zones, or else deflect them. The more discrete mylonites must therefore have developed towards the later stages in the (m) scale zone's history. Time separation is therefore negligible

between formation of the various structural elements and a progressive localisation of strains is inferred.

at C20154349,

Similar relationships exist 2km SW of Dunfanaghy along the eastern shores of Port Lough, in a roadside quarry exposure of thinly bedded pelites. Here F2 folds with thrust middle limbs are seen some 10-15m above a major ductile thrust. By virtue of the nature of the exposure, both top and bottom of the folds' axial planes and the surrounding non-folded rock can be observed (see Fig 4.3). The mylonitic S2m fabric of the major thrust becomes less intense and steepens dip by some 20° up section to become the penetrative axial planar S2 cleavage in the exposure. Within the domain of individual folds, the cleavage again intensifies towards the mid limb where fabric parallel high strain zones displace cut offs of beds. This cleavage intensification and the attendant displacements seem to be bound within the extent of the folds, although in some cases they 'leak' beyond the fold for short distances. Long thin quartz veins are frequently intruded along these displacement surfaces, and again, generally contained within the folds' jurisdiction. Impurity trails within these veins record a gradual thrust sense opening at a shallow angle to the cleavage and displacement across the veins cannot be accounted for solely by restoring the vein walls along the opening trails. This indicates that the veins were intruded into the displacement zones during movement. Indeed, shearing of the trails at the vein margins confirms cleavage-parallel thrust displacement. Shear bands which occasionally deform the veins are restricted to the folds and are therefore interpreted to result from shearing within the developing ramp segment. Displacement of cutoffs decreases up and down the high strain zones from a central maximum, indicating a forward and rearward propagation along the axial planes.

Again, the folds and cleavage must pre-date intensification

of the cleavage and the development of cutoff displacements. Since the veins are cleavage parallel, are within the high strain zones, have opening trails which verge in the same direction as the axial planar cleavage and become thrust sense sheared themselves, the veins must have been formed during the displacement of bedding cutoffs. Clearly these veins were intruded during the latter part of strain and displacement localisation history. It is interesting to note here that augened quartz vein material was present within the (m) scale mylonite of the previous exposure description and that this exposure is lacking in the discrete (cm) scale mylonites. The shear bands are the latest structures to be developed. Since these are restricted to the fold shear zone, they are considered to be a consequence of movements on individual ramps.

Significantly, some of these structures are developed in alignment with one another, suggesting that individual ramp segments may propagate towards each other and coalesce to form single larger ramps.

In a coastal exposure in northern Breaghy Head, thickly bedded quartzites are folded by a large F2 fold and intruded by thin metadolerite sheets (Fig 4.4). The metadolerites are intruded within high strain zones parallel to the fold's axial planar S2 cleavage in a similar way to the veins described above. Passing through gentle-steep-gently inclined bedding, these sheets must post-date the main buckling stage of the fold development, but record several important aspects of the structure's later history.

The metadolerite sheets contain a cleavage parallel to that in the surrounding quartzites and are cloaked by an intensified version of the same cleavage. This would suggest intrusion during intensification of the mid limb fabric. At their tips, the sheets



are clearly seen to intrude along the cleavage planes and discrete cleavage-parallel shears (Fig 4.4). This suggests intrusion at a time when mid limb fabric intensification was generating discrete shearing and displacement of cut offs. As with the veins described above from the quarry exposure, continued shearing must have led to a build up of strains, leading to formation of a fabric internal to the sheets and to further intensification of the existing external fabric. Extensional crenulations which deform the internal fabric indicate that the sheets were sites of thrust displacement. Following this, the internal fabrics were deformed by flexural slip-shearing of bedding (Fig 4.4), indicating that the fold structure underwent a tightening phase. Close to the sheets, cleavage-parallel (mm) scale quartz veins with (mm) scale spacing are arranged in dense swarms. These are deformed by the flexural shearing, but play host to discrete cleavage parallel thrust mylonites which displace bedding and deform the flexural shear structures. This suggests that although the development of a mid limb thrust did not reach maturity at this locality (as it has at locality 40, map 2 (see Fig 3.9a)), discrete thrusts were still developing during the last stages of the fold tightening phase. These are the last structures to develop in the exposure.

We can see that the different structural elements described from the examples above share a common development sequence, summarized in Fig 4.5. This begins with a mesoscopic asymmetric fold and its axial planar cleavage. Increase in intensity of this cleavage (strain) in the mid limb is the next logical step, providing a smooth strain gradient backdrop against which the other structures and discrete strains are seen. During this stage at least some mylonite develops, but what is readily apparent is that strain becomes localised onto discrete planes which displace stratigraphy. This modifies the original smooth strain gradient to a more 'dog tooth' character (cf. Fig 2.14), and records the

localisation of displacement. It is at this stage when fluids or melts may become injected along these discrete zones; separation of the hangingwall from footwall presumably being a response to resulting heightened local strain rate and pressure of the intruding fluid; motion across the zone may create 'decompression' by effectively relieving the stress across the zone, thus enabling injection of pressured fluids into the zone. The fabric parallel slippage and mylonite development continues, however, deforming these discrete structures and veins. This would make these features difficult if not impossible to recognise in ductile thrusts of high displacement. The latest structures to develop are the discrete hangingwall and footwall mylonites and shear bands.

Fabric slip ramps are therefore characterised by the propagation of a fabric parallel thrust outwards from the mid limb of an asymmetric fold. Individually developing ramps may propagate towards each other and coalesce, thereby generating larger ramp structures which may ultimately become incorporated into the trajectory of a major ductile thrust. This is analogous to some thrust faults in foreland thrust and fold belts (eg. Ellis & Dunlap 1988).

#### **4.1.2 Fold Ramps**

As described above, the penetrative deformation folds may be considered as being shear zones, kinematically equivalent to thrust ramps. Fabric slip ramps are characterised by the localisation of displacement and strain and the propagation of a ductile thrust ramp outwards from the mid limb. By comparison, (as will be described below), 'fold ramps' ramp material from flat tip to flat tip, so that thrusts propagate towards the fold mid limb.

At 612200, locality 56 map 2, grey and micaceous limestones in the hangingwall of (bt2) are pervaded by platy S2m. The mylonites decrease intensity away from the thrust contact, (from cleavage spacing of less than 1mm to a spacing of several mm) in a series of low cliff exposures approximately 4-5m above the thrust. These exposures contain a number of (m) scale recumbent folds with axial planar S2m (see Fig 3.23).

The S2m intensifies (to spacing less than 1mm from the 'background' state) into zones of discrete (10-20cm) very high strain within the fold normal limbs, forming discrete shear zones (thrusts) at the lower and upper part of the fold axial planes. These shear zones are associated with fine fabric parallel quartz veins and shear bands, so that they are similar to the shear zones found within fabric slip ramps. The intensity of the shear zone S2m, however, decreases towards the central portion of the mid limbs so that the thrust shear zones effectively tip out in these areas. This is the reverse of the strain pattern associated with fabric slip ramps.

For most of their visible length, the discrete shear zones are bedding parallel and therefore have thrust flat geometry. As the folds are approached, however, bedding becomes overturned, attenuated towards and cut off against the shear zones so that the shear zones climb (ramp) section with thrust displacement. As the central portion of the mid limb is approached both up and down the axial plane, however, the shear zone S2m decreases intensity to 'background' as cut off displacements decrease and overturned bedding is less sharply attenuated. This strongly suggests that the shear zones (thrusts) tip both up and down the axial plane towards the central portion of the fold mid limb and further suggests that the thrusts may propagate towards one another through the fold.

A large scale example of a fold ramp is exposed in sea cliffs on the SE shore of Marble Hill Bay (845126 map 1). These cliffs are dominated by overturned SE dipping limestones and transition beds, folded by the Errigal Syncline (see chapter 1), the hinge of which runs NE-SW through Marble Hill Bay and non exposure inland. The overturned limestones, pelites, calc pelites and silts are pervaded by S2 fabrics and are host to two ramping ductile thrusts. These thrust structures are found within a major easterly verging fold pair (Fig 4.6). Both thrusts are associated with marked increase in S2 and S2m intensity into a (m) scale shear zone. Both thrusts (especially the higher of the two) are also associated with isoclinal overturning and sharp attenuation of bedding. Quartz veining, both fabric parallel and cross cutting tension gashes are spatially associated with the shear zones which also contain streaked and augened vein material.

The higher of the two thrusts places a hangingwall flat onto a footwall flat at the western end of the exposure, and maintains a hangingwall flat geometry towards the east whilst ramping at a progressively higher angle to bedding in the footwall. The thrust, and therefore the ramp, however, maintains a smooth trajectory of less than  $30^{\circ}$  with respect to the flat.

The lower of the two thrusts has a more complicated structure and geometry. At the eastern end of the exposure, the thrust has a flat on flat geometry. Moving westwards, the thrust ramps briefly in the footwall before returning to flat on flat geometry. Further west the thrust develops a hangingwall ramp on footwall flat geometry briefly (Z Fig 4.6), before a ramp on ramp geometry. At this position the S2m decreases intensity, veins are lost and bedding displacements across the thrust decrease. The thrust shear zone disappears as the S2m is lost into a broad zone of isoclinal and recumbent folds between the anticlinal hinge (X Fig 4.6), and the synclinal hinge (Y Fig 4.6). The implication here

is that the thrust has propagated towards the fold pair mid limb (similar to the fold ramp structures described from locality 56 above). Also present in this exposure is a large open anticlinal refold of the lower thrust. This may represent buttressing deformation in the form of layer parallel shortening in response to the fold ramp structure locking up. The development of this structure is summarised in Fig 4.7.

The generation of fold ramps must proceed with the development of the regional pervasive S2 cleavage. S2 must then intensify into discrete bedding parallel zones of localised strain, to form thrust flat shear zones. These thrust flats, developed as isolated dislocations would then propagate outwards from their point of origin. In order to maintain displacement continuity, it is likely that an asymmetric fold will develop between convergently propagating flat tips, especially where the tip stress fields interact. In this situation, the thrust tips would propagate towards one another through the fold to form a single larger thrust from originally separate 'cells'.

#### 4.2 Vein array Ramps

Unlike the two fold associated ramp styles described above, 'vein array ramps' are developed within zones of climbing tension gash vein arrays.

At 691200, locality 6 map 2, limestones and micaceous limestones are in thrust contact with quartzites. The thrust has a hangingwall flat on footwall ramp geometry. Platey S2m in the limestones is parallel to the contact which dips approximately 35° to the SE with respect to sub horizontal bedding in the footwall quartzites which is easily traced to within 1m of the thrust. If there is a footwall synclinal deflection of bedding into the thrust it is obscured by S2m and intense veining and must be

sharp. S2 intensifies towards the thrust contact, but has a narrow expression in both hangingwall and footwall. In the immediate hangingwall, (as discussed in chapter 3), this may be a response to the crystalline (recrystallised) nature of the limestone. Higher in the hangingwall, the limestones become micaceous and are host to a (m) scale zone of intense platy S2m which cuts across and is seen at the zone's lower margin to shear out the S2 in the 'lower' limestone. This intra-limestone thrust shear zone is orientated at a lower (20-25°) angle with respect to the footwall bedding. This S2m within this zone produces C shears of the earlier S2 and displaces quartz veins towards the NNW. This feature is interpreted as a hangingwall short cut (Knipe, 1985), which lowers the active ramp angle (Fig 4.8).

The hangingwall and footwall are pervaded by (mm) to (cm) scale quartz veins, which are extremely dense in the footwall, especially closer to the thrust contact, being numbered in thousands. These veins fall into two fairly distinct groups: long tension gashes and swarms of veins sub-parallel to the limestone-quartzite thrust contact. The tension gashes appear to form multiple sets of shallowly to moderately north-westerly dipping veins. There are a large number of mutually cross cutting and inter-connectivity relationships between individual veins, indicating contemporaneity. The majority of the cross cutting relationships, however, indicate that the oldest tension gash veins have the steeper dips and the youngest veins the shallower dips. The thrust parallel veins also cross cut and are cut by individual tension gashes, indicating negligible time separation between the development of each vein group. The S2m parallel veins in the hangingwall short cut shear zone are not seen to be cut by any tension gashes, suggesting that they are the latest veins to develop in the exposure.

A number of solitary R-2 shear bands are developed and

restricted to the footwall quartzites. These deform tension gashes, but are also cross cut by these veins in certain places, indicating development synchronous with the latter part of the veining history. Also restricted to the footwall are a number of minor NW vergent intrafolial folds and discrete bedding parallel thrust shears which also deform and in places are cross cut by tension gash veins.

The shear bands, folds and bedding parallel thrust shears are developed towards the latter part of vein generation and may represent deformation associated with incipient 'collapse' of the footwall prior to the development of the hangingwall short cut.

The features described above indicate that the  $35^{\circ}$  ramp angle may be too high to remain stable during ductile thrusting in the Breaghy Head area. Although incorporated into the thrust profile, such footwall ramps may hinder further thrust motion, such that short-cutting or footwall collapse aids mechanical expediency.

A smaller scale example of a Vein array ramp is to be found in the hangingwall of the Dunfanaghy Slide (at 280227, map 1), where the whole of the ramp segment is exposed. Here, a quartzite bed within pelitic and silty lithologies contains a zone of climbing tension gash arrays within which a discrete thrust ramp is developed, causing displacement of the bed.

As Fig 4.9 illustrates, the majority of the tension gashes are contained within the ramp region and show progressive steepening of veins followed by cross cutting of these veins by new generations of lower angle tension gashes. The later tension gashes also tend to be shorter structures than the earlier ones and are preferentially located within the central region of the vein array zone. It is within the central region of this zone of vein arrays that the discrete thrust is developed. This thrust

takes the form of a discrete (max. 5mm thick) zone of mylonite which thins and thickens erratically upwards and downwards, being knife sharp in some places, suggesting a fracture separation origin.

The above structures suggest that *vein array* ramps are generated by progressive localisation of displacement in the ramp region, and that prior to the separation of the hangingwall from the footwall, the deformation is essentially 'brittle flow'. This may suggest that the generation of this ramp style involves rheological control (ie. relatively high competency) and anomalous strain rates.

#### 4.3 Summary

Three frontal to oblique ramp styles have been identified in the Breaghy Head ductile thrust system. These are here named "fabric slip ramps", "fold ramps" and "*vein array* ramps". Ramps associated with fold development, especially fabric slip ramps, appear to be the more commonly developed frontal to oblique ramp styles in the Breaghy Head area, transtensional ramps being less frequently developed. All three ramp styles display displacement/strain localisation histories and are an integral part of the coalescent propagation of isolated flat and ramp thrust dislocation 'cells'. In order of increasing occurrence in the Breaghy Head area:

(1) In '*vein array* ramps', the ramp is generated in a zone of climbing tension gash vein arrays, with early deformation essentially brittle flow. The veining history shows an increasing density of veins in a central zone, the youngest veins appearing to concentrate in this central zone where they crosscut a series of earlier generations of tension gash veins. This represents a zone of strain (displacement) localisation within which a discrete



mylonitic thrust dislocation develops. The 35° ramp angle which appears to be characteristic of these structures, however, is apparently unstable such that *vein array* ramps appear to be susceptible to lock-up, creating a type of "buttressing" deformation in which the footwall begins to flatten and collapse towards the foreland in an attempt to achieve a lower, more stable ramp angle. This buttressing and collapse deformation is manifest by the dense generation of secondary structures (intrafolial folds, shear bands, layer parallel shears) which move the footwall away from the ramp. This deformation seems to be inefficient, and may be circumvented by the development of footwall or hangingwall short-cut dislocations which are better able to accommodate the displacement (strain) rate (cf. Knipe, 1985).

(2) Fold-associated ramps which result from coalescent propagation of isolated thrust flat dislocation cells (fold ramps) maintain displacement continuity by ramping bed length as relay structures between flat tips. the geometry of the folding between the flat tips is akin to that frequently described as 'intrafolial', (fold amplitude and hinge tightness decreases up and down the axial plane towards the flat tips), and S2m decreases intensity and increases dip away from the flat tips to become non-mylonitic S2, axial planar to the inter-flat tip F2 folds.

These structures develop as the adjacent flat-tip strains begin to interact and therefore the ramps post date the flats in the structural sequence. The ductile thrust dislocations propagate towards each other through the fold to create a flat-ramp-flat thrust trajectory.

(3) Fold-associated ramps which initiate as ramp-attitude thrust dislocation cells in their own right (fabric slip ramps) develop by progressive localisation of shear strain in F2 fold mid limbs. This leads to development of mylonitic S2m in the mid

limb, parallel to surrounding non-mylonitic axial planar S2. A central (m) scale mylonite zone is flanked by narrower (cm) scale mylonite zones, visible as intensification of S2 relative to "background" S2 strains. This produces a "dog-tooth" strain profile across the mid limb similar to that seen in thrust-flat tectonic slides (see chapter two and Figs 2.14, 2.15). The fabric slip ramps therefore represent 'small' thrust-ramp attitude tectonic slides in their own right. Displacement of mid limb markers takes place across these mylonite zones parallel to the surrounding axial planar S2 fabrics.

The geometry of fabric slip ramps is apparently precise. The fold hosting the ramp dislocation is 'intrafolial' and non cylindrical in style, with amplitude and hinge-tightness decreasing in all directions along the axial plane from a central maxima. The mid limb S2m zone is contained within the fold and the displacement of mid limb markers across the S2m zone has finite limits, decreasing in all directions along the zone from a central maxima. The fabric slip ramps therefore represent isolated thrust dislocation cells.

Propagation of the dislocation cell (fabric slip ramp) is in all directions outwards from and parallel with the mid limb S2m zone. Several fabric slip ramps are seen to be developed in alignment in some exposures and some appear to be hybrids of more than one original fabric slip ramp. This suggests that large fabric slip ramps may be developed by coalescence of a number of smaller dislocation cells.

Development of flexural shear deflection and thinning of S2 at discrete bedding parallel shears, similar to that described by Trayner & Cooper (1984), is occasionally seen in fabric slip ramp folds. This flexural shearing along bedding appears late in the mid limb strain history, reflecting a change in the dominant



deformation process from pervasive straining to more localised displacement processes, which culminate in the generation of discrete mid limb mylonitic dislocations.

As the thrust displacement localises and has to be accommodated by a progressively narrower mid limb S2m dislocation zone, anomalously high shear strain rates may be generated within the zone. This is evidenced by the presence of S2m parallel veins which are intruded into the mid limb late in the strain localisation history. This indicates that as the localisation process reaches an advanced stage, further propagation of the fabric slip ramp outwards from the mid limb S2m zone may, at least in part, be by brittle fracture. This is analogous to shear zone tips described by Simpson (1983). These S2m parallel veins and fractures (also noted in thrust flats, chapters 2 & 3), indicate that the ductile thrusts may become partially seismic dislocations.

Both fabric slip ramps and fold ramps are developed parallel with S2 where S2 is inclined ( $20 - 30^{\circ}$ ) with respect to bedding and the S2m of bedding parallel flats. They therefore have a 'true' ramp attitude. Once incorporated into a mature 'shaped' thrust trajectory, however, it would be very difficult to tell whether a fold related ramp originated as a fold ramp or a fabric slip ramp. Accurate displacement variation measurements along the thrust (similar to that of Ellis & Dunlap 1988), however, might identify fabric slip ramps as displacement 'highs' and fold ramps as displacement 'lows'.

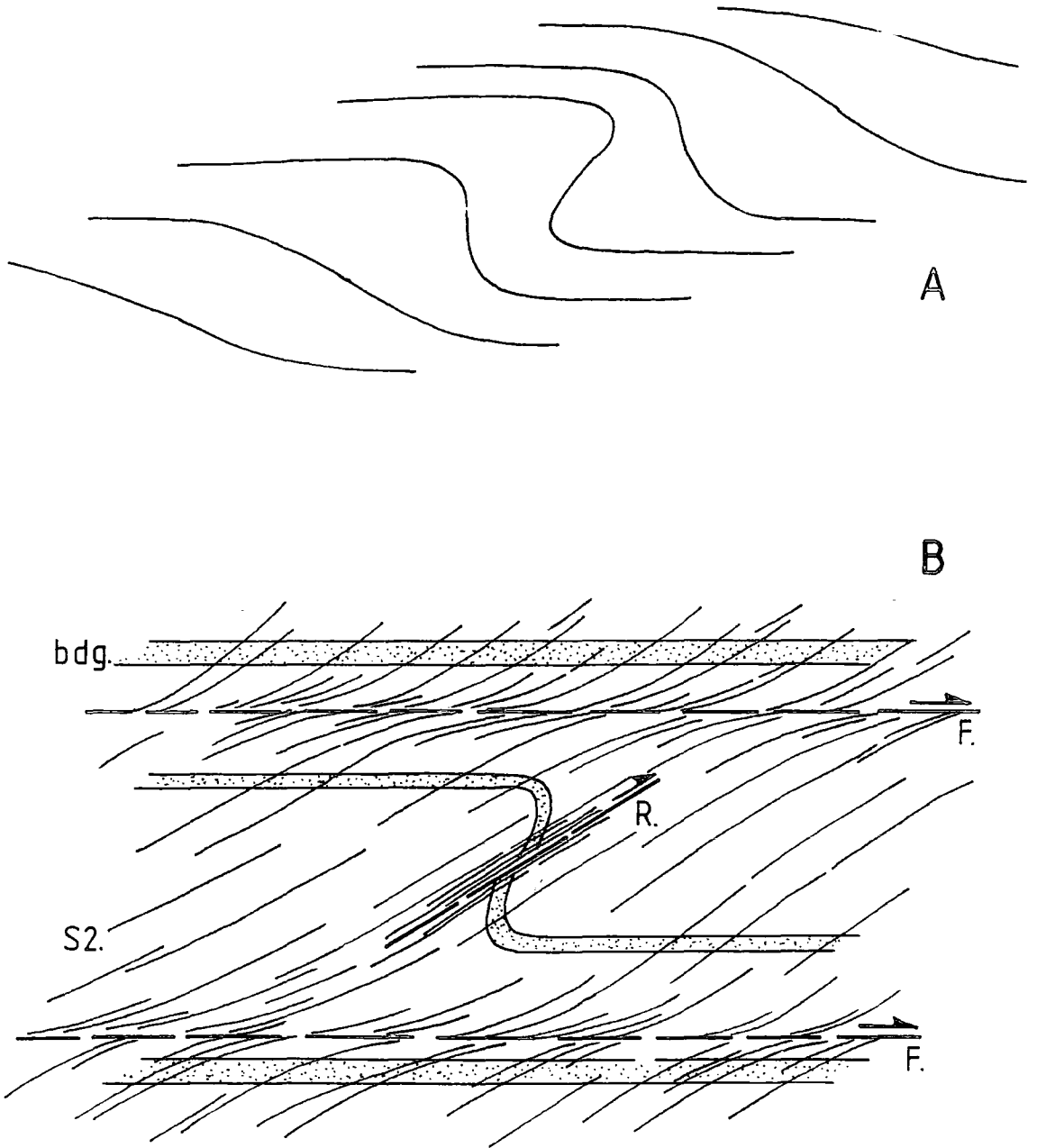
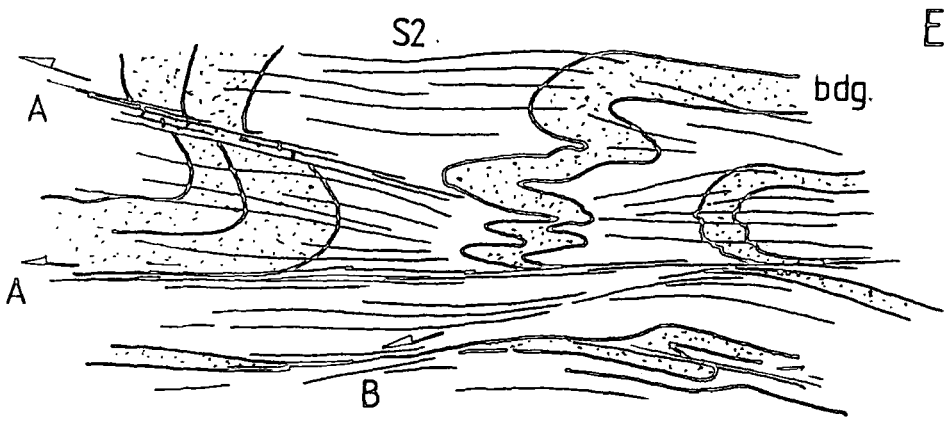


**Figure 4.1** Schematic diagrams illustrating the morphology of penetrative deformation folds in the Breaghy Head area. (A) Note that the amount of upward and forward displacement of the anticlinal hinge relative to the synclinal hinge decreases up and down the axial surface. (B) Bedding (bdg) displacement in a fold mid-limb, parallel to the fold axial planar cleavage (S2). The cleavage and therefore the displacement is oblique to bedding and therefore bedding parallel flats. The displacement in the fold mid-limb therefore has a ramp attitude with respect to flat-parallel datum lines (bedding). Note that S2 intensifies towards both ramps and flats. (R) ramp, (F) flat.

1.  
W



2.  
E

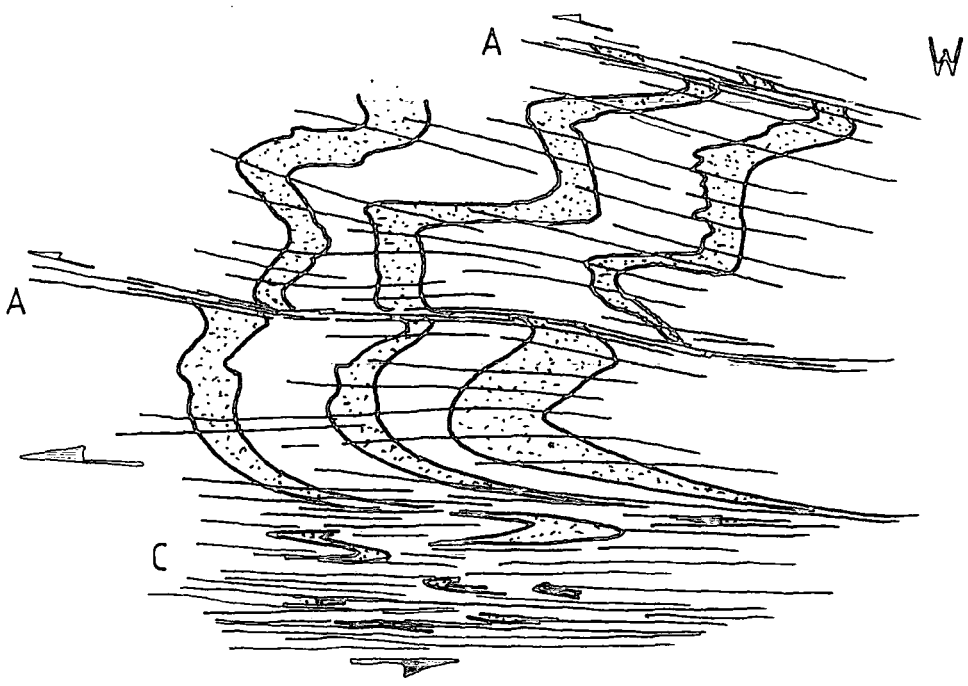
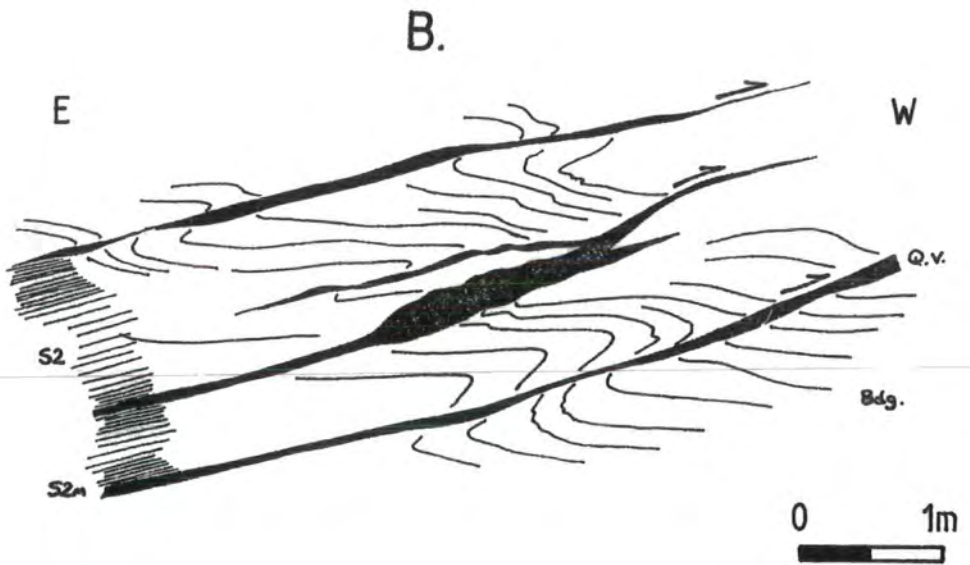
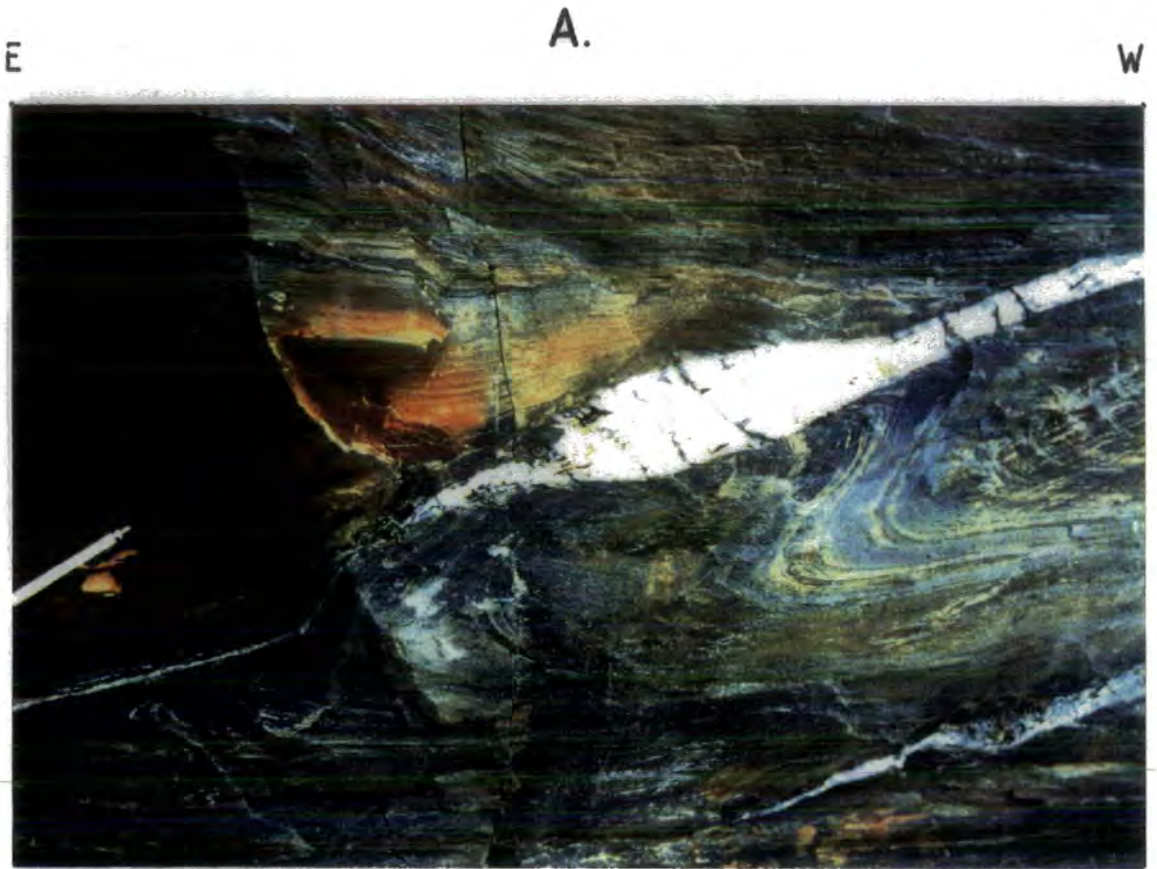
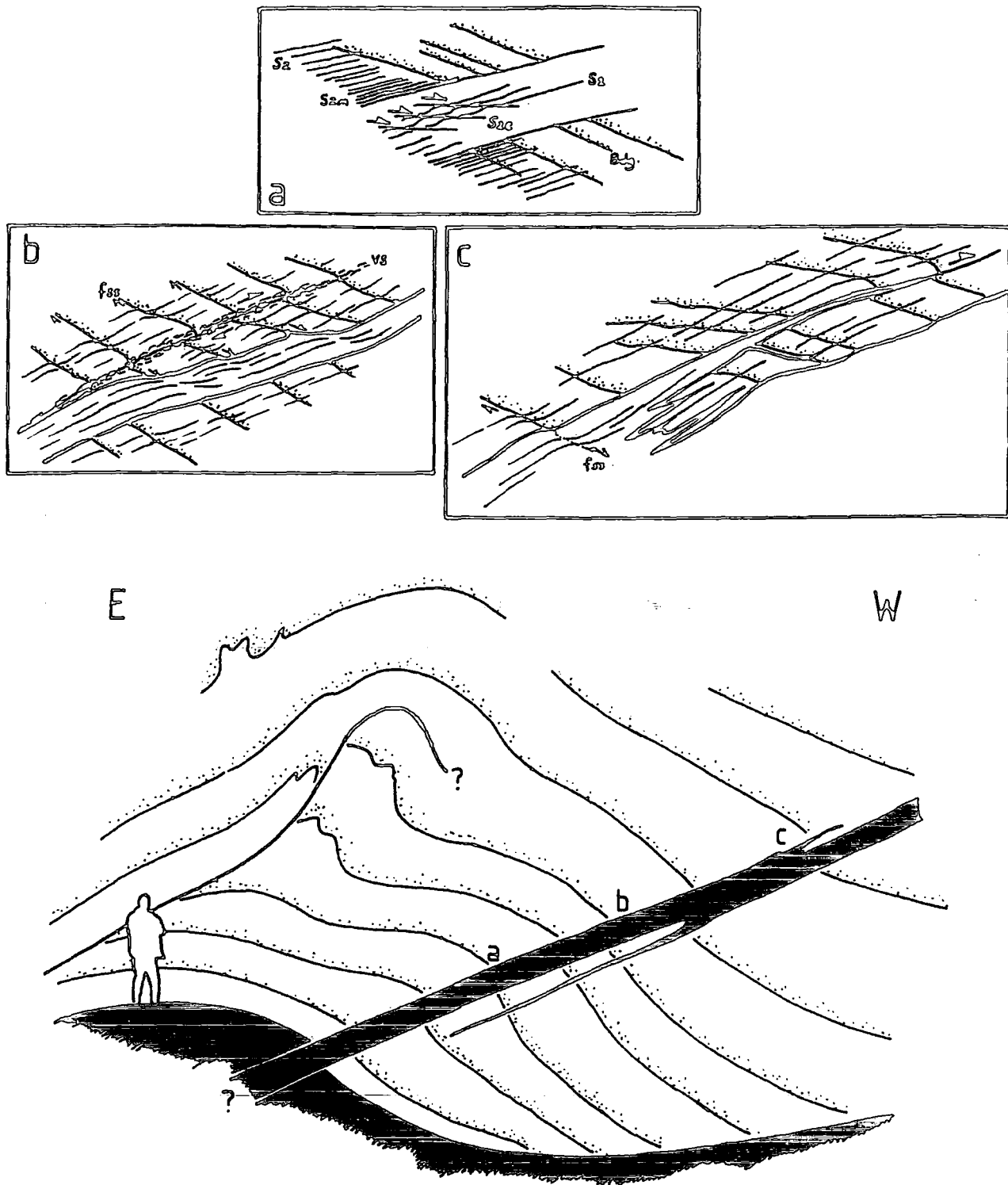


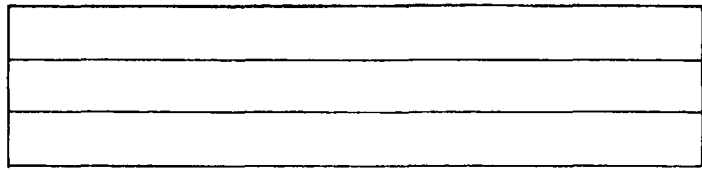
Figure 4.2 Simplified field sketches of examples of fabric slip ramps. (1) Within pelitic quartzites west of Dunfanaghy at 200186, maps 1 & 2. The main (m scale) ramp mylonites lie 1-2m below this example, which illustrates discrete (cm scale) zones of S2m across which bedding cut offs record (m) scale displacements. These zones alternately link with or are deflected by shear bands associated with the main ramp mylonites. (2) Within mixed pelites, silts and thin quartzites near Sandhill at 496145, maps 1 & 2. Illustrated from this example is the anticlinal mid limb portion of a fabric slip ramp. Strain (fabric intensity) increases towards the base of the diagram as bedding becomes overturned and attenuated into the mid limb's (m) scale mylonite. This (m) scale mylonite contains rootless recumbent minor fold hinges and augened remnant quartz vein material. Above this mylonite, more discrete (cm scale) mylonite zones displace bedding cut offs. (A) Displacements of bedding across discrete (cm scale) mylonite zones (S2m). (B) Shear bands deflect and/or link with discrete S2m zones (C) Main (m scale) ramp mylonites.



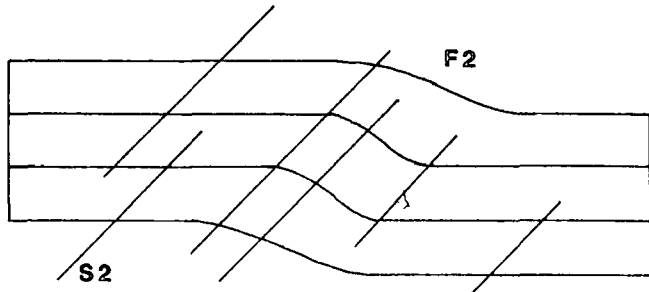
**Figure 4.3** (A) Photograph of a minor fabric slip ramp in pelites in a roadside quarry near Port Lough, 2km SW of Dunfanaghy. Note the presence of a quartz vein within the mid limb displacement zone. (B) Simplified field sketch of some more examples from the same quarry, occurring in a swarm. A number of the fabric slip ramps in this quarry occur in alignment, suggesting that they may propagate forwards and rearwards towards one another and coalesce to form single larger ramps. This may be the case with the uppermost ramp in the diagram which appears to be a composite of two individual ramp segments, each with a central displacement maximum. Note also shear banding in the central ramp and shear - thinning of the vein in the lowermost ramp, indicating continued displacement across the ramp.



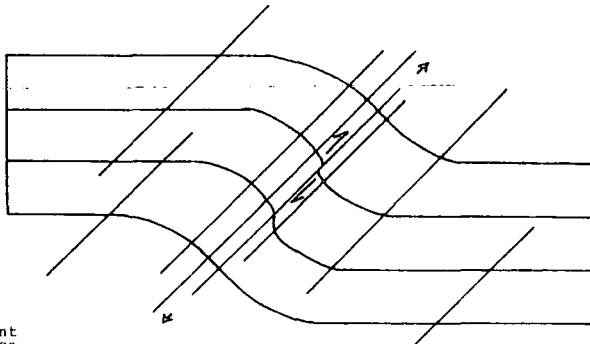
**Figure 4.4** Schematic field sketches summarizing structural relationships in a fabric slip ramp in quartzites at 610235, maps 1 & 2, west of Curragh Harbour. The mid limb of the fold at this locality is intruded by several thin S2-parallel metadolerite sheets. (A) The metadolerite sheets are intruded within and parallel to zones of intensified S2 in the quartzites. The metadolerites contain S2 parallel to that in the quartzites, and extensional crenulations indicative of north-westerly directed overshear. (B) Dense swarms of fine S2 parallel quartz veins emanate from the metadolerite margins. These vein swarms (vs) contain discrete (cm scale) mylonites which thrust displace bedding. These discrete thrusts also displace bedding-parallel flexural slip shears (fss) which deflect S2 in the quartzites and metadolerite. (C) Metadolerite is clearly seen to be intruded along S2 cleavage planes, S2 parallel shears and occasional bedding planes.



1

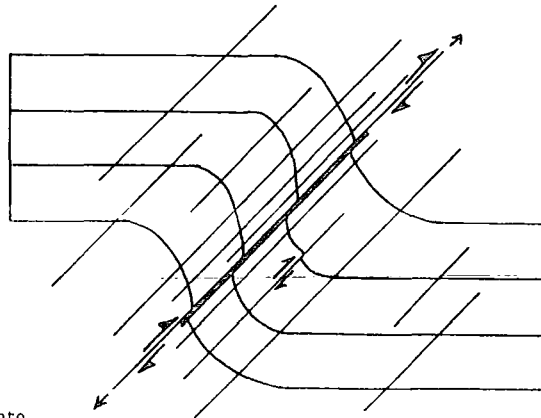


2



3

Increase in intensity of S2 in mid limb and localisation of displacement onto discrete S2 parallel zones of S2m.



4

Continued localisation of displacement onto a mid limb S2m mylonite zone (thrust). This thrust propagates forwards and rearwards along the S2 trajectory. Veins or igneous sheets may intrude parallel to S2 as displacement localisation peaks.

**Figure 4.5** Sequential diagram summarising the development of a fabric slip ramp during progressive displacement localisation.



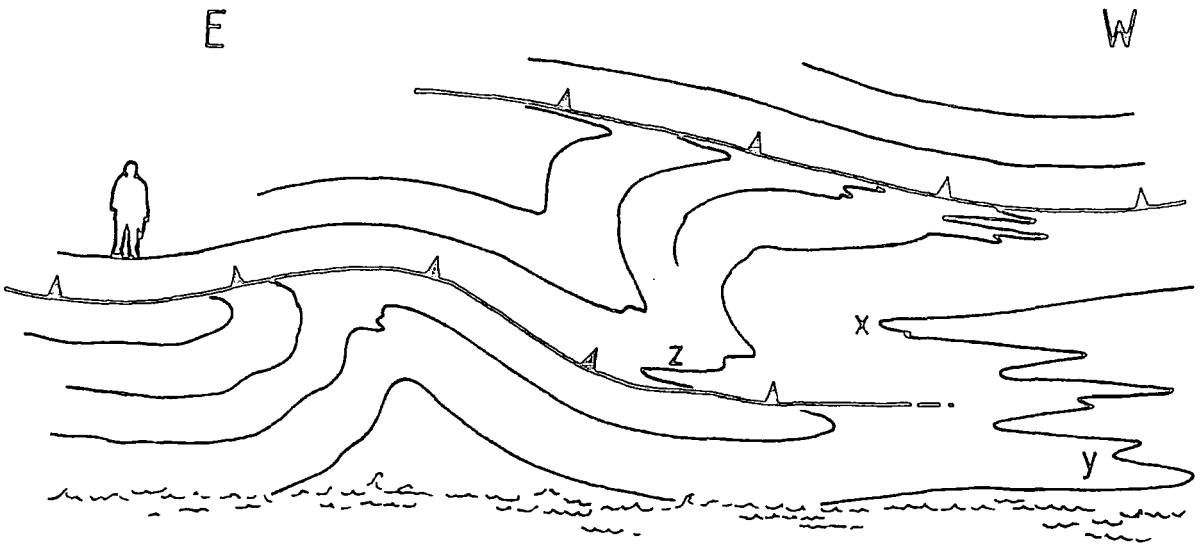


Figure 4.6 Simplified field sketch of a large scale example of a fold ramp in sea cliffs along the SE shore of Marble Hill Bay (845126, maps 1 & 2). X,Y,Z referred to in text discussion.

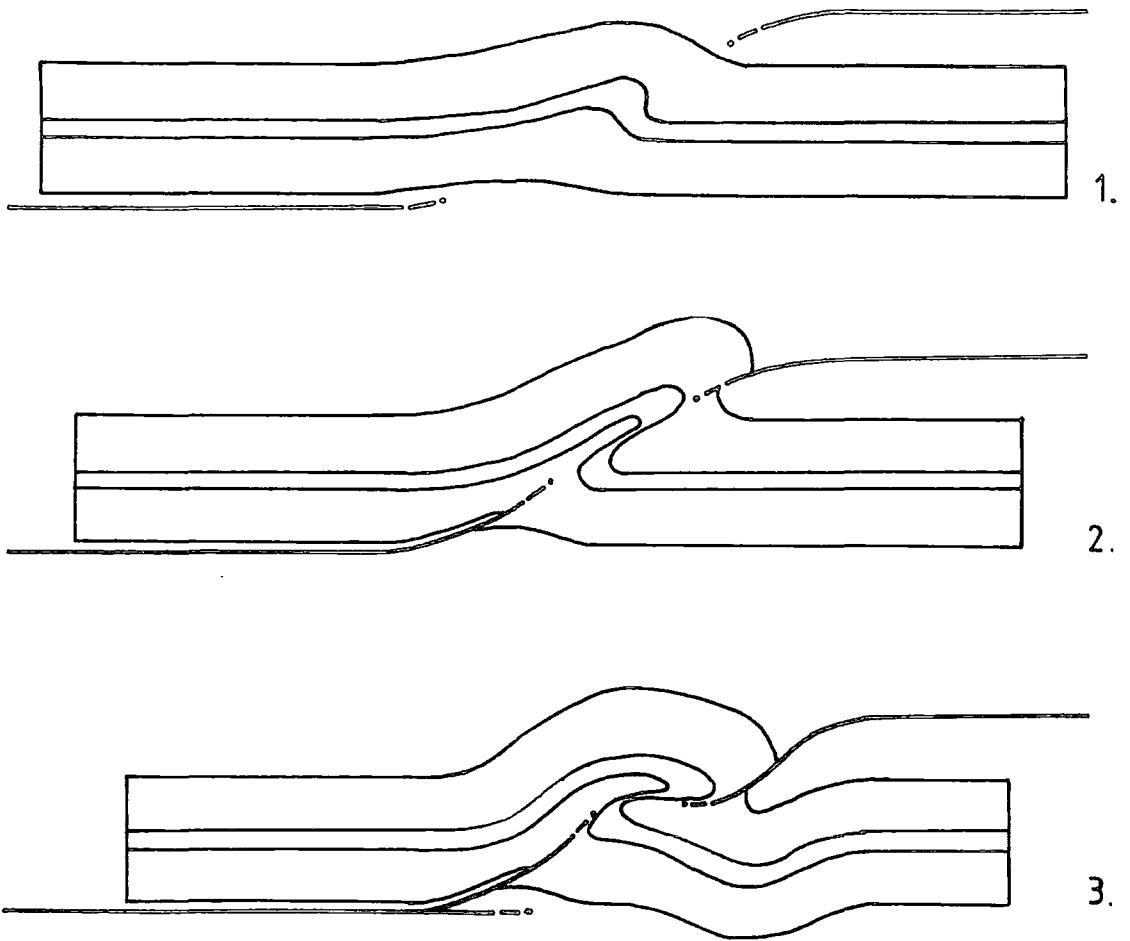
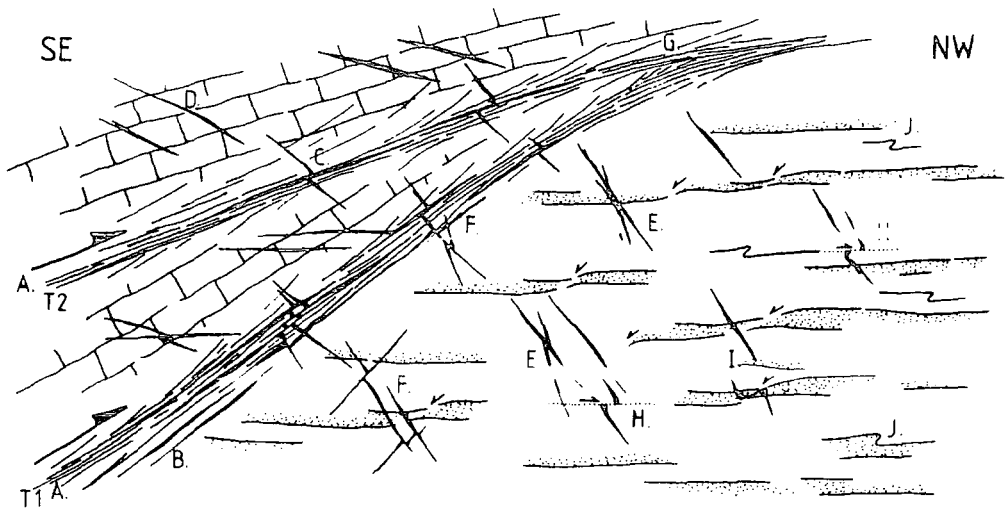


Figure 4.7 Summary diagram illustrating the development of a fold ramp. (1 & 2) Propagation of two flats towards one-another. The generation of a fold maintains displacement continuity between the lower and upper flats which may propagate into each other through the fold to form one larger thrust from separate "cells". (3) Re-folding of the fold ramp during buttressing and incipient footwall collapse.



**Figure 4.8** Schematic diagram illustrating structural relationships in the region of a vein array ramp located at 691200, maps 1 & 2. The exposure is approximately 4m high and 8-10m long. Two thrusts T1 & T2 dip towards the SE and emplace limestones onto sub-horizontal footwall quartzites. (A) Narrow (m scale) S2/platey S2m zones. (B) Thin (mm-cm scale) S2m parallel veins, become dense close to thrust contact, representing up to 50% rock volume. (C) Last veins in exposure parallel to S2m of upper thrust T2. (D) Arrays of thin (mm-cm scale) north-westerly inclined veins have shallower dip and lower density in the limestones. (E) Arrays of thin (mm-cm scale) north-westerly inclined veins have steeper dip and higher density in the quartzites. Also steep to sub vertical veins in quartzites cut by younger shallower vein sets. (F) Mutual cross cutting of inclined veins and those parallel to S2m of lower thrust T1. (G) S2/S2m of thrust T1 deformed by S2/S2m of thrust T2. (H) Sub-horizontal, bedding parallel shears in quartzites displace veins towards the NW. (I) Mutual cross cutting of R2 shear bands and veins in quartzites. (J) NW vergent intrafolial folds in quartzites.

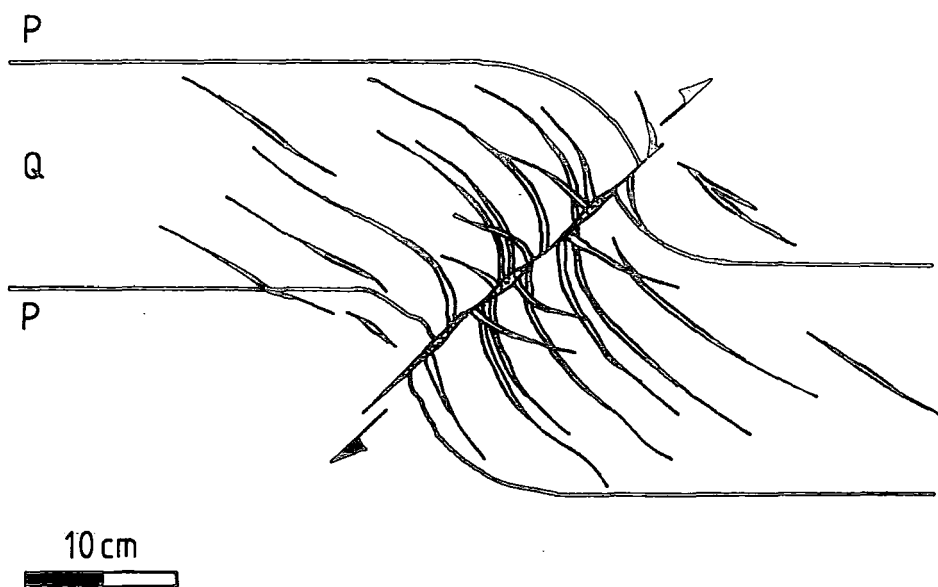


Figure 4.9 Simplified field sketch of a small scale example of a *Vein array* ramp at Dunfanaghy Harbour, 280227, maps 1 & 2. (P) pelites (Q) Quartzite bed. See text for details.

## CHAPTER 5

### PROPAGATION OF TECTONIC SLIDES AND THE GENERATION OF "SHAPED" DUCTILE THRUSTS

It has been shown (chapters 2 & 3) that within the present study area, continuum D2 ductile thrusting has been responsible for the development of a locally complex fold-fabric history of structures previously categorised into D2, D3, D4 & D5 (Hutton 1979a, 1982, 1983). In the Breaghy Head area, D2 is seen to contain the "penetrative deformation" fabrics and folds (D2 & D3 of Hutton op. cit.), related directly to ductile thrusts, and to contain the "non-penetrative" fabrics and folds (D4 & D5 of Hutton op. cit.), related indirectly to the ductile thrusts, chiefly as hangingwall strains of local kinematic significance. The development of the latter structures has been described in chapters 2 & 3. This chapter aims to address the development of the 'penetrative deformation' structures in relation to the propagation and movement of D2 ductile thrusts.

#### 5.1 History

The ductile thrusts of the Dunfanaghy - Breaghy Head area conform to the definition of tectonic slides proposed by Hutton (1979b). Tectonic slides form a distinct class of dislocation formed as part of the penetrative deformation stages in many mid crustal thrust zones (Hutton 1979b, Sanderson 1982, Platt & Behrmann 1986, Holdsworth 1989).

As discussed in detail by Hutton (1979b), "tectonic slides" (Fleuty 1964), were first identified by Bailey (1910) in the

Scottish Dalradian. Bailey's work was based on the recognition and correlation of stratigraphic sequences, with which he was able to infer the existence of major recumbent fold hinges where these stratigraphic sequences were symmetrically repeated. Bailey noted that the stratigraphic repetitions across the fold hinges were often incomplete, with formations excised or thinned against both sides of clearly mappable dislocations (slides) which gradually crossed the stratigraphy in the fold limbs. This led Bailey (1910) to suggest that slides were developed in fold limbs in response to the folding process.

Fleuty (1964) stressed this causal relationship between major folds and tectonic slides, proposing the rigid definition:

"A slide is a fault formed in close connection with folding, which is broadly conformable with a major geometric feature (either fold limb or axial surface) of the structure, and which is accompanied by thinning and/or excision of members of the rock succession affected by the folding."

As Hutton (1979b) points out, however, many tectonic slides do not appear to be related to major folds. Indeed, Bailey (1922, 1938) modified his earlier definition of slides to account for their occurrence in the absence of major folds, comparing major Dalradian slides and folds to Alpine thrusts and nappes, such that slides were considered to be an integral part of the deformation rather than a mechanical product of the folding process alone.

Hutton (1979b) emphasised the connection between tectonic slides and the penetrative deformation within which they are contained. The high strain fabrics of tectonic slides are orientated at only low angles to the surrounding lower strain pervasive cleavages of the same age, at clear variance to the

expected 45° angular relationship and underformed walls of 'classical' shear zones (cf. Ramsay & Graham 1970). This led Hutton (1979b) to suggest that tectonic slides are generated by intensification and modification of (principally) the regional pervasive fabrics, and to propose the following redefinition:

"A tectonic slide is a fault which forms in metamorphic rocks prior to or during a metamorphic event. It occurs within a zone of coeval penetrative (ie microscopic) deformation that represents an intensification of a more widespread, often regionally developed deformation phase. Within this zone of high strain slides may lie along and be sub-parallel to (although they will cross-cut on a large scale) the boundaries of lithological, tectonic and tectonic-metamorphic units".

The observations and discussions contained within this chapter and chapters 2, 3, & 4 provide a strong case for retention of this definition.

## **5.2 D2 "Associated" structures**

As described in chapters 2 & 3, the ductile thrusts in the Breaghy Head area are syn-metamorphic (greenschist facies) high strain mylonitic dislocations which duplicate stratigraphy with linked thrust geometries similar to those described from foreland thrust zones. The mylonites contain shear sense indicators which support thrust sense dislocation of the stratigraphy across the mylonitic zones. In addition, the ductile thrust high strain zones and the inter-thrust low strain horses contain "associated" structures, considered to be diagnostic of tectonic slides (cf. Hutton 1979b, Rathbone et al 1983, Fig. 5.1). These structures are now discussed with special reference to the Breaghy Head ductile thrusts:

### 5.2.1 Kinematic classification of F2 folds.

As noted in chapters 2 & 3 and Fig 5.1, minor intrafolial folds are seen to become tight to isoclinal with sheath closures and rootless geometries with increasing strain as ductile thrusts are approached. These folds often verge towards the W or NW, but also towards the E, and hinges become rotated towards parallelism with the D2 stretching lineation as strain increases towards the ductile thrust contacts. Whilst these folds often deform thinned bedding, they are also seen to fold S<sub>2m</sub>, some with axial planar cleavage indistinguishable from the S<sub>2m</sub> which they fold. These minor intrafolial folds appear to be restricted to the ductile thrust high strain zones, and were clearly formed after the ductile thrust strain profiles had been established. These structures are therefore considered to represent a distinct class of F2 folds related to local flow perturbations within and reworking of the mylonitic banding during ductile thrust motion (cf. Bell 1978, Bell & Hammond 1984, Evans & White 1984), and will not be discussed further. Other, larger penetrative deformation folds which fold bedding outside the S<sub>2m</sub> zones of the ductile thrusts or which S<sub>2m</sub> dislocates (see chapter 4) require more detailed consideration:

The chronology of deformation events in the study area (Hutton 1977a, 1977b, 1982, 1983) was first described and ordered at exposures of major tectonic slides (Mickey's Hole and Dunfanaghy) and subsequently correlated outwards from these localities (Hutton 1983, pers. comm. 1986). These two exposures are therefore the basis for the regional chronology of deformation events described by Hutton (op. cit.). This followed standard procedure for structural investigation in metamorphic polyphase deformation belts, based on the suggestion that the pelitic lithologies in these exposures might contain the most



complete record of the regional polyphase fold and fabric history. R-1 extensional crenulations are well developed in these exposures, and were therefore interpreted as a SE verging cleavage post-dating S2 (at a time when extensional crenulations were poorly understood), and formed the basis for D3 in the chronology, being correlated with E & SE verging folds and cleavage in surrounding rocks regionally (Hutton pers. comm. 1986). In the Breaghy Head area, this cleavage is restricted to the D2 thrust high strain zones and demonstrably an extensional crenulation cleavage (this chapter and chapters 2 & 3).

Significantly, westerly vergent folds and easterly vergent folds (F2 and F3 respectively in the sense of Hutton op. cit.) are geometrically identical (Hutton 1977a, this work chapters 3 & 4). This work has shown that both the westerly and easterly vergent folds share a common axial planar S2 cleavage which is indistinguishable despite orientation. These observations strongly suggest that both fold sets are D2 in age. The westerly and easterly vergence of the folds cannot be explained as vergence reversals across major fold hinges, since the required younging reversals and symmetrical repetitions of stratigraphy are absent. Indeed, both westerly and easterly vergent folds are seen to occupy the same stratigraphic and/or structural level in some exposures with notable absence of fold interference relationships. Thus the westerly and easterly verging folds in the study area appear to be mutually exclusive in 3D space, such that "F3" folds are not seen to refold F2 folds. These observations further suggest contemporaneous (D2) formation of the westerly and easterly verging folds.

In addition to having axial planar S2 cleavage, both westerly and easterly verging folds are seen to host D2 ductile thrust ramps (chapters 3 & 4). This confirms a D2 age for these structures and strongly suggests that their orientation is an

original feature associated with the development of D2 ductile thrusts.

As described in chapter 3, folds shown to be intimately associated with rare backthrusts possess an easterly vergent axial planar cleavage which crenulates S2, however this cleavage is seen to be in mutual cross-cutting (conjugate) relationship with S2 (eg. Fig 3.14). Both fabrics are therefore of D2 age with negligible temporal separation. Similar conjugate fold and fabric relationships associated with forethrusts and backthrusts have been described from other thrust belts (eg. Morley 1986, Seago & Chapman 1988). Indeed, spatially and temporally localised polyphase structure sequences are not uncommon within foreland thrust belts (eg. Butler 1982b, Coward & Potts 1983). The E to SE vergent conjugate cleavage to S2 is therefore here termed "conjugate S2". The E & SE verging 'conjugate S2' and attendant folds therefore represent a distinct class of D2 structure, restricted in development to the immediate vicinity of rare backthrusts and are therefore not considered further.

It is now possible to examine the relationship between D2 ductile thrusts and "primary" S2 and F2 folds (ie those remaining in the data set after removal of small scale intrafolial folds and 'conjugate' structures) with confidence. As described above, the westerly and easterly vergence of these structures appears to be an original feature which is clearly not related to larger scale F2 structures or polyphase deformation. Passive rotation of the fold hinges towards the X direction during progressive shearing (cf. Sanderson 1973, Escher & Watterson 1974, Rhodes & Gayer 1977, Bell 1978, Cobbold & Quinquis 1980) to explain the vergence pattern is also precluded since the high strains required are absent. Thus, primary F2 folds form a distinct class of D2 structures which must be intimately associated with ductile thrusting in the area. In view of the above arguments, this

association must pertain specifically to forethrusts.

### 5.2.2 "Primary" F2 folds

"Primary" F2 folds (defined above), with dislocated mid limbs have been described in some detail in chapters 3 & 4. Some of these folds have become incorporated into mature 'shaped' ductile thrust profiles, now present as hangingwall anticlines and footwall synclines. Some of these folds form structures which connect leading and trailing tip lines of adjacent ductile thrust flats, and others, now present in the hangingwalls of the thrusts appear to have escaped direct incorporation into the thrust profiles and instead host isolated thrust ramp dislocation "cells". In view of the strong association between D2 ductile thrust ramps and F2 folds, it is suggested that the majority of primary F2 folds may potentially have nucleated ramps for incorporation into through-going ductile thrust profiles.

As described in chapter 4, the thrust dislocation of primary F2 fold limbs is parallel to the axial planar S2, across zones of S2 parallel S2m. The parallelism of the S2 and dislocating S2m presents an apparent paradox, since it implies shearing along the axial planar cleavage, which is generally regarded as representing the XY plane of the strain ellipsoid and therefore a plane of no shear strain. This problem has been addressed by Ghosh (1982), who demonstrated that axial planar cleavage may rotate as a material plane to deviate from the orientation of the XY plane of the strain ellipsoid if the deformation is characterized by a combination of pure shear and simple shear. This angular deviation will always be small, being less than 5° for simple shear and even less for combined pure and simple shear.

Under these conditions, the axial planar cleavage becomes a plane of shearing and may potentially accrue considerable fabric-parallel

shear strains, even though the angular deviation from the XY plane is only slight. This style of deformation in the F2 fold mid limbs is evidenced by the shallowly oblique thrust-sense impurity trails observed in S2m - parallel quartz veins described in chapter 4, where the instantaneous stretching azimuth is clearly outside the cleavage plane.

It is important to note that the angular deviations between S2 and the XY plane of the strain ellipsoid discussed above are too small to be resolved by field measurement. For the purposes of this discussion, we may therefore consider F2 fold mid limb ramp S2m to be parallel to the axial planar S2 in the hinges and normal limbs, as described in chapters 3 & 4. It is also appropriate to note here that S2-bedding intersection lineations are parallel to F2 hinges, such that S2 is, within the bounds of field resolution, an authentic axial planar cleavage. The D2 ductile thrust ramps may therefore be considered to be 'axial planar' to primary F2 folds.

"Facing" is defined by Shackleton (1958), Lisle (1985) and in discussion by Holdsworth (1988) as follows:

1. Fold Facing: the direction, normal to the fold axis, along the fold axial plane, and towards the younger beds.
2. Cleavage facing: the direction, normal to the bedding plane intersection, along the cleavage plane, and towards the younger beds.
3. Fault Facing: the direction, normal to the bedding plane intersection, along the fault plane and towards the younger beds.

In view of the parallelism of the ductile thrust ramps and

the axial planar S2 found within the ramp-hosting primary F2 folds, the axial plane, cleavage plane and fault plane in the above definitions are in this case equivalent reference planes. Since, as noted earlier, the majority of primary F2 folds may potentially have nucleated ramps, it is possible to consider primary F2 fold facing data as representative of the potential range of D2 ductile thrust ramp facing directions.

In Fig 5.2, So, S2 and S2m, D2 stretching lineation and, following a technique described by Holdsworth (1988), primary F2 fold facing data are presented stereographically. A number of important features are evident in the facing stereonet (Fig. 5.2d):

1. All downward facing primary F2 folds have a W to NW facing azimuth, suggesting an axis of rotation orthogonal to the D2 ductile thrust transport direction. These folds' downward facing can be attributed in the field (chapter 3), to buttressing deformation or thrust folding caused by movement of underlying thrusts during continuum D2 thrusting.

2. Holdsworth (1988) indicates that in areas of deformation dominated by sheath folding, the lines of facing should plot about a great circle coincident with the mean axial plane of that folding. This geometrical restriction must reflect the rotation of hinges towards the X direction within the axial plane, a condition of the sheath folding process (cf. Escher & Watterson 1974). As Fig 5.2d shows, however, the lines of facing of primary F2 folds in the Breaghy Head area are not coincident with any particular great circle.

3. The primary F2 facing azimuths show a broad bimodal distribution with respect to the mean D2 thrust transport direction, one cluster facing from SW to NW and one from E to

NE. Those folds hosting examples of D2 thrust ramps (bold azimuth arrows) are restricted to the NW and NE, with facing azimuths forming a more acute angle with the NNW transport direction than the non-ramp hosting primary F2 folds. Significantly, the majority of D2 thrust ramp hosting folds face to the NW in a frontal thrust orientation.

The easterly and westerly vergence and facing pattern of primary F2 folds in the Breaghy Head area cannot be attributed to a sheath folding process involving rotation of hinges towards the X direction within the S2 plane. This is geometrically untenable (Fig 5.2d) and (as noted earlier), there is insufficient strain in the rocks hosting the folds to have accomplished the required rotations.

In view of the above, it is suggested that these folds formed with hinges close to their present orientations with only modest rotational modification. The vergence and facing pattern of primary F2 folds must therefore reflect gross inhomogeneity in the D2 deformation. Significantly, the D2 strain inhomogeneity which the D2 ductile thrusts represent has been described in chapters 2 & 3.

As described in chapters 2, 3 & 4, the primary F2 folds and D2 ductile thrusts are kinematically intimate. It would appear that the development of the primary F2 fold orientations are related to the development of the D2 ductile thrusts, indeed it has been shown in chapter 4 that primary F2 folds are intimately related to the process of D2 ductile thrust ramp propagation. It is therefore suggested in the absence of any identified post D2 refolds (chapter 3), that the primary F2 fold vergence and facing pattern and the D2 deformation inhomogeneity this represents is a direct result of D2 ductile thrust propagation.

### 5.2.3 D2 strain, S2 cleavage and bedding

As described and discussed in chapters 2 & 3, D2 strain increases towards D2 ductile thrust contacts. The strain was estimated in the field qualitatively from S2 spacing, nature and intensity, and where possible quantitatively from measurement of porphyroblast (chiefly pyrite) pressure shadows. The strain was found to increase exponentially towards the thrust contacts in under 20m from "background" strains to  $1 \times 10^1$  in excess of 8 or 9 closest to the D2 thrust contacts. This clearly indicates localisation of D2 strains and displacement at the D2 ductile thrust contacts so that the majority of thrust displacement is carried along these thin high strain zones, as evidenced by the sharp lithological breaks across the thrust contacts. Indeed, this D2 strain localisation around the thrust planes enables mylonite (thrust) bound low strain horses to be identified. The D2 thrusts therefore represent dislocation-related inhomogeneity in the D2 deformation.

In detail, the D2 ductile thrust strain profiles are apparently not simple exponential increases towards the thrust contacts, since the presence of localised bands of high shear strain or thin zones of intense S2m offsetting markers form an integral part of the strain profile in some thrusts. This superimposes on the smooth exponential strain profiles a 'dog-tooth' pattern of strain 'highs' (cf. Fig 2.14).

The S2 cleavage becomes mylonitic as D2 thrust contacts are approached such that S2 is transitional with S2m. Indeed, as Hutton (1983) noted, platy S2m is a diagnostic feature of D2 ductile thrusts.

S2 is seen to curve asymptotically towards parallelism with the D2 thrust planes as they are approached, such that S2m is

parallel or sub-parallel to the thrust planes. Thus, (a) S2m will be shallowly SE dipping, parallel to D2 thrust flats and oblique to steeper SE dipping S2, (b) S2m will be steeper SE, easterly and westerly dipping parallel to D2 thrust ramps where S2m will be less oblique or sub-parallel to S2 (as indicated in chapter 4). These relationships are reflected in Fig 5.2b.

As S2 swings towards parallelism with D2 thrust planes, the angle between S2 and bedding decreases from 20-30° towards parallelism as the thrust planes are approached, the thrust flats being parallel or sub-parallel to bedding (cf. Figs 5.2a & b). Bedding thickness is also progressively reduced towards the D2 thrust planes to become obliterated by the high strains such that platy S2m and S2m related mineral banding is the only recognisable pervasive planarity closest to the D2 thrust contacts.

The thickness of the D2 ductile thrust high strain zones (mylonite and intensely cleaved rock) is noted to be greater in the hangingwalls of D2 thrusts. The high strain zones are generally less than 20m thick (this thickness is laterally variable, such that 20m is an approximate maximum). This indicates further spatial inhomogeneity of D2 thrust related strain.

#### **5.2.4 D2 stretching lineation**

The D2 stretching lineation, representing the X direction of the strain ellipsoid is contained within the S2 cleavage planes which represent the XY plane of the D2 strain ellipsoid (cf. Figs 5.2b & c). As a general feature of the Breaghy Head D2 ductile thrusts, the stretching lineation (X2) intensifies towards the thrust contacts as the host S2 intensifies in the same direction.



Hutton (1977a, 1979b) noted intensification of contemporaneous stretching lineation as a diagnostic feature of tectonic slides, aiding their field recognition, but also noted (Hutton 1979b, pers. comm. 1989) that this feature is absent from some tectonic slides, suggesting that this may be a result of syn- or post-tectonic annealing of the mylonites. In the case of the Breagh Head D2 ductile thrusts, a qualitative estimate of X2 strength indicates that the relative intensification of X2 towards the thrust contacts is sometimes conspicuously variable along strike. A change of lithology would be expected to accompany this if an along strike variation in annealing (secondary recrystallization) were responsible, since:

1. A pure quartzite and pure limestone might be expected to undergo secondary recrystallization at different rates and to different finite grain sizes under the same (greenschist) metamorphic conditions.

2. The presence of a second phase (eg. mica) is known to suppress migration of grain boundaries during recrystallization (eg. Drury & Urai 1990). This effect is noted in limestone exposures where pure limestone bands are seen to have a larger grain size with saccharoidal crystalline texture and less distinct S2m planes and stretching lineation development than adjacent micaceous limestone bands where grain size is submicroscopic with intensely developed S2m and X2 (eg. -localities 5 & 6 and along the SE shore of Marble Hill Bay, chapter 3, maps 1 & 2).

The lateral variation in X2 intensification towards D2 thrust contacts noted above, however, appears to take place within identical lithologies along strike (eg. within quartzite beds and within metadolerite between localities 7 & 9 west of Dunrudian, maps 1 & 2). If variation in secondary recrystallization is not responsible for the lateral variation in

X2 intensity, it must represent an original feature developed during the D2 ductile thrusting process. This may imply lateral variation in the finite extension in the X direction of the D2 strain ellipsoid. The intensification of X2 towards the D2 thrust contacts is an integral part of the D2 thrust high strain zones, therefore any lateral variation in the X2 intensity must have developed during the strain profile development and subsequent displacement history of the D2 ductile thrusts.

### 5.2.5 Tectonic schists

At some exposures of D2 ductile thrust contacts, a thin (cm scale) zone of "tectonic schist" separates hangingwall and footwall, the best examples of which are exposed at Mickey's Hole and Lishagh (Figs 2.9 & 2.15a).

This tectonic schist is a mineralogical hybrid of the hangingwall and footwall lithologies, containing small lenses and rootless fold hinges of wall rock lithology and/or vein quartz within the hybrid schistose matrix. This represents locally developed metamorphic and mechanical mixing of the adjoining hangingwall and footwall lithologies at the thrust contact. This requires to some degree the 'shaving' and fragmentation of wallrock asperities (as indicated by the presence of the porphyroclasts of wall rock lithologies), suggesting local pseudo-brittle behaviour along the thrust contact such that the thrust motion is carried along the knife sharp plane this represents. Indeed, as noted in chapter 3, brittle fractures are associated with the tip zone of a D2 ductile thrust at locality 88, (maps 1& 2, Fig 3.40) and the presence of S2m parallel brittle fractures within D2 thrust ramps has been described in chapter 4. The presence of these fractures and tectonic schists at some localities suggests that D2 ductile thrust propagation may, at least in part, proceed along brittle fractures.

### 5.2.6 Boudinage

In section 5.2.1, F2 folds have been categorised into minor intrafolial F2 folds resulting from flow perturbations within the S2m banding, 'conjugate' F2 folds related to rare D2 ductile backthrusts and 'primary' F2 folds related to the D2 ductile forethrusts which dominate the D2 deformation in the Breaghy Head area. In section 5.2.2 the nature and orientation pattern of 'primary' F2 folds bear testimony to inhomogeneity in D2 contractional deformation associated with the D2 ductile thrusting process. The presence of D2 boudinage and shear bands must further indicate inhomogeneity in the D2 deformation, since the contractional and extensional deformation must coexist kinematically. An examination of the geometry, orientation and relationship of boudinage to D2 strain leads to further insight into the nature of D2 ductile thrust propagation and motion.

As noted in chapters 2 & 3, boudinage is contained within the higher strain zones approaching D2 ductile thrust contacts. The rheological control to this boudinage is evident in the fact that metadolerite sheets and quartzites between pelites in thinned bedding are boudinaged, as are the more quartz or calcite rich microlithons between the more mica rich planes of S2m cleavage. Thus, as noted in chapter 2 & 3, where boudinage is well developed, the individual boudins become smaller and more frequent, or denser as D2 ductile thrust contacts are approached. Certainly, where small scale boudinage of S2m is concerned, the timing is late in the local deformation history since the required rheological anisotropy is only present once S2m is well developed. Boudinage of bedding becomes smaller as bedding thickness is reduced towards thrust contacts. This suggests boudinage formation either during or after the main phase of D2 ductile thrust strain profile development.'

There is little dispute as to the D2 age of these structures, however, since firstly, S2 is locally intensified around individual boudins, both within the boudinaged competent unit margins and within the enclosing less competent unit. Secondly, some boudins internally contain R2 shear bands or domino rotations (Fig 2.17), some individual boudin necks nucleate R2 shears where the rheological contrast is strong (eg. metadolerite sheet within banded pelites, silts and thin quartzites, Fig 3.13), and some individual boudin necks nucleate R1 shears where the rheological contrast is weaker (eg. quartzites within pelites and spaced mica-rich S2 planes, Fig 3.33). These 'internal' and 'neck' shear bands are consistent with D2 shear bands and extensional crenulations in surrounding rocks.

The boudins are generally of symmetrical geometry with long axes lying close to perpendicular to the local D2 stretching lineation (X2). The orientation of these boudins with respect to the mean X2 direction is illustrated in Fig 5.3. Significantly, those boudins containing or nucleating shear bands are also those with long axes closest to perpendicular to the mean X2 direction.

The boudinage is generally contained within the rheological banding, be it within S2/S2m close to the D2 thrust contacts, thinned bedding (sub-parallel to S2 closer to the D2 thrust contacts, or acutely oblique to S2 further away from the contacts) or else metadolerite sheets or quartzite beds on the margins of the D2 thrust high strain zones. Where boudinage is well developed, the host banding is parallel or sub-parallel to the nearby D2 thrust contact. In the absence of 'chocolate tablet geometries, the boudinage must therefore represent a non-flattening (stretching) deformation within the banding parallel to the thrust contacts, with a component of NW directed overshear parallel to the transport direction of the D2 thrusts.

Although not uncommon, this boudinage is not ubiquitously developed, being not only confined to the D2 thrust high strain zones, but also laterally restricted within them. Clearly, the stretching deformation that the boudins represent is temporally and spatially localised. This indicates further inhomogeneity in the ductile thrust related D2 deformation.

Furthermore, although boudinage is seen to intensify towards D2 thrust planes, it is never seen to deform them. This suggests that the stretching deformation which the boudins represent is detached at the thrust planes to which they intensify. D2 boudinage in the Breaghy Head area must, therefore, be related spatially and temporally to the motion of individual D2 thrusts.

#### 5.2.7 Syn-tectonic quartz veins

Quartz veins are not uncommonly developed in the Breaghy Head area. The majority of these veins are demonstrably D2 in age. For example in chapter 3, steeply inclined swarms of thin planar quartz veins were shown to be developed over D2 thrust culminations and in chapter 4, dense zones of thin climbing planar vein arrays were shown to be developed within vein array ramps. These two vein types have already been discussed and are not, therefore, considered further in the following discussion.

Three main kinematically important types of D2 age quartz veins exist in the Breaghy Head area:

1. Rod-like veins with irregular or lozenge shaped cross sections hosted by D2 boudin necks (chapters 2 & 3).
2. Moderately to shallowly inclined thin planar veins present as tension gash arrays indicating NW directed overshear in sympathy with the D2 thrust shear sense (chapters 2 & 3).

3. Thin planar veins parallel or subparallel to S2/thinned bedding or S2m in the D2 thrust high strain zones in both flats and ramps which are sometimes quite dense close to the thrust contacts (chapters 2, 3 & 4).

Mutual cross-cutting and interconnectivity of veins of the three main types can be identified in the field (chapters 2 & 3, Fig 2.21), indicating that the three main vein types must be of D2 age, since the boudinage within the area has been shown to be of D2 age, the three vein types are shown to have a close spatial and kinematic relationship to D2 thrust structures and high strain zones, and the planar veins within the thrust high strain zones closer to the thrust contacts are often folded by minor intrafolial F2 folds or displaced by C, P, R1 & R2 shears (eg. Figs 2.5 & 3.5).

The minor F2 intrafolial folding of some planar veins, often with rootless geometries, and the presence of augen remnants of vein quartz within the D2 thrust S2m zones suggests quartz vein formation in the thrust high strain zones when the thrust hangingwalls and footwalls were being pervasively strained, possibly prior to the host thrust high strain zones achieving maturity. As discussed above, however, D2 boudinage formation appears to have taken place after or as the D2 thrust high strain zones achieved maturity. The connectivity between boudin necks and planar veins, the presence of relatively undeformed S2m parallel planar veins with oblique impurity (opening) trails indicative of NW directed overshear and the displacement of planar veins by discrete secondary shears all suggest vein formation during or just after a change in the thrust related deformation from pervasive straining to more localised displacement processes.

It appears therefore, that quartz vein formation was initiated by planar veins developed within the rocks closest to

the thrust contacts, presumably representing transient high strain rate events (cf. Knipe & Wintsch 1985, Knipe 1989), within the developing thrust mylonite zones. Vein formation then appears to have continued, progressively spreading into the thrust wall rocks as the D2 thrust deformation process changed from pervasive wall rock straining to more localised displacement processes, with the synchronous formation of both planar vein types and boudinage related veins across the entire width of the thrust high strain zone profile.

### 5.3 D2 Secondary fabrics

This group of minor structures includes R2 'domino' hard band rotations, C & P shears, R1 & R2 extensional crenulations and shear bands (Figs 2.4, 2.8, 2.9, 2.10, 2.11, 2.12). These structures have been described and discussed in detail in chapters 2 & 3, where their value as kinematic (shear sense) indicators was established. It is not intended to repeat those arguments here. The following discussion is biased towards R1 & R2 extensional crenulations since they are commonly developed, and as will be demonstrated, kinematically revealing.

#### 5.3.1 Secondary fabric timing

Interconnectivity of C, P & R1 shears is well developed at some localities (eg. Fig 2.12). This, together with the mutually cross-cutting and rare conjugate relationships between R1 & R2 extensional crenulations (chapter 2), clearly demonstrates that C, P, R1 & R2 shears are contemporaneously developed. The D2 age of R1 & R2 extensional crenulations (and therefore D2 age of C & P shears) is in little doubt for the following reasons:

1. As noted above, both R1 & R2 shears and R2 'domino' rotations are contemporaneously developed with D2 boudinage at some localities.

2. The D2 thrust high strain zones represent pervasive (i.e. microscopic) straining of the thrust hangingwall and footwall rocks. This involves mobilization and recrystallization of micas and quartz into cleavage planes and microlithon microfold hinges respectively in the non-mylonitic S2 zones, and quartz grain size reduction with subgrain development, mica growth and thinning at crystal tips, feldspar fracturing/minor subgrain development and feldspar break-down to muscovite & quartz in the mylonitic (S2m) zones closest to the thrust contacts which host much of the extensional crenulation cleavage.

Since extensional crenulation cleavages (ecc) represent extensional microshears which deform host S2/S2m, the ecc must be developed after the D2 thrust high strain zones have become established, implying ecc development after pervasive crystal-plastic deformation processes have ceased. Thin section investigation, however, indicates that the same mylonite-related crystal plastic deformation processes outlined above are active within the ecc "curvature domains" (Fig 2.10), but diffusional migration of quartz into microlithon microfold hinges is absent. Recovery (secondary recrystallization) textures are also noted in thin section to be common to both ecc planes and the host S2/S2m (eg. quartz grain boundary migration to form larger crystals with triple point boundaries and crossfabric mica porphyroblast growth (eg. large biotites at Mickey's Hole)).

In summary, the ecc and host S2m share common microstructural deformation processes and recrystallization textural history, indicating negligible temporal separation between S2m maturity and ecc development. The ecc must therefore be developed later in the



local S2m history, marking a change from pervasive straining to more localised displacement processes.

3. The geometry of the Breaghy Head ecc/shearbands and the microstructural deformation mechanisms associated with them are consistent with shear zone 'contemporary' secondary fabrics described from ductile deformation zones around the world (eg. Platt & Vissers 1980, White et al 1980, Hutton 1982, Law et al 1984, Platt 1984, Weijemars & Rondeel 1984, Kelley & Powell 1985, Brunel 1986, Platt & Behrmann 1986, White et al 1986, Behrmann 1987, Dennis & Secor 1987, Butler & Prior 1988).

The above arguments clearly place the Breaghy Head ecc (and therefore C & P shears and R2 'dominoes') within D2. More specifically, the ecc appear to be developed as the D2 ductile thrust deformation proceeds from pervasive thrust wall rock straining to more localised displacement processes.

### 5.3.2 Extensional crenulation orientation

Extensional crenulation (ecc) orientational data collected in the field was only qualitative for the following reasons:

1. The ecc planes are defined by asymptotic curvature and thinning of the host S2/S2m into the extensional microshears which the ecc planes represent. The ecc planes often gently anastomose, especially in the strike direction and/or curve asymptotically towards parallelism with the host S2 fabric, especially in the S2m zones. Accurate field measurement of ecc is therefore precluded by the general absence of clearly defined planar cleavage surfaces.

2. Until fieldwork was almost completed, the significance of ecc was considered to be purely in relation to shear sense determination. Only crude estimates of ecc strike or ecc microlithon microfold plunges were therefore made in the field in order to supply a quadrant to the shear sense indicated by the microlithon asymmetries (see map 2). If additional kinematic significance had been attached to these structures earlier in the fieldwork, additional efforts would have been made to obtain a reliable quantitative data set for the ecc.

### 5.3.3 Extensional crenulation geometry and flow partitioning

If extensional crenulation cleavages (ecc) are viewed purely as shear sense indicators, they might be perceived as only a kinematic spin-off of D2 ductile thrusting. There is greater depth to the kinematic significance of ecc, however, and to highlight this it is necessary to examine the causative processes responsible for ecc development in D2 ductile thrust high strain zones. It is therefore of value to briefly recap and categorise the salient features of R1 and R2 ecc:

#### R1 Extensional crenulations:

1. There is no evidence of pressure solution along R1 ecc planes.
2. The R1 ecc are extensional microshears which deform the S2 host fabric and define the ecc planes. The microlithon structure is therefore that of open microfolds of S2 fabrics with NW dipping limbs which are thinned (with respect to the SE dipping limbs), as they curve asymptotically into the ecc planes (microshears) which they define (Figs 2.10, 2.11). This produces a 'tail' or 'fish' microlithon geometry which is maintained across the exposure width of ecc zones (Fig 2.9).

3. R1 ecc planes are sometimes seen to clearly displace passive markers (eg. distinct discrete S2/S2m parallel mineral bands or fine S2/S2m parallel quartz veins) towards the NW (mm or cm scale). These displacements are not equal across the ecc zone and occasionally differ markedly across adjacent ecc planes.

4. Multiple sets of R1 ecc may be developed in some exposures, with the later set being wider spaced than the earlier set. The later set cross-cuts the earlier set at a higher angle, but individual later ecc planes are seen to link with the earlier planes in a similar way to fault systems. This suggests negligible temporal separation between the sets and rotation of the ecc planes top towards the SE during movement.

5. R1 ecc are occasionally folded by open minor F2 folds, a rare gentle axial planar crenulation may be present which is only seen in thin (mm scale) micaceous partings represented by S2/S2m or ecc planes. The trace of the ecc planes around these folds appears to be more geometrically coherent than the trace of the S2 fabric in the ecc microlithons around these folds. This may suggest that it is the ecc anisotropy which is being folded, (i.e. shortening along the R1 ecc planes (Fig 2.13)).

## **R2 Extensional crenulations**

1. Similar to R1 ecc, R2 ecc are extensional microshears which deform host S2/S2m fabrics. R2 ecc microlithons are also open microfolds of host S2 fabrics, but with SE dipping limbs (defining ecc planes) being thinned with respect to NW dipping limbs and curving asymptotically into the ecc planes which they define, however, the microfolds have tighter, sharper hinges than those of R1 ecc counterparts (Fig 2.10).

2. S2 in the R2 ecc microlithons dips NW and would therefore verge SE with respect to surrounding bedding. S2 verges towards the NW in surrounding rocks unaffected by the R2 ecc. This suggests that the R2 ecc planes and the S2 fabrics in the microlithons have rotated top towards the NW 'domino fashion' during R2 ecc development and motion.

3. R2 ecc planes are sometimes clearly seen to displace passive markers towards the SE.

4. Gentle crenulations of the S2 fabrics in the microlithons are occasionally present with axes sub-parallel to the R2 ecc planes. This gives a superficial contractional appearance, however, similar to R1 ecc, 'tail' asymmetry is maintained across exposure width. This may suggest weak postslip shortening orthogonal to the R2 planes where these crenulations are developed.

### Miscellaneous

1. Where R1 & R2 ecc developed together in a given exposure, R2 always cross cuts earlier R1 generations. In some rare isolated positions of these exposures, phacoidal (conjugate) interference geometries exist (cf. Figs 2.10, 2.11), suggesting R2 initiation towards the latter part of R1 activity.

2. Later ecc are always wider spaced than earlier ecc generations.

Lister & Williams (1979, 1983) suggest that the flow within shear zones may be spatially partitioned. As Behrmann (1987) notes, the formation of extensional crenulations requires local partitioning of flow into either simple shear plus spin or coaxial stretching plus spin.

A rheologically "hard band" (eg. metadolerite sheet) within a D2 ductile thrust high strain zone will promote local flow partitioning into rotation of the hard band and slip along it's boundaries, consistent with the former flow partitioning model (ie. simple shear plus spin). The development of cross-band R2 'domino' shears (eg. Fig 2.8), may in part help to facilitate the hard band rotation.

Other hard band related secondary extensional fabrics are closely associated with boudinage of the hard band, manifested as R2 dominos within boudins and ecc or large isolated shear bands emanating from the boudin necks. The crystallization and shearing of the boudin vein quartz within the intra-boudin domino and neck shear band planes (eg. Figs 2.17, 3.13, 3.31, 3.33), clearly indicates synchronous secondary fabric and boudinage development. This negates potential argument that the secondary fabrics may have nucleated on pre-existing boudins or visa-versa. This clearly indicates that the intra-boudin dominos, neck ecc and shear bands are developed in response to flow partitioning which involves coaxial stretching of the hard bands, more consistent with the latter flow partitioning model (coaxial stretching plus spin).

Platt (1984) has examined the potential of the coaxial stretching plus spin flow partitioning model for the development of ecc in detail (Fig 5.4). - Platt (1984)-provides two end-member cases for the precise nature in which the coaxial stretching plus spin flow partitioning may take place with respect to ecc. In the context of the Breaghy Head/Horn Head area, this would be either:

1. Flow is partitioned into slip parallel to S2/S2m, stretching parallel to S2/S2m and spin (top to the NW). This predicts that R1 should rotate towards the shear plane and S2/S2m, promoting multiple R1 ecc sets, such that low angle R1 are cross-cut by higher angle R1. R2 should also rotate towards the shear plane and S2/S2m under these conditions or:

2. Flow is partitioned into slip along R1 ecc, shortening along R1 ecc planes and spin (top of the NW). This predicts that R1 ecc should rotate away from the shear plane and S2/S2m, and R2 should rotate towards the shear plane and S2/S2m. Shortening orthogonal to R2 planes should quickly develop.

As Platt indicates, the true situation will lie between (1) and (2) above. In all respects, the detailed geometrical attributes of the D2 ecc, summarized above, are consistent with those predicted by the coaxial stretching plus spin flow partitioning model for ecc development of Platt (1984).

#### **5.4 Propagation of tectonic slides and the generation of 'shaped' ductile thrusts.**

The D2 ductile thrusts of the Breaghy Head area have been shown (chapters 2, 3 & 4) to have ramp-flat geometries with long bedding-parallel flats, smooth shallow lateral ramps and shorter 20-30° frontal to oblique ramps parallel to surrounding S2. Shallow frontal ramps may be present, however, since the ramp angles are probably below the resolution of field observation (especially in view of the restricted down-dip extent of exposure), their recognition has been treated with caution. The D2 ductile thrusts have also been shown to have a complicated sequence, with both piggy-back and break-back sequences identified.

Chapter 4 strongly indicates that ramps and flats may be developed separately as a consequence of ductile thrust dislocation cell propagation, such that mature D2 ductile thrusts result from coalescent propagation of:

1. Bedding parallel (flat) dislocation cells which propagate towards one another through 'fold ramps' which maintain displacement continuity between adjacent flat tips as the adjacent leading and trailing tip strains interact. A flat-ramp-flat thrust geometry is generated as the dislocation cells coalesce (Fig 4.7).

2. Ductile thrust ramp dislocation cells ('fabric slip ramps') are generated within the mid limbs of primary F2 folds parallel to the axial planar S2 between thrust flats (Figs 4.1, 4.5). These fabric slip ramp dislocation cells propagate in all directions along S2 from a central point and will therefore potentially link with flats of different structural level.

#### **5.4.1 Propagation of D2 thrust flats: a rheological control**

As described above and in chapters 2, 3 & 4, S2 intensifies to become S2m in the vicinity of the D2 ductile thrust contacts, such that the thrusts are represented by discrete mylonitic dislocations of the stratigraphic package contained within identifiable high strain shear zones.

Hutton (1979b) noted that the regional D2 strain in NW Donegal is of plane strain character, but deviates to non-plane strain within the high strain zones approaching the major Dunfanaghy and Mickey's Hole tectonic slides. In both cases, the tectonic slides bring into sharp thrust contact hangingwall pelitic lithologies and footwall quartzites, and in both cases the pelitic lithologies record exponentially increasing oblate strains, whilst the quartzites record exponentially increasing

prolate strains as the thrust contact is approached. This, and the low angle of regional S2 fabrics to major tectonic slide planes (statistically less than  $10^\circ$ ) in NW Donegal, are significant departures from "classic" shear zones (cf. Ramsay & Graham 1970), where the shear zone cleavage is developed at  $45^\circ$  to the shear plane at the shear zone margins and the strain pattern is a gradual increase of plane strain towards the shear plane in both hangingwall and footwall. This led Hutton (1979b) to conclude that the tectonic slides in NW Donegal represent local intensification and modification of the regional S2 at the boundaries between different lithologies. The different lithologies on either side of the boundary are believed to have experienced correspondingly different strain paths during the intensification of S2, leading to the development of a strain discontinuity at the lithological boundary, inducing a dislocation to develop and thereby enabling separation of the two strain ellipsoid types. Hutton (1983) suggested that once such a dislocation is developed, it "...may be able to propagate along the axis of the shear zone into rocks of non-contrasting lithology". This supports and is analogous to the suggestion above that the Breaghy Head D2 ductile thrust flats originate as dislocation cells which propagate outwards from a central point of origin.

The nature of strain refraction at lithological boundaries has been investigated by a number of authors. Theoretical modelling by Cobbold (1983) and Treagus (1983, 1988) has shown that for layered Newtonian mediums, finite strain ellipsoids refract and show higher values within the less competent units, such that: "the ratio of layer parallel finite shear strain across a boundary is equal to the inverse viscosity ratio." (Treagus & Sokoutis 1992). In layered power law mediums, however, the finite shear strain ratio across the boundaries does not follow a constant relationship with the viscosity ratio (Cobbold 1983).



Treagus & Sokoutis (1992) in their investigation of strain variation across rheological boundaries discuss in review of key literature, the nature of rock rheology. It would appear that despite certain problems with comparing laboratory creep experiments with naturally deforming rocks, such comparisons indicate that rocks are essentially non-linear materials which characteristically deform by power law flow.

The multi and single layer laboratory models of Treagus & Sokoutis (1992) use a variety of model materials of both Newtonian and power law rheology. These models highlight rheological control of strain inhomogeneity, indicating the following:

1. Deformation of closely spaced banding of different rheology leads to overall Newtonian behaviour in which strain refracts sharply at the boundaries and strain is uniform within the bands, suggesting that the close spacing of the rheological banding effectively smooths the rheological influence on shear stress to produce a constant shear stress across the multilayer zone. This would be analogous to minor lithological boundaries within the study area (eg. quartzite - pelite intercalations within the Sessiagh-Clonmass formation).

2. When isolated single layers or (more pertinent to this discussion), single rheological boundaries are deformed, shear stress gradients are generated across the rheological boundaries. The resultant strain refraction across the rheological boundary is characterised by strain rate and finite strain intensification towards the boundary within the less competent material. This would be analogous to major, formation scale lithological boundaries within the study area (eg. the Ards Quartzite - Sessiagh-Clonmass formation boundary).

Naturally deforming rocks, as noted above, are believed to deform according to power law flow, such that a linear shear stress increase across a lithological (rheological) boundary produces a non-linear increase in shear strain rate, resulting in finite strain refraction across the boundary with exponential strain intensification towards the boundary. This is consistent with observations of hangingwall dominance and general character of strain and S2 intensification towards D2 ductile thrust flat contacts in the Breaghy Head area discussed above. Indeed, Hutton (1979b) suggested that major tectonic slides may be generated within zones of intensified regional contemporary cleavage at major lithological boundaries (specifically S2 at the Ards Pelite/Ards Quartzite and Ards Quartzite/Sessiagh-Clonmass formation boundaries in the present study area).

The planar mineralogical segregation which S2 fabrics represent creates an anisotropy in the rock which intensifies and rotates towards parallelism with the D2 thrust planes, becoming mylonitic (involving strong grain size reduction and crystal axis alignment) as the thrust planes are approached. The formation of these features represent geometric, recrystallisation and reaction enhanced flow softening mechanisms (Poirier 1980, White et al 1980), which have been spatially localised at major lithological (rheological) boundaries in the study area, in response to the process outlined above. These flow softening mechanisms promote further D2 deformation localisation by effectively reducing the load (stress) bearing capacity of the rocks at the lithological boundaries (Fig 5.5).

D2 strain localisation onto major lithological boundaries necessitates that orogenic shortening becomes progressively accommodated by thrust motion across progressively narrowing (localising) zones within major lithological boundary zone

rocks. The development of a thrust dislocation within such lithological (rheological) boundary zone rocks is almost inevitable.

That this D2 thrust flat dislocation should nucleate and develop from a dislocation cell which propagates outwards from a central point of origin is a logical conclusion. The host lithological boundary must have finite area within which any dislocation would be spatially restricted. The temporal and spatial diachroneity which characterises orogenic deformation may also impose a spatial restriction on the potential area over which a rheological boundary hosted thrust dislocation may develop at any given time, since only part of a spatially significant lithological boundary may be contained within the rock volume undergoing active pervasive deformation. Furthermore, the strength of rheological contrast across such a boundary is likely to be spatially variable, controlled by facies variations within inter-formation transition beds and specific mineralogical content of the rocks; for example the arkosic content of quartzites, or the proportional second phase content (cf. Olgaard 1990). These considerations dictate that isolated areas of a lithological boundary will preferentially localise and intensify D2 strains, such that development of a mature D2 ductile thrust flat is accomplished through coalescent propagation of spatially isolated dislocation cells. Indeed, compelling evidence consistent with growth of D2 ductile thrusts from coalescent propagation of dislocation cells has already been presented and discussed above and in chapters 3 and 4.

#### 5.4.2 Flow kinematics associated with dislocation cells

Eshelby (1973) examined the concept of dislocation cells, suggesting that faults might be considered as Somigliana dislocations in which the dislocation is an isolated planar entity with a finite boundary or "tip line" which demarcates the outer edge of the slipped region, within which the magnitude of displacement across the dislocation is spatially variable (Fig 5.6a). The tip line of a Somigliana dislocation is ideally *elliptical* with a centrally located displacement maxima (Fig 5.6b). Contours of both the finite and incremental displacements associated with real faults produce broadly *elliptical* patterns on a fault plane projection, (eg. Archuleta 1984, Barnett et al 1987, Price 1988, Sibson 1989, Walsh & Watterson 1989, 1991; Fig 5.6c).

Pertinent to this discussion is the effect which localising D2 strain and displacement onto a discrete plane as a dislocation cell has on flow patterns, since it is changes in flow patterns which lead to *inhomogeneous* strains and generation of new structures:

Kinematics is the consideration of the "geometry of motion of systems of particles, without any regard for associated forces." (Means 1990). Consider the motion behaviour of a system of marker particles within a deforming medium. At any instant in time, each individual particle has a *definite* velocity and movement direction, which can be defined as a velocity vector. When this is considered together with the velocity vectors of a large number of neighbouring particles, the pattern of vectors defines the velocity field. The velocity vector of the individual particle and the overall pattern of vectors (velocity field) can be viewed as the vectorial summation of three aspects of motion; translation, rotation or spin and distortion or stretch (Fig 5.7). Some success has been achieved in explaining the development of structural

features by considering the way in which flow can be partitioned into these various components (eg. Lister & Williams 1983, Platt 1984), as discussed above.

The relativity of motion must also be considered, however, since the motion of particles can only be observed with respect to a fixed reference point. The choice of reference point effects the nature of particle motion observed and therefore the kinematic conclusions drawn.

Consider the velocity field associated with a graphical model of a simple shear zone. In Fig 5.8a, the reference point lies at the centre of the shear zone, such that particles occupying the centre line of the shear zone are stationary with respect to each other. Flow velocity therefore appears to decrease towards the shear zone centre line. This can be re-plotted, however, to illustrate the velocity field with respect to a reference point along the lower margin of the shear zone (Fig 5.8b). Here particles occupying the lower edge of the shear zone are stationary with respect to each other and flow velocity appears to increase towards the top edge of the model.

The uni-directional velocity gradient inherent in Fig 5.8b would enable any anomalies in the velocity field to be more readily observed and interpreted than the bi-directional gradient of Fig 5.8a would allow. A reference point is therefore chosen at the lower edge of the shear zone model in Figs 5.8c & d to highlight anomalies in the flow velocity generated by a lithological boundary hosted dislocation cell. This reveals a zone of anomalously high flow velocity centred on the dislocation cell.

In an informative discussion, Talbot & Jackson (1987) explain the connections between a number of flow related concepts and strain, highlighting the use of stream lines as an illustrative

tool in this respect. In summary, stream lines are defined as lines, at any point along which the tangent is the velocity vector; the pattern of stream lines therefore defines the geometry of the velocity field. The stream line spacing reflects flow velocity with closer spacing indicating higher velocity; it therefore follows that parallel stream lines reflect uniform flow, whilst non-uniform accelerating or decelerating flow is intimated by converging or diverging stream lines respectively.

Following the study of Hansen (1971), Talbot & Jackson (1987) indicate that there is a strong relationship between changes in the stream line spacing in the direction of flow and the strain ellipsoid shapes which are produced (illustrated in Fig 5.9 for incompressible mediums). This leads to the conclusion that accelerating flow (converging stream lines) produces prolate strain types, whilst decelerating flow (diverging stream lines) produces oblate strain types. This fundamental relationship is unaltered by a dilational component to the deformation, therefore although the rock types of the Breaghy Head area are not incompressible materials, Fig 5.9 is a valid illustration of the relationship between D2 flow behaviour and strain. Significantly, the change from plane to non plane D2 strain approaching D2 ductile thrusts and the co-existence of contractional and extensional structures within the D2 strain in the Breaghy Head area has been described in detail above.

The behaviour of flow against a time frame also classifies flow types into steady and unsteady flow. In the case of steady flow, the velocity at any point does not vary over time, with particle movement paths and stream lines following an identical track. The integrity of straight parallel markers is maintained during flow, and whilst inherited structures in these markers may grow, no new structures may form. This implies that steady flow produces homogeneous strain. In the case of unsteady flow, the

stream lines can depart from the particle paths in direction or velocity. Stream lines in unsteady flow can therefore cross markers parallel to previous stream lines and form new structures in those markers. This implies that unsteady flow produces inhomogeneous strain. It should be noted that inhomogeneity is a characteristic of the D2 deformation in the Breaghy Head area which has been described in detail above.

As discussed above, stress gradients appear to be generated at the boundaries between lithologies of differing rheological property. The strain refraction which develops across such a boundary is characterised by a gradient of increasing shear strain rate and finite strain towards the boundary within the less competent lithology. The shear strain rate (and therefore finite strain) within this boundary zone increases with each additional strain increment, enhanced by flow softening mechanisms. This flow pattern dictates that the anomalous boundary strain zone becomes narrower (ie. strain and displacement localises) over successive strain increments. As discussed, strain and displacement localisation will be spatially and temporally variable, focused by rheological control onto specific areas of the lithological boundary. A dislocation cell may develop within such an area if strain rate and finite strain becomes sufficiently anomalous to enable separation of hangingwall and footwall across a discrete plane.

This is equivalent to stating that the boundary zone rocks in the less competent lithology within a developing dislocation cell represent a zone of increasingly anomalous high flow velocity (cf. Fig 5.8). Stream lines within the less competent unit must therefore become closer spaced as the developing dislocation cell is approached. The stream lines must therefore converge as flow accelerates across the trailing edge of the developing dislocation cell and diverge as flow decelerates across the leading edge in

the flow direction (Figs 5.8c, d & 5.10). This indicates that extensional strains and structures develop across the trailing edge, whilst contractional strains and structures develop across the leading edge. Flow velocity gradients must also exist orthogonal to the flow direction across the lateral margins of the developing dislocation cell. The development of wrench shear strains at the lateral margins are an inescapable consequence of these velocity gradients.

With general emphasis on the generation of folds, dislocation cells have been invoked elsewhere in the literature to explain similar strain patterns and structural associations to those predicted above; in both the foreland areas of thrust belts (eg. Coward & Kim 1981, Coward 1982, Fischer & Coward 1982, Coward & Potts 1983, Williams & Chapman 1983), and more recently, within thrust belt internal zones (eg. Ridley 1986, Holdsworth 1990, Alsop & Holdsworth 1993). The D2 deformation in the Breaghy Head area is implicitly contractional, but also contains extensional structures. If the development of dislocation cells is responsible for the coexistence of these structures within the D2 deformation, a dislocation cell must display testable kinematic coherence which links the predicted contractional and extensional zones at the leading and trailing edges respectively.

#### **5.4.3 D2 extensional structures: support for a dislocation cell model**

The zone of maximum stream line convergence must lie inside the tip line of a developing dislocation cell, since flow accelerates across the trailing edge (Figs 5.8c, d & 5.10). By definition, the stream lines must converge towards a narrow point close to the lithological boundary within the anomalous high flow velocity zone. In the context of the Breaghy Head area, this predicts that extensional strains should be restricted to the high



strain rocks inside the trailing edge of any developing D2 ductile thrust dislocation cell; a further prediction being that the extensional strains are compelled to intensify towards the thrust plane (Fig 5.10). The converging stream lines must cross both bedding and S2, which in addition to deflecting these markers towards the thrust plane, predicts that new structures will develop which deform and extend these planar markers.

The salient features of D2 boudinage, shear bands and extensional crenulations in the Breaghy Head area are consistent with these predictions. As described above, these extensional structures are contained within the high strain zones which mantle the D2 ductile thrusts and intensify towards the thrust planes. These structures are kinematically and temporally intimate, such that boudins, shear bands and extensional crenulations have been observed at a number of exposures to form combination structures. Although demonstrably of D2 age, these structures deform and extend both bedding and S2 cleavage. Detailed evidence presented and discussed above and in chapters 2 & 3 indicates that these structures are developed during the later stages of local D2 thrust strain profile development, as accommodation of displacement across the shear zone changes from pervasive straining to more localised displacement processes. Indeed, D2 boudinage of bedding, S2 & S2m within a number of well exposed transects across D2 thrusts is seen to intensify towards the thrust planes (ie. individual boudins become smaller and more frequently developed). However, the thrust planes (defined by a lithological break or tectonic schist) towards which the boudinage structures intensify is never seen to be deformed by or contained within the boudins. This strongly suggests that the extensional flow which the boudinage and extensional fabrics represent is effectively detached at the thrust plane.

It is therefore suggested that D2 boudinage, shear bands and extensional crenulations within the Breaghy Head area are representative of structures formed within the extensional strain zones, generated by flow acceleration across the trailing edge of developing thrust dislocation cells. Indeed, the zone of maximum stream line convergence should map out as a line inside the trailing edge of the dislocation cell, similar to a great circle path on a stereonet. This line must, therefore, be sub-orthogonal to the transport direction for much of it's length (Fig 5.11). This may explain why (as noted above), the majority of boudin neck axes, especially those associated with shear bands and extensional crenulations, are orientated orthogonal to the local D2 stretching lineation.

#### 5.4.4 Implications for D2 stretching lineations

The D2 stretching lineation is contained within the S2 cleavage plane and therefore taken to represent the X direction of the D2 strain ellipsoid. As described above, this stretching lineation (X2) intensifies with the S2 cleavage as strain increases towards the D2 thrust planes, but in some areas this X2 intensification is laterally variable. As discussed above, Platt (1984) has suggested that extensional crenulations might be generated as a result of flow partitioning involving stretch parallel to the host fabric. This suggests the X dimension of the strain ellipsoid within such regions of a shear zone becomes anomalously elongated with respect to that in the surrounding rock volume. Where the host cleavage represents only a relatively weak layered anisotropy, the formation of extensional secondary fabrics will be suppressed (Platt & Vissers 1980). Under these conditions, the penetrative cleavage (S2) and especially the X2 stretching lineation can be expected to intensify to accommodate the stretch component of the flow partitioning. In view of these arguments, X2 can be expected to undergo anomalous intensification over a broad

area within the extensional strain area inside the trailing edge of a developing dislocation cell. This may explain much of the lateral variation in X2 intensification towards D2 thrust planes.

In Fig 5.2c, D2 stretching lineation data displays a conical dispersal about a main cluster indicating mean plunge towards  $165^{\circ}$  and therefore D2 thrust transport towards the NNW. Outboard of this, some data plunge to the north and west, and can be attributed in the field to locally developed structures (eg. thrust breaching or buttressing deformation, chapter 3). At the lateral and oblique tip lines of thrust shear zones, the addition of thrust normal (wrench) shear strains to the dominant thrust (transport) parallel shearing will cause deviation in the strain ellipse orientation (discussed in detail by Sanderson 1982, Coward & Potts 1983). In addition to contemporary cleavage strike swings, this predicts that stretching lineations may deviate from parallelism with the thrust transport direction across the lateral to oblique edges of dislocation cells; although the permissible limit of angular deviation from parallelism may be debatable (cf. Sanderson 1982, Ridley 1986). This may, therefore, explain at least some of the mean centred conical dispersal of the D2 stretching lineation data (Figs 5.2c, 5.11).

#### **5.4.5 Implications for propagation of D2 thrust ramps**

The D2 ductile thrusts of the Breaghy Head area have been shown to have 'shaped' geometries, with long bedding parallel flats separated by smooth shallow lateral ramps and shorter more frontal to oblique ramps (chapters 2, 3 & 4). The shorter ramps are preserved as hangingwall anticlines, footwall synclines or remnant complex zones of climbing vein arrays. At a number of localities, ramps have escaped direct incorporation into mature thrust profiles and have been preserved 'frozen' at an early or intermediate stage of development. As described in chapter 4, this

has enabled three distinct ramp styles to be identified, each with a different mode of formation; 'vein array ramps' (characterised by complex zones of climbing vein arrays), 'fold ramps' and 'fabric slip ramps' (both primary F2 fold hosted). Described in detail in chapter 4, the salient features of primary F2 folds and S2/S2m relationships associated with the latter (fold hosted) D2 thrust ramp structures have provided compelling evidence for the existence of D2 ductile thrust dislocation cells. Indeed, mesoscopic dislocation cells of this type have been directly observed. In the absence of post D2 refolds in the Breaghy Head area (chapter 3), the gross patterns of S2 dip and S2/F2 vergence and facing also support the dislocation cell model of thrust propagation in terms of larger (map) scale considerations:

As illustrated in Fig 5.8, a developing dislocation cell will generate a zone of anomalously high flow velocity, producing trailing edge convergence and leading edge divergence in the stream line pattern (Fig 5.10). By definition, the stream lines must diverge away from the anomalous high velocity zone within an increasingly broad zone as flow decelerates across the leading edge. The region of maximum stream line divergence must, therefore, lie above or outside the tip line. Furthermore, the diverging stream lines of a bedding parallel dislocation cell must transect bedding (Fig 5.10), such that bedding above or outside the tip line will be deflected away from the thrust plane and deformed by newly generated contractional structures. The development of primary F2 folds and D2 thrust ramps in the Breaghy Head area are consistent with these predictions. Contractional strains should increase within a broad zone away from the high strain rocks towards and across the leading edge of any developing D2 ductile thrust dislocation cell, such that the trace of maximum contractional strain (primary F2 folds, D2 ramps), should follow or lie just outside the leading edge tip line (Fig 5.11).

Detailed field observations (this and chapters 2, 3 & 4), have clearly demonstrated the kinematic and temporal intimacy between primary F2 folds and D2 ductile thrusts in the Breaghy Head area. Primary F2 folds are generally found between D2 ductile thrust flats and clearly deflect bedding upwards and forelandwards, such that these structures are kinematically equivalent to thrust ramps. As discussed above, primary F2 fold facing can be considered equivalent to D2 forethrust ramp facing, since ramps develop parallel to the fold axial planar S2. An arcuate range of primary F2 fold facing directions from NW (frontal) to SW and NE (oblique to lateral) has been identified (Fig 5.2d).

The non mylonitic S2 which is axial planar to primary F2 folds is seen to shallow towards thrust flats by some 20-30° and intensify transitionally to become bedding parallel mylonitic S2m (chapters 2 & 3, Figs 5.2a & b). F2 fold hosted ramps are developed parallel to the fold axial planar S2 and are therefore formed between flats with a 'true' ramp attitude of 20-30° to the flats. Ramp hosted S2m is therefore locally developed parallel to S2 at up to 20-30° to the bedding parallel thrust flat S2m (Fig 5.2b). Maximum S2 dips exceed those of S2m, since S2 within a hangingwall flat in contact with a footwall ramp will always have a steeper dip than the S2 fabrics in the footwall ramp (eg. Fig 3.39). The S2 and S2m data show a range of strike directions consistent with thrust flat, frontal and oblique to lateral ramp orientations (Fig 5.2b).

The S2/S2m dip and primary F2 fold facing data clearly indicate an arcuate range of D2 ductile forethrust ramp orientations in the Breaghy Head area, similar to that predicted by the trace of maximum stream line divergence (contractional strain) in Fig 5.11. Similar arcuate fold and/or ramp orientation

trends have been recognised elsewhere in both the foreland and internal parts of thrust belts and attributed to the leading edge of dislocation cells (eg. Fischer & Coward 1982, Coward & Potts 1983, Ridley 1986, Holdsworth 1990).

The above evidence supports the dislocation cell model and clearly indicates that primary F2 folds and fold hosted D2 thrust ramps are developed at the leading edge tip line to bedding parallel (thrust flat) dislocation cells. Indeed, as described above and in chapters 3 & 4, this relationship has been directly observed in mesoscopic field examples of D2 thrust dislocation cells. Fold ramps, for example, are observed to result from the coalescent propagation of D2 ductile thrust flat dislocation cells from different structural levels. These structures are therefore effectively tip line folds through which the dislocation cell thrust propagates away from the lithological boundary along the S2 trajectory, similar to propagation of thrusts through tip folds in foreland areas of thrust belts (eg. Fischer & Coward 1982, Williams & Chapman 1983).

Unlike the converging stream lines at the trailing edge of a dislocation cell, the diverging stream lines at the leading edge will be sub-parallel to or cross S2 at an acute angle (Fig 5.10). This suggests that rather than being deformed by the development of new structures, S2 and existing S2 parallel structures are more likely to intensify and amplify respectively. The intensification and modification of S2 to S2m in primary F2 fold mid limbs in fabric slip ramps may fulfil this prediction. As discussed above, Ghosh (1982) has indicated that axial planar cleavage may rotate through small angles to become a shear plane of the strain ellipsoid during pure or simple shear deformation. At the leading edge of a dislocation cell, the small angular deviation of the stream lines from parallelism with the S2 trajectory and addition of contraction to the shearing strain would satisfy these conditions

and may therefore promote the rotation and shearing suggested by Ghosh.

#### 5.4.6 Lateral structures

As noted above, Sanderson (1982) and Coward & Potts (1983) have discussed in detail the interaction between thrust (transport) parallel shear strain and additional thrust normal (wrench) strains developed at the oblique to lateral tip lines of thrust shear zones. This deformation produces arcuate fold and contemporary cleavage orientation patterns, such that folds are generated with axes sub-parallel or at acute angles to the X direction of the strain ellipsoid. As noted above, such arcuate S2 and F2 orientation trends are identified in the Breaghy Head area, where ambient D2 strains are insufficient to bring F2 axes into parallelism with X2 by passive rotation (cf. Escher & Watterson 1974, Cobbold & Quinquis 1980).

Watkinson (1975) indicates experimentally that folds generated close or parallel to the X direction are characteristically cylindrical in geometry. This implies that from the frontal to lateral areas of a thrust shear zone, fold geometry should change from asymmetric to symmetric. These relationships have been identified in the field (eg. Rattey & Sanderson 1982, Ridley 1986). Conversely, maintenance of fold asymmetry through the frontal to lateral thrust tip line has also been observed in both the foreland and internal zones of thrust belts (eg. Coward & Potts 1983, Holdsworth 1990). This appears to be the case in the Breaghy Head area, since primary F2 folds are characteristically asymmetric with inclined axial planar S2, regardless of axis orientation (described above and in chapters 2, 3 & 4).

In view of the evidence presented above, SW & NE facing and verging primary F2 folds in the Breaghy Head area may be

considered representative of the wrench strains developed at the leading oblique to lateral edges of dislocation cells. The majority of fold hosted ramps are of frontal to oblique orientation (chapters 3 & 4, Fig 5.2d). A number of fold hosted ramps have also, however, been identified with more lateral orientations (chapter 3, Figs 3.19, 3.22, 5.2d). Some of these lateral folds may therefore mature into through-going inclined lateral ramps, such that a dislocation cell may develop leading edge frontal, oblique and lateral ramp segments, all potentially dislocating primary F2 fold mid limbs.

As discussed above and in chapter 4, however, most of the lateral ramps observed and mapped in the Breaghy Head area are smooth structures, which are apparently unrelated to F2 folding. At a number of localities, these lateral ramps are observed to contain a combination of S2 parallel vein swarms, cross S2 planar vein arrays and extensional structures (eg. Fig 3.5). In the context of a D2 thrust dislocation cell, these relationships suggest a position towards the trailing edge, where the lateral ramp is transitional with the development of extensional structures inside the trailing edge tip line. Supporting evidence for such transitions is provided by the salient relationships between inclined planar vein arrays and boudinage in the Breaghy Head area.

A component of D2 thrust sheet differential shearing is expressed at a number of localities by the development of en-echelon planar vein arrays. In most cases, the centre line of the array is developed at an acute angle to the X2 direction, with constituent veins developed at more oblique intermediate angles. This is illustrated by Fig 5.3b, in which the mean vein strike directions lie close to  $55^{\circ}$  to the mean X2 direction ( $165^{\circ}$ ).

As described above, the majority of D2 boudins have neck long



axes orientated orthogonal to the local X2 direction and may form combination structures with shear bands. Those boudins with neck axes orientated at intermediate angles to the X2 direction, however, show a clear tendency to form combination structures with planar vein arrays (see Fig 2.21). Furthermore, in some examples, the boudin forms the dominant structure, whilst in other examples it is the planar en-echelon veins which form the dominant structure. Symmetrical boudinage and en-echelon vein arrays therefore appear to represent end members in a continuous series, in which the 'mid range' is represented by the combination structures. It is suggested that these relationships reflect the transition between lateral ramps and the extensional strains developed inside the trailing edge tip lines of D2 thrust dislocation cells.

### 5.5 Summary

It has been shown that penetrative deformation (ie. syn-metamorphic) westerly and easterly vergent folds and axial planar fabrics in the Breaghy Head area share a similar (D2) age. It has also been shown (chapter 3), that 'post-metamorphic' folds and fabrics within the Breaghy Head area can be related to local hangingwall straining processes (eg. thrust stacking). There is, therefore, a general absence of identifiable post-D2 structures in the Breaghy Head area.

There is a clear spatial, temporal and kinematic intimacy between the propagation and motion of D2 ductile thrusts and the development of both contractional and extensional D2 structures. A thrust dislocation cell model has been proposed to best explain these observations, the orientational data and the kinematic co-existence of contractional and extensional flow during the propagation and motion of the D2 ductile thrusts in the Breaghy Head area. Indeed, D2 ductile thrust dislocation cells have been

directly observed (see chapter 4).

In terms of the structures produced by this process in the Breaghy Head area, it would appear, therefore, that a transition may exist between frontal, oblique and lateral F2 fold hosted ramp segments developed towards the leading edge of D2 thrust dislocation cells. The lateral F2 fold hosted ramp segments are likely to be transitional with the smoother ramps which form the majority of the lateral structures observed and mapped in the Breaghy Head area. Where prominent veining is associated with mature examples of these lateral ramps, complicated mutual cross-cutting and inter-connectivity relationships exist between inclined and S2 parallel planar veins, with early inclined vein arrays deformed by movement of the thrust. This suggests that en-echelon vein arrays are developed during the early stages of the ramp development in a similar fashion to vein array ramps (chapter 4). As indicated by the boudinage/planar vein combination structures, these lateral ramp structures may be transitional with the extensional strains developed inside the trailing edge tip line of D2 thrust dislocation cells. These relationships are summarised in Fig 5.12.

The development and growth of these dislocation cell related structures and structural patterns may rely to some extent on the dislocation cell tip line propagation rate. This would need to be slower than the rate at which the related structures can grow to accommodate its displacement, since a prerequisite for the generation of these structures by the dislocation cell model is the presence of tip line associated accelerating or decelerating flow. As the tip line propagates outwards, the zones of accelerating and decelerating flow will migrate with it, such that a region subject to accelerating or decelerating flow will subsequently be contained within the tip line and therefore subject to steady state flow conditions. Any existing structures

or those inherited from the passage of the tip line may amplify under the steady state flow conditions (ie. parallel stream lines), or else be abandoned and carried passively, but no new structures may form. The presence of S2m parallel veining and brittle fracturing emanating from some ductile thrust tip lines into surrounding non folded or extended rocks (chapters 3 & 4), may provide evidence for this.

Primary & Conjugate F2 folds: D2 thrust ramps hosted by those folds with hinges orthogonal to the X2 direction.

Intrafolial minor F2 folds (a) become smaller & more frequently developed, (b) hinges tighten & rotate towards parallelism with X2, (c) develop rootless & sheath geometries closest to thrust plane.

Bedding progressively thins, angle between bedding & S2 progressively reduced.

Bedding obliterated: platy S2m is only pervasive planar fabric.

S2 fabrics progressively shallow (asymptotically) towards parallelism with thrust plane.

S2 transitional towards thrust contact with S2m.

Thrust contact enclosed in mantle of thrust parallel platy S2m.

Progressive intensification of X2: becomes exponential in S2m zone closest to thrust contact.

D2 strain increases exponentially.

Local peaks in exponential strain profile (thin zones of intense S2m).

Tectonic schist may be present at thrust contact.

Symmetrical boudins become smaller & more frequently developed. Boudins hosted by rheological banding (extension parallel to thrust flats). Where long axes orthogonal to X2, necks may host R1 and/or R2 shears.

Vein quartz in boudin necks, tension gashes & thinned bedding/S2 fabric-parallel veins: the former being the dominant vein type developed away from the thrust contact, the latter vein type being dominant closest to the thrust contact.

Dense swarms of S2m parallel quartz veins of multiple generations, may be relatively undeformed, folded, dislocated or reduced to vein quartz augen.

Shear zone secondary fabrics.

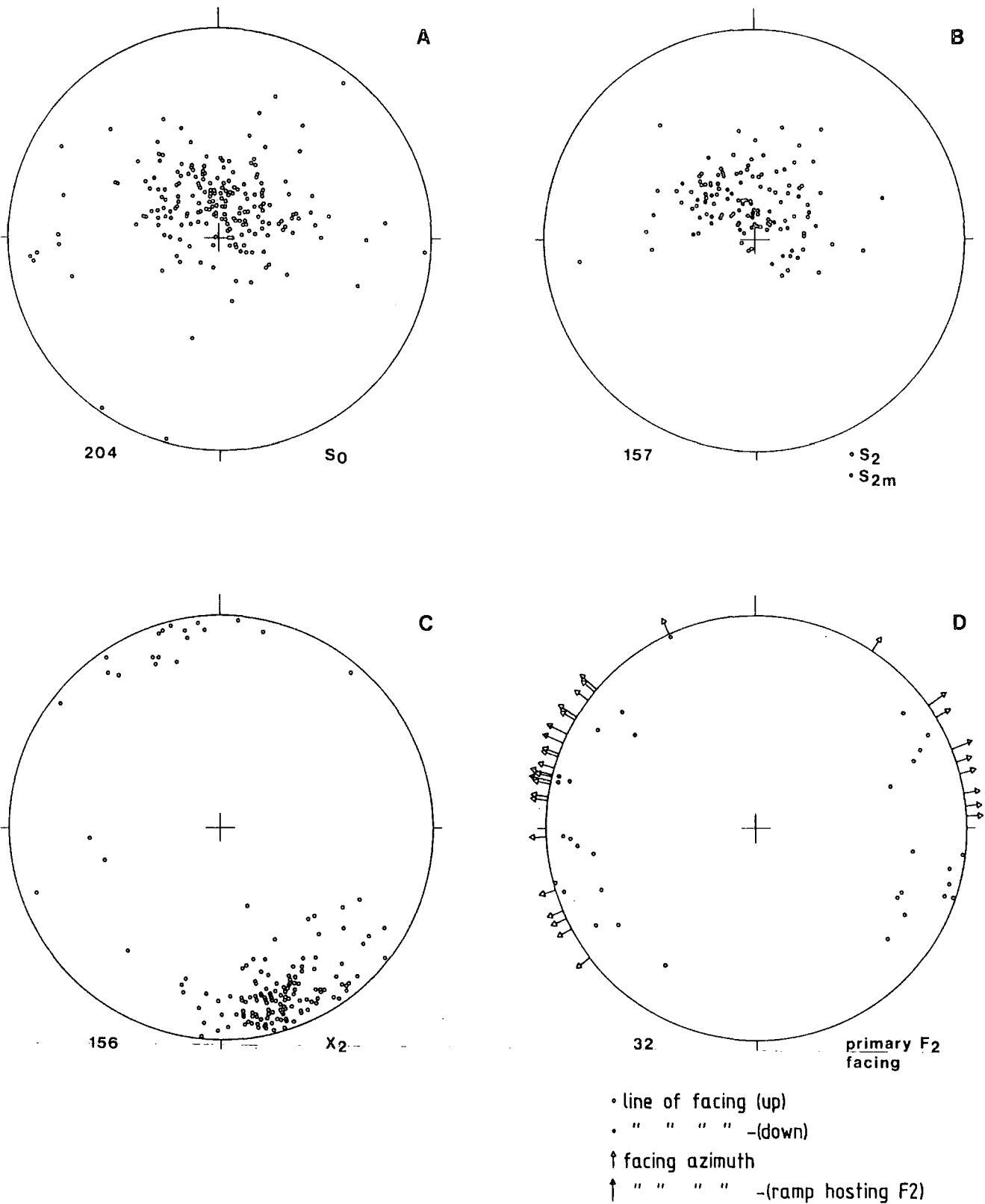


**Figure 5.2** Lower hemisphere equal area stereographic plots of passive marker and primary D2 structures in the Breaghy Head area. (a) Bedding ( $S_0$ ), (b) Non mylonitic ( $S_2$ ) and mylonitic ( $S_{2m}$ ) cleavage, (c) D2 stretching lineation ( $X_2$ ), (d) Facing data of primary  $F_2$  folds and D2 ductile thrust ramp-hosting primary  $F_2$  folds, plotted according to a technique described by Holdsworth (1988).

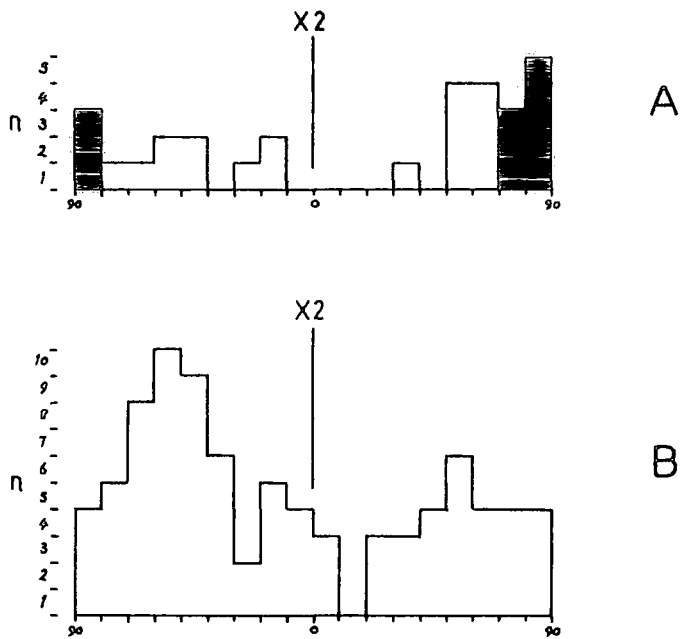


Figure 5.3 Histograms of: (a) Orientation of D2 symmetrical boudin neck axes with respect to the mean D2 stretching lineation azimuth ( $165^\circ$ ). Boudin neck orientations nucleating R2 shear bands are black ornamented. (b) Strike directions of planar quartz veins which are inclined with respect to S2.

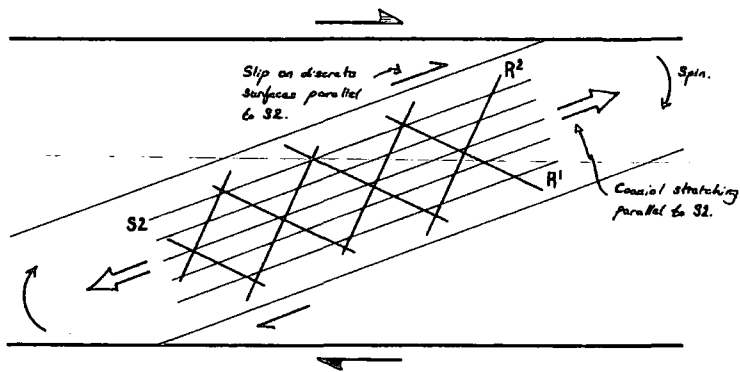


Figure 5.4 Development of R1 & R2 extensional crenulation cleavages within a shear zone in response to flow partitioning as envisaged by Platt (1984).

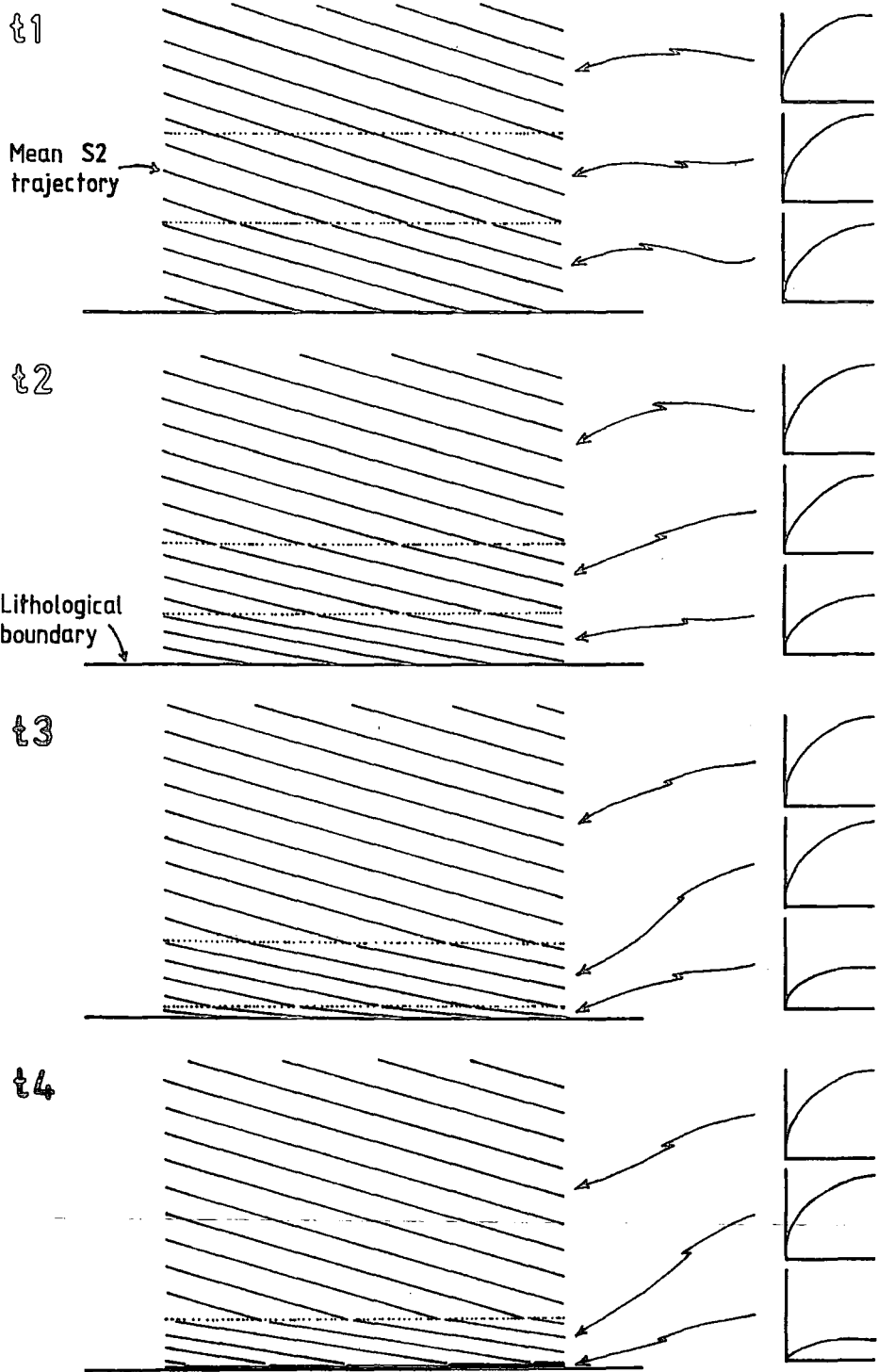
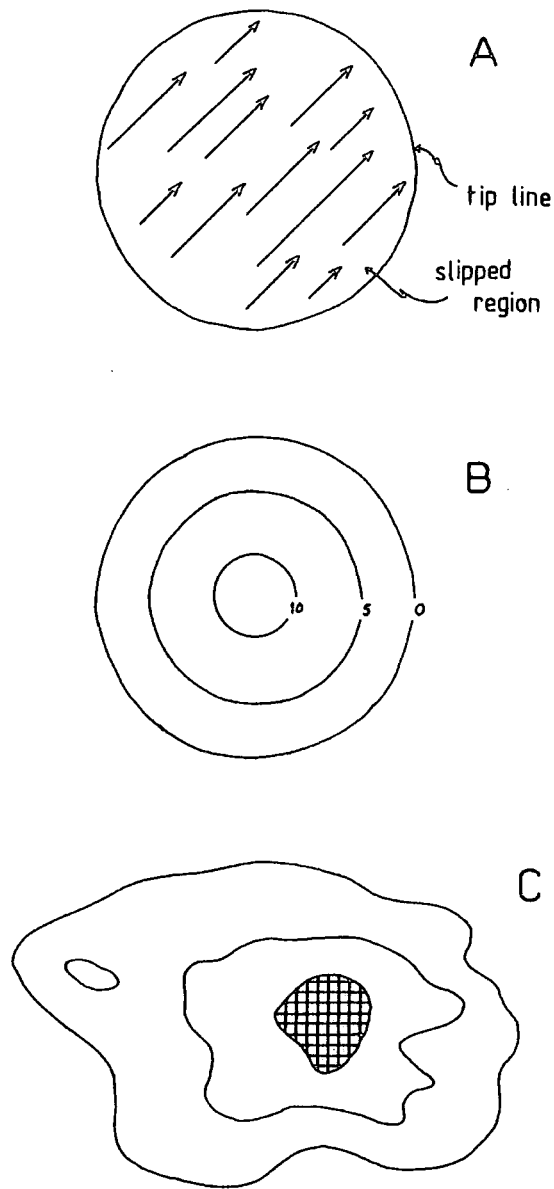


Figure 5.5 Schematic diagram illustrating the nature and evolution of power law stress-strain behaviour approaching a hypothetical rheological (lithological) boundary under constant applied shear strain rate, over successive strain increments (t1-t4). Individual graphs represent mean rheological behaviour within given zones approaching the boundary (V=shear stress, H=shear strain). A thrust dislocation develops within the boundary rocks at t4.



**Figure 5.6** Somigliana dislocations: (a) After Eshelby (1973), (b) Ideal dislocation with central displacement maxima and symmetrically disposed displacement contours decreasing to zero at the encompassing tip line, (c) A hypothetical representation of a displacement pattern associated with a more realistic Somigliana dislocation occurring in nature.



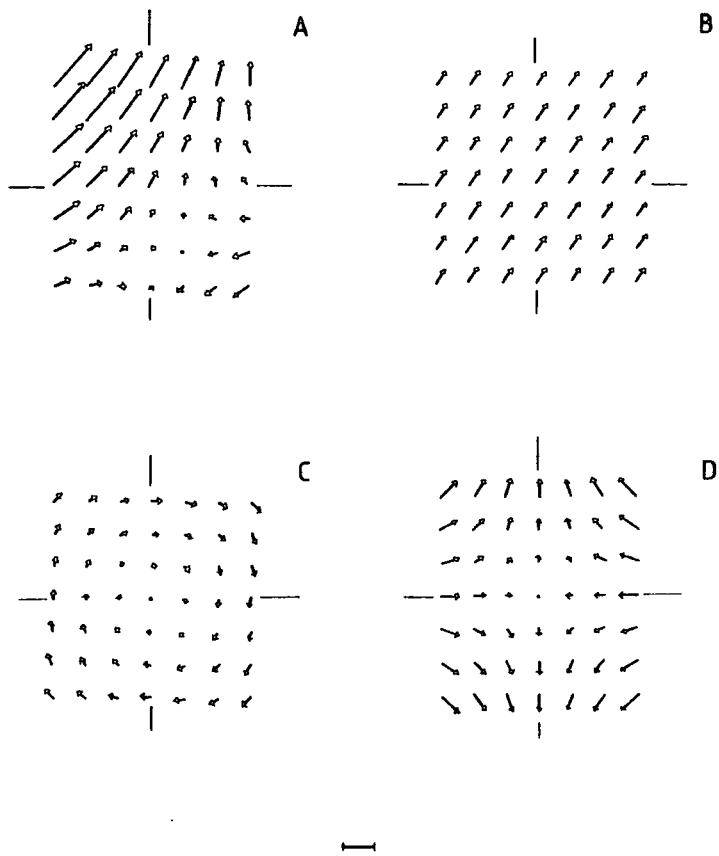
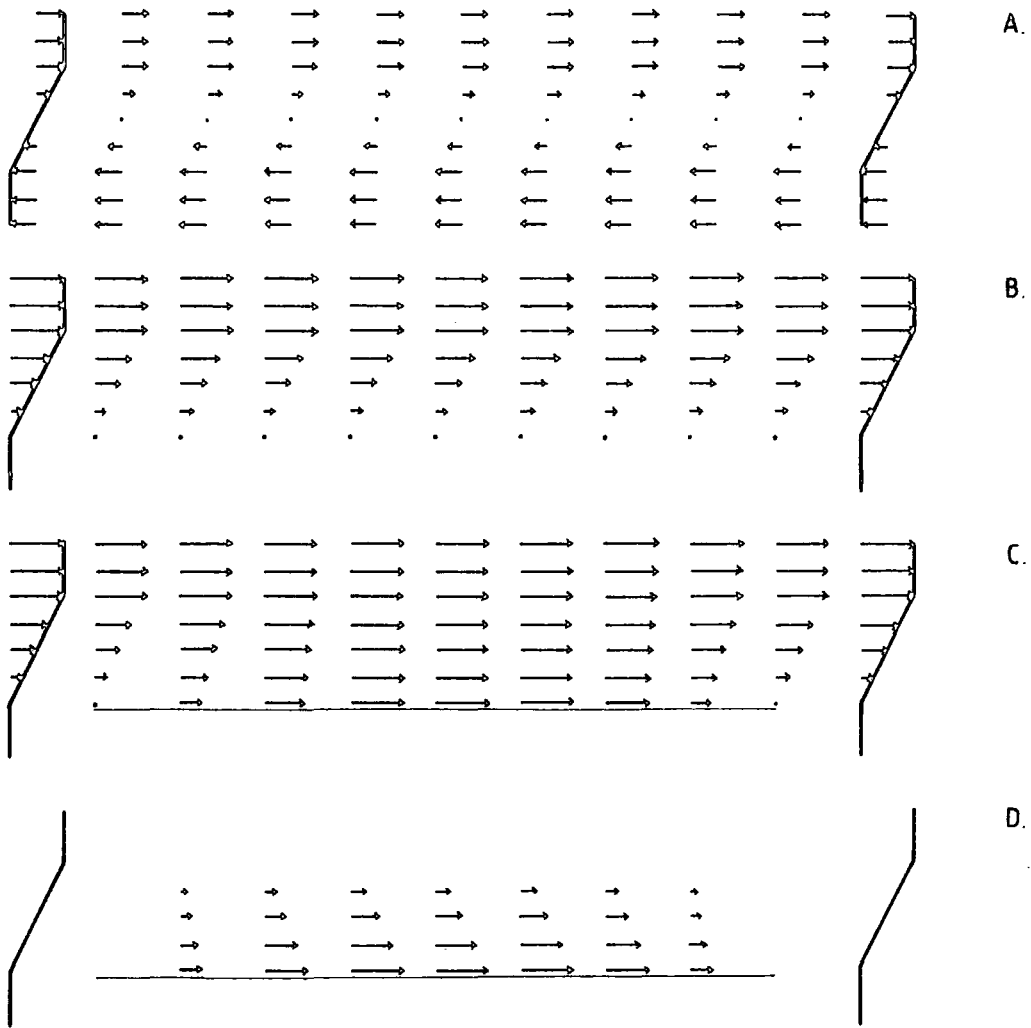


Figure 5.7 A velocity field (a), and its components (b-d) of translation, spin and stretch: the total velocity at any point is derived from vectorial summation of these velocity components at that position. The scale bar represents unit distance and velocity. (after Means 1990).



**Figure 5.8** Graphical models of simple shear zone velocity fields. (a) Total velocity field with central reference point, (b) Total velocity field with lower margin reference point. The choice of reference point alters perceived relative motion and therefore kinematic observations. In the case of (b) the lower margin reference point simplifies the velocity field. This would highlight and ease kinematic interpretation of any anomalous zones within the velocity field. (c) Total velocity field of a simple shear zone with a lower margin dislocation cell, (d) Anomalous velocity field associated with the lower margin dislocation cell (c minus b); note that flow accelerates and then decelerates from left to right.

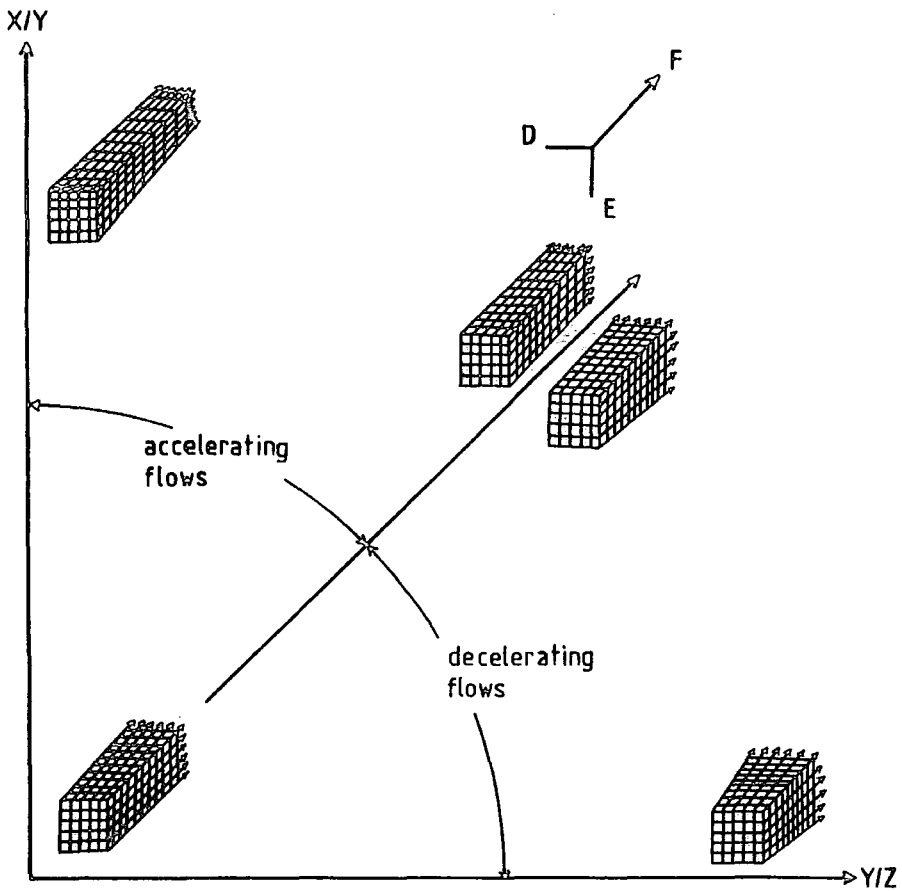


Figure 5.9 Stream tubes (bundles of stream lines), illustrating qualitatively the flow geometries of an incompressible fluid with respect to three orthogonal flow axes (D, E & F), where F represents the flow direction. Unit volume cubes at the front distort to other shapes downstream (into the page as arrowed). Spheres imagined within the cubes will therefore distort to strain ellipsoids downstream. The stream bundles are arranged on a Flinn graph to illustrate the relationship between stream line geometry and strain type. Accelerating flow (converging stream lines) can be seen to produce prolate strains, whilst decelerating flow (diverging streamlines) produces oblate strains. (after Talbot & Jackson 1987; modified from Hansen 1971).

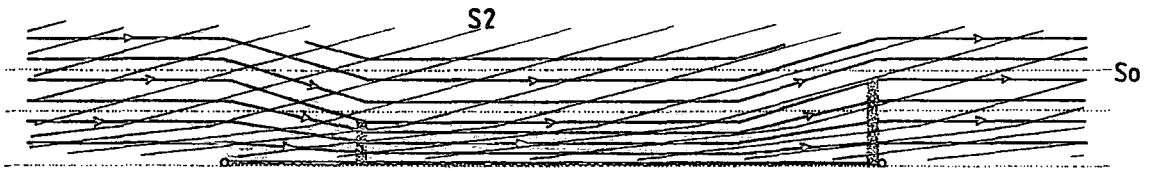


Figure 5.10 Graphical model of a bedding parallel shear zone with a lower margin dislocation cell, showing changes in the pattern of stream lines in the flow direction. Shaded areas represent zones of maximum stream line convergence (extension) and divergence (contraction).

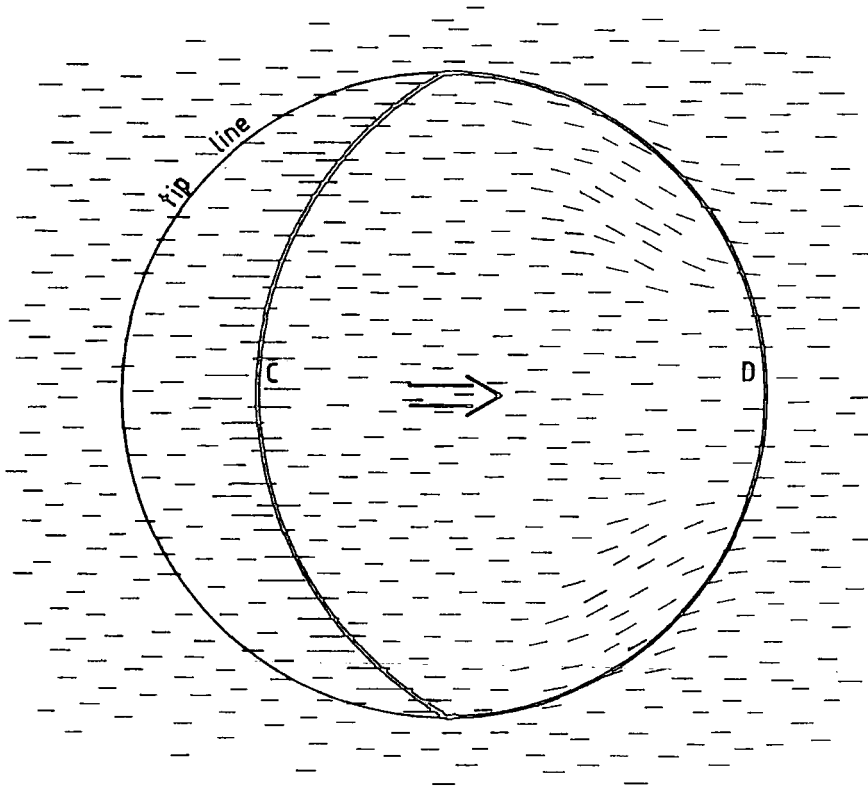
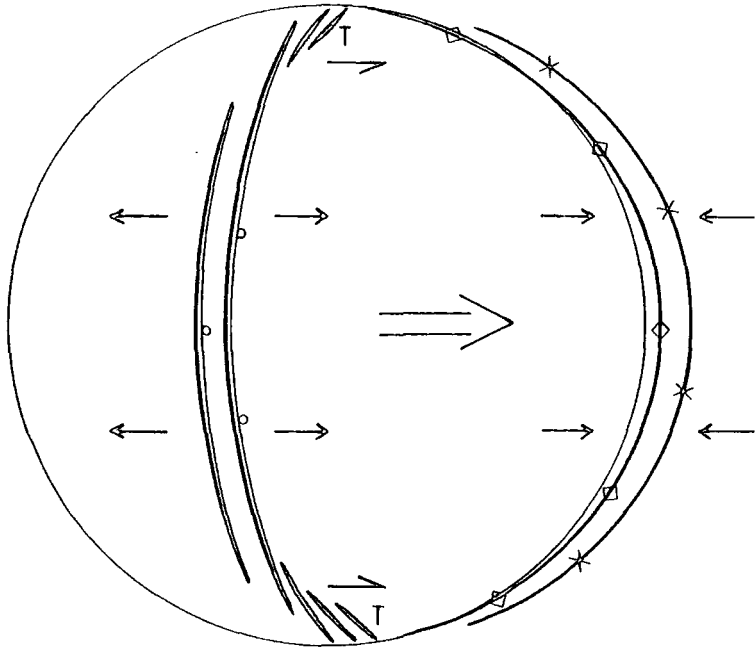


Figure 5.11 Plan view of a model dislocation cell, onto which zones of maximum stream line convergence (C) and divergence (D) have been mapped as bold lines. Large arrow indicates transport direction. Dashed lines indicate distribution of stretching lineation (X2) orientations; longer lines represent area of potential X2 intensification. See text for details.



**Figure 5.12** Plan view of a model ductile thrust dislocation cell, summarising expected distribution and orientation of structures developed in response to movement of the cell (compare with Figs 5.10 & 5.11). Large arrow indicates hangingwall transport direction, smaller arrows and half arrows indicate zones of leading contraction, trailing extension and lateral differential shearing. Bold lines with cross and diamond symbols indicate primary F2 folds. Large thin bold crescent symbols indicate boudinage; laterally transitional with tension gash vein arrays (T). Lollipop symbols superimposed on crescents indicate region where boudinage, shear bands and extensional crenulations may coexist. Ramps may develop throughout and parallel to the primary fold trace and be transitional with the lateral tension gash zones. See text for details.

## CHAPTER 6

### DISCUSSION AND CONCLUSIONS

Chapters 1 to 5 inclusive have described the evidence for the presence of a D2 ductile thrust imbricate zone within the Sessiagh Clonmass formation rocks of the Dunfanaghy - Breaghy Head area. Much discussion has already been provided internal to these chapters and within the summarizing remarks at their close. It is not intended to repeat those discussions here, but rather to broaden the discussion of some of the salient implications and conclusions.

#### 6.1 Section Restoration and D2 Ductile Thrust Displacement in the Breaghy Head area

It has been demonstrated in chapters 2 & 3 that the Sessiagh Clonmass sequence in the Dunfanaghy - Breaghy Head area contains a well defined D2 ductile thrust imbricate zone which repeatedly duplicates a relatively simple limestone - quartzite transition - quartzite stratigraphic package. The imbricates detach from a major stratigraphy parallel tectonic slide located at the Ards Quartzite - Sessiagh Clonmass formation boundary. These mid crustal D2 ductile thrusts have ramp/flat geometries, sequence histories and gross strain patterns similar to thrusts within foreland fold and thrust belts. A ball-park estimate of the cumulative displacement of the Breaghy Head imbricates can be made from maps 1 & 2 to exceed 4km.

The D2 ductile thrusts have been shown to have 'shaped' geometries, with long flats and shorter ramps developed at up to 30° to the flats (chapters 3, 4 & 5). The D2 thrust sequence has also been well defined (chapter 3), such that it is possible to construct a sequentially restored section in order to provide a more accurate cumulative minimum displacement estimate for the Breaghy Head D2 thrusts, in excess of 6km.

The minimum estimate for shortening associated with the Errigal Syncline, the trace of which runs through Marble Hill bay, is in excess of 1.5km. Total D2 shortening in the Breaghy Head area therefore exceeds 7.5km (70%).

The section restoration is included with maps 1 & 2 at the rear of this thesis. The section line (Fig 6.1) has been chosen to maximise constraint during construction from exposures lateral to the line and to incorporate geometrical and kinematic observations intrinsic to chapter 3. Salient constraining observations are indicated on the section.

As shown in chapter 5, the D2 ductile thrusts appear to result from coalescent propagation of thrust dislocation cells. This implies the presence of bi-directional displacement gradients along the thrusts within the section line. Initial attempts to estimate likely displacement gradients were hampered by lateral and down dip exposure limitations which preclude systematic measurement of down dip and strike parallel displacement patterns associated with individual thrusts. Considerable difficulty also exists in estimating the position of dislocation cell centre points. Significant and cumulative errors would therefore arise if displacement gradients were incorporated into the section; the restoration is therefore constructed to conserve individual thrust displacement.

The growth of D2 ductile thrusts from intensification and localisation of D2 strain and S2 cleavages (chapter 4 & 5), suggests that lithologies closest to the thrusts should display an exponential component of *shear plane parallel extension* towards the thrust planes. This would be expressed as a loss of cross sectional area in the near-thrust lithologies on the section. This shortening, although difficult to estimate, would be contained within the thrust parallel high strain zones which are generally about 20m thick (chapter 3), and is therefore assumed to have negligible effect on the section restoration at the scale of construction.

The section restoration is sequential, with removal of imbricates in reverse order to that of development as identified in chapter 3. The construction technique uses a combination of slip-line and vertical shear methods in order to preserve geometrical features (eg. ramps), which appear to be retained during D2 ductile thrust displacement (chapter 3).

## **6.2 D2 Ductile Thrust Dislocation Cells**

The Breaghy Head D2 ductile thrusts display patterns of intensifying strain and minor structures generally regarded as being diagnostic of the much broader thrust shear zones (tectonic slides) which typify deformation within metamorphic parts of mountain belts (cf. Hutton 1979b, Rathbone et al 1983, Figs 2.22, 5.1). This commonality of structural associations implies that the Breaghy Head D2 ductile thrusts and their broader larger scale counterparts must share similar generative and propagative processes.

As discussed in detail in chapter 5, there is a clear spatial, temporal and kinematic intimacy between the propagation and motion of D2 ductile thrusts and the development of both



contractional and extensional D2 structures. A thrust dislocation cell model has been proposed to best explain these observations, the orientational data and the kinematic coexistence of D2 thrust related contractional and extensional flow in the Breaghy Head area. Graphical modelling of flow characteristics associated with dislocation cells appears to predict the D2 structural patterns observed. Indeed, D2 ductile thrust dislocation cells have been directly observed (chapter 4).

The dislocation cell model is similar to the tectonic slide generative model of Hutton (1979b, 1983) in suggesting that a major rheological (lithological) boundary might focus D2 strains, ultimately leading to thrust separation across the boundary. As discussed in chapter 5, the shear stress gradient created across a strong rheological (lithological) boundary may cause focusing (localisation) of D2 strains at the boundary within the less competent lithology. The resulting thrust dislocation would propagate outwards from a central point of origin. In the case of the Breaghy Head imbricates, the strong rheological contrast across the boundary between the massive Ards Quartzite and the calcareous to pelitic lower section of the Sessiagh Clonmass formation is seen as a good example of this rheological strain focusing process.

The emphasis on rheological control inherent in the model suggests that strain localisation leading to discrete ductile thrust development would be less efficient in the case of weaker rheological boundaries, since any shear stress gradients created would be correspondingly weaker. A ductile thrust shear zone associated with such a boundary is therefore likely to be broader in its finite state than ductile thrusts developed at stronger rheological boundaries (cf. Alsop & Hutton 1993).

Since ductile thrusts appear to grow from coalescent propagation of dislocation cells, the strain profile thickness (shear zone width) associated with a mature through going ductile thrust may change spatially as a function of the strength of the original hangingwall and footwall rheological contrast. This may in part explain the approximate 10-30m range of D2 ductile thrust high strain zone thickness variation in the Breaghy Head area (chapter 3).

### **6.3 Implications for Polyphase Deformation**

Described in detail in chapters 2, 3 & 5, this work has shown that the D2 deformation within the Dunfanaghy - Breaghy Head area is kinematically more complex than envisaged by Hutton (1977a, 1983) and contains fabrics and folds previously interpreted as D3, D4 & D5 structures (cf. Hutton op. cit.):

#### **6.3.1 Penetrative Deformation Structures**

The westerly and easterly verging and facing penetrative deformation folds and fabrics within the study area were separated into D2 & D3 respectively, principally on the basis of vergence (Hutton 1977a, 1983, pers. comm. 1986). As described and discussed in detail in chapters 4 & 5, however, this work has shown that these structures are intimately associated with D2 ductile thrust ramp development, such that fold vergence and facing in this case is related to ramp orientation. Some folds, however, contain axial planar fabrics which are conjugate to S2 and are clearly related to rare D2 backthrusts (chapters 3 & 5). Both westerly and easterly verging and facing penetrative deformation folds and fabrics are therefore contained within the D2 thrust related deformation.

Clearly, easterly vergent D2 folds and fabrics related to westerly dipping forethrust ramps and rare backthrusts might easily be mistaken for regional D3 structures (as defined by Hutton op. cit.). Whilst D3 structures are not found to exist within the study area, D3 structures are developed elsewhere within the Dalradian of Donegal (cf. Alsop 1987, Alsop & Hutton 1993).

### **6.3.2 Local Polyphase Deformation Histories**

The shear zones which separate R2 domino hard band rotation blocks are responsible for the local generation of strain slip fabrics, which emanate from the shear zones into the surrounding less competent lithologies. The block rotation also creates open folding of the surrounding rocks with axial planar crenulation cleavage at the block corners. The size of the folds and the extent of the fabrics is governed by the size of the domino blocks involved (see Fig 2.8). These folds, strain slip and crenulation fabrics are essentially 'non-penetrative' in character and would be D4 & D5 structures in the sense of Hutton (op. cit.). These structures are, however, clearly an integral part of D2 kinematic structure development.

Steeply dipping 'non-penetrative' strain slip crenulation cleavages (previously interpreted as S4 & S5), are also locally developed in association with culmination wall extension zones analogous to hangingwall drop faults in foreland thrust and fold belts (Figs 3.36 & 3.37).

A local polyphase history of 'non-penetrative' folds and axial planar contractional crenulation cleavages (previously interpreted as D3 & D4 structures) is developed and restricted to the rear of the Middle Town ductile thrust stack, in response to imbricate back-steepening (Figs 3.36, 3.39).

Upright contractional 'non-penetrative' folds and axial planar crenulation fabrics (previously interpreted as D4 & D5 structures) are also locally developed and restricted to the region of D2 ductile thrust footwall ramps (eg. Figs 4.6, 4.7) and the forethrust - backthrust complex at Curragh Harbour (Figs 3.11 3.15). These are interpreted as an expression of D2 buttressing deformation (cf. Fig 3.18).

Clearly, there is strong potential for generation of local polyphase fold and fabric histories during continuum D2 ductile thrusting. This implies that the D3, D4 & D5 deformation events of Hutton (1977a, 1979a, 1982, 1983) may not be as regionally ubiquitous as previously indicated.

This work also indicates that peak metamorphism may not be an entirely reliable criteria for temporal separation of structures and should therefore be used with caution. It is suggested that the local kinematic significance of a given 'non-penetrative' structure (with respect to surrounding penetrative deformation structures) should be evaluated in order to establish the significance of relative temporal separation.

### **6.3.3 D2 Thrust and Fold Sequence**

As described in detail in chapter 3, a clear D2 thrust sequence has been established for the Breaghy Head area. Both piggy back and break back thrust sequences have been identified, such that individual D2 ductile thrusts and F2 folds are seen to breach and/or fold previous thrusts in the sequence and some thrusts are clearly seen to originate from the hangingwall of the previous thrust in the sequence. Thus D2 structures deform other D2 structures to create local polyphase deformation sequences entirely composed of D2 structures. This is analogous to local polyphase deformation histories within foreland thrust and fold

belts (eg. Butler 1982b).

The breaching action of thrust (bt1) in particular, has significant implications for polyphase deformation. This thrust cuts across the Curragh Harbour anticline and therefore structures previously interpreted as D3, D4 & D5 (Hutton op. cit.). This thrust therefore provides independent evidence for the containment of these structures within D2.

#### **6.4 Metamorphic Implications**

Whilst in general the effects of syn-D2 greenschist metamorphism appear to be spatially and therefore temporally concentrated towards D2 ductile thrusts, the local presence of "non-penetrative" structures within the D2 thrusting deformation (chapter 3), implies sharper spatial and temporal metamorphic inhomogeneity. Although more complicated metamorphic discussion of these implications is outside the scope of this work, the following are indicated:

##### **6.4.1 Spatial and Temporal focusing of Greenschist Metamorphism**

The S2 & S2m fabrics which intensify towards D2 ductile thrusts are characteristically associated with mineral growth, crystal-plastic deformation and secondary recrystallisation indicative of syn-peak greenschist facies metamorphism (chapters 2 & 5, also Hutton 1977a). This mineral growth is seen to become more marked as a function of S2 fabric intensification, such that the peak greenschist metamorphic effects are spatially focused towards D2 ductile thrusts in the Breaghy Head area.

As described and discussed in chapters 4 & 5, the propagation of D2 ductile thrusts is a direct result of D2 strain/cleavage localisation and intensification, suggesting a temporal as well as

spatial association between individual thrust development and greenschist facies mineral growth. Indeed, chemically evolving and changing mineral growth within mylonites has been shown to be induced by active straining (Wintsch & Knipe 1983, Knipe & Wintsch 1985). This implies that during thrust motion, metamorphic mineral growth within D2 thrust plane S2m may continue after it has ceased in the thrust hangingwall and footwall S2 (as a function of the strain localisation history). The clear identification of a thrust sequence (chapter 3), therefore indicates diachronous coexistence of D2 deformation and peak metamorphism.

#### **6.4.2 D2 'Non-Penetrative' Fabrics**

As described above and in chapters 2, 3 & 5, the D2 deformation also contains a number of fabrics (previously interpreted as S3, S4 & S5), which are essentially 'non-penetrative' crenulations of S2 with little or no associated mineral growth. These include R1 & R2 extensional crenulations, C & P shears, strain slip and contractional fabrics associated with domino block rotations, culmination wall extensional fabrics and contractional fabrics associated with imbricate back-steepening and buttressing structures. These fabrics, some of which are axial planar to folds, have therefore been shown to reflect local kinematic processes associated with and therefore intimate to individual D2 ductile thrusts.

Clearly, all these fabrics are generated as or after D2 thrust shear zone displacement strains become localised into discrete thrust planes; that is (according to the metamorphic focusing effects outlined above), outside the zones of active mineral growth. Strain localisation-driven focusing of metamorphic fluid and ionic flow into the thrust planes may provide an additional explanation for the lack of mineral growth associated with these fabrics.

As discussed in chapter 5, a developing D2 thrust plane becomes increasingly less able to support loads (stress) and can therefore be regarded as a low stress feature during motion. It is suggested that this may generate sufficient pressure gradients within the metamorphic fluids to cause channelling of fluid flow into the thrust plane from the hangingwall and footwall, leading to preferential mineral growth within the thrust plane S2m. Furthermore, stress gradients associated with some structures (eg. between hinge and limb regions of folds), appear to result in metamorphic mineral growth concentration and composition gradients within those structures as a consequence of ions migrating along stress-sympathetic pressure gradients in the metamorphic fluid (cf. Gresens 1966, Cosgrove 1976).

### **6.5 Structure and Age of Metadolerite Intrusives**

The timing of metadolerite sill-like intrusions in NW Donegal with respect to contractional deformation phases, and their significance with respect to similar basic sheet intrusives within the Scottish Dalradian belt has been a subject of recent debate (cf. Hutton 1979d, Elsdon 1986). The majority of metadolerite sills in the region are concordant with the stratigraphy and at some localities clearly deformed by D2 structures, whilst some sills transgress stratigraphy and cut through or are contained within D2 structures (McCall 1954, Rickard 1962, Pitcher & Berger 1972, Hutton 1977a, 1979d, Elsdon 1986). This has led to the suggestion that two temporally disparate suites of metadolerite intrusions are present in NW Donegal; a pre-orogenic suite and a syn-orogenic suite (Pitcher & Berger 1972 and references therein, Hutton 1979d, Elsdon 1986).

Contrary to this suggestion, however, the metadolerites variously interpreted as pre-D2, syn-D2 and post-D2 in NW Donegal all share a common (originally quartz dolerite) composition and no

cross-cutting relationships between the sills have so far been described.

#### **6.5.1 Evidence for Pre-orogenic Intrusion?**

Elsdon (1986) has shown that the major Rough Point metadolerite sill is inverted with host stratigraphy within the mid limb of a major recumbent F2 fold in the hangingwall of the Horn Head thrust, suggesting pre-D2 intrusion. Furthermore, Elsdon shows that this sill is geochemically indistinguishable from basic intrusives within the SW Scottish Highlands, interpreted as being intruded into unlithified sediments during the rifting phase of the Dalradian basin development (Graham 1976).

As described by Elsdon (1986), the country rocks adjacent to the northern (top) contact of the Rough Point sill contain a zone of disrupted metasediments, in which pelite rafts are contained within a massive medium grained crystalline matrix. The rafts have sharp and bedding-parallel and orthogonal boundaries, and many contain bedding-parallel and orthogonal fractures and veins of the matrix material. The matrix and rafts share a common geochemical and mineralogical composition, such that the matrix is highly disrupted metasediment (pelite), not metadolerite (Elsdon 1986). The metadolerite sill makes a sharp, laterally continuous conformable planar contact with the country rocks and no metasediment rafts are seen to be contained within the sill. Similar relationships are noted at the contact of the regionally significant Mam sill, several kilometres to the SW; the sill-top structures described as 'volatile escape' features in chapter 3 are also analogous. These contact relationships are unlike the pillowed chilled margins, fluidized sediment veins and dense population of intra-intrusive wispy to globular xenoliths of fluidized sediment described as indicative of magma - wet sediment interaction (cf. Kokelaar 1982, Walker & Francis 1987, Leat &



Thompson 1988).

In the absence of any well developed D1 structures in the area, the timing of metadolerite intrusions with respect to D1 is unknown. This work has shown, however, that the majority of the sill-like metadolerite sheet intrusions within the study area have been duplicated across a suite of previously unrecognised D2 ductile thrusts (chapter 3, maps 1 & 2). These metadolerite sheets have therefore acted as passive markers to the thrusting deformation in much the same way as the metasediments; it is significant that the sills occupy similar stratigraphic levels within adjacent thrust sheets in the imbricate stack. At some localities, the metadolerites are seen to be cut out against thrusts, where they host S2 fabrics which show intensity gradients (S2 'background' to platy S2m) of similar style to the cleavage/strain gradients seen approaching D2 thrusts within the metasediments which host the intrusives (also Hutton 1979d). This appears to suggest intrusion of the metadolerites prior to D2 deformation, however, this may represent an over simplification of the true situation:

### **6.5.2 Evidence for Syn-D2 Intrusion**

Clearly, the metadolerite sills in NW Donegal were intruded after the host sediments had been lithified. The mineralogy of hornfels spots in the country rocks marginal to some of the larger metadolerite sills is composed of biotite, muscovite, quartz and iron oxides; grain size increases outwards from the core to the margins of the spots where large biotites are prominent (Fig 2.3, also McCall 1954). Significantly, this mineral assemblage is identical to that characteristic of the peak (syn-D2) metamorphism described above, the growth of which define the regional penetrative S2 fabrics. Careful examination of thin sections of hornfels spots indicates that the randomly orientated muscovites

and biotites contained within the spots have the same clean, colour and pleochroism characteristics as those outside the spots which define the S2 cleavage (see Fig 2.3). This may suggest syn-D2 hornfelsing of the sill margins; the presence of fresh garnets within the outer margins of the spots may support this (Fig 2.3). The indication here is a negligible temporal separation between metadolerite intrusion and onset of D2 thrusting and folding.

Indeed, strong evidence exists for syn-D2 intrusion of metadolerite sills within the study area. As described in chapter 3, for example, a thin (cm scale) metadolerite sheet is seen to be intruded during and parallel to 'primary' S2 generation within the developing D2 Curragh Harbour forethrust - backthrust complex (Fig 3.14).

Further evidence for syn-D2 intrusion comes from a thin boudinaged metadolerite sheet contained within the western limb of the Curragh Harbour anticline. The necks of the boudins, which have a pronounced ovoid or 'rugby ball' geometry, are filled with interlocking masses of quartz and dark green chloritic material which in the field strongly resembles the boudinaged metadolerite (which is also chloritized). The quartz and chloritic masses within the neck veins are apparently mutually exclusive in 3D space, with only intermittently developed thin zones of minor intermixing at their boundaries. These masses are also crudely polarized, such that patches of the chloritic material are concentrated towards and in contact with metadolerite boudins and the quartz patches are concentrated towards the interior of the neck veins. Although the quartz and chloritic masses appear to form a texture crudely reminiscent of pegmatites, the boundaries between the quartz and chloritic masses are irregular to rounded or even reneform in character. At some positions, small sub-spherical 'blob'-like patches of quartz are seen to be

enclosed within but towards the margins of chlorite masses and visa versa, in what appears to be an extension of the irregular contact relationship between the masses. These relationships may indicate D2 boudinage of the metadolerite sheet prior to its full crystallization, and therefore a syn-D2 age for the intrusion. This would require pull-apart of the metadolerite sheet by fracturing the solidified margins, thus enabling escape/extrusion of unsolidified magma from the core of the sheet into the boudin neck areas where it would interact (immiscibly ?) with rapidly crystallizing quartz rich fluid. A thin 'beaded' sliver of metadolerite which emanates from the intrusive/country rock contact and crosses one of the boudin necks for some distance may represent a remnant of the solidified margin. Evacuation of magma from inside the sheet close to the boudin necks might also explain the pronounced ovoid boudin geometry.

At 610235 (maps 1 & 2), thin metadolerite sheets are clearly seen to be intruded within the mid limb area parallel to the axial planes of evolving F2 hosted D2 thrust ramps, at a specific point in the kinematic history of the structures (chapter 4, Fig 4.4, also Hutton 1979d). Of significance is the relationship between these thin sheets and the much larger sill beneath:

This larger (40m+ thick) intrusive is contained within the hangingwall to a D2 ductile thrust which is downward facing in the western limb of the Curragh Harbour anticline (chapter 3, Figs 3.15, 3.17, locality 50, map 2). West of (50), a second D2 ductile thrust emplaces limestones and a thin sequence of transition beds onto this sill, such that the top of the sill is pervaded by high strain S2m fabrics related to the thrust. This thrust climbs stratigraphic section in the hangingwall towards 610235 (maps 1 & 2) to the west, to bring transition beds and quartzites into thrust contact with the large sill beneath the fold structure described above (Fig 4.4). The mid limb metadolerite sheet within

this fold passes through the thrust into the larger sill beneath, where its margins rapidly become indecipherable from the surrounding metadolerite. Approximately 100m further to the west, the thrust climbs section in the footwall away from the top of the large sill; here another thin metadolerite sheet crosses the thrust and, again, appears to 'vanish' into the sill beneath.

These relationships indicate that although intrusion of the large sill at this locality appears to pre-date movement of the D2 ductile thrusts above and below it, the core of the sill may not have completely solidified and therefore acted as the magma source for the thin syn-D2 metadolerite sheets. A negligible temporal separation between intrusion of the sill and the motion of the two thrusts is clearly implied. Good evidence for this occurs at 590226 (maps 1 & 2), where the sill, which is exposed at the base of the cliffs to the east, turns sharply to transgress stratigraphy and cuts across the thrust. S2 cleavage pervades the contact metadolerite here and to the south, although this is visibly weaker than that developed at 610235 (maps 1 & 2) or the base of the sill exposed within a blow hole at (61), map 2. This sill is cut out against and pervasively deformed by break-back thrust (bt2) to the SW at locality (60), map 2. Significantly, the thrusts above and below the sill described above are among the earliest to develop in the Breaghy Head area, whilst (bt2) is considerably later in the thrust sequence (chapter 3).

### **6.5.3 Temporal Interaction between Metadolerite Intrusions and D2 Thrusting**

Estimates of plate convergence and individual thrust displacement rates within foreland areas of thrust belts range between 5-10km/my (eg. Burbank & Reynolds 1988, Allen et al 1991). Estimated cooling times for dolerite sheet intrusives under greenschist conditions range from 1-10 years for a sill 1m thick

to between 1000 and 10,000 years for a sill 100m thick (R. England & S. Day pers. comm. 1989). This indicates that a thrust would only achieve 5-50m displacement in the time it would take a 50m thick sill to intrude and cool to a completely solid state; (the upper limit for sill thickness in the Breaghy Head area is approximately 50m).

The majority of the D2 ductile thrusts in the Breaghy Head area (including the thrusts immediately above and below the sill described above) have map measurable minimum displacements of several 100m to 1km+ (maps 1 & 2). This indicates that there is sufficient time to accommodate intrusion and cooling of a metadolerite sill within a thrust sheet prior to development of the next thrust in the sequence. Clearly, in view of the above observations, D2 thrust imbrication and/or F2 folding of a metadolerite sill does not prove pre-regional D2 age of intrusion; rather it indicates intrusion prior to the particular D2 thrust or fold structures locally involved. Thus the intrusion of sills during regional D2 deformation, at different times and places within the evolving D2 thrust stack explains why apparently pre-D2, syn-D2, and post-D2 relationships are all associated with the sills in NW Donegal.

## **6.6 Significance of Dalradian Basin Extensional Faults**

The broad thrust sense shear zones (tectonic slides) which typify the penetrative deformation within the Dalradian belt show clear kinematic and spatial association with contractional folds and fabrics of the same generation (ie. the slides are clearly contractional structures). The considerable stratigraphic dislocations which many of these structures represent, however, are apparently extensional (ie. the slides emplace younger rocks onto older rocks, often with marked stratigraphic excision).

In order to account for this, Soper & Anderton (1984) suggested that the Ballachulish and Fort William slides may represent Dalradian basin extensional growth faults which have undergone incomplete inversion during penetrative contractional deformation. Anderton (1988) modified and expanded this interpretation to encompass the entire Dalradian belt, at the expense of detailed precluding structural observations, and has therefore come into strong criticism (cf. Roberts & Treagus 1990).

Alsop (1987) invokes the presence of an original Dalradian basin extensional fault to explain stratigraphic excision across a major tectonic slide in Central Donegal. In this case, however, Alsop suggests that the slide cuts across the basin fault to emplace younger rocks onto older. A similar suggestion has been made in chapter 3 to best explain the tectonic interleaving by forethrusts and backthrusts of the Ards Quartzite and Sessiagh Clonmass rocks and the buttressing deformation seen in the Curragh Harbour area.

### **6.7 Other Discrete Ductile Thrust Imbricate Zones within the Dalradian Belt**

The D2 ductile thrusts in the Breaghy Head - Dunfanaghy area are, by Dalradian standards, unusually discrete tectonic slides. It has been suggested that the reason for this might be the strong rheological contrast across the Ards Quartzite - Sessiagh Clonmass formation boundary. This rheological contrast and the lithological variability of the Sessiagh Clonmass formation may also promote rapid strain localisation over spatially restricted areas of the boundary (see chapter 5), leading to multiple imbricate development.

This imbricate zone is not unique within the Dalradian belt. Significantly, another discrete ductile imbricate stack has been

identified within Appin Group rocks of identical stratigraphic level and lithological composition near Loch Creran in the Scottish Dalradian (Litherland 1980, 1982). Although less complicated than the Breaghy Head ductile thrust zone, field checking of the Loch Creran imbricates during this study revealed similar patterns of intensifying strain and minor structures over similar 10-30m thick high strain zones within similar lithologies.

## **6.8 Regional Implications and Concluding Remarks**

The trace of the Errigal Syncline runs through Marble Hill bay, with the long normal limb exposed to the north of the bay and the steep limb exposed to the south. This syncline folds the D2 ductile thrust detachment surface and one of the highest (most southerly) thrusts. This indicates later displacement on a lower (sub-Ards Pelite) detachment and therefore a regional D2 piggy back thrust sequence.

Recently, Hutton (pers. comm. 1993, re: Hutton & Alsop in prep.) suggested that major D2 tectonic slides with excellent regional down-dip exposure (principally between and west of Ards Point and Dunlewy Lough, Fig 6.2), record many tens of kilometres displacement and have a clear piggy back sequence of development. The diachrony and inhomogeneity of D2 deformation and greenschist facies metamorphism indicated for the Dunfanaghy - Breaghy Head area may therefore be applied at a regional scale.

In addition to describing ductile thrust geometry, this thesis has described processes leading to generation and propagation of 'shaped' ductile thrusts and development of local polyphase deformation histories during continuum ductile thrusting. These processes may apply to larger scale tectonic slides within the Dalradian and the metamorphic parts of other mountain belts.

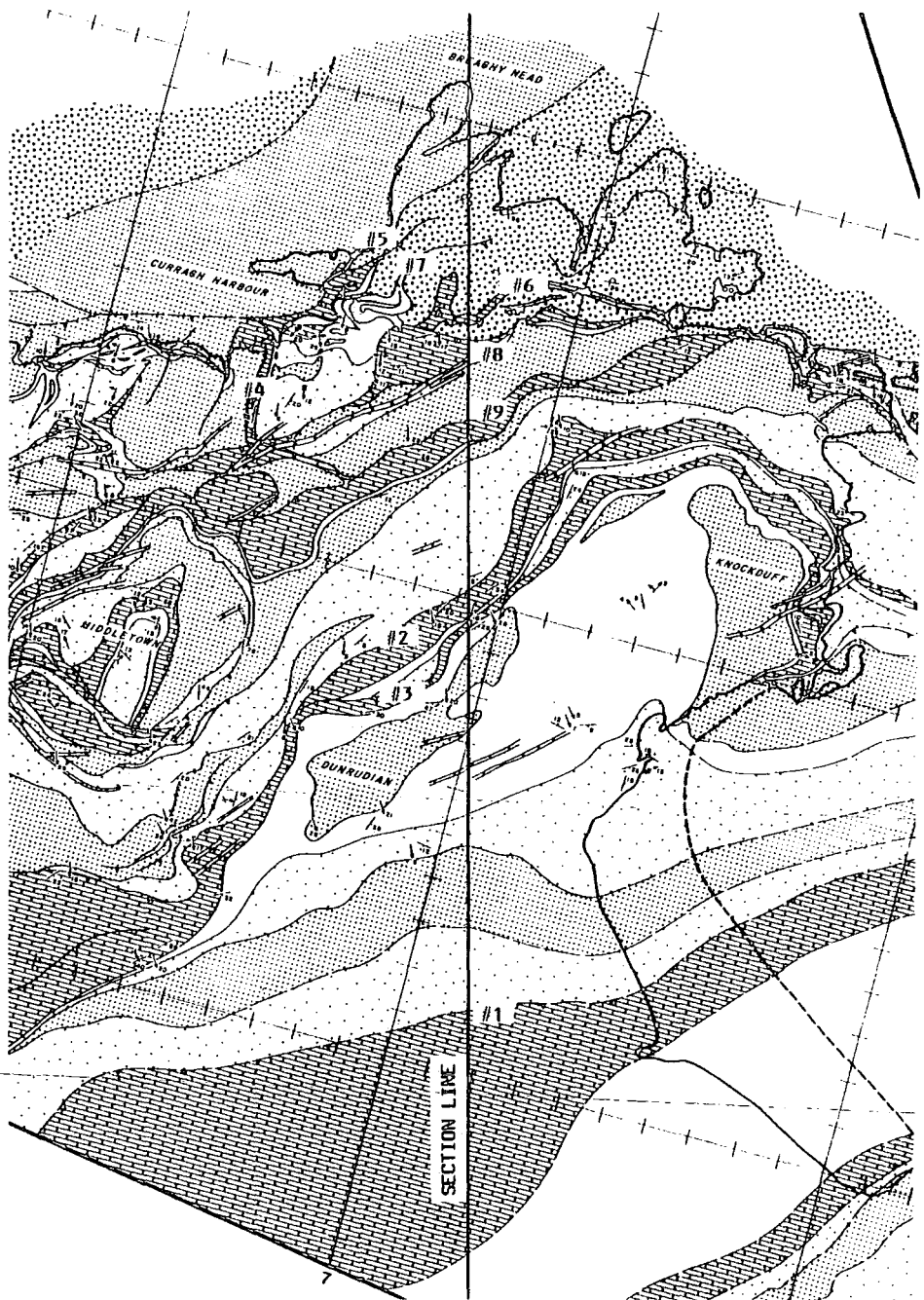


Figure 6.1 Map trace of restored section line (cf. maps 1 & 2). Numbers refer to thrust sequence identified in chapter 3, as indicated in the sequential section restoration.



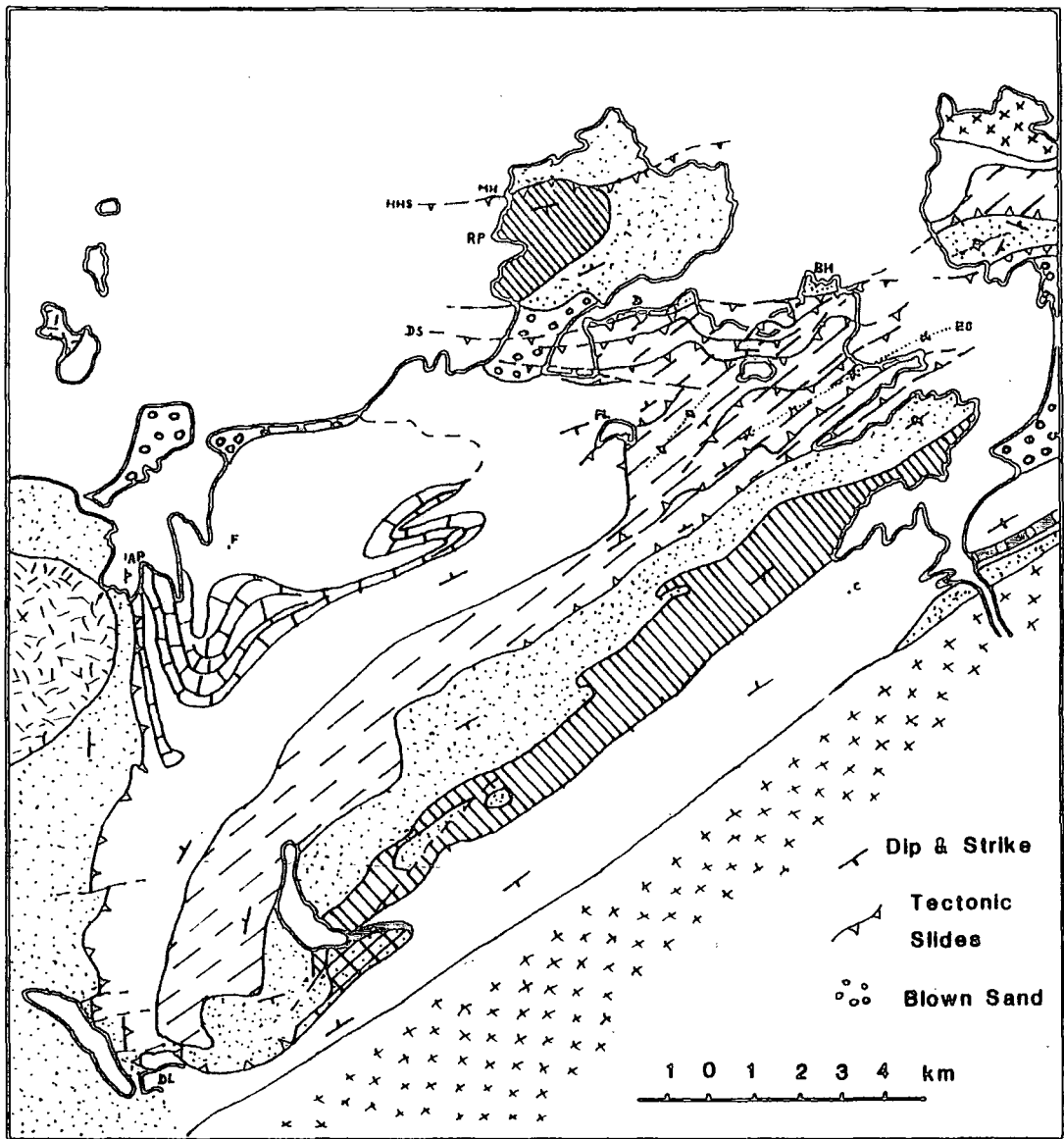


Figure 6.2 Regional map of NW Donegal modified from Fig 1.6 to incorporate D2 structures identified by this work in the Dunfanaghy - Breaghy Head area. (Ornament as for Fig 1.1).  
 AP: Ards Point, BH: Breaghy Head, C: Creeslough, D: Dunfanaghy, DL: Dunlewy Lough, DS: Dunfanaghy Slide, ES: Errigal Syncline, F: Falcarragh, HHS: Horn Head Slide, MH: Mickey's Hole, PL: Port Lough, RP: Rough Point.

## REFERENCES

ALLEN, P.A., CRAMPTON, S.L. & SINCLAIR, H.D. 1991. The inception and early evolution of the North Alpine Foreland Basin, Switzerland. *Basin Research*, 3, 143-163.

ALSOP, G.I. 1987. The Dalradian of Central Donegal, Ireland: An example of a polyphase mid-crustal thrust zone. Unpublished Ph.D. thesis, Durham University. U.K.

ALSOP, G.I. & HOLDSWORTH R.E. 1993. The distribution, geometry and kinematic significance of Caledonian buckle folds in the western Moine Nappe, northwestern Scotland. *Geological Magazine*, 130, 353-362.

ALSOP, G.I. & HUTTON, D.H.W. 1993. Major southeast-directed Caledonian thrusting and folding in the Dalradian rocks of mid-Ulster: implications for Caledonian tectonics and mid-crustal shear zones. *Geological Magazine*, 130, 233-244.

ANDERTON, R. 1988. Dalradian slides and basin development: a radical interpretation of stratigraphy and structure in the SW and Central Highlands of Scotland. *Journal of the Geological Society of London*, 145, 669-678.

ARCHULETA, R.J. 1984. A faulting model for the 1979 Imperial Valley earthquake. *Journal of Geophysical Research*, 89, 4559-4585.

BAILEY, E.B. 1910. Recumbent folds in the schists of the Scottish Highlands. *Quarterly Journal of the Geological Society of London*, 66, 586-620.

BAILEY, E.B. 1922. The structure of the Southwest Highlands of Scotland. Quarterly Journal of the Geological Society of London, 78, 82-131.

BAILEY, E.B. 1938. Eddies in mountain structure. Quarterly Journal of the Geological Society of London, 94, 607-625.

BARNETT, J.A.M., MORTIMER, J., RIPPON, J.H., WALSH, J.J. & WATTERSON, J. 1987. Displacement geometry in the volume containing a single normal fault. American Association of Petroleum Geologists Bulletin, 71, 925-937.

BEACH, A. 1981. Some observations on the development of thrust faults in the Ultradauphinois zone, French Alps: In: McCLAY, K.R. & PRICE, N.J. (eds), Thrust and Nappe tectonics. Geological Society of London Special Publication, 9, 329-334.

BEHRMANN, J.H. 1987. A precautionary note on shear bands as kinematic indicators. Journal of Structural Geology, 9, 659-666.

BELL, T.H. 1978. Progressive deformation and reorientation of fold axes in a ductile mylonite zone: The Woodroffe thrust. Tectonophysics, 44, 285-320.

BELL, T.H. & HAMMOND, R.L. 1984. On the internal geometry of mylonite zones. Journal of Geology, 92, 667-686.

BLISS, G.M., GRANT, P.R., MAX, M.D. & DIVER, W.L. 1978. Sedimentary and diagenetic features in the Sessiagh Clonmass formation of the Dalradian Ballachulish Sub-Group in Donegal. Geological Survey of Ireland Bulletin, 2, 189-204.

BOYER, S.E. & ELLOITT, D. 1982. Thrust systems. American Association of Petroleum Geologists Bulletin, 66, 1196-1230.

BOYER, S.E. & MITRA, G. 1988. Relations between deformation of crystalline basement and sedimentary cover at the basement/cover transition zone of the Appalachian Blue Ridge Province: In: MITRA, G. & WOJTAL, S. (eds), Geometries and Mechanisms of thrusting. Geological Society of America, Special Paper, 222, 119-136.

BRUNEL, M. 1986. Ductile thrusting in the Himalayas: Shear sense criteria and stretching lineations. *Tectonics*, 5, 247-265.

BURBANK, D.W. & RAYNOLDS, R.G.H. 1988. Stratigraphic keys to the timing of thrusting in terrestrial foreland basins: applications to the Northwestern Himalaya: In: KLEINSPEHN, K.L. & PAOLA, C. (eds), *New Perspectives in Basin Analysis*. Springer Verlag, New York. 331-351.

BUTLER, R.W.H. 1982a. The terminology of structures in thrust belts. *Journal of Structural Geology*, 4, 239-245.

BUTLER, R.W.H. 1982b. A structural analysis of the Moine Thrust Zone between Loch Eriboll and Fionaven, NW Scotland. *Journal of Structural Geology*, 4, 19-29.

BUTLER, R.W.H. 1982c. Hangingwall strain: a function of duplex shape and footwall topography. *Tectonophysics*, 88, 235-246.

BUTLER, R.W.H. 1987. Thrust sequences. *Journal of the Geological Society of London*, 144, 619-634.

BUTLER, R.W.H. 1989a. The influence of pre-existing basin structure on thrust system evolution in the Western Alps: In: COOPER, M.A. & WILLIAMS, G.D. (eds), *Inversion Tectonics*. Geological Society of London Special Publication, 44, 105-122.

BUTLER, R.W.H. 1989b. Thrust evolution within previously rifted regions: an example from the Vercors, French Sub-Alpine chains. *Memoria Societa Geologica Italiana*, 389, (in press).

BUTLER, R.W.H. & PRIOR, D.J. 1988. Anatomy of a continental subduction zone: the Main Mantle Thrust in Northern Pakistan. *Geologische Rundschau*, 77, 239-255.

COBBOLD, P.R. 1983. Kinematic and mechanical continuity at a coherent interface. *Journal of Structural Geology*, 5, 341-349.

COBBOLD, P.R. & QUINQUIS, H. 1980. Development of sheath folds in shear regimes. *Journal of Structural Geology*, 2, 119-126.

COOPER, M.A. & TRAYNER, P.M. 1986. Thrust-surface geometry: implications for thrust-belt evolution and section balancing techniques. *Journal of Structural Geology*, 8, 305-312.

COSGROVE, J.W. 1976. The formation of crenulation cleavage. *Journal of the Geological Society of London*, 132, 155-178.

COWARD, M.P. 1982. Surge zones in the Moine thrust zone of NW Scotland. *Journal of Structural Geology*, 4, 247-256.

COWARD, M.P. & KIM, J.H. 1981. Strain within thrust sheets: In: McCLAY, K.R. & PRICE, N.J. (eds) *Thrust and Nappe Tectonics*. Geological Society of London Special Publication, 9, 275-292.

COWARD, M.P. & POTTS, G.J. 1983. Complex strain patterns developed at the frontal and lateral tips to shear zones and thrust zones. *Journal of Structural Geology*, 5, 383-399.

COWARD, M.P. & SMALLWOOD, S. 1984. An interpretation of the Variscan tectonics of SW Britain: In: HUTTON, D.H.W. & SANDERSON, D.J. (eds), Variscan tectonics of the North Atlantic region. Geological Society of London Special Publication, 14, 89-102.

DAHLSTROM, C.D.A. 1970. Structural geology in the eastern margin of the Canadian Rocky Mountains. Bulletin of Canadian Petroleum Geology, 18, 332-406.

DENNIS, A.J. & SECOR, D.T. 1987. A model for the development of crenulations in shear zones with applications from the Southern Appalachian Piedmont. Journal of Structural Geology, 9, 809-817.

DRURY, M.R. & URAI, J.L. 1990. Deformation related recrystallization processes. Tectonophysics, 172, 235-253.

ELLIS, M.A. & DUNLAP, W.J. 1988. Displacement variation along thrust faults: implications for the development of large faults. Journal of Structural Geology, 10, 183-192.

ELSDON, R. 1986. Petrology, structure and age of the Rough Point sill, Donegal. Geological Journal, 21, 151-168.

ELSDON, R. & TODD, S.P. 1989. A composite spessartite - appinite intrusion from Port na blagh, county Donegal, Ireland. Geological Journal, 24, 97-112.

ESCHER, A. & WATTERSON, J. 1974. Stretching fabrics, folds and crustal shortening. Tectonophysics, 22, 223-231.

ESHELBY, J.D. 1973. Dislocation theory for geophysical applications. Philosophical Transactions of the Royal Society of London, A274, 331-338.

EVANS, D.J. & WHITE, S.H. 1984. Microstructural and fabric studies from the rocks of the Moine Nappe, Eriboll, NW Scotland. *Journal of Structural Geology*, 6, 369-389.

FISCHER, M.J. & COWARD, M.P. 1982. Strains and folds within thrust sheets: An analysis of the Heilam sheet, N.W. Scotland. *Tectonophysics*, 88, 291-312.

FLEUTY, M.J. 1964. Tectonic Slides. *Geological Magazine*, 101, 452-456.

GHOSH, S.K. 1982. The problem of shearing along axial plane foliations. *Journal of Structural Geology*, 4, 63-67.

GILLCRIST, R., COWARD, M.P. & MUGNIER, J.L. 1987. Structural inversion and its controls: examples from the Alpine foreland and the French Alps. *Geodinamica Acta*, 1, 5-34.

GRAHAM, C.M. 1976. Petrochemistry and significance of Dalradian metabasaltic rocks of the SW Scottish Highlands. *Journal of the Geological Society of London*, 132, 61-84.

GRESENS, R.L. 1966. The effect of structurally produced pressure gradients on diffusion in rocks. *Journal of Geology*, 74, 307-321.

HANMER, S. 1986. Asymmetric pull aparts and foliation fish as kinematic indicators. *Journal of Structural Geology*, 8, 111-122.

HANSEN, E. 1971. *Strain facies*. Springer Verlag. New York.

HARRIS, A.L. & PITCHER, W.S. 1975. The Dalradian Supergroup: In: HARRIS, A.L., HOLLAND, C.H. & LEAKE, B.E. (eds), *A correlation of the precambrian rocks of the British Isles*. Geological Society of London Special Report, 6, 52-75.

HOLDSWORTH, R.E. 1988. The stereographic analysis of facing. *Journal of Structural Geology*, 10, 219-223.

HOLDSWORTH, R.E. 1989. The geology and structural evolution of a Caledonian fold and ductile thrust zone, Kyle of Tongue region, Sutherland, northern Scotland. *Journal of the Geological Society of London*, 146, 809-823.

HOLDSWORTH, R.E. 1990. Progressive deformation structures associated with ductile thrusts in the Moine Nappe, Sutherland, N Scotland. *Journal of Structural Geology*, 12, 443-452.

HUTTON, D.H.W. 1977a. The structure of the Lower Dalradian rocks of the Creeslough area, Co. Donegal, with special reference to tectonic slides. Unpublished Ph.D. Thesis, Queen's University Belfast.

HUTTON, D.H.W. 1977b. A structural cross-section from the aureole of the Main Donegal Granite. *Geological Journal*, 12, 99-122.

HUTTON, D.H.W. 1979a. Dalradian structure in the Creeslough area, NW Donegal, Ireland: In: HARRIS, A.L., HOLLAND, C.H. & LEAKE, B.E. (eds), *The Caledonides of the British Isles-reviewed*. Geological Society of London Special Publication, 8, 239-241.

HUTTON, D.H.W. 1979b. Tectonic slides: A review and reappraisal. *EarthScience Reviews*, 15, 151-172.

HUTTON, D.H.W. 1979c. The strain history of a Dalradian slide: using pebbles with low fluctuations in axis orientation. *Tectonophysics*, 55, 261-273.



HUTTON, D.H.W. 1979d. Metadolerite age relationships in the Dalradian of Northwest Donegal, Ireland and their orogenic significance. *Geological Journal*, 14, 171-178.

HUTTON, D.H.W. 1981. Tectonic slides in the Caledonides: In: McCLAY, K.R. & PRICE, N.J. (eds), *Thrust and Nappe tectonics*. Geological Society of London Special Publication, 9, 261-265.

HUTTON, D.H.W. 1982. A tectonic model for the emplacement of the Main Donegal Granite, NW Ireland. *Journal of the Geological Society of London*, 139, 615-631.

HUTTON, D.H.W. 1983. Deformational history of an area with well-developed tectonic slides; Dalradian rocks of Horn Head, NW Irish Caledonides. *Transactions of the Royal Society of Edinburgh: Earth Sciences*, 73, 151-171.

IYENGAR, S.V.P., PITCHER, W.S. & READ, H.H. 1954. The plutonic history of the Maas area, Co. Donegal. *Quarterly Journal of the Geological Society of London*, 110, 203-228.

KELLEY, S.P. & POWELL, D. 1985. Relationships between marginal thrusting and movement on major, internal shear zones in the Northern Highland Caledonides, Scotland. *Journal of Structural Geology*, 7, 161-174.

KILROE, J.R. & NOLAN, J. 1891. Northwest and Central Donegal. *Memoir of the Geological Survey of Ireland*.

KNILL, D.C. & KNILL, J.L. 1961. Time relations between folding, metamorphism and the emplacement of granite in Rosguill, County Donegal. *Quarterly Journal of the Geological Society of London*, 117, 273-302.

KNIPE, R.J. 1985. Footwall geometry and the rheology of thrust sheets. *Journal of Structural Geology*, 7, 1-10.

KNIPE, R.J. 1989. Deformation mechanisms - recognition from natural tectonites. *Journal of Structural Geology*, 11, 127-146.

KNIPE, R.J. & WINTSCH, R.P. 1985. Heterogeneous deformation, foliation development, and metamorphic processes in a polyphase mylonite: In: THOMPSON, A.B. & RUBIE, D.C. (eds), *Metamorphic reactions - kinetics, textures and deformation*. *Advances in physical geochemistry*, 4, Springer Verlag, New York.

KOKELAAR, B.P. 1982. Fluidization of wet sediments during the emplacement and cooling of various igneous bodies. *Journal of the Geological Society of London*, 139, 21-33.

LAW, R.D., KNIPE, R.J. & DAYAN, H. 1984. Strain path partitioning within thrust sheets: microstructural and petrofabric evidence from the Moine Thrust Zone at Loch Eriboll, northwest Scotland. *Journal of Structural Geology*, 6, 477-497.

LEAT, P.T. & THOMPSON, R.N. 1988. Miocene hydrovolcanism in NW Colorado, USA, fuelled by explosive mixing of basic magma and wet unconsolidated sediment. *Bulletin of Volcanology*, 50, 229-243.

LISLE, R.J. 1985. The facing of faults. *Geological Magazine*, 122, 249-251.

LISTER, G.S. & SNOKÉ, A.W. 1984. S-C mylonites. *Journal of Structural Geology*, 6, 617-638.

LISTER, G.S. & WILLIAMS, P.F. 1979. Fabric development in shear zones: theoretical controls and observed phenomena. *Journal of Structural Geology*, 1, 283-298.

LISTER, G.S. & WILLIAMS, P.F. 1983. The partitioning of deformation in flowing rock masses. *Tectonophysics*, 92, 1-33.

LITHERLAND, M. 1980. The stratigraphy of the Dalradian rocks around Loch Creran, Argyll. *Scottish Journal of Geology*, 16, 105-123.

LITHERLAND, M. 1982. The structure of the Loch Creran Dalradian and a new model for the SW Highlands. *Scottish Journal of Geology*, 18, 205-225.

McCALL, G.J.H. 1954. The Dalradian geology of the Creeslough Area, Co. Donegal. *Quarterly Journal of the Geological Society of London*, 110, 153-175.

McCALLIEN, W.J. 1937. The geology of the Rathmullan district, Co. Donegal. *Proceedings of the Royal Irish Academy*, 44B, 45-59.

MEANS, W.D. 1990. Kinematics, stress, deformation and material behavior. *Journal of Structural Geology*, 12, 953-971.

MITRA, G. & ELLIOTT, D. 1980. Deformation of basement in the Blue Ridge and development of the South Mountain Cleavage: In: WONES, D.R. (ed), *Caledonides in the U.S.A.*, Proceedings IGCP Symposium, Blacksburg Virginia. Virginia Polytechnic Institute and State University Department of Geological-Sciences, Memoir, 2, 307-311.

MORLEY, C.K. 1986. Vertical strain variations in the Osen-Roa thrust sheet, Northwestern Oslo Fjord, Norway. *Journal of Structural Geology*, 8, 621-632.

OLGAARD, D.L. 1990. The role of second phase in localizing deformation: In: KNIPE, R.J. & RUTTER, E.H. (eds), Deformation mechanisms, Rheology and Tectonics. Geological Society of London Special Publication, 54, 175-181.

PARK, R.G. 1969. Structural correlation in metamorphic belts. Tectonophysics, 7, 323-338.

PHILLIPS, G.N. 1987. Metamorphism of the Witwatersrand gold fields: conditions during peak metamorphism. Journal of Metamorphic Geology, 5, 307-322.

PITCHER, W.S. & BERGER, A.R. 1972. The geology of Donegal: a study of granite emplacement and unroofing. Wiley, New York.

PITCHER, W.S. & SHACKLETON, R.M. 1966. On the correlation of certain lower Dalradian successions in Northwest Donegal. Geological Journal, 5, 149-156.

PLATT, J.P. 1984. Secondary cleavages in ductile shear zones. Journal of Structural Geology, 6, 439-442.

PLATT, J.P. & BEHRMANN, J.H. 1986. Structures and fabrics in a crustal scale shear zone, Betic Cordillera, SE Spain. Journal of Structural Geology, 8, 15-33.

PLATT, J.P. & LEGGETT, J.K. 1986. Stratal extension in thrust footwalls, Makran accretionary prism: Implications for thrust tectonics. American Association of Petroleum Geologists Bulletin, 70, 191-203.

PLATT, J.P. & VISSERS, R.L.M. 1980. Extensional structures in anisotropic rocks. Journal of Structural Geology, 2, 397-410.

POIRIER, J.P. 1980. Shear localization and shear instability in materials in the ductile field. *Journal of Structural Geology*, 2, 135-142.

PRICE, R.A. 1988. The mechanical paradox of large overthrusts. *Geological Society of America Bulletin*, 100, 1898-1908.

PULVERTRAFT, T.C.R. 1961. The Dalradian successions and their relationships in the Churchill district of Co. Donegal. *Proceedings of the Royal Irish Academy*, 61B, 255-273.

RAMSAY, R.G. & GRAHAM, R.H. 1970. Strain variation in shear belts. *Canadian Journal of Earth Sciences*, 7, 786-813.

RAMSAY, R.G. & HUBER, M.I. 1987. The techniques of modern Structural Geology, volume 2: Folds and Fractures. Academic Press, London.

RATHBONE, P.A., COWARD, M.P. & HARRIS, A.L. 1983. Cover and basement: a contrast in style and fabrics: In: HATCHER, R.D., WILLIAMS, H. (Jr.) & ZIETZ, I. (eds), *Contributions to the tectonics and geophysics of mountain chains*. Geological Society of America Memoir, 158, 213-223.

RATTEY, P.R. & SANDERSON, D.J. 1982. Patterns of folding within nappes and thrust sheets: examples from the Variscan of southwest England. *Tectonophysics*, 88, 247-267.

RHODES, S. & GAYER, R.A. 1977. Non-cylindrical folds, linear structures in the X-direction and mylonite developed during translation of the Kalak Nappe Complex of Finnmark. *Geological Magazine*, 114, 329-341.

RICKARD, M.J. 1962. Stratigraphy and structure of the Errigal area, County Donegal, Ireland. Quarterly Journal of the Geological Society of London, 118, 207-236.

RIDLEY, J. 1986. Parallel stretching lineations and fold axes oblique to a shear displacement direction - a model and observations. Journal of Structural Geology, 8, 647-653.

ROBERTS, J.L. & TREAGUS, J.E. 1990. Discussion on Dalradian slides and basin development: a radical interpretation of stratigraphy and structure in the SW and Central Highlands of Scotland. Journal of the Geological Society of London, 147, 729-731.

ROERING, C. & SMIT, C.A. 1987. Bedding-parallel shear, thrusting and quartz vein formation in Witwatersrand quartzites. Journal of Structural Geology, 9, 419-427.

RUTTER, E.J. 1986. On the nomenclature of mode of failure transitions in rocks. Tectonophysics, 122, 381-387.

SANDERSON, D.J. 1973. The development of fold axes oblique to the regional trend. Tectonophysics, 16, 55-70.

SANDERSON, D.J. 1982. Models of strain variation in nappes and thrust sheets: a review. Tectonophysics, 88, 201-233.

SANDERSON, D.J. & MARCHINI, W.R.D. 1984. Transpression. Journal of Structural Geology, 6, 449-458.

SEAGO, R.D. & CHAPMAN, T.J. 1988. The confrontation of structural styles and the evolution of a foreland basin in central SW England. Journal of the Geological Society of London, 145, 789-800.

SHACKLETON, R.M. 1958. Downward-facing structures of the Highland Border. Quarterly Journal of the Geological Society of London, 113, 361-392.

SIBSON, R.H. 1989. Earthquake faulting as a structural process. Journal of Structural Geology, 11, 1-14.

SIMPSON, C. 1983. Displacement and strain patterns from naturally occurring shear zone terminations. Journal of Structural Geology, 5, 497-506.

SIMPSON, C. & SCHMID, S.M. 1983. An evaluation of criteria to deduce the sense of movement in sheared rocks. Geological Society of America Bulletin, 94, 1281-1288.

SOPER, N.J. & ANDERTON, R. 1984. Did the Dalradian slides originate as extensional faults? Nature, 307, 357-360.

TALBOT, C.J. & JACKSON, M.P.A. 1987. Internal kinematics of salt diapirs. American Association of Petroleum Geologists Bulletin, 71, 1068-1093.

TRAYNER, P.M. & COOPER, M.A. 1984. Cleavage geometry and the development of the Church Bay Anticline, Co. Cork, Ireland. Journal of Structural Geology, 6, 83-87.

TREAGUS, S.H. 1983. A theory of finite strain variation through contrasting layers, and its bearing on cleavage refraction. Journal of Structural Geology, 5, 351-368.

TREAGUS, S.H. 1988. Strain refraction in layered systems. Journal of Structural Geology, 10, 517-527.

TREAGUS, S.H. & SOKOUTIS, D. 1992. Laboratory modelling of strain variation across rheological boundaries. *Journal of Structural Geology*, 14, 405-424.

WALKER, B.H. & FRANCIS, E.H. 1987. High-level emplacement of an olivine-dolerite sill into Namurian sediments near Cardenden, Fife. *Transactions of the Royal Society of Edinburgh: Earth Sciences*, 77, 295-307.

WALSH, J.J. & WATTERSON, J. 1989. Displacement gradients on fault surfaces. *Journal of Structural Geology*, 11, 307-316.

WALSH, J.J. & WATTERSON, J. 1991. Geometric and kinematic coherence and scale effects in normal fault systems: In: ROBERTS, A.M., YIELDING, G. & FREEMAN, B. (eds) *The Geometry of Normal Faults*. Geological Society of London Special Publication, 56, 193-203.

WATKINSON, A.J. 1975. Multilayer folds initiated in bulk plane strain with axis of no change perpendicular to the layering. *Tectonophysics*, 28, I7-I11.

WEIJERMARS, R. & RONDEEL, H.E. 1984. Shearband foliation as an indicator of sense of shear: Field observations in Central Spain. *Geology*, 12, 603-606.

WELBON, A. 1988. The influence of intrabasinal faults on the development of a linked thrust system. *Geologische Rundschau*, 77, 11-27.

WHITE, N.J. & HUTTON, D.H.W. 1985. The structure of the Dalradian rocks in West Fanad, County Donegal. *Irish Journal of Earth Sciences*, 7, 79-92.



WHITE, S.H., BRETAN, P.G. RUTTER, E.H. 1986. Fault zone reactivation: kinematics and mechanisms. Philosophical Transactions of the Royal Society of London. A317, 81-97.

WHITE, S.H., BURROWS, S.E., CARRERAS, J., SHAW, N.D. & HUMPHREYS, F.J. 1980. On mylonites in ductile shear zones. Journal of Structural Geology, 2, 175-187.

WILLIAMS, G.D. & CHAPMAN, T.J. 1983. Strains developed in the hangingwalls of thrusts due to their slip/propagation rate: a dislocation model. Journal of Structural Geology, 5, 563-571.

WILLIAMS, P.F. 1985. Multiply deformed terrains: problems of correlation. Journal of Structural Geology, 7, 269-280.

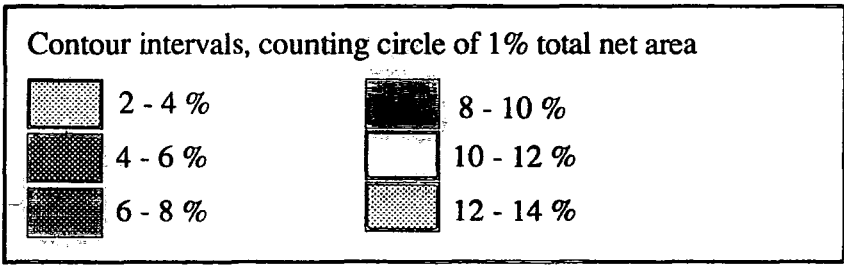
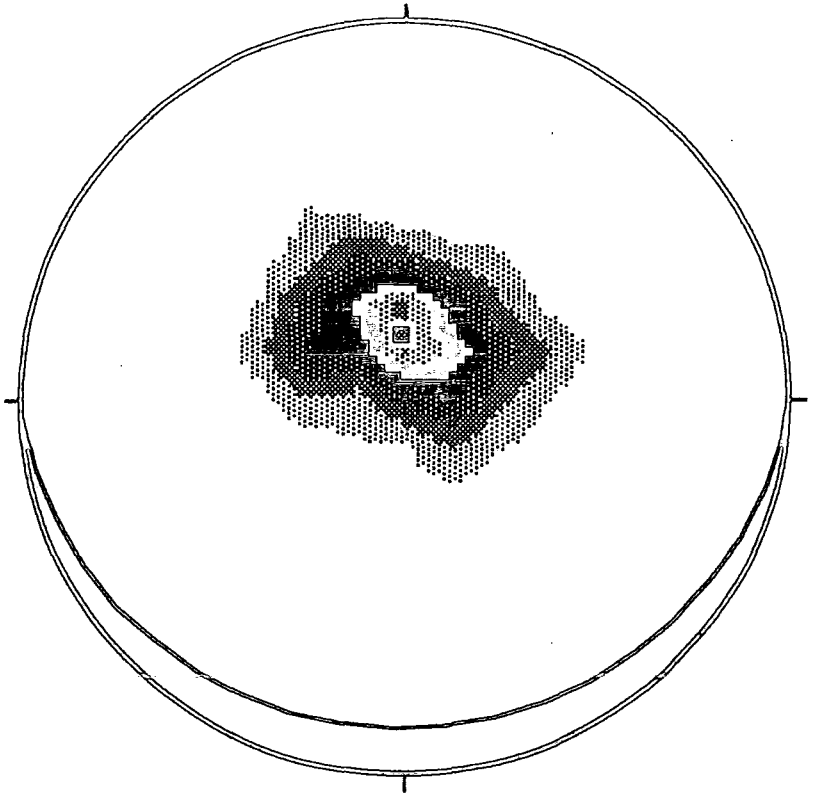
WINKLER, H.G.F. 1967. Petrogenesis of metamorphic rocks. Springer Verlag, New York.

WINTSCH, R.P. & KNIPE, R.J. 1983. Growth of a zoned plagioclase porphyroblast in a mylonite. Geology, 11, 360-363.



Figure 5.2e

Contoured plot of poles to S0 (bedding) planes



N : 236

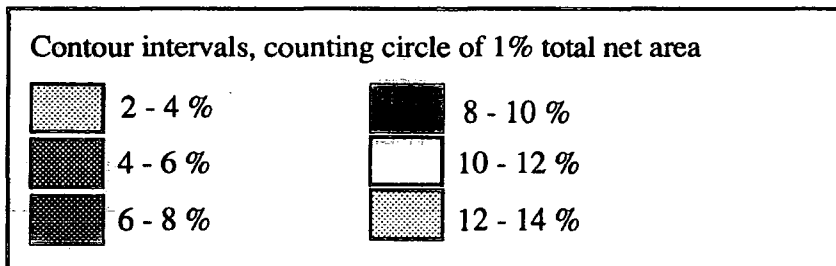
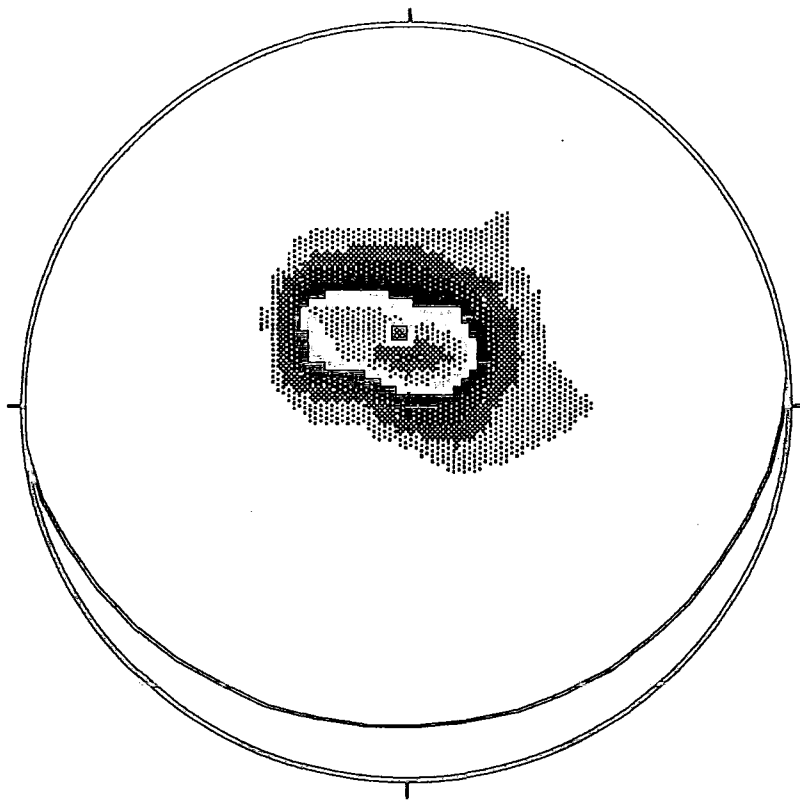
Equal area projection

Mean strike and dip : 087/14S



Figure 5.2f

Contoured plot of poles to S2 (cleavage) planes



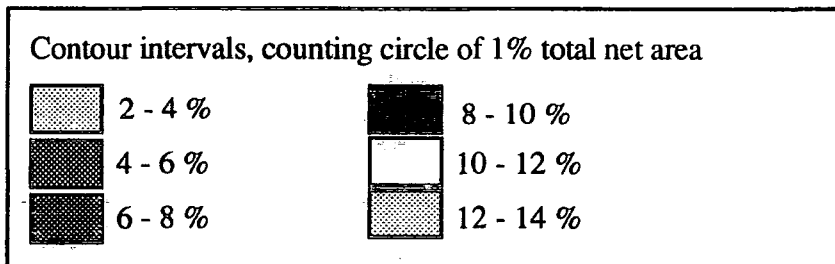
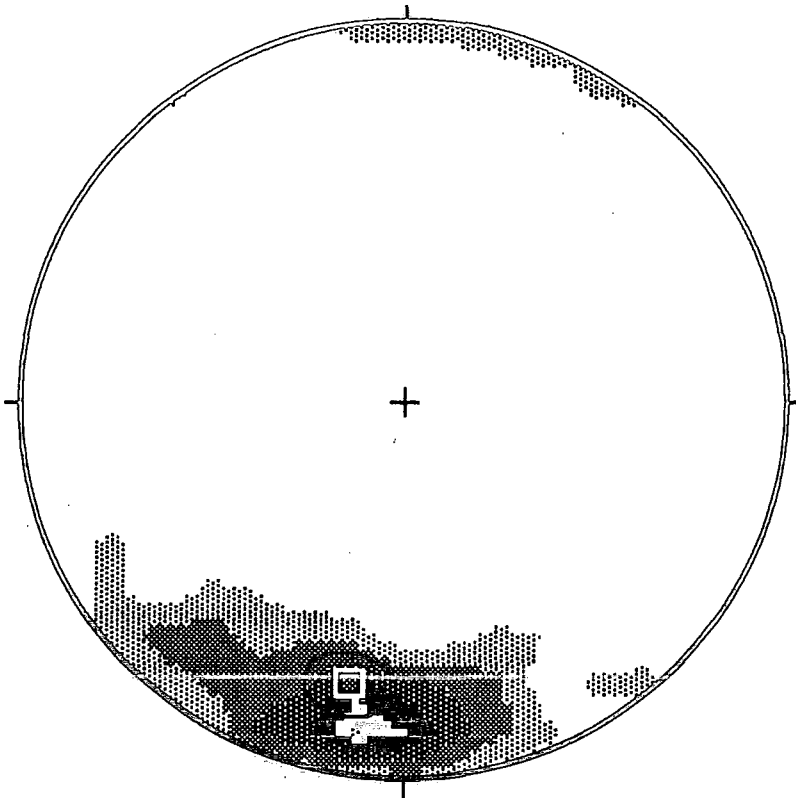
N : 230

Equal area projection

Mean strike and dip : 087/15S

Figure 5.2g

Contoured plot of F2 (minor fold) axes



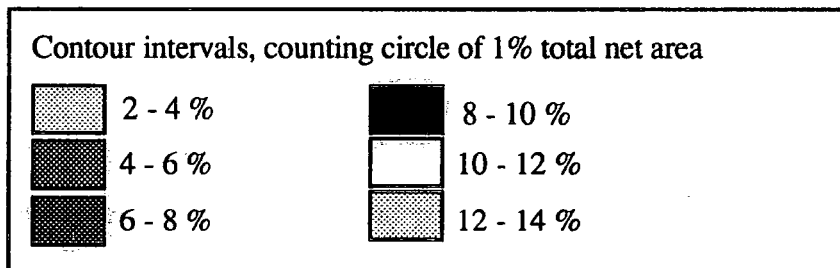
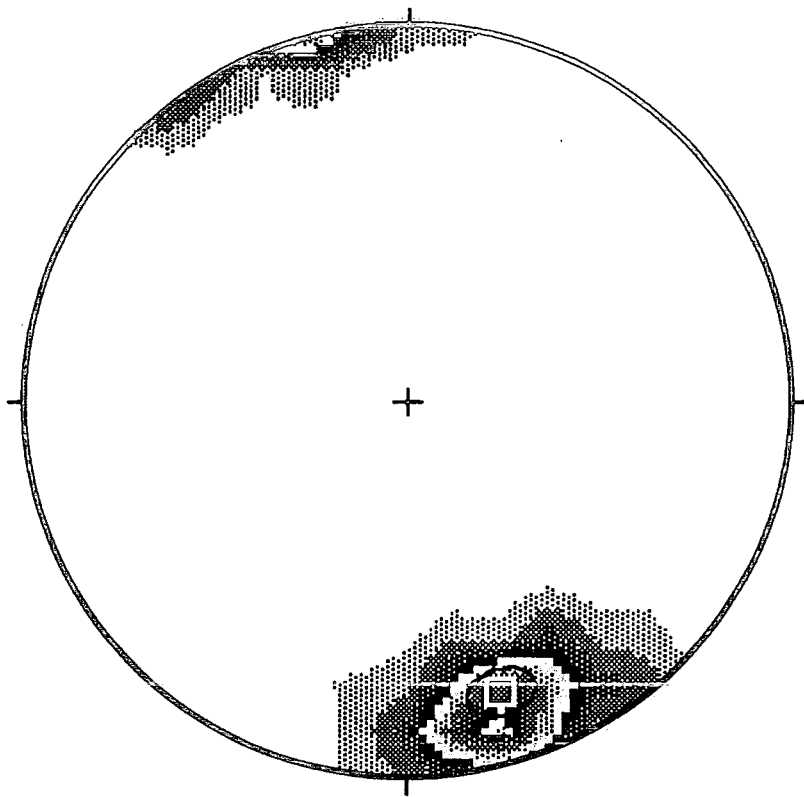
N : 156

Equal area projection

Mean vector : 20/167

Figure 5.2h

Contoured plot of D2 (mineral stretching) lineations



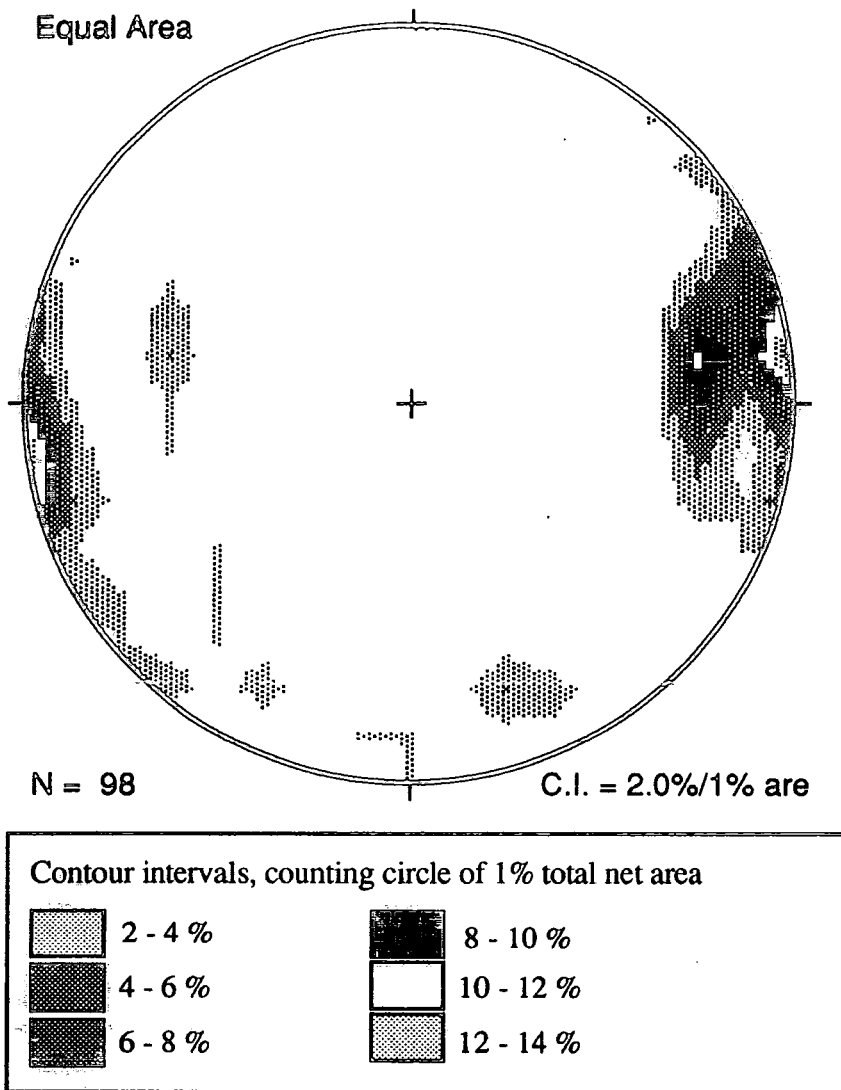
N : 199

Equal area projection

Mean vector : 20/167

Figure 5.2i

Contoured plot of D2 (boudin) axes



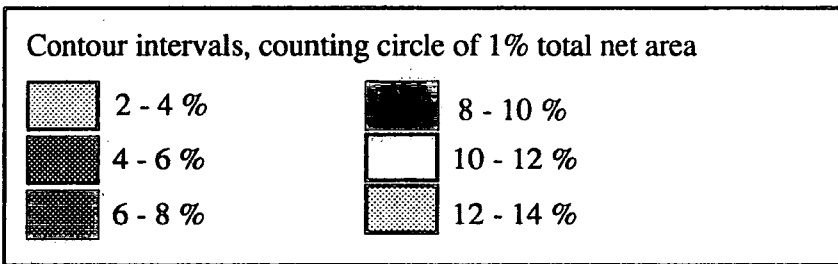
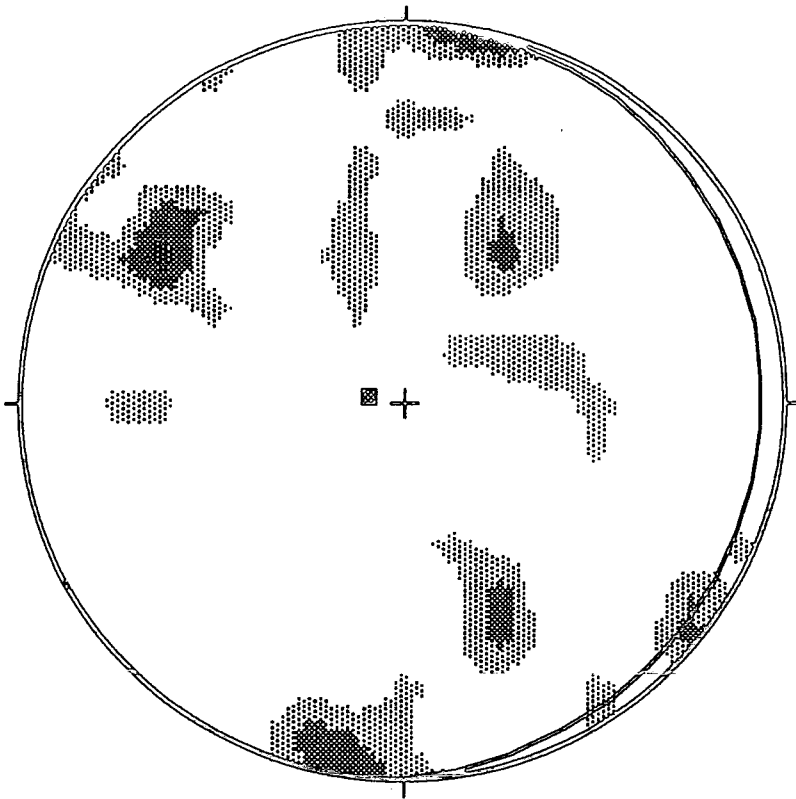
N : 98

Equal area projection

Mean vector : 3/82

Figure 5.2j

Contoured plot of D2 planar veins



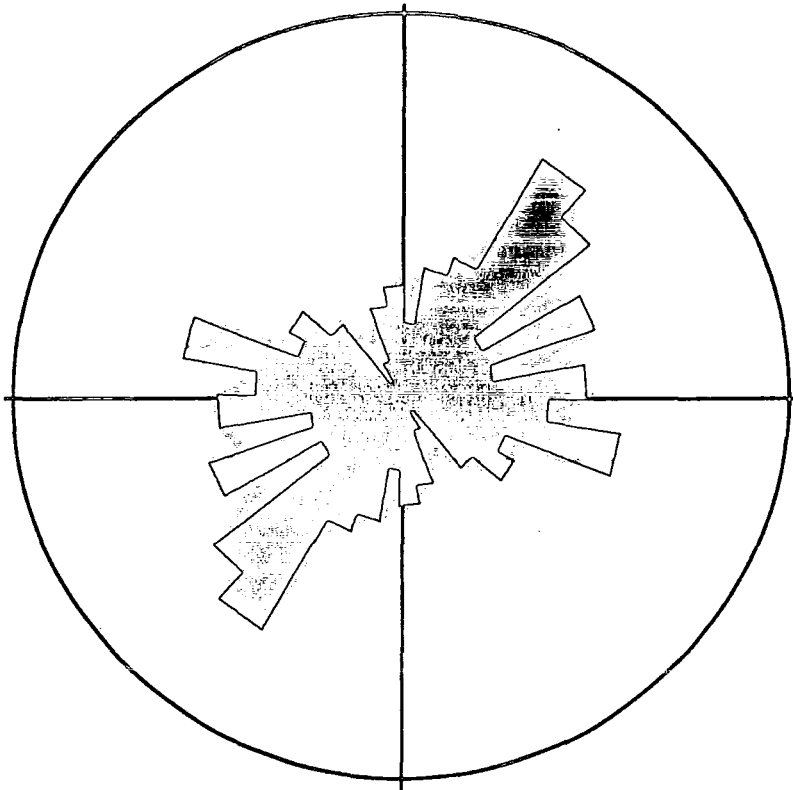
N : 79

Equal area projection

Mean strike and dip : 009/7E

Figure 5.2k

Rose diagram of strike directions of D2 planar veins



N : 260

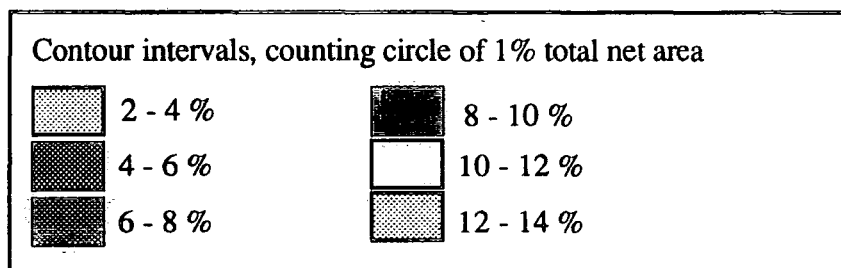
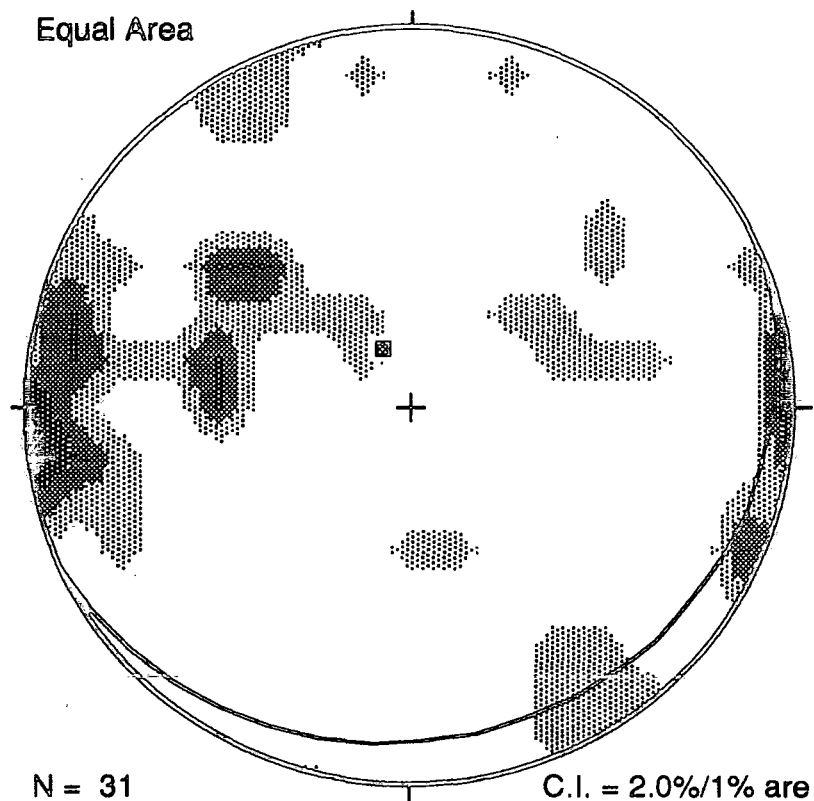
Circle perimeter : 8%

Mean strike trend : NNE-SSW (033-213)



Figure 5.21

Contoured plot of poles to non-penetrative cleavage planes



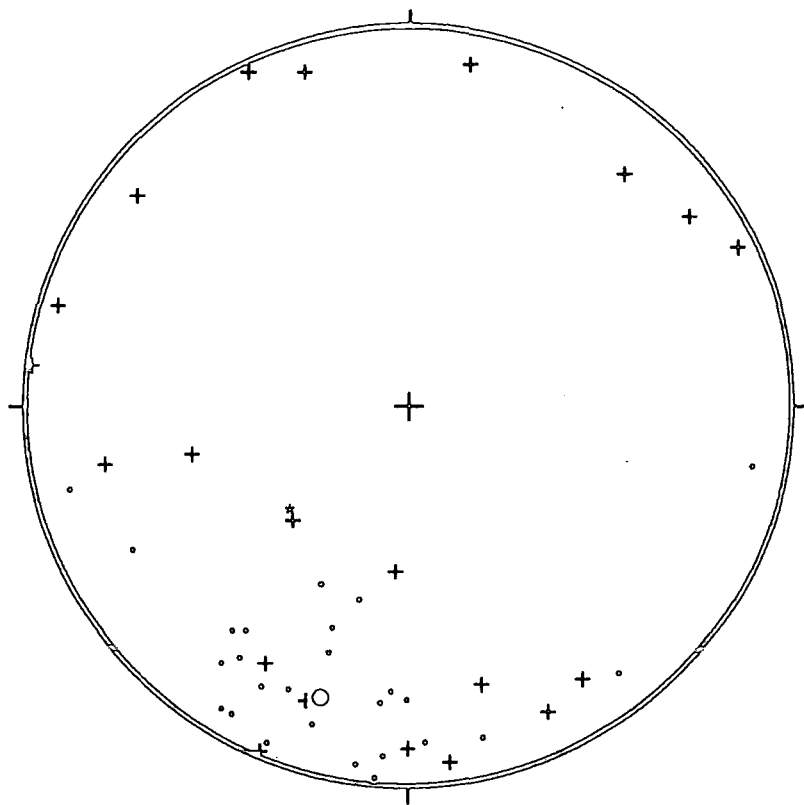
N : 31

Equal area projection

Mean strike and dip : 066/14S

Figure 5.2m

Composite scatter plot of non-penetrative fold axes and non-penetrative crenulation lineations on S2 or S0



. : Fold axes  
+ : Crenulation lineations

N (axes) : 26

N (lineations) : 20

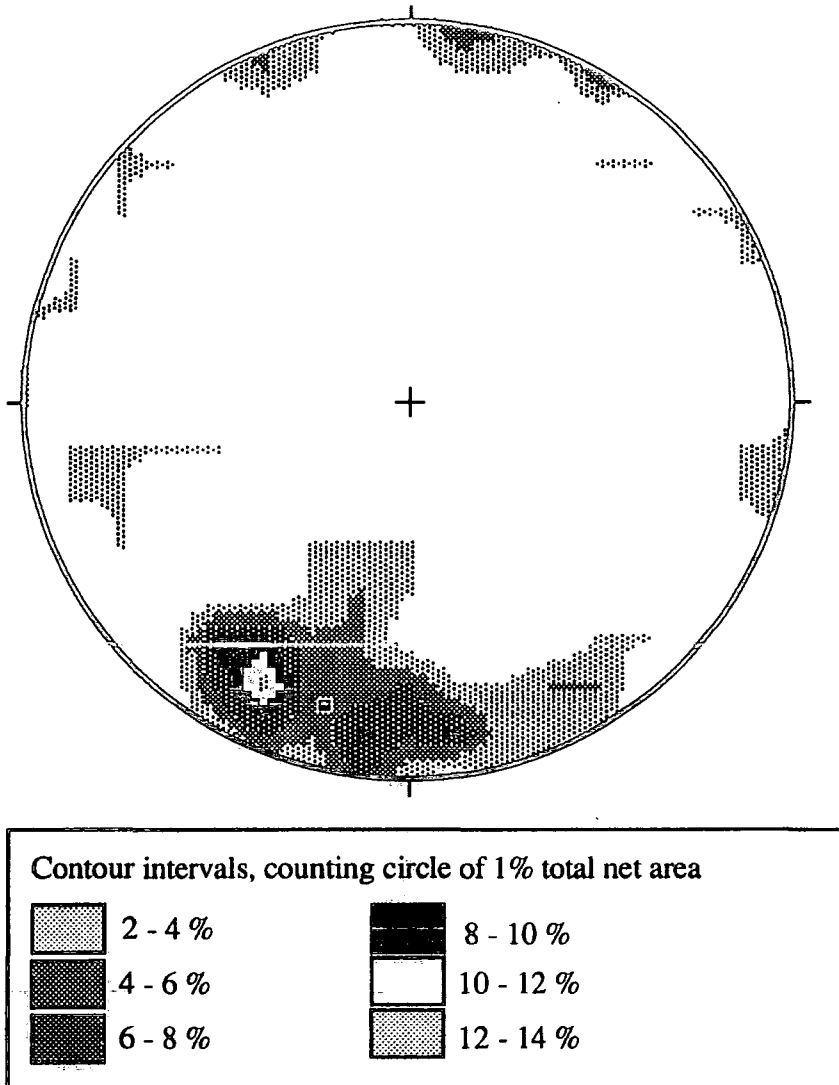
Equal area projection

Mean vector, axes,  $\circ$  : 21/196

Mean vector, lineations,  $\star$  : 56/226

Figure 5.2n

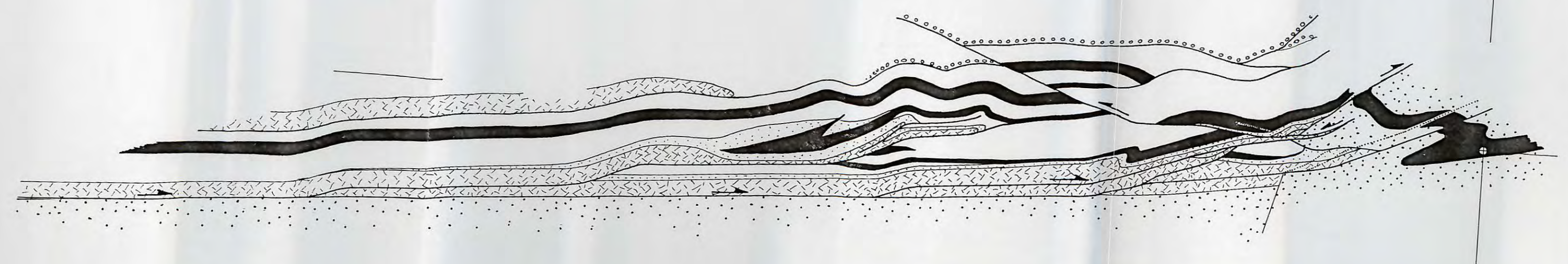
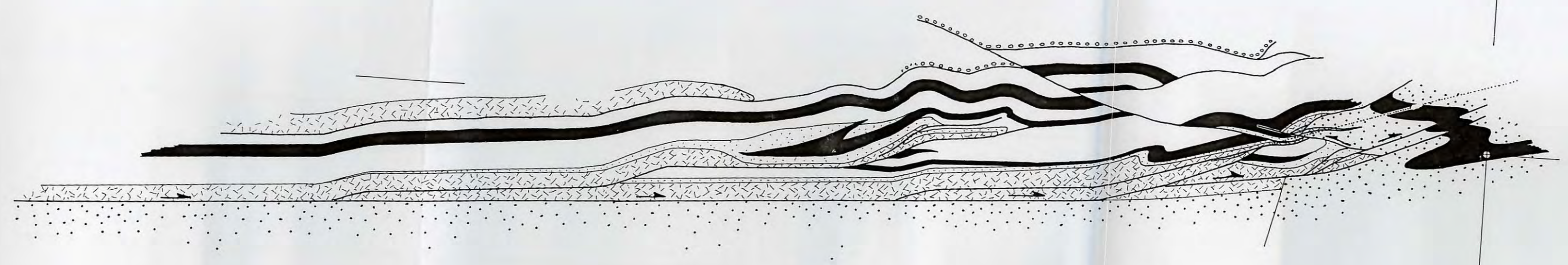
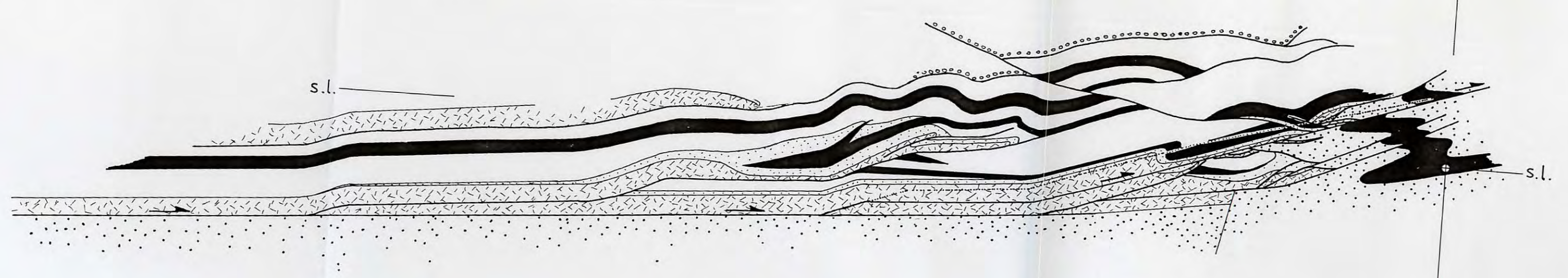
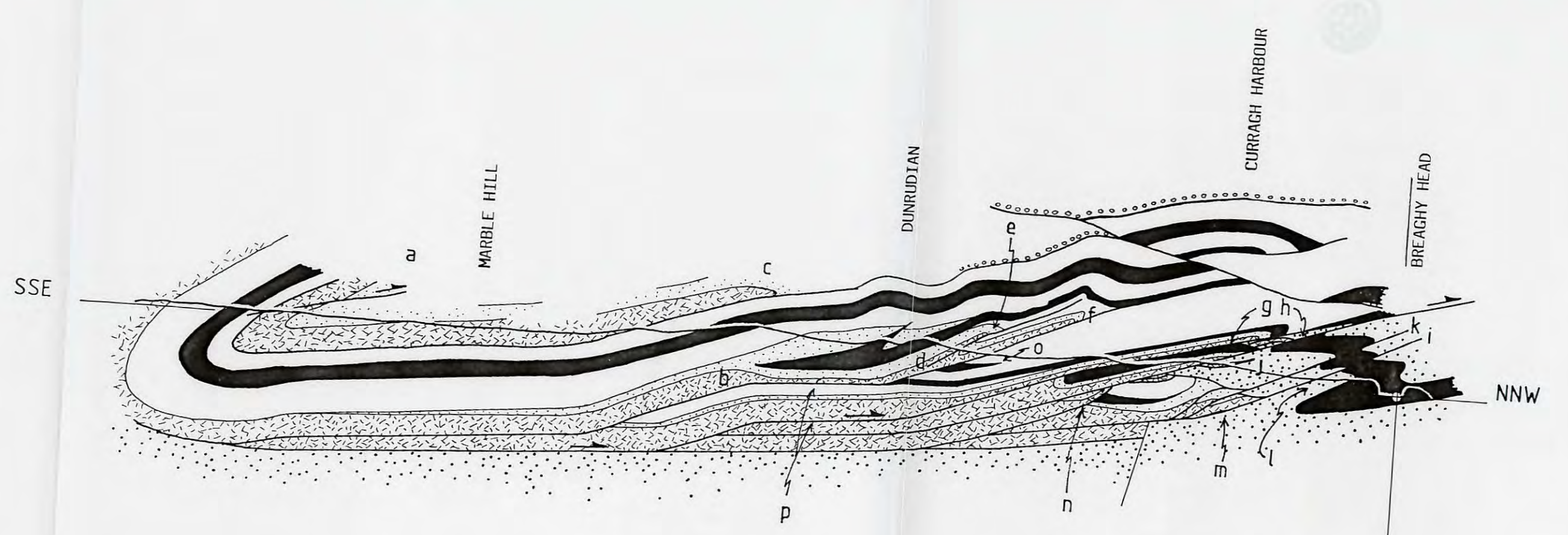
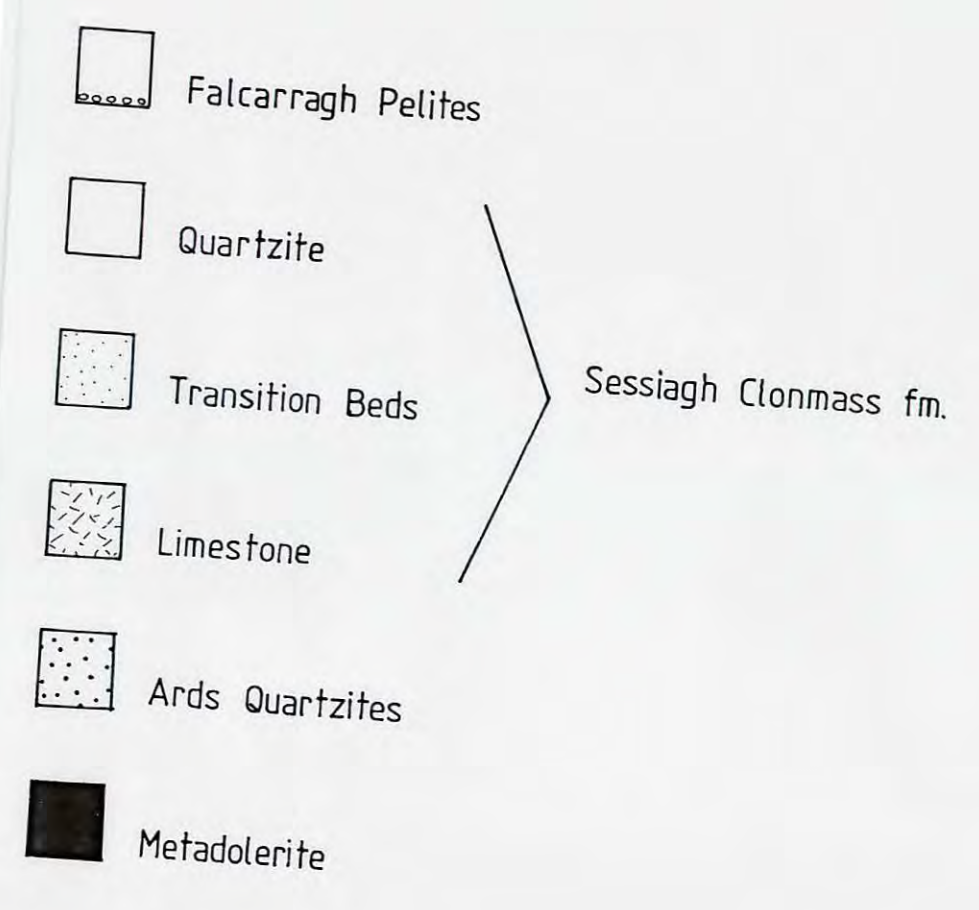
Composite contoured plot of non-penetrative fold axes and non-penetrative crenulation intersection lineations



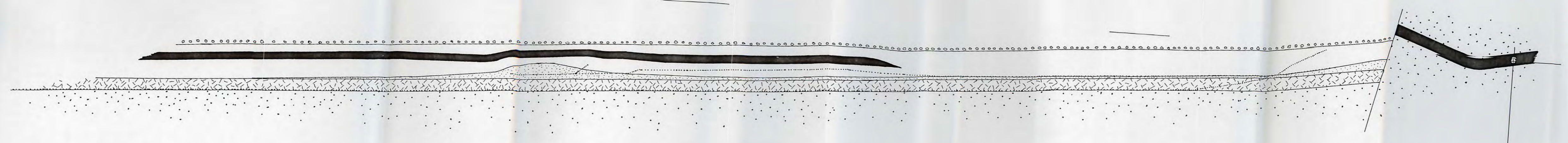
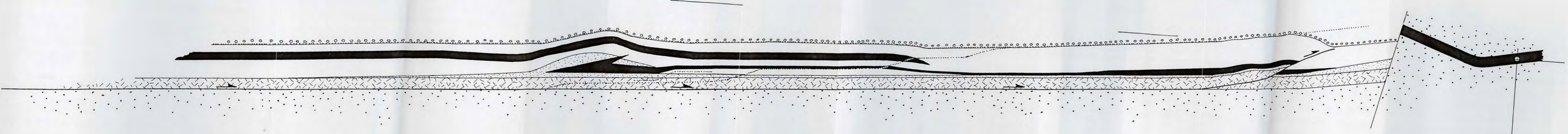
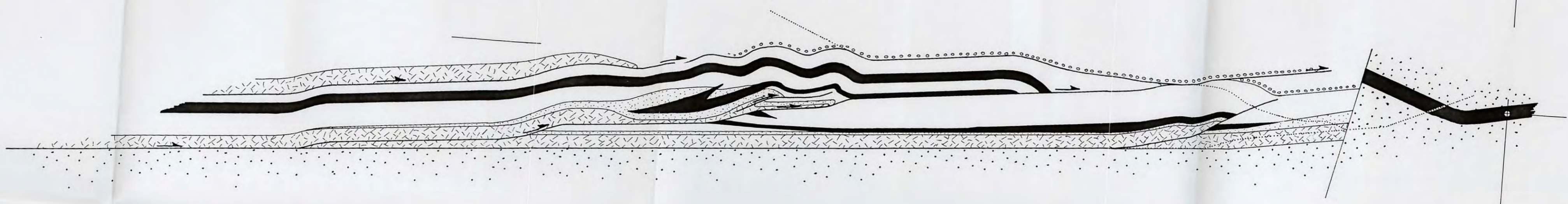
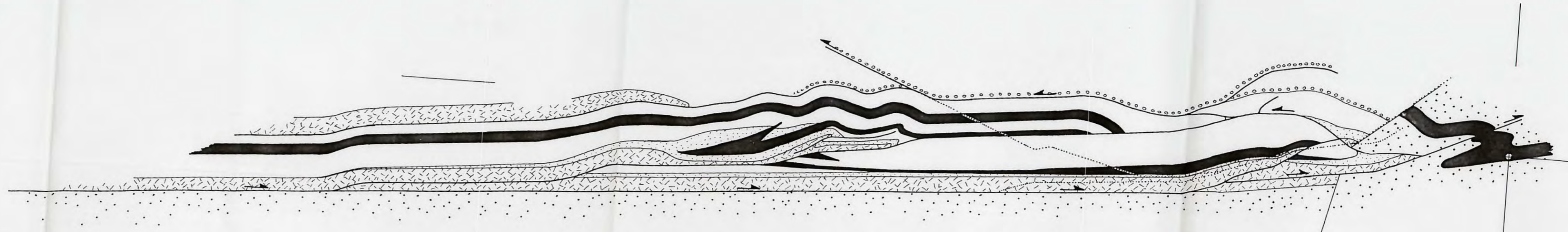
N : 46

Equal area projection

Mean vector : 17.6/195.5



- (a) Errigal Syncline.
- (b) Hangingwall ramp; constrained by exposures E of Sessiagh Lough.
- (c) Thrust #2; minimum displacement constrained by projection from exposures S of Sessiagh Lough to E of Marble Hill.
- (d) Branch point exposed NW of Dunrudian.
- (e) Thrust #4; minimum displacement constrained by exposures N of Knockduff to N of Dunrudian.
- (f) Thrust #3; minimum displacement constrained by exposures Knockduff to N of Sessiagh Lough.
- (g) Thrust #9 (bt3); minimum displacement constrained by hangingwall ramp N of Knockduff and footwall ramp S of Curragh Harbour.
- (h) Thrust #8 (bt1); minimum displacement constrained by exposures NW of Middle Town to E of Curragh Harbour.
- (i) Thrust #5.
- (j) Thrust #6.
- (k) Thrust #7.
- (l) Breached major F2 folds indicated and constrained by prevailing younging directions and folds exposed in the N Bregagh Head area.
- (m) Forethrust/backthrust complex exposed in Curragh Harbour area.
- (n) Folded thrust #1; cut-off against thrust bt1 to S of Curragh Harbour.
- (o) Metadolerite sill pinch-out exposed to N of Dunrudian.
- (p) Flats constrained by exposures and prevailing dip E of Knockduff.
- (q) Footwall ramps constrained by prevailing surface dip changes.



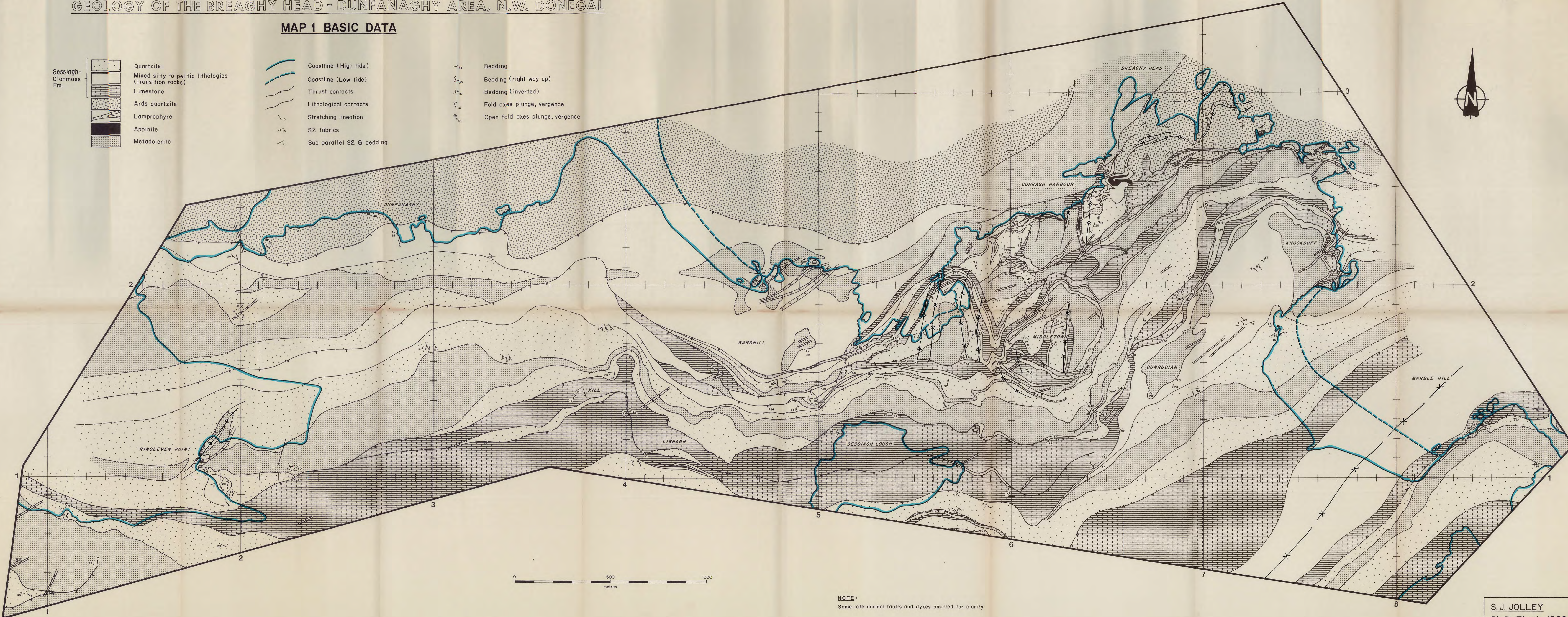
GEOLOGY OF THE BREAGHY HEAD - DUNFANAGHY AREA, N.W. DONEGAL

MAP 1 BASIC DATA

- Sessiagh-Clonmass Fm.
- Quartzite
  - Mixed silty to pelitic lithologies (transition rocks)
  - Limestone
  - Ards quartzite
  - Lamprophyre
  - Appinite
  - Metadolerite

- Coastline (High tide)
- Coastline (Low tide)
- Thrust contacts
- Lithological contacts
- Stretching lineation
- S2 fabrics
- Sub parallel S2 & bedding

- Bedding
- Bedding (right way up)
- Bedding (inverted)
- Fold axes plunge, vergence
- Open fold axes plunge, vergence

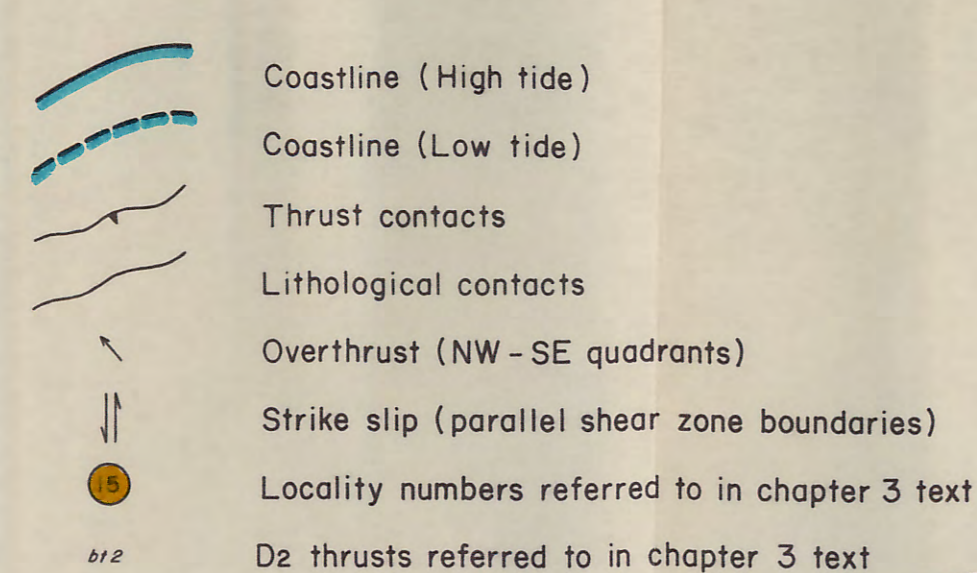
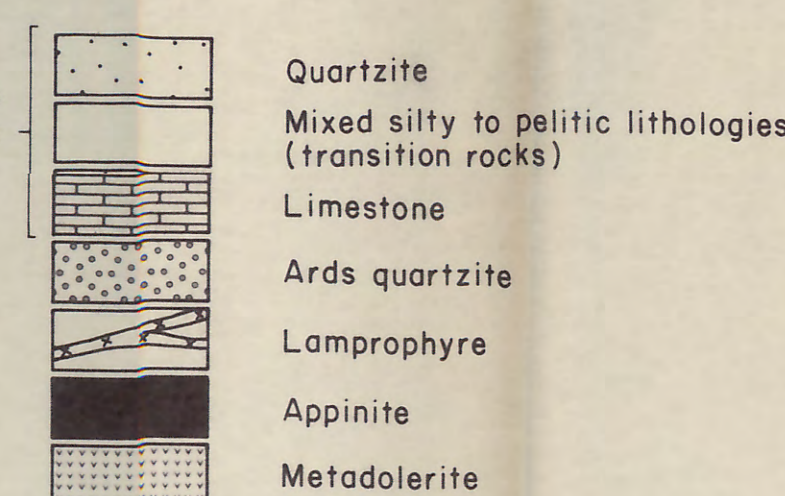


NOTE:  
Some late normal faults and dykes omitted for clarity

GEOLOGY OF THE BREAGHY HEAD - DUNFANAGHY AREA, N.W. DONEGAL

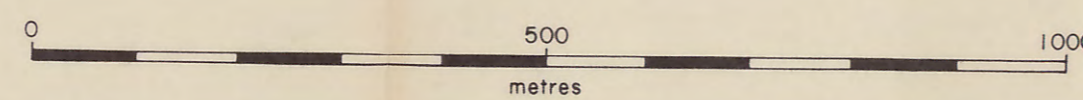
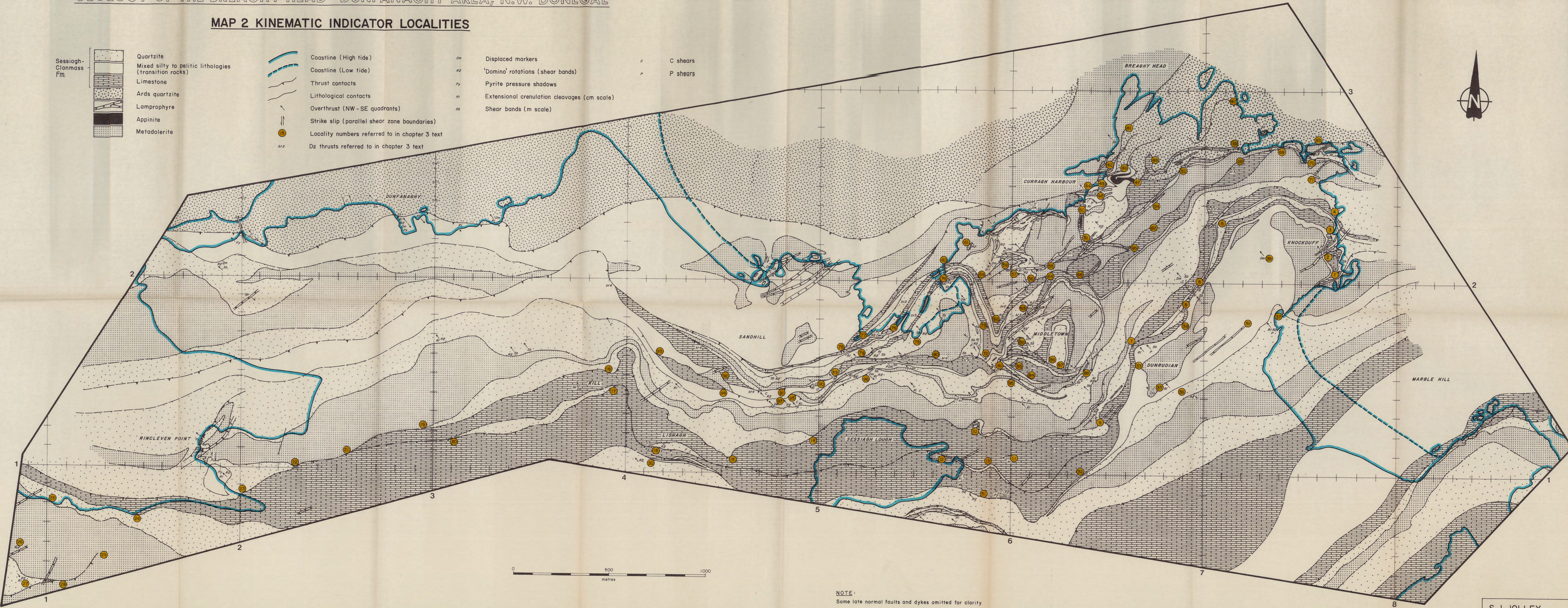
MAP 2 KINEMATIC INDICATOR LOCALITIES

Sessiagh-Clonmass Fm.



*dm* Displaced markers  
*rz* 'Domino' rotations (shear bands)  
*py* Pyrite pressure shadows  
*ri* Extensional crenulation cleavages (cm scale)  
*sb* Shear bands (m scale)

*c* C shears  
*p* P shears



NOTE:  
 Some late normal faults and dykes omitted for clarity

S. J. JOLLEY  
 Ph.D. Thesis 1992